UNIVERSITY OF SOUTHAMPTON

FACULTY OF MEDICINE

CLINICAL AND EXPERIMENTAL SCIENCES

Modelling the Airway Epithelial–Mesenchymal Trophic Unit in Asthma

by

Alison Rachel Hill, MRes, BSc (Hons)

A thesis submitted for the degree of
Doctor of Philosophy

September 2016

UNIVERSITY OF SOUTHAMPTON

ABSTRACT

FACULTY OF MEDICINE

Thesis for the degree of Doctor of Philosophy

Modelling the Airway Epithelial-Mesenchymal Trophic Unit in Asthma

By Alison Rachel Hill

Local exchange of information between human bronchial epithelial cells (HBECs) and fibroblasts allows them to work together as an epithelial-mesenchymal trophic unit (EMTU) that controls tissue homeostasis and co-ordinates inflammatory and repair responses to stimuli. In asthma, human rhinovirus (HRV) and eosinophil major basic protein (MBP) are agents which cause epithelial disruption and are associated with disease exacerbation. I hypothesised that HRV or MBP challenge of BECs induces cellular cross-talk with the underlying fibroblasts, to co-ordinate EMTU proinflammatory and repair responses.

An EMTU co-culture model incorporating polarised HBECs (16HBE14o$^-$) and fibroblasts (MRC5), on the upper and lower surfaces of nanoporous membranes respectively, were apically challenged with double-stranded RNA (dsRNA, viral mimetic) or poly-L-arginine (pLArg, an MBP mimetic). Epithelial physical barrier properties were determined by transepithelial resistance (TER) and FITC-dextran diffusion measurements. Cytokine, matrix metalloprotease (MMP) and growth factor release was determined by ELISA or Luminex® assay. Fibroblast responses were assessed by immunofluorescent staining for α-smooth muscle actin (α-SMA) and proliferation assays. The response of a primary EMTU co-culture model comprising differentiated HBECs and fibroblasts challenged with HRV16 were also investigated.

Ionic but not macromolecular permeability of the epithelium was significantly increased after challenge of the EMTU model with dsRNA or pLArg. Proinflammatory responses of the EMTU models were next investigated and demonstrated that while dsRNA or pLArg induced polarised IL-6, CXCL8 and GM-CSF release, only dsRNA induced CXCL10 release. These mediators were synergistically enhanced in the basolateral compartment of the EMTU model compared to HBEC or fibroblast monocultures. DsRNA and pLArg also induced IL-1α release in the EMTU model and HBEC monocultures but not fibroblasts. Blockade of IL-1 signalling with IL-1 receptor antagonist (IL-1Ra) abrogated dsRNA- and pLArg-dependent basolateral IL-6 and CXCL8 responses. However, only fibroblasts were responsive to stimulation with exogenous IL-1α. These data were confirmed in the primary EMTU model where HRV16 induced IL-1α, IL-6, CXCL8 and CXCL10 release and IL-1Ra significantly reduced HRV16-dependent IL-6 and CXCL8. The effect of dsRNA and pLArg on repair responses within the EMTU models were next investigated. Apical MMP-9, MMP-2, and VEGF release were also induced by dsRNA and pLArg stimulation of the polarised EMTU model which was confirmed in the primary EMTU model following HRV16 infection. DsRNA and pLArg stimulation of the polarised EMTU model also increased fibroblast α-SMA expression, via a mechanism involving TGF-β, whilst having minimal effects on fibroblast proliferation.

Cellular cross-talk within the EMTU model synergistically enhanced basolateral inflammatory responses and activated fibroblast differentiation following viral- or MBP-stimulation. Inflammatory responses were mediated by HBEC-derived IL-1α activation of fibroblasts, whilst fibroblast differentiation was mediated by TGF-β. These mediators may have important consequences in promoting inflammation and remodelling in viral-induced or eosinophil/MBP-associated exacerbations of chronic lung diseases such as asthma.

Table of Contents

List of tables

List of figures

Publications

IL-1α mediates cellular cross-talk in the airway epithelial mesenchymal trophic unit.

Hill AR, Donaldson JE, Blume C, Smithers N, Tezera L, Tariq K, Dennison P, Rupani H, Edwards MJ, Howarth PH, Grainge C, Davies DE, Swindle EJ.

Tissue Barriers. 2016 Jun 28;4(3)

(Attached in Appendix B)

Oral presentations

'Role for IL-1α in viral-induced inflammatory responses in an epithelial-fibroblast co-culture model of the airway mucosa'
12/2014 British Thoracic Society winter conference, London, UK

'Poly(I:C)-activated epithelial cells enhance IL-6 release in a co-culture model of the epithelial-mesenchymal trophic unit'
06/2014 Faculty of Medicine Research Conference, University of Southampton

Poster presentations

'Viral stimulation of bronchial epithelial cells activates repair and remodelling responses in a co-culture model of the airway mucosa'
04/2016 European Respiratory Society (ERS) Research Seminar: New developments in *in vitro* models of the pulmonary epithelium, Berlin, Germany

'Role for IL-1α in viral-induced inflammatory responses in an epithelial-fibroblast co-culture model of the airway mucosa'
09/2015 ERS International Congress, Amsterdam
03/2015 Wessex Immunology Group spring meeting, University of Southampton
03/2015 ERS Lung Science Conference, Estoril, Portugal

'MMP-9 release is suppressed in a co-culture model of the airway mucosa at baseline and after exposure to eosinophil major basic protein (MBP)- or viral-mimetics'*
06/2015 Faculty of Medicine Research Conference, University of Southampton

DECLARATION OF AUTHORSHIP

I, Alison Rachel Hill declare that this thesis and the work presented in it are my own and has been generated by me as the result of my own original research.

Modelling the airway epithelial–mesenchymal trophic unit in asthma

I confirm that:

1. This work was done wholly or mainly while in candidature for a research degree at this University;
2. Where any part of this thesis has previously been submitted for a degree or any other qualification at this University or any other institution, this has been clearly stated;
3. Where I have consulted the published work of others, this is always clearly attributed;
4. Where I have quoted from the work of others, the source is always given. With the exception of such quotations, this thesis is entirely my own work;
5. I have acknowledged all main sources of help;
6. Where the thesis is based on work done by myself jointly with others, I have made clear exactly what was done by others and what I have contributed myself;
7. [Delete as appropriate] None of this work has been published before submission [or] Parts of this work have been published as: [please list references below]:

Signed:.....

Date: .....

Acknowledgements

Firstly I would like to thank the Gerald Kerkut Charitable Trust, not only for their financial support for this work, but also for organising such enjoyable away days. These meetings were a great opportunity to present and discuss my project, for which I am very grateful.

The completion of this thesis would also not have been possible without the support and guidance of my supervisors. I would especially like to thank Dr. Emily Swindle, who has always been really approachable, on-hand to discuss things and has always taken the time to give detailed feedback. I am also thankful for her encouragement to apply for travel grants and go to conferences, which has been a really great part of the PhD experience. I would also like to thank my second supervisor, Professor Donna Davies, whose depth of knowledge and experience has been invaluable.

Within the Faculty of Medicine I would like to thank Liku Tezera for his help and advice on Luminex® assays. I would also like to thank the clinicians who collected the bronchial brushings and biopsies including, Dr. Patrick Dennison, Dr. Hitasha Rupani and Yvette Thirlwall. In particular I would like to thank Prof. Peter H Howarth, Dr. Kamran Tariq, Prof. Ratko Djukanovic and Dr. Tim Hinks who are the principal investigators on the following studies: "Investigation of Pathophysiological Mechanisms in Airway Diseases such as Asthma and COPD" (REC no. 05/Q1702/165),"Investigation of gastro-oesophageal reflux disease (GORD) in asthma" (REC no. 13/SC/0182), "*Ex vivo* modelling of infection and therapeutics in airways disease" (REC no. 09/H0504/109), and "Cross sectional study IL-17) in asthma 10/H0504/2.

I would also like to thank past and current members of the Brooke lab for their assistance and technical advice. In particular, I would like to thank Dr. Cornelia Blume, who did a lot of my initial lab training and has been one of my go-to people for technical advice. I would also like to thank our technicians, Dr. Natalie Smithers and Graham Berreen who work incredibly hard to keep the lab running smoothly. In addition, I would like to thank them for processing the bronchial brushings and biopsy samples and for their help with establishing and maintaining the ALI cultures. I would also like to thank Dr. Emily Swindle for training me to work with HRV, allowing me to use some of her HRV16 stocks and to assay some of her virally-infected ALI supernatants and freeze-

thaw samples. Finally I would like to thank my fellow PhD students, particularly Charlene Akoto, who not only ran some MSD samples for me, but also sits next to me in the office and has been there to share grumbles and successes. My time in the Brooke lab would also not have been the same without my lunch buddies. Special mentions go to Lyndsy Ambler and Richard Latouche who have been good friends to me from the start.

From a non-academic perspective, I would like to thank all of my friends and family. I would particularly like to thank my fellow PhD friends, past housemates and past and current members of the Southampton University Concert Band, who have made Southampton a fun place to live. Special mentions go to Lyndsy Ambler, Natt Day, Kate Packwood, Natasha Denton, Sarah Chitty, Dan Prichard and Dr. Aleks and Miriam Dubas. I would also especially like to thank my Mum and Dad, who have been there for me throughout my PhD. Thank you for supporting me in all of my endeavours. I hope I've done you proud.

Finally I would like to thank my wonderful partner, Jacob Povall, for his support, particularly over the last year and stressful months of writing. Thank you for your incredible patience. You always know just what to say to make things better and have never stopped believing in me. I cannot thank you enough.

Definitions and Abbreviations

2D	two dimensional
ADAM33	a disintegrin and metalloprotease 33
AEA	aspirin exacerbated asthma
AJ	adherens junction
ALI	air-liquid interface
ANOVA	analysis of variance
APCs	antigen presenting cells
ATS	American Thoracic Society
b.d	below detection
BALF	bronchoalveolar lavage fluid
BEBM	bronchial epithelial cell basal medium
BEC	bronchial epithelial cell
BEGM	bronchial epithelial cell growth medium
bFGF	basic fibroblast growth factor
BHR	bronchial hyper-responsiveness
BSA	bovine serum albumin
BTS	British Thoracic Society
CF	cystic fibrosis
CFTR	cystic fibrosis conductance regulator
COPD	chronic obstructive pulmonary disease
CPE	cytopathic effect
DAMPS	damage associated molecular patterns
DAPI	4',6-diamidino-2-phenylindole
DCs	dendritic cells
DMEM	Dulbecco's modified eagle's medium
DMSO	dimethyl sulfoxide
DNA	deoxyribonucleic acid
dsRNA	double stranded RNA
ECM	extracellular matrix
EDTA	ethylenediaminetetraacetic acid
EdU	5-ethynyl-2´-deoxyuridine
EGF	epidermal growth factor
EGFR	epidermal growth factor receptor
EIA	exercise induced asthma
ELISA	enzyme linked immunnosorbent assay
em	emission wavelength
EMT	epithelial-mesenchymal transition
EMTU	epithelial-mesenchymal trophic unit
EPO	eosinophil peroxidase
ET-1	endothelin-1
ex	excitation wavelength
FBS	fetal bovine serum
Fc	fragment crystallisable
FcεRI	high-affinity IgE receptor
FDA	Food and Drug Administration
FITC	fluorescein isothiocyanate
FP	fluticasone propionate
GINA	Global Initiative for Asthma
GM-CSF	granulocyte macrophage-colony stimulating factor
GPCRs	G protein coupled receptors
GWAS	genome-wide association studies
HASM	human airway smooth muscle cells
HBEC	Human bronchial epithelial cell
HBSS	Hank's balanced salt solution

HDM	house dust mite
HEPES	N-(2-hydroxyethyl)piperazine-N'-(2-ethanesulfonic acid)
HGF	hepatocyte growth factor
HLF	human lung fibroblast
HRV	human rhinovirus
ICAM-1	intercellular adhesion molecule-1
ICS	inhaled corticosteroid
IFNAR2	human interferon α/β receptor chain 2
IFNs	interferons
Ig	Immunoglobulin
IGF-1	insulin-like growth factor-1
IKKα/β	IκB kinase
IL	interleukin
IL-1R1	IL-1 receptor 1
IL-1R2	IL-1 receptor 2 (decoy receptor)
IL-1Ra	IL-1 receptor antagonist
IL-1RAcp	IL-1 receptor accessory protein
IL-1RN	IL-1 receptor antagonist gene
INT tetrazolium salt	2-(4-iodophenyl)-3-(4-nitrophenyl)-5-phenyl-2H-tetrazolium chloride
IP-10	interferon-γ induced protein 10
IPF	Idiopathic pulmonary fibrosis
IPS-1	IFN-promoter stimulator 1
IRF	interferon regulatory factor
ISGF-3	IFN-stimulated gene factor 3
ISGs	IFN-stimulated genes
ISRE	IFN-stimulated response element
ITS	insulin-transferrin-selenium
IκB	Inhibitor of NF-κB
JAK	Janus kinase
JAM	junctional adhesion molecule
kb	kilobases
LABAs	long acting β_2 agonists
LDH	lactate dehydrogenase
LDL	low-density lipoprotein
L-Glut	L-glutamine
LPS	lipopolysaccharide
LTRAs	leukotriene receptor antagonists
LTs	leukotrienes
MBP	major basic protein
MC	mast cell
MDA-5	melanoma differentiation-associated protein-5
MEM	minimum essential medium
MHC	major histocompatibility complex
MMP	matrix metalloproteinase
MOI	multiplicity of infection
MSD	Meso Scale Discovery
Mw	molecular weight
MyD88	myeloid differentiation primary response gene 88
NADPH	nicotinamide adenine dinucleotide phosphate
NEAA	non-essential amino acids
NF-κB	nuclear factor κ-light-chain-enhancer of activated B cells
NK cell	natural killer T cell
NLRs	nod-like receptors
NPG	Nature Publishing Group

OCS	oral corticosteroids
ORMDL3	orosomucoid 3
P/S	penicillin/streptomycin
PAMPS	pathogen associated molecular patterns
PBS	phosphate buffered saline
PDGF	platelet-derived growth factor
PE	phycoerythrin
PFA	paraformaldehyde
PGE_2	prostaglandin E_2
PKR	protein kinase R
pLArg	poly-L-arginine
poly(I:C)	polyinosinic-polycytidylic acid
PRRs	pattern recognition receptors
RA	retinoic acid
REC	research ethics committee
RIG-1	retinoic acid-inducible gene-1
RLRs	RIG-like receptors
RNA	ribonucleic acid
ROS	reactive oxygen species
rpm	revolutions per minute
RPMI	Roswell Park Memorial Institute 1640 Medium
RSV	respiratory syncytial virus
RT	room temperature
SABAs	short acting β_2 agonists
SCF	stem cell factor
SD	standard deviation
ST2	IL-33 receptor
STAT	signal transducer and activator of transcription
Strep-HRP	streptavidin conjugated to horseradish-peroxidase
Strep-PE	streptavidin conjugated to phycoerythrin
SV40	simian virus 40
$TCID_{50}$	tissue culture infective dose 50%
TER	transepithelial resistance
TGF	transforming growth factor
Th2	type 2 T helper
TIMP	tissue inhibitor of metalloproteinase
TIR	toll/interleukin-1 receptor
TJS	tight junctions
TKB1	TRAF family member-associated NF-κB-binding kinase 1
TLRs	toll-like receptors
TMB	3,3'-,5,5-tetramethylbenzidine
TNF	tumour necrosis factor
TRAF	TNF receptor associated factor
TRIF	TIR-domain-containing adapter-inducing interferon-β
TSLP	thymic stromal lymphopoietin
TX-100	Triton™ X-100
UTR	Untranslated region
UV	ultra-violet
VCAM-1	vascular cell adhesion molecule-1
VEGF	vascular endothelial growth factor
VNTR	variable number tandem repeat
VP	viral protein
VPg	Viral protein genome-linked
WHO	World Health Organization
ZO	zona occluden
α-SMA	α-smooth muscle actin

1. Introduction

1.1 Asthma background

1.1.1 Asthma definition

Asthma is a condition of the conducting airways characterised by chronic inflammation, distinct structural and functional changes and bronchial hyper-responsiveness (BHR) to a variety of stimuli [1, 2]. BHR is where inhaled agents from the environment trigger contraction of the smooth muscle that surrounds the airway wall, causing a narrowing of the lumen and breathing difficulty. Symptoms of asthma therefore include coughing, wheezing, shortness of breath and tightness in the chest [3, 4].

1.1.2 Asthma prevalence

In the world, over 334 million people of all ages are affected by asthma [5] and it is the most common non-communicable disease among children [6]. In Europe, asthma affects 30 million people under the age of 45. The UK has the 2nd highest prevalence of asthma in Europe [7] where 5.4 million people are currently receiving treatment; 1 in 11 children (1.1 million) and 1 in 12 adults (4.3 million) [8]. While the prevalence of asthma has remained unchanged since the late 1990s, the burden of asthma in the UK remains high. For example, in 2014, 73046 people were admitted to hospital (of which 30,194 were children) and 1,216 people died (of which 40 were children) due to their asthma [8-10]. Many of these hospital admissions are avoidable and as many as 90% of deaths are preventable with complacency in asthma care and poor disease management being a factor [9]. However, even with optimum treatment and management, approximately 5-10% of asthmatic subjects are still non-responsive to the two main therapies of β-agonists and corticosteroids [11, 12]. Therefore there is a need for novel treatments and better management for asthma.

1.1.3 Asthma pathology

1.1.3.1 Th2 Inflammation

One of the characteristic pathologies of asthma is chronic airway inflammation. In the majority of cases, this is driven by inappropriate T helper 2 (Th2) cell-driven (allergic) responses to normally innocuous antigens. Allergic sensitisation occurs when dendritic cells (DCs) activate an adaptive Th2 immune response against an allergen (Figure 1.1.3-1A). These cells reside beneath the bronchial epithelium and extend projections between human bronchial epithelial cells (HBECs), towards the luminal surface. Expression of pattern recognition receptors (PRRs) allows them to survey the airway. Recognition of allergen by DCs leads to its uptake and processing for presentation at the cell surface in the context of major histocompatibility complex (MHC) class II molecules. Allergen-MHC class II complexes are recognised by naive T cells via the T cell receptor. This interaction, along with DC-derived cytokines and the engagement of cell-surface co-stimulatory molecules, promote T cell proliferation and differentiation into effector Th2 cells [13]. These cells guide the differentiation of B cells into plasma cells which secrete antibodies [13, 14]. In addition, Th2 cells secrete cytokines such as interleukin (IL)-4 and IL-13, which promote class switching from immunoglobulin (Ig)G to IgE. This allergen-specific IgE binds to the high-affinity IgE receptor (FcεRI) receptor expressed on the surface of mast cells (MCs) in a process called MC sensitisation.

The immediate type-I hypersensitivity reaction occurs when the allergen is re-encountered and binds and cross-links allergen-specific IgE on the MC surface (Figure 1.1.3-1B). This activates the release of MC granule contents such as histamine and *de novo* synthesis of cysteinyl leukotrienes (LTs), which induce airway smooth muscle (ASM) contraction, oedema and mucus production resulting in a sharp decline in lung function within the first hour after allergen re-exposure. This is known as the early phase of the allergic response and is followed by the late phase allergic response where there is an influx of effector cells via the release of newly generated proinflammatory mediators including, IL-4, IL-13, IL-5, IL-9 and granulocyte macrophage-colony stimulating factor

(GM-CSF). These are generated from MCs and Th2 cells and recruit other effector leucocytes, such as eosinophils. This leads to a more sustained decline in lung function, lasting several hours or days. In the asthmatic airway this late phase can develop into chronic inflammation and airway remodelling [13].

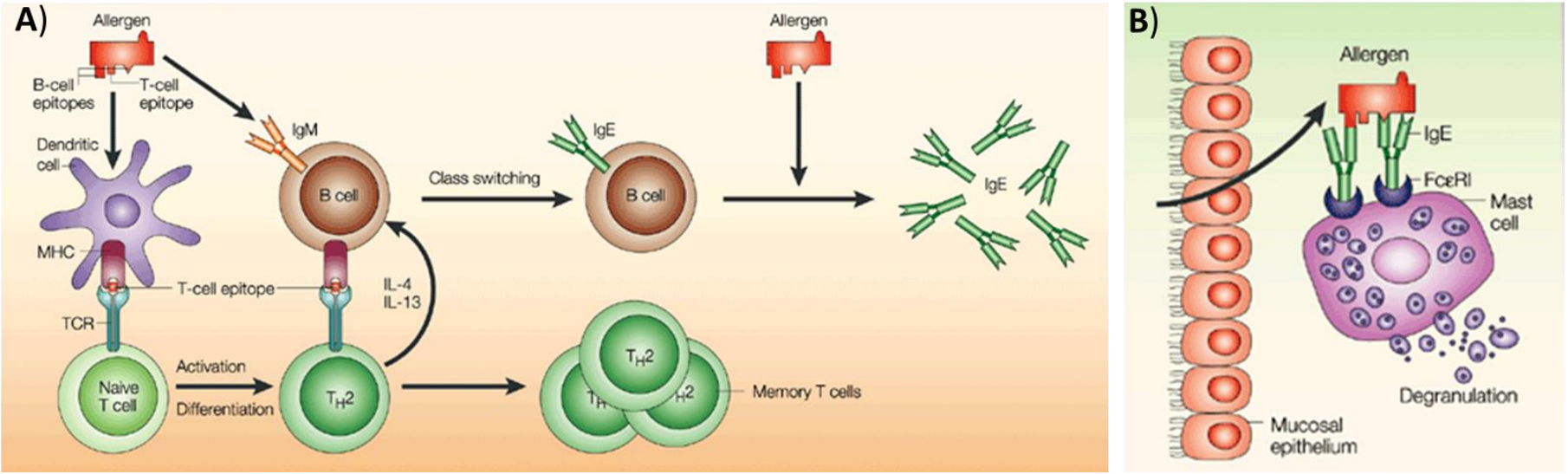

Figure 1.1.3-1 Schematic representation of allergic sensitisation and type I hypersensitivity reactions.

(A) Primary exposure to allergens leads to their uptake by mucosal DCs. DCs present antigens to naive T cells and activate differentiation into Th2 cells. Fully differentiated Th2 cells secrete IL-4 and IL-13 and provide co-stimulatory signals to B cells, leading to their activation and production of IgE antibody. IgE then binds to FcεRI expressed on the surface of MCs. (B) When agents to which a person has been sensitised are re-encountered and bind to IgE on the MC surface, MCs are activated to release their granule contents and synthesise inflammatory mediators. Together these granule contents and inflammatory mediators induce BHR and drive eosinophilic inflammation, leading to lung function decline. Figure reproduced from reference [15] with permission from the Nature Publishing Group (NPG).

1.1.3.2 Airway remodelling

In addition to chronic airway inflammation, asthma is characterised by changes in the normal composition and structural organisation of the airways (Figure 1.1.3-2), termed airway remodelling [16]. These changes include alterations to the epithelium such as epithelial cell shedding, loss of ciliated cells and goblet cell hyperplasia resulting in increased mucus production. Beneath the asthmatic epithelium, the basement membrane is thickened and there is increased collagen deposition. This enhanced extracellular matrix (ECM) protein deposition is a consequence of the increased number of activated fibroblasts called myofibroblasts which disrupt the normal balance between ECM synthesis and breakdown towards ECM deposition leading to subepithelial fibrosis. Other characteristics of airway remodelling are angiogenesis and increased smooth muscle mass [17, 18]. These structural changes ultimately cause thickening of the airway wall leading to non-specific BHR, airflow obstruction, increased stiffness and eventually lung function decline [19, 20].

It has previously been widely assumed that airway remodelling in asthma is driven by chronic inflammation. This is because immune cells such as MCs, eosinophils and neutrophils, release mediators which are damaging to the surrounding structural cells. In addition, these cells release a range of pro-fibrotic cytokines and growth factors. For example, eosinophils are a source of transforming growth factor (TGF)-β [21]. However, airway remodelling has been observed in childhood asthma, in the relative absence of inflammation, from the age of 4 [19, 22]. Furthermore, bronchoconstriction promotes remodelling in the absence of inflammation. For example, methacholine-induced bronchoconstriction in human volunteers, increased epithelial TGF-β expression, collagen deposition and basement membrane thickening in bronchial biopsies [23]. For these reasons, it is now widely accepted that airway remodelling occurs in parallel with, rather than as a consequence of inflammation [1].

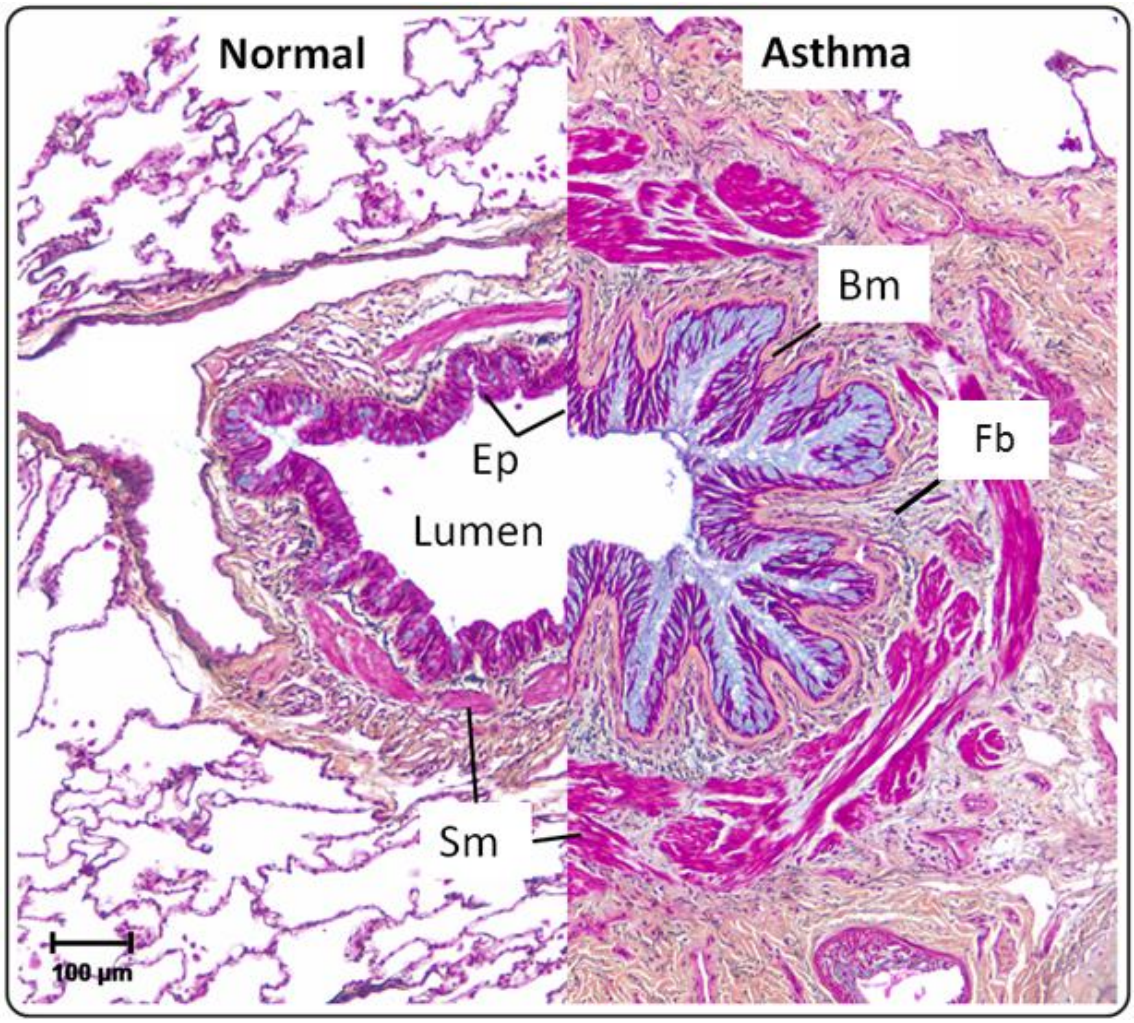

Figure 1.1.3-2 Comparison in airway structure between the normal and asthmatic airway.

Images are cross-sections of medium-sized airways from a normal individual and a severe asthmatic patient, stained using Movat's pentachrome stain. In asthma, there is a narrowing of the airway lumen, mucus hypersecretion (blue) by the epithelium (Ep), basement membrane (Bm) thickening, increased subepithelial fibrosis (Fb) and increased smooth muscle (Sm) mass. Reproduced from reference [24] with permission from Dove Medical Press.

1.1.4 Asthma exacerbations

Worsening and life-threatening symptoms are known as an asthma exacerbation or attack. Common causes of exacerbations include inhaled environmental agents, which can trigger severe airway constriction and inflammation. For example, as described in section 1.1.3.1, inhaled allergens can cause worsening of asthma symptoms by activating allergic reactions. However, the most frequent cause of asthma exacerbations is the common cold, caused by human rhinovirus (HRV) infection. Exacerbations caused by HRV are particularly severe in nature, and patients often require hospitalisation [14].

1.1.4.1 HRV biology

HRV is a positive sense, single-stranded, non-enveloped, ribonucleic acid (RNA) virus of the picornavirus family [25, 26]. The HRV genome is approximately 7.2 kilobases (kb) and consists of a single gene, with a single open reading frame, joined to a 5' untranslated region (UTR) (Figure 1.1.4-1). The 5' UTR contains structural and sequence elements necessary for gene translation and is attached to a short viral priming protein (VPg), which serves as a primer for genome replication [25, 27]. The viral genome is translated as a polyprotein which is processed into structural (P1) and non-structural proteins, including those involved in protein processing and genome replication (P2 and P3) (Figure 1.1.4-1). Structural proteins include viral protein (VP) 1, VP2, VP3 and VP4 which assemble into an icosahedral structure to form the viral capsid (Figure 1.1.4-2). VP4 is internal and functions in anchoring the RNA core to the capsid. VP1-3 are external and exposed to the host antibody response. Variations in VP1-3 therefore determine the viral serotype, of which there are over 100 [25]. The serotypes are classed into groups (HRV-A,-B or -C) based on their genetic homology. The groups can then be subdivided further based on which receptor they use for cell entry. For example, the major group encompasses 90% of the known serotypes of the HRV-A and -B families, which use intercellular adhesion molecule-1 (ICAM-1) as their cell entry receptor [28, 29]. The minor group encompasses 10 HRV-A and HRV-B serotypes, which use the low-density lipoprotein (LDL) receptor. The cellular receptor for HRV-C serotypes was recently identified as cadherin-related family member 3

(CDHR3) [30]. HRV-A and HRV-C cause the most severe illness in infants and are most likely to cause severe disease [31].

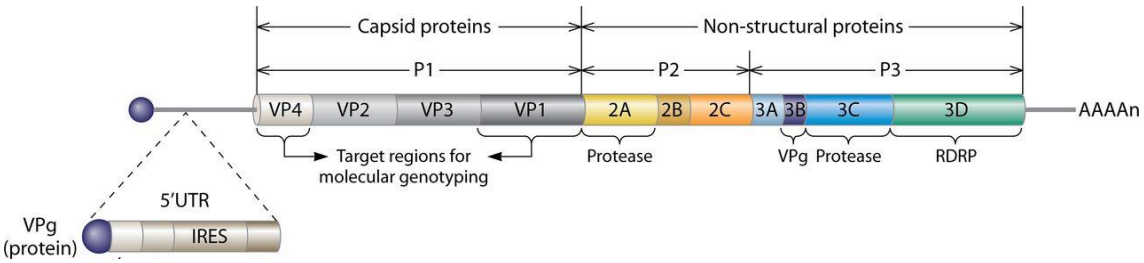

Figure 1.1.4-1 Structure of the HRV genome [25].

The 5' end of the viral genome consists of a 5' UTR which is attached to the VPg protein and contains structural and sequence elements necessary for gene translation such as the internal ribosomal entry site (IRES). The translated region contains genes for structural proteins (VP1-4) and non-structural proteins including viral proteases involved in protein processing, and proteins involved in genome replication such as VPg and RNA-dependent RNA polymerase (RDRP). Reproduced from reference [25] with permission from the American Society for Microbiology

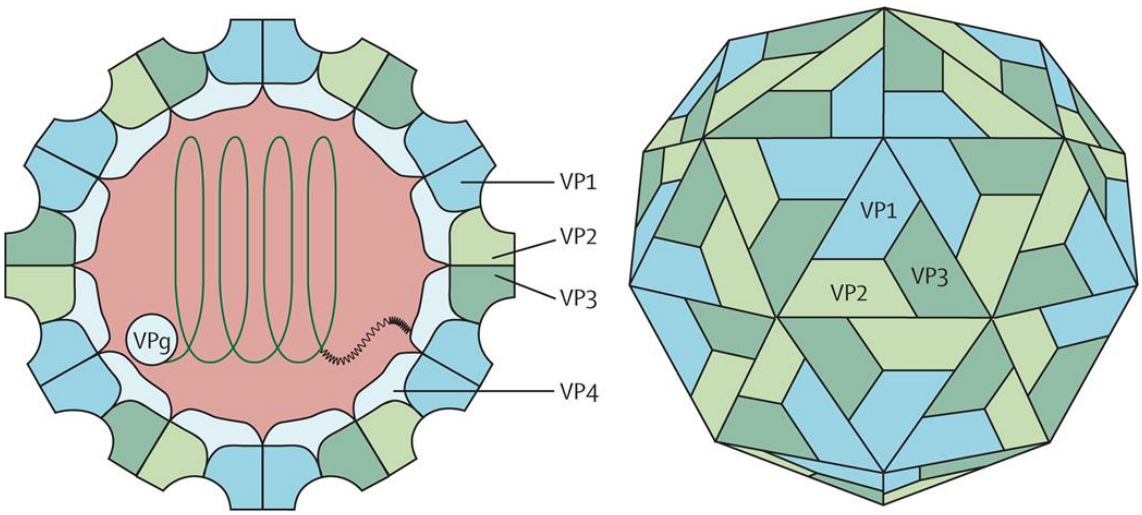

Figure 1.1.4-2 HRV virion structure.

The HRV capsid is composed of four structural viral proteins (VP1-VP4), of which VP1, VP2, and VP3 are external. VP4 is internal and functions in anchoring the RNA genome to the capsid. Reproduced from ViralZone:www.expasy.org/viralzone with permission of the Swiss Institute of Bioinformatics.

1.1.4.2 HRV and asthma

HRV infection is the most frequent cause of common cold symptoms in adults [25, 29]. Typically symptoms are limited to the upper respiratory tract and include rhinorrhoea and nasal obstruction, which are associated with a neutrophilic inflammatory response, increased vascular permeability and mucus hypersecretion [29]. Individuals with asthma or other chronic respiratory lung diseases tend to have more frequent upper and lower respiratory symptoms [32]. Lower respiratory symptoms include cough, shortness of breath, chest tightness and wheezing, all of which are also clinical features of acute asthma [29]. Several studies have shown that infants with wheeze following HRV infection have an increased risk of subsequent asthma suggesting that HRV could play a role in asthma development [33, 34]. The mechanisms behind why HRV is associated with an increased risk of asthma development are unclear. It has been suggested that in childhood, when the airways and immune system are still developing, they may be more vulnerable to HRV infection and the effects of viral-induced cytokines and growth factors. Alternately, HRV infection in early life may reveal a pre-existing tendency for asthma development. In reality, the role of HRV in asthma development may be a combination of these theories or even more complex [26].

In addition to its association with asthma development in childhood, HRV is also associated with asthma exacerbations. Viral infections are responsible for approximately 85% of asthma exacerbations in children and of these HRV accounts for two thirds [35]. Interestingly, seasonal peaks in asthma exacerbations correspond to peaks in HRV infection with increases in spring and autumn, when children return to school [36]. This suggests that the association between HRV and asthma exacerbation is causal [26]. However in inoculation studies, HRV alone did not trigger asthma exacerbations in subjects with stable asthma, indicating other factors contribute to HRV-induced exacerbations including allergens, pollutants, stress and co-infections [26, 37]. While allergy appears to be the strongest risk factor for viral-induced exacerbations in stable asthmatics those with unstable asthma may be more at risk [26].

1.1.5 Asthma treatments

Current asthma treatments are unable to alter the natural course of the disease and offer only limited amelioration of viral-induced asthma exacerbations [14, 38, 39]. However, in the majority of patients they are able to control the clinical symptoms and minimise future risk of exacerbations by targeting disease pathology. For example, therapies can be broadly classified into reliever and preventer treatments which aim to reverse bronchoconstriction and suppress inflammation respectively [11, 12]. Some of the commonly used treatments are described below:

1.1.5.1 β_2-agonists

β_2-agonists are a reliever medication. They are one of the most commonly prescribed treatments for asthma and are often used in combination with corticosteroids. This class of drugs work by binding β_2-adrenergic G protein coupled receptors (GPCRs) on airway smooth muscle cells, leading to activation of adenylyl cyclase and generation of intracellular cyclic adenosine monophosphate (cAMP). This in turn activates signalling pathways, resulting in a reduction in intracellular Ca^{2+} and the activation of K^+ channels, with the consequent hyperpolarisation of airway smooth muscle, producing muscle relaxation [40, 41]. Muscle relaxation leads to widening of the airway lumen which relieves episodes of BHR [41].

There are 2 classes of β_2-agonists- short acting β_2 agonists (SABAs) and long acting β_2-agonists (LABAs). As the name suggests, SABAs (e.g. salbutamol) provide rapid symptom relief and short term prophylactic protection (4-6h) against bronchoconstriction. SABAs are therefore mainly used as a reliever therapy for the treatment of acute asthma exacerbations [40, 42]. In contrast, LABAs (e.g. salmeterol and formoterol) provide sustained bronchodilation (12h) and are therefore used as a long acting reliever therapy usually in combination with an inhaled corticosteroid (ICS) for poorly controlled asthma [40, 42]. However, in some patients regular use of LABAs leads to tolerance to their bronchoprotective effects and reduced asthma control [41].

1.1.5.2 Corticosteroids

Corticosteroids are a preventer medication. They are the most effective anti-inflammatory therapy for asthma and are the first-line treatment for adults and children with persistent asthma. This class of drugs work by suppressing multiple inflammatory genes that are activated in the asthmatic airways, leading to a reduction in inflammation, asthma symptoms and exacerbations [43]. Corticosteroids are typically administered by inhaler which reduces the systemic side effects observed with oral corticosteroids (OCS) [43]. While most patients respond to low doses of ICS (e.g. budenoside or fluticasone propionate), patients with severe disease may require higher doses or regular treatment with OCS (e.g. dexamethasone) [42, 43]. Patients that require regular OCS treatment are described as steroid refractory, while patients that are resistant to ICS and OCS are described as corticosteroid resistant [43].

1.1.5.3 LT receptor antagonists (LTRAs)

LTRAs (e.g. montelukast) are an alternative first-line therapy and an add-on treatment for asthma [44]. This class of drugs work by blocking the effects of cysteinyl LTs which are powerful smooth muscle contractile agents released by MCs upon allergen challenge [44]. In addition to their bronchoconstrictive effects, LTs also exert pro-inflammatory effects acting as an eosinophil chemoattractant and inducing cytokine production from lymphocytes [44]. LTRAs therefore act as both a bronchodilator and an anti-inflammatory therapy and significantly improve lung function, asthma symptoms and quality of life. Many stimuli, including allergens and viral infection, can initiate LT production suggesting that patients with allergen or viral-induced asthma exacerbations may be responsive to LTRAs [12, 44].

1.1.5.4 Asthma treatment levels

In order to assist clinicians in the treatment of asthma, organisations such as the Global Initiative for Asthma (GINA), the British Thoracic Society (BTS) and the American Thoracic Society (ATS), produce treatment guidelines based on the severity of asthma symptoms (Table 1.1.5-1). These phenotypes include mild intermittent, mild persistent, moderate persistent and severe persistent

[45]. However, this has limitations since someone may have severe disease but their symptoms may be well controlled. Alternatively patients with the same severity of disease (e.g. mild persistent) may respond differently to the same treatment. In addition, asthma symptoms may fluctuate over time and treatments may need to be reviewed and adjusted accordingly. Therefore, asthma severity is assessed according to the treatment level required to achieve good symptom control [42] and patients can step up or down the treatment level depending on their symptoms. However, some patients (approximately 5-10%), do not achieve good symptom control even with the maximum level of treatment and are described as having severe, persistent/uncontrolled asthma [7, 11, 12, 42]. One potential reason for this, is that although current therapies treat the inflammation and BHR in asthma, their effects on structural remodelling of the airways are limited [46]

Table 1.1.5-1 Overview of treatment levels required to control symptoms and minimise future risk for asthma of different severities [42, 45].

Treatment Step	Asthma severity	Treatments
1	Mild intermittent	SABAs as needed Consider low dose ICS
2	Mild intermittent	SABAs as needed Low dose ICS
3	Mild persistent	SABA as needed Moderate dose ICS + LABA. (add LTRAs if control inadequate)
4	Moderate persistent	SABAs as needed High dose ICS/LTRA + LABA.
5	Severe persistent	SABAs as needed High dose ICS/LTRA + LABA + OCS.

1.1.6 Asthma phenotypes and endotypes

Asthma has traditionally been classified according to clinical symptoms, disease pathology and symptom control, resulting in 4 phenotypes (mild intermittent, mild persistent, moderate persistent and severe persistent asthma), each having either an allergic (Th2) or non-allergic (non-Th2) inflammatory component [45]. However, asthma is a heterogeneous disease involving multiple genetic and environmental interactions over the life course and as mentioned in section 1.1.5 there is heterogeneity in responses to treatment. Therefore several new approaches to classifying asthma have been developed. Haldar *et al* were the first to use multivariate cluster analysis and identified 5 distinct phenotypes of asthma based on symptoms and eosinophilic inflammation in patient populations, which traditionally had been classified as mild to moderate [47]. A further 5 distinct phenotypes were identified for severe asthma which had some overlap with those described by Haldar *et al.* [48].

Currently, asthma is broadly associated with either a Th2 (allergic) eosinophilic inflammatory phenotype or non-Th2 (non-allergic), typically neutrophilic, inflammatory phenotype [49, 50]. However, within these phenotypes there are a variety of differences including the age of onset, symptom severity and asthma triggers (Figure 1.1.6-1).

Th2 asthma phenotypes are strongly linked to atopy and allergy and involve type I hypersensitivity reactions and eosinophilic inflammation [49]. They can be further divided into 4 subphenotypes; early onset asthma, late onset asthma, aspirin exacerbated asthma (AEA) and exercise induced asthma (EIA). Early-onset asthma, occurring in childhood (before 12 years of age), ranges from mild-severe and is linked to atopy [49, 51-53]. Late onset asthma, occurs after the age of 12 (often age 20 or later) and is typically severe, eosinophilic and not linked to atopy [49, 51-53]. AEA is a recognised subphenotype of late onset asthma which is highly eosinophilic and is characterised by life-threatening non-IgE mediated responses to aspirin [49]. Finally EIA is a milder form of Th2 asthma where exacerbations are triggered in response to sustained exercise [49]. The majority of patients with Th2-associated asthma are particularly responsive to corticosteroid treatment [54, 55], which

suppresses inflammation and activates eosinophil apoptosis. However, there are some severe phenotypes for which corticosteroids are ineffective [49]. Recently there has been some success in the development of novel therapeutics that target the pathological mechanisms underlying these severe Th2 phenotypes. These include humanised monoclonal antibodies that bind to and block the activities of key markers of Th2-associated inflammation. For example, anti-IgE (Omalizumab) recognises the fragment crystallisable (Fc) region of free IgE and prevents its binding to FcεRI on MCs, basophils and DCs. As a consequence, MC degranulation is prevented leading to improved symptoms, reduced exacerbations and reduced corticosteroid use, without loss of asthma control in severe allergic asthma patients [56, 57]. Another successful monoclonal antibody therapy is anti-IL-5 (mepolizumab), which prevents free IL-5 from binding to its receptor on the surface of eosinophils, preventing terminal differentiation and survival, resulting in reduced eosinophilia and exacerbations in severe persistent eosinophilic asthma [58, 59].

Non-Th2 asthma phenotypes have an absence of Th2 inflammation and tend to be late in onset, non-atopic and associated with neutrophilic inflammation [12, 60]. Although the cause of neutrophilic inflammation is not fully understood, Th17 cells are reported to play a role. This asthma phenotype is also associated with non-allergic environmental factors such as smoking, particulate air pollution, occupational exposures and viral or bacterial infection [49, 61]. Non-Th2 asthma is also associated with co-morbidities including obesity and hormonal imbalances which may explain the development of a later onset asthma phenotype in women (obese, non-eosinophilic) [49, 62]. In contrast, to patients with Th2 asthma, patients with non-Th2 asthma generally respond poorly to corticosteroid therapy [55, 63] and this treatment may even promote neutrophilia [64-67].

Asthma phenotypes can be further classified based on the pathological mechanisms behind the disease known as endotypes. For example, Woodruff *et al* were able to differentiate between Th2-high and Th2-low asthma based on the gene expression of *CLCA1*, *POSTN* and *SERPINB2* [68] and regulation by IL-13 [69] revealing a Th2-high population which were responsive to ICS and predicted responsiveness to anti-IL-13 therapy [70]. Defining asthma phenotypes and endotypes will not only allow more targeted treatment and

improved asthma management for individual patients, but also enable the development of targeted novel therapies [71].

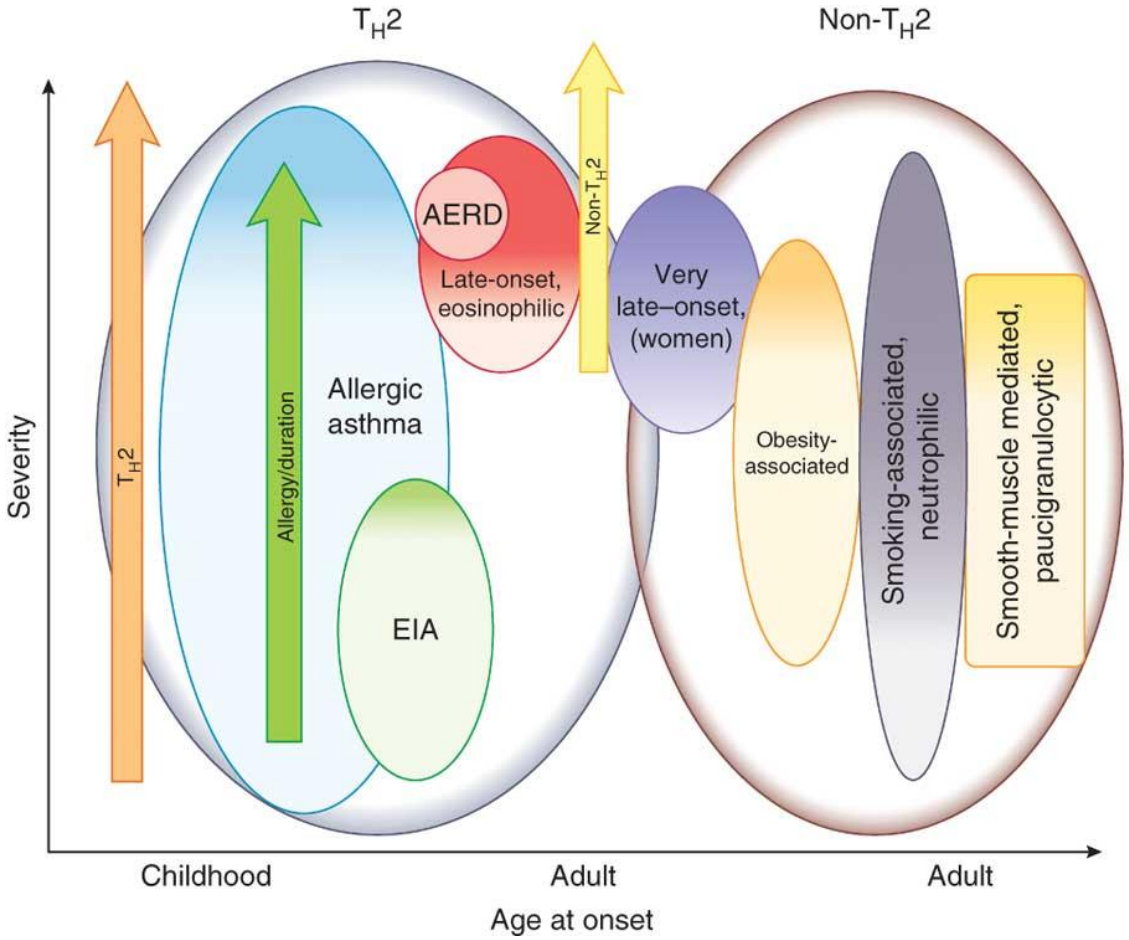

Figure 1.1.6-1 Theoretical grouping and overlap of emerging asthma phenotypes proposed by Wenzel *et al.* [49].

Phenotypes can be broadly separated into Th2- and non-Th2-associated asthma. Th2-associated asthma can be late or adult in onset and contains several subphenotypes including classic allergic asthma, mild exercise induced asthma (EID) and more severe late-onset eosinophilic asthma which can be exacerbated by aspirin in some patients (aspirin-exacerbated respiratory disease (AERD). Non-Th2 asthma is usually adult in onset and subphenotypes are obesity-associated, smoking-related, smooth muscle-mediated or very late in onset in women. While inflammation is generally neutrophilic in non-Th2 asthma, an absence of inflammatory processes is observed in the paucigranulocytic subtype Reproduced from reference [49] with permission from the NPG.

1.1.7 Genetics of asthma

The many phenotypes and endotypes of asthma highlight the disease complexity and the need to understand the interplay between multiple genetic and environmental factors. Recent studies have identified several asthma susceptibility genes including *ADAM33*, *PHF11*, *DPP10*, *GPR154*, *ORMDL3,* and *CYFIP2* [1, 14]. In most cases the biological function of these genes and their contribution to the development of asthma are still poorly understood but some genes are associated with allergy and expressed in the structural cells of the airway.

The asthma susceptibility genes associated with allergy and Th2 inflammation include genes for antigen presentation (*HLA-DRB1, HLA-DQB1*), T cell differentiation (*IL2RB, GATA3*), Th2 cytokines (*IL4*, *IL13*), IL-4 signalling (*IL4RA, STAT6*) and subunits of the high affinity IgE receptor (*FCERIA*, *FCERIB*) [14, 72].

1.1.7.1 Epithelial-associated asthma susceptibility genes

Several independent, unbiased genome-wide association studies (GWAS) have identified a large number of asthma susceptibility genes that are localised to the epithelium. These include genes associated with epithelial barrier functions (*MUC8, PCDH1, CDHR3, GPR154)* [1, 14, 73], and inflammatory mediators including thymic stromal lymphopoietin (*TSLP*) [74] and the IL-1 family of cytokines *(IL33, IL1RL1(ST2), IL18R1, IL1RN)* [75, 76]. The association of TSLP, IL-33 and its receptor (ST2) with asthma suggests a role for the epithelium in driving allergic sensitisation as these cytokines are known to activate DCs and promote Th2 cell differentiation [77-79]. TSLP and IL33 expression are also increased in HBECs from asthmatic compared to healthy donors [80-82]. The association of the IL-1α and IL-1β receptor antagonist gene (*IL1RN)* [76] with asthma suggests a central role of the epithelium in driving inflammation. In one study, patients with the A2 allele of the *IL1RN* gene had significantly lower serum IL-1 receptor antagonist (IL-1Ra) levels [83] which may lead to increased IL-1 signalling and inflammation.

Another epithelial gene strongly associated with asthma is the gene encoding orosomucoid 3 (*ORMDL3*) [75]. While the exact role of epithelial ORMDL3 in asthma is still unclear, ORMDL3 expression is induced by allergen and Th2 cytokines [84]. Overexpression of ORMDL3 in primary HBECs *in vitro* induces

chemokine and matrix metalloproteinase (MMP) expression suggesting a role for this gene in inflammation and remodelling [84]. This is supported by increased inflammation and remodelling in the airways of mice overexpressing ORMDL3 [85].

The product of another asthma susceptibility gene, *CDHR3,* was recently identified as the cellular receptor for serotype group C HRVs (HRV-C) [30, 86]. In addition, asthma-associated polymorphisms in *CDHR3* enhance viral binding and increase progeny yields *in vitro* [30, 86]. These polymorphisms may therefore have important consequences in asthma and could explain why HRV-C causes particularly severe exacerbations of disease [31].

1.1.7.2 Mesenchymal-associated asthma susceptibility genes

A number of asthma susceptibility genes are also associated with repair and remodelling and include *ADAM33, CHI3L1, PDE4D, SMAD3* and *PLAUR*. [75, 87-90]. A disintegrin and metalloprotease 33 (ADAM33) is a membrane-anchored MMP that has diverse functions including shedding of cell surface proteins such as cytokines and growth factors and their receptors, that could potentially promote airway inflammation and remodelling in asthma. Studies in mice demonstrate a potential *ADAM33* gene-environment interaction that could contribute to asthma pathogenesis, as transgenic *ADAM33* expression enhanced inflammatory and remodelling responses to HDM allergen [91]. In addition to the role of ADAM33 in cell-cell and cell-matrix interactions, other mesenchymal asthma susceptibility genes include genes involved in tissue remodelling (*CHI3L1*), degradation of ECM (*PLAU*R), mediating TGF-β signalling (*SMAD3*) and airway smooth muscle contractility (*PDE4D*) [75, 87-90, 92].

1.2 The bronchial epithelium

1.2.1 Epithelial cell functions

The identification of epithelial and mesenchymal asthma susceptibility genes suggests that the structural cells of the airway are key players in asthma pathology. In addition, as the interface between the external environment and the internal tissue of the lung, HBECs are in a key position to mediate gene-environment interactions. The functions of HBECs in health and disease are therefore of considerable interest. HBECs line the conducting airways in a pseudostratified epithelium, which functions in protecting the internal mileu of the lungs by forming physical, chemical and immunological barriers to the external environment (Figure 1.2.1-1).

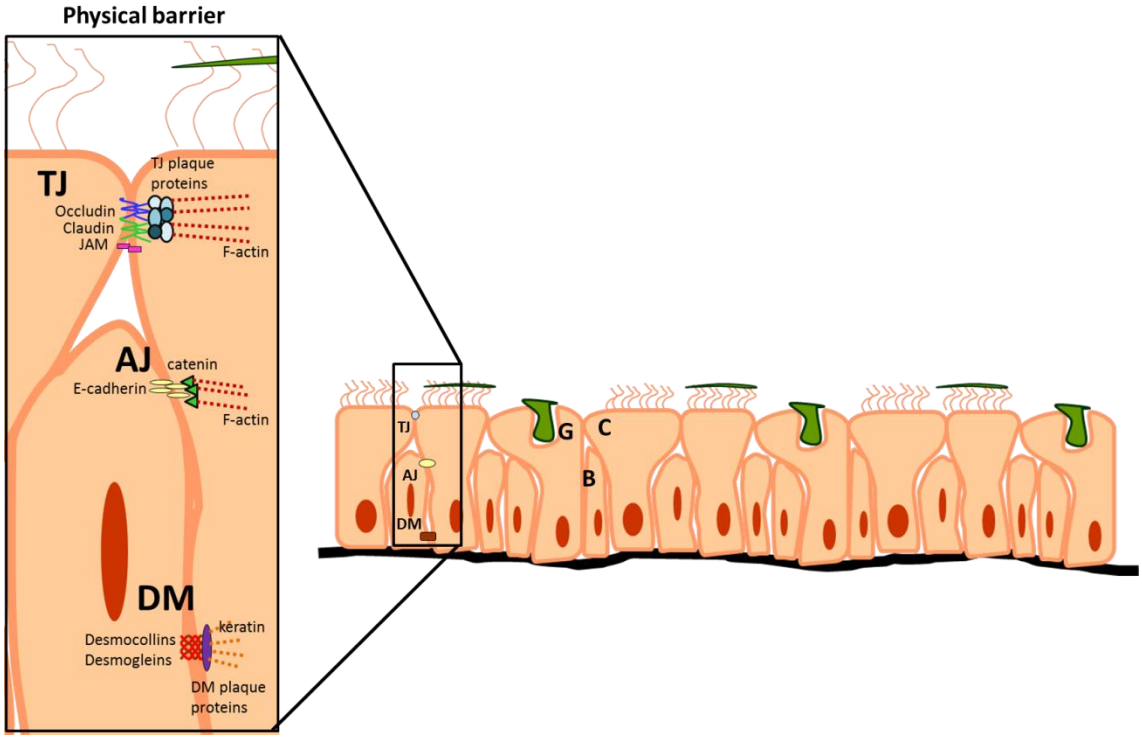

Figure 1.2.1-1 Schematic of the pseudostratified bronchial epithelium [1, 93]. The bronchial epithelium is comprised of ciliated (C), goblet (G) and basal cells (B), which line the airway lumen and protect the internal mileu of the lung. Cells form a physical barrier by the formation of three different types of cell-cell contacts: tight junctions (TJs), adherens junctions (AJs) and desmosomes (DMs). Goblet cells also secrete mucus which traps inhaled agents, and is removed by the action of ciliated cells. Epithelial cell secretions also contain host defence molecules which form a chemical barrier. The immunological barrier refers to the ability of the epithelium to promote inflammatory responses by the expression and activation of PRRs as well as the ability to interact with cells of the adaptive immune system.

1.2.1.1 The physical barrier

HBECs provide a physical barrier to the external environment by forming macromolecular protein complexes which seal the cells together, preventing the passage of molecules and ions. These complexes also give polarity to the cells, regulate epithelial permeability and maintain tissue integrity by connecting to the actin cytoskeleton [1]. HBECs form three types of cell-cell contacts: tight junctions (TJs), adherens junctions (AJs) and desmosomes (Figure 1.2.1-1).

TJs are the most apical junctional complexes and are composed of integral membrane proteins, whose extracellular domains form tight links with similar proteins on adjacent cells [93]. This forms a selectively but variably permeable barrier to the passage of ions and solutes via the paracellular pathway [94]. In addition, it forms a barrier between the apical and basolateral regions of the plasma membrane, preventing the diffusion of membrane proteins and glycolipids, and maintaining cell polarity [93, 94]. Proteins of the TJ include integral membrane proteins with 2 extracellular domains and 4 transmembrane domains, including occludin, tricellulin and members of the claudin family (of which there are at least 24) [95]. In contrast the TJ protein, junctional adhesion molecule (JAM), has 1 extracellular and 1 transmembrane domain [95]. The differential expression and properties of the integral membrane proteins confers distinctive ionic permeabilities to the TJs in which they are found [1, 94]. This is particularly determined by the extracellular domains, while the intracellular, C-terminal domain binds to membrane-associated scaffolding proteins which links them to the cell cytoskeleton and stabilises the TJ complex [93, 94]. Scaffolding proteins include the zona occluden (ZO) molecules (ZO-1-3) cingulin and 7H6 [1, 95]. A variety of signalling molecules and proteins, that play roles in regulating proliferation and differentiation, also associate with the TJ protein scaffold [1, 96]. TJs therefore have more than just a physical function.

Below and in close apposition to TJs are AJs, which are important in the development of the epithelial layer and TJ assembly [1, 94]. AJs mediate cell-cell adhesion via interactions between E-cadherin proteins. These are transmembrane glycoproteins, whose extracellular domains interact with E-cadherins on adjacent cells in a Ca^{2+}-dependent manner [97]. The cytosolic

domains of E-cadherin are linked to the actin cytoskeleton by adaptor proteins including, α- and β-catenin [93]. These linkages are not only essential for strong adhesion but also mechanically connect adjacent cells [93, 97]. In addition, β-catenin and other proteins that associate with the cytosolic domains of cadherins, such as p120-catenin and epidermal growth factor receptor (EGFR), are signalling molecules important in the regulation of proliferation and differentiation [93, 97].

Desmosomes are the most basal cell-cell contacts and provide strong adhesion between cells via specialised desmosomal cadherins; desmocollins and desmogleins [93]. The cytosolic domains of these proteins are linked to the keratin cytoskeleton by adaptor proteins including γ-catenin, plakoglobin, plakophilin and desmoplakin [93]. This interaction contributes to the cohesive and mechanical strength of the epithelium [98].

In addition to cell contacts, epithelial secretions also contribute to the physical barrier. For example goblet cells secrete mucus, the main components of which are the mucins MUC5B and MUC5AC [99]. These molecules are highly charged and oligomerise to form a viscoelastic gel that traps inhaled agents, which are then removed by the mucocilliary escalator. This process is supported by serous cell secretions which hydrate the airway surface, and provide a fluid matrix for the gel-forming mucins and other macromolecules [100].

1.2.1.2 The chemical barrier

Epithelial cell secretions also form a chemical barrier that detoxifies noxious particles inhaled from the environment. For example, mucus contains a variety of molecules involved in host defences. These include soluble IgA and antimicrobial components such as defensins, cathlecidins, lysozyme, lactoferrin, secretory phospholipase A2 and secretory leukocyte protease inhibitor [99]. The mechanisms by which these antimicrobials provide protection include disruption of bacterial cell walls and membranes, sequestering microbial nutrients and acting as decoys for microbial attachment. In addition to antimicrobials, mucus also contains antioxidants such as reduced glutathione, antioxidant enzymes, uric acid, vitamins C and E

and proteins such as albumin, transferrin, ceruloplasmin and lactoferrin. These antioxidants protect against the effects of ambient oxygen as well as exogenous oxidants from air pollutants such as ozone, sulphur dioxide, oxides of nitrogen and diesel exhaust particles [101].

1.2.1.3 The immunological barrier

Finally, the airway epithelium forms an immunological barrier. For example, epithelial cells contribute to humoral immunity by actively transporting immunoglobulins (IgA, IgM and IgG) to the luminal surface, where they coat invading pathogens [1]. This can either neutralise pathogen infectivity and/or target the pathogen for destruction by Fc-receptor expressing phagocytes [1, 13].

HBECs also contribute to cellular immunity by the release of cytokines and chemokines, which promote or suppress the activation of innate and adaptive immune responses as appropriate. For example, under normal conditions HBECs constitutively secrete anti-inflammatory mediators such as prostaglandin E_2 (PGE_2) and IL-10, which help suppress inflammation at baseline [102, 103]. In the presence of pathogen associated molecular patterns (PAMPs) or damage associated molecular patterns (DAMPS), activation of innate PRRs induces proinflammatory cytokine and chemokine release. These mediators may have important autocrine or paracrine effects on the surrounding structural cells (underlying fibroblasts) and leucocytes. For example, cytokines and chemokines released by the epithelium can regulate DC precursor recruitment (e.g.CCL2 and CCL13) and maturation (e.g. type I interferon (IFN), IL-15, GM-CSF) [1]. In addition, HBECs recruit mature DCs by the production of CCL20 and can also influence the polarisation of DC-mediated T cell responses [104]. For example, HBEC-derived TSLP and IL-33 upregulate DC expression of Th2 cytokines, MHC, and co-stimulatory molecules [77-79, 104]. In addition to DCs, HBEC-derived cytokines also affect the recruitment and survival of other immune cell types. For example, HBECs express CCL11, CCL5 and GM-CSF [105-107], which are chemotactic and prosurvival factors for eosinophils, as well as stem cell factor (SCF) [108, 109], which is a chemotactic and prosurvival factor for MCs.

As well as forming an immunological barrier by the release of soluble mediators, HBECs can also physically interact with immune cells and participate

in adaptive immunity by the expression of MHC class I, co-stimulatory, and inhibitory molecules [110, 111]. Expression of MHC and co-stimulatory molecules is required for the physical interaction, detection and destruction of virally infected cells by cytotoxic lymphocytes [13]. In addition these molecules allow HBECs to present antigen to naive T cells at the site of infection and promote Th1 differentiation.

1.2.2 Epithelial interactions with inhaled environmental agents

Epithelial cells form a barrier against the inhaled external environment, and so are the first cells to encounter asthma triggers such as allergens (e.g. pollen or house dust mite (HDM)), air pollutants (e.g. cigarette smoke) and infectious agents (e.g. bacteria and viruses). Many of these asthma triggers cause epithelial barrier disruption and activate PRRs, leading to initiation of inflammatory and repair responses that restore tissue homeostasis.

HBECs are the main hosts for replication of viruses such as HRV, which disrupt barrier functions and activate innate immune responses. HRVs are the most common cause of asthma exacerbations and infection in infancy is associated with subsequent asthma development [33-35]. In addition, the epithelial asthma susceptibility gene, *CDHR3*, is the gene for the cellular receptor for HRV-C [30, 86]. Epithelial interactions and innate responses to HRV are therefore of particular interest and are described in more detail below.

1.2.2.1 Epithelial interactions with HRV

HRVs interact with HBECs via receptors expressed on the cell surface. As mentioned in section 1.1.4.1, the cellular receptors for major, minor and group C HRVs are ICAM-1, LDL and CDHR3 respectively [28-30]. Once bound to their cellular receptor, HRVs are internalised into endosomes (Figure 1.2.2-1). Acidification of the endosomal compartment leads to release of HRV RNA, which is translated by host cell ribosomes and replicated to produce additional copies of the viral genome (Figure 1.2.2-1) [26]. Once sufficient quantities of positive strand RNA and capsid protein have been synthesised, new virions are assembled and released by cell lysis (Figure 1.2.2-1).

Infection and replication of HRV within HBECs induces dissociation of epithelial TJ proteins, leading to disruption of epithelial barrier functions [112]. In addition, HRV activates the release of mediators involved in epithelial repair such as MMPs, ECM components and growth factors [113-116]. Viral replication also activates innate PRRs and immune responses. For example, replication of the viral genome involves copying the positive-strand RNA genome to form a double stranded RNA (dsRNA) intermediate of positive and negative strand RNA [117] which is recognised by host cell PRRs, leading to activation of innate responses (Figure 1.2.2-2) [118, 119]. PRRs include the toll like receptors (TLR)s (e.g. TLR3 and TLR7) which are transmembrane proteins that can detect viral RNA outside the cell or within endosomal compartments. Rig like receptors (RLRs) (e.g. retinoic acid-inducible gene-1; RIG-1 and melanoma differentiation-associated protein-5; MDA-5) are responsible for cytosolic dsRNA recognition. Viral dsRNA in the cytoplasm can also activate the RNA activated kinase, protein kinase R (PKR). Together the activation of these receptors and PKR triggers signalling cascades which induce translocation of nuclear factor κ-light-chain-enhancer of activated B cells (NF-κB) and IFN regulatory factor (IRF)3/7 to the nucleus, where they initiate expression of proinflammatory cytokines and IFNs respectively (Figure 1.2.2-2). These proinflammatory cytokines include IL-6 and CXCL8 which are important in leucocyte chemotaxis and activation. Viral-induced IFNs include the type I IFNs, IFN-α and IFN-β, and the type III IFN, IFN-λ (IL-29) [119, 120]. Type I and III IFNs induce an antiviral state in neighbouring cells by binding to the type I and type III IFN receptor respectively (Figure 1.2.2-2) [119, 120]. This leads to activation of Janus kinase (JAK)/signal transducer and activator of transcription (STAT) signalling and formation of the IFN-stimulated gene factor 3 (ISGF-3) complex (Figure 1.2.2-2) [119]. The ISGF-3 complex translocates to the nucleus where it binds the IFN-stimulated response element (ISRE) and initiates expression of IFN-stimulated genes (ISGs). These include several anti-viral proteins, chemokines (e.g. CXCL10) and IRF-7, which is responsible for a positive feed-back loop by initiating a second wave of IFN synthesis. Epithelial-derived IFNs may also have paracrine effects and induce IFN release and anti-viral responses by other cell types. For example, type I IFNs activate natural killer (NK) T cells, which are a source of the type II IFN, IFN-γ [13].

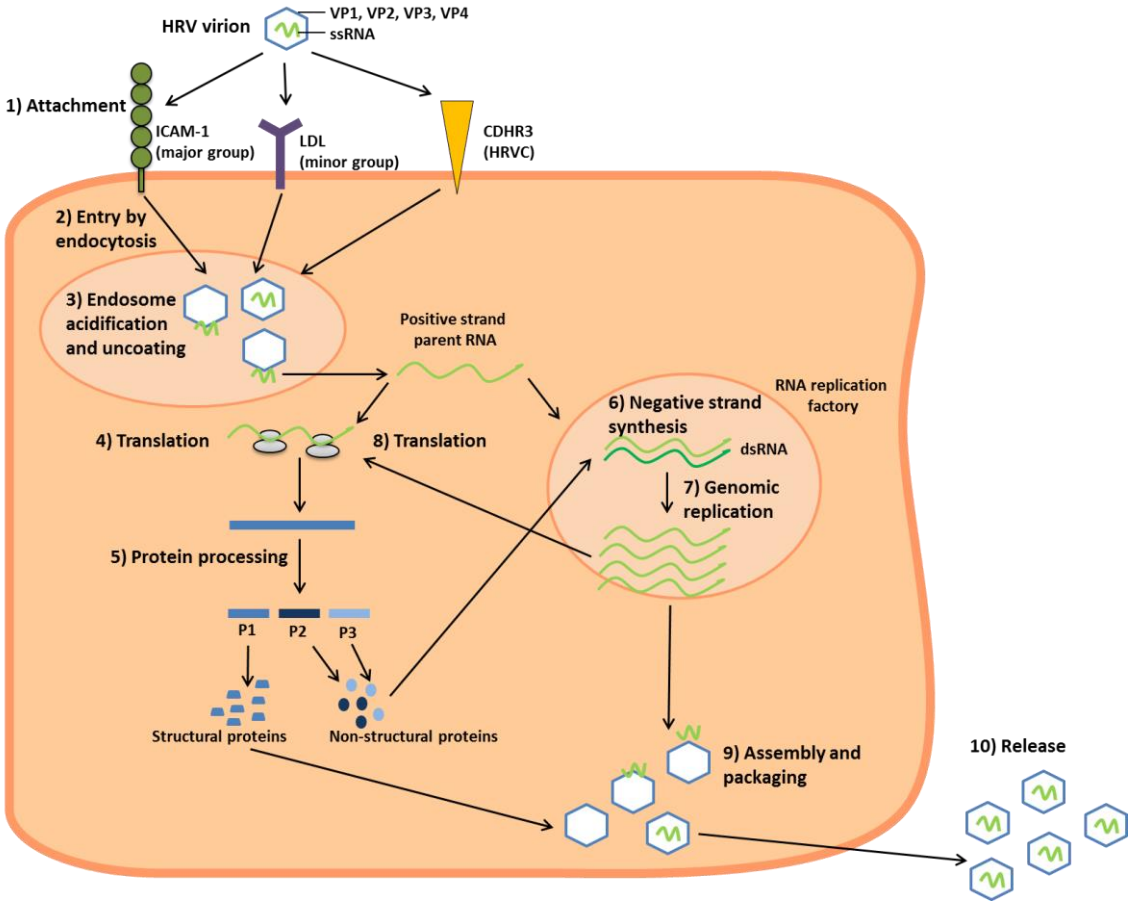

Figure 1.2.2-1 Overview of the HRV replication cycle.

1) HRV binds to one of three cellular receptors (depending on its serotype and subgroup) 2) and is internalised by endocytosis. 3) Acidification of the endosome leads to structural changes in the capsid and uncoating of the viral genome. The RNA genome crosses into the cytosol 4) where it is translated into a single polyprotein by host cell ribosomes. 5) The polyprotein is processed into structural (P1) and non-structural proteins, including those involved in protein processing and genome replication (P2 and P3). 6) The non-structural protein, viral RNA polymerase, copies the positive strand parent RNA to form negative strand RNA. 7) Negative strand RNA is copied to produce additional positive strand RNA 8) for translation of more viral proteins 9) or for packaging into new virions. Newly synthesised virions are released by cell lysis, although some strains can be released in the absence of cytopathic effect [25, 117]

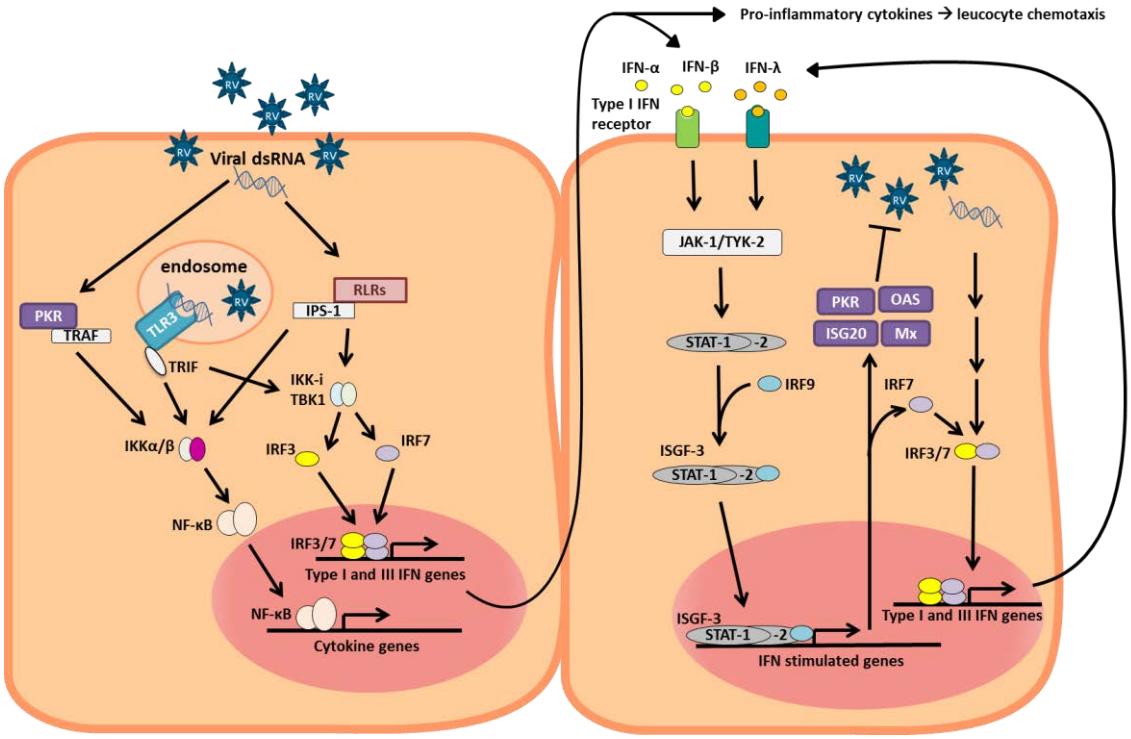

Figure 1.2.2-2 Schematic of epithelial responses to HRV infection.

DsRNA produced during replication of the viral genome is detected by endosomal (TLRs) and cytoplasmic (RLRs) PRRs, and also activates the antiviral protein, PKR. TLR3 and RLRs, trigger signalling cascades via the adaptor proteins TIR-domain-containing adaptor-inducing IFN-β (TRIF) and IFN-promoter stimulator 1 (IPS-1) respectively. Downstream of these adaptor proteins are inducible IκB kinase (IKK-i) and TRAF family member-associated NF-κB-binding kinase 1 (TBK1), which phosphorylate IRF3 and IRF7 leading to their translocation to the nucelus and activation of type I and III IFN gene expression. The TRIF and IPS-1 adaptors also activate IκB kinase (IKKα/β), which frees NF-κB from its regulatory domain, allowing it's translocation to the nucleus and activation of cytokine gene expression. Activation of PKR by dsRNA also activates IKKα/β, via the TNF receptor associated factor (TRAF) adaptor protein, leading to cytokine gene expression. Expression and release of cytokines and type IFNs leads to leucocyte chemotaxis and activates antiviral responses in neighbouring cells. For example, activation of the IFN receptor induces expression of numerous ISGs via the JAK/STAT signalling pathway. These include several anti-viral proteins and IRF-7, which amplifies the IFN response

1.2.3 The epithelium is dysregulated in asthma

As described above, HBECs express genes associated with asthma susceptibility, form a barrier against and interact with environmental asthma triggers such as HRV, suggesting that these cells play a key role in asthma pathology [2, 75] and there is an increasing body of evidence suggesting that epithelial cell functions are dysregulated in the asthmatic airway.

1.2.3.1 Epithelial barrier functions are disrupted in asthma

One of the most important functions of HBECs is to provide a protective barrier to the external environment. However, in the asthmatic airways, this barrier is disrupted. For example, in biopsies and HBEC cultures from asthmatic patients, TJ immunostaining is patchy and irregular compared to biopsies from healthy subjects, where TJ proteins are localised to distinct focal areas [121]. The physical barrier is therefore disrupted and HBEC cultures from asthmatic donors have increased ionic and macromolecular permeability [121]. The physical barrier is also disrupted in terms of the barrier provided by goblet cell secretions. For example, in the asthmatic airway, goblet cell hyperplasia and mucus hypersecretion is observed, which may lead to mucus plugging of the lumen [122]. Bronchial secretions also provide an important chemical barrier. However, in asthma, these secretions contain lower levels of antioxidant enzymes, and consumption of antioxidants is increased [123]. Epithelial secretion of mediators that contribute to the immunological barrier is also dysregulated in asthma. For example, constitutive epithelial expression of cytokines and chemokines involved in immune cell recruitment is increased including CCL2 (DC precursor chemoattractants) [124], CCL17 (T cell chemoattractant) [125] and CCL11 (eosinophil chemoattractant and prosurvival factor) [126]. A number of proinflammatory mediators are also induced following epithelial stimulation with asthma triggers, including CCL20, CCL5, GM-CSF and CXCL10 [127-129]. Furthermore, epithelial expression of mediators that promote DC-mediated allergic inflammation (TSLP and IL-33) is also increased in asthma [80, 82].

Evidence suggests that in allergic asthma, Th2 inflammation promotes or augments disruptions in epithelial barrier functions. For example, the Th2

cytokine, IL-13 disrupts TJs and induces goblet cell hyperplasia [1, 130]. IL-13 and other Th2 cytokines including IL-5, IL-3 and GM-CSF also drive eosinophilia by promoting eosinophil differentiation, activation and survival [13]. In the asthmatic airway, eosinophils localise to the epithelium and airway lumen, where they may cause significant disruption to the epithelial barrier by releasing a variety of highly toxic proteins free radicals, and inflammatory mediators from intracellular granules (Table 1.2.3-1) [13, 131-134]. The predominant constituent of these granules is major basic protein (MBP), which is highly cytotoxic and has been shown to damage the airway epithelium, and reduce ciliary activity *in vitro* [135, 136]. In addition, MBP activates epithelial release of proinflammatory [137] and pro-fibrotic mediators [138, 139].

Table 1.2.3-1 Summary of eosinophil granule contents [13]

Class of product	Contents	Biological effects
Enzymes	Eosinophil peroxidase (EPO)	Toxic to targets and triggers histamine release from MCs
	Eosinophil collagenase	Remodels connective tissue matrix
Toxic proteins	MBP	Toxic to parasites and mammalian cells and triggers histamine release from MCs
	Eosinophil cationic protein (ECP)	Toxic to parasites and neurotoxic
	Eosinophil-derived neurotoxin (EDN)	Cytotoxic
Cytokines	IL-3, IL-5 and GM-CSF	Amplify eosinophil production by bone marrow and cause eosinophil activation
Chemokines	CXCL8	Promotes influx of leucocytes
Lipid mediators	LTs C_4, D_4 and E_4	Cause smooth muscle contraction and increase vascular permeability and mucus secretion
	Platelet-activating factor	Attracts leucocytes, amplifies production of lipid mediators and activates neutrophils, eosinophils and platelets

1.2.3.2 The asthmatic epithelium is more susceptible to disruptions in tissue homeostasis

In the asthmatic airway, dysregulated barrier functions may increase epithelial susceptibility to disruptions in tissue homeostasis by allowing increased penetration of environmental agents between the cells, leading to increased activation of PRRs and epithelial damage. Compared to healthy HBECs, asthmatic HBECs are more susceptible to oxidant-induced apoptosis and barrier disruption by agents including cigarette smoke and proteases from the allergenic fungus, *Alternaria alternata* [121, 140, 141]. In addition, biopsies from asthmatic patients show evidence of epithelial damage as they stain strongly for EGFR, an epithelial marker of stress and injury [142]. This increased epithelial damage may activate the release of epithelial alarmins and mediators of inflammation and repair. For example, epithelial expression of Th2 promoting cytokine IL-33 [80, 82] and the pro-fibrotic growth factor TGF-β_2 [143, 144] is increased in asthma.

The epithelium may be particularly susceptible to the effects of HRV in asthma. For example, asthma-associated polymorphisms in the HRV-C receptor, CDHR3, enhance viral binding and increase progeny yields *in vitro* [30, 86]. In addition, expression of the major group HRV receptor, ICAM-1 is increased on the surface of asthmatic epithelial cells [14, 145]. Susceptibility to viral infection may also be increased due to epithelial cell shedding and loss of ciliated cells, leading exposure of basal cells, which are more susceptible to HRV infection [146]. Similarly goblet cells, which are increased in the asthmatic epithelium, are also more susceptible to infection [147]. Once infected, asthmatic cells are less able to mount an anti-viral response, as the production of anti-viral mediators (type I and III IFNs) by asthmatic HBECs is impaired [148, 149]. As a consequence, replication and release of virus progeny is higher in these cells. Conversely, HRV induces epithelial release of proinflammatory mediators, which may be enhanced in allergic asthma by underlying Th2 inflammation [26, 150]. HRV infection can also promote Th2 inflammation by inducing the Th2 promoting cytokines, TSLP, IL-33 and IL-25 [31, 151]. Finally, as described earlier, HRV is a common cause of asthma exacerbation. During an exacerbation, smooth muscle contraction produces compressive forces which activate structural cells to release mediators of remodelling, including growth factors and MMPs [22]. These mediators include

TGF-β which is released from asthmatic but not healthy epithelial ALI cultures *in vitro* following compression [152]. Taken together these data show that HRV may promote inflammation and remodelling and have important consequences in asthma, where the epithelium is more susceptible to infection.

1.3 The epithelial-mesenchymal trophic unit

The bronchial epithelium releases a range of inflammatory and repair mediators in response to disruption by inhaled environmental agents. These mediators may have important autocrine and paracrine effects on immune cells, as described in section 1.2.1.3, and also on structural cells. For example, fibroblasts lie within ECM in close proximity to the basolateral epithelial surface, in a layer known as the attenuated fibroblast sheath. These cells are important structural elements that maintain homeostasis of the airway connective tissue. For example, they regulate the balance of ECM by the secretion of collagen and other ECM components which build up the matrix. In addition, they secrete MMPs and their inhibitors (tissue inhibitors of MMPs; TIMPS), the balance of which regulates matrix degradation.

While fibroblasts are important structural elements, their close proximity to the epithelium allows them to act as sentinel cells that receive and send information to epithelial and inflammatory cells through direct cell-cell contact or indirectly through the secretion of cytokines, chemokines and growth factors [153]. In this way fibroblasts may support the function of HBECs to transfer signals from the environment into deeper areas of the tissue. It has therefore been suggested that epithelial and mesenchymal cells work together as a unit; a concept described as the epithelial-mesenchymal trophic unit (EMTU) [153]. Local exchange of information within the EMTU is thought to have an important influence over the local microenvironment and an essential role in maintenance of tissue homeostasis and co-ordination of inflammatory and repair responses to stimuli.

In the asthmatic airway chronic inflammation and structural remodelling indicate that tissue homeostasis is disrupted and that the EMTU is dysregulated (Figure 1.3.1-1). In addition, as described in sections 1.1.7.1

and ⁋1.2.3, several asthma susceptibility genes have been identified in the epithelium and HBEC functions are dysregulated in asthma. This may influence the ability of HBECs to signal to underlying fibroblasts. Furthermore, fibroblast responses and signalling to the epithelium may be altered since several asthma susceptibility genes have also been identified in the mesenchyme (⁋1.1.7.2). Together, altered epithelial-fibroblast signalling may lead to increased/persistent activation of EMTU inflammatory and repair responses including increased expression and secretion of various cytokines, chemokines, growth factors and pro-fibrotic mediators. This may ultimately cause structural changes within the airways and contribute to the pathogenesis of asthma. The co-ordination of EMTU inflammatory and repair responses in health and disease is therefore discussed in more detail below.

1.3.1 EMTU inflammatory and repair responses

1.3.1.1 EMTU inflammatory responses

As described in section ⁋1.2.1, HBECs form a barrier to the external environment. Evidence suggests that fibroblasts support these functions. For example in co-culture, fibroblasts reduce the ionic permeability of the epithelium and support epithelial proliferation and differentiation by the release of factors such as hepatocyte growth factor (HGF) [154, 155]. Fibroblasts also express cytokine receptors and PRRs that recognise DAMPs, suggesting that they are responsive to HBEC-derived signals and can contribute to the immunological barrier [156, 157]. In the asthmatic EMTU, disruption of epithelial barrier functions (see section ⁋1.2.3) may lead to increased release of DAMPS and inflammatory mediators, which activate the underlying fibroblasts, leading to enhanced inflammation. For example, epithelial IL-33 expression is increased in asthma [80] and can activate eotaxin production by fibroblasts [156]. Pro-inflammatory cytokines such as tumour necrosis factor (TNF)-α, IL-1β and IL-4 have also been shown to induce TSLP expression by fibroblasts [158, 159]. Epithelial-derived IL-1α is another important activator of fibroblasts and induces fibroblast CXCL8 and IL-6 release [157, 160, 161]. Fibroblast responses to epithelial mediators may be further enhanced in the asthmatic airway where there are increased numbers of subepithelial fibroblasts [17, 18]. An enhancement in EMTU inflammatory

responses in asthma may promote immune cell recruitment and retention, as well as allergic inflammation [80, 82]. In addition, increased epithelial barrier disruption in asthma could lead to increased penetration of environmental agents. These agents may not only act directly on fibroblasts but also on DCs, leading to allergic sensitisation. In summary, disruption of HBEC functions and increased fibroblast activation may lead to increased EMTU activation and promote chronic (allergic) inflammation in asthma.

1.3.1.2 EMTU repair responses

In addition to activation of inflammation, epithelial barrier function disruption in asthma may also lead to increased epithelial damage and the increased release of mediators that promote epithelial repair. For example, these include growth factors, MMPs and ECM components that together promote downregulation of TJs, allowing cell migration, and epithelial proliferation to re-seal the barrier. Fibroblasts also respond to epithelial-derived growth factors. For example, HBEC-derived basic fibroblast growth factor (bFGF), platelet-derived growth factor (PDGF), endothelin-1 (ET-1) and insulin-like growth factor-1 (IGF-1), induce fibroblast proliferation [138, 162, 163]. In addition, the epithelium releases TGF-β; a potent inducer of fibroblast differentiation into a specialised repair, myofibroblast phenotype [162-164]. These cells secrete high levels of ECM proteins and growth factors which accumulate to form a temporary barrier and promote epithelial repair respectively [165]. Myofibroblasts are also characterised by expression of contractile α-smooth muscle actin (α-SMA) fibres, important for wound closure. Once epithelial barrier functions are restored, the temporary structural changes are resolved. Part of this process is due to myofibroblast apoptosis or de-differentiation. Additionally, factors that oppose the pro-fibrotic effects of TGF-β, such as epidermal growth factor (EGF), stimulate the production of MMPs that degrade ECM.

Interestingly, structural changes in the asthmatic airway are similar to the temporary changes that occur during the immediate response to tissue injury, which include basement membrane thickening, subepithelial fibrosis and ECM deposition [166]. However, in the asthmatic airway these changes are not temporary, suggesting that there is increased activation of repair responses

and a lack of resolution, i.e. a chronic wound response [17]. Consistent with this, the levels of factors involved in repair and remodelling are altered in the asthmatic airway. For example, MMPs and their inhibitors, which have important roles in regulating the balance of ECM accumulation and degradation, are increased in asthmatic bronchoalveolar lavage fluid (BALF), although the overall MMP/TIMP ratio is decreased [167-169]. In addition, pro-fibrotic growth factors such as TGF-β, bFGF and vascular endothelial growth factor (VEGF) are also increased in the asthmatic airway [170-173]. These mediators have the potential to activate fibroblast repair responses. For example, in recent *in vitro* studies, fibroblast α-SMA and collagen expression was increased in co-cultures with asthmatic compared to healthy HBECs, and was mediated by TGF-β [174, 175]. While these studies used healthy fibroblasts, evidence also suggests that fibroblast responses to epithelial-derived mediators are enhanced in asthma. For example, asthmatic fibroblasts have enhanced predilection for TGF-β-induced myofibroblast differentiation [176]. Together, disruption of HBEC functions and dysregulation of fibroblast responses may lead to increased activation EMTU repair responses and promote airway remodelling in asthma.

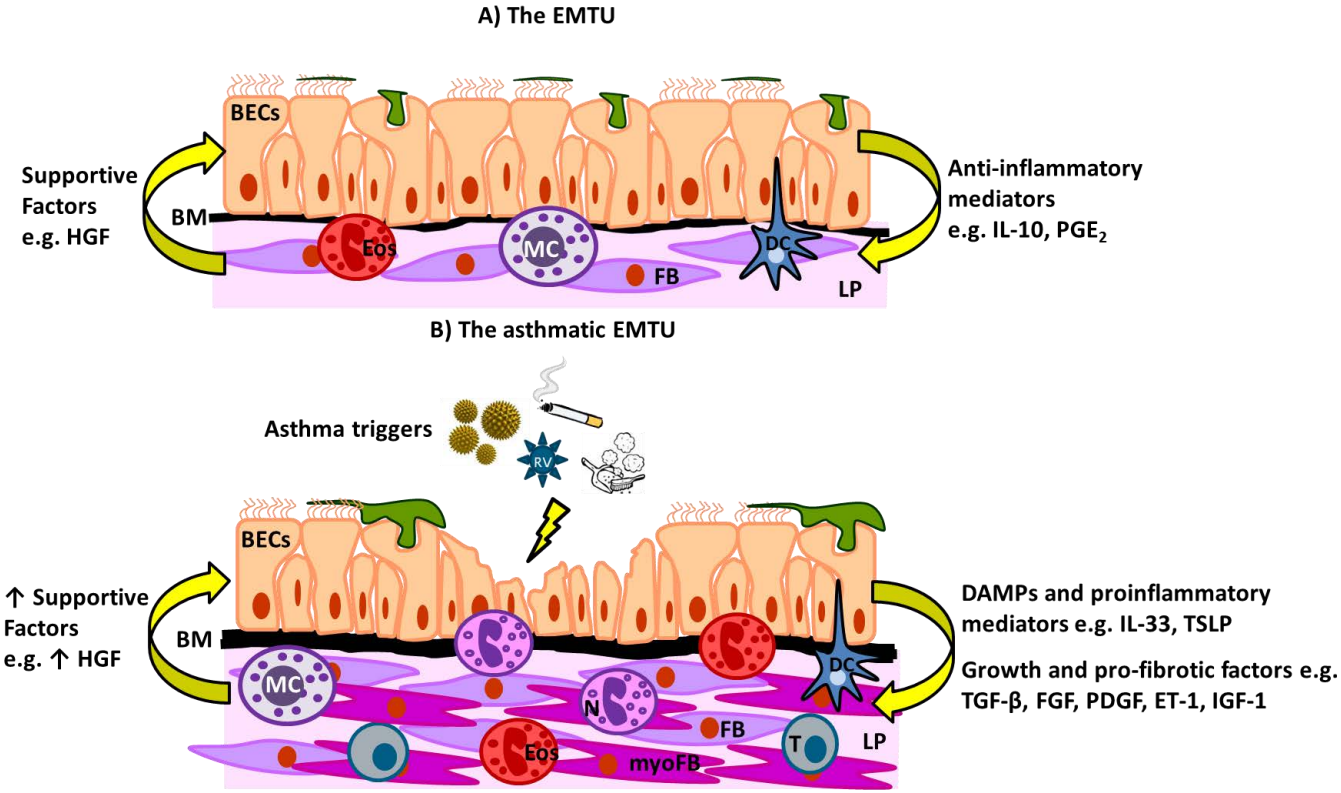

Figure 1.3.1-1 Schematic of the airway EMTU and the airway EMTU in asthma.
(A) *In vivo* HBECs are in close proximity to a layer of stellate fibroblasts (FB) that reside within the lamina propria (LP). FBs receive and send information to HBECs and inflammatory cells [153], which work together to maintain homeostasis by supporting each other's functions and suppressing inflammation and remodelling at baseline. (B) Inflammation and remodelling suggest that the EMTU is dysregulated in asthma. Defects in HBEC function increase susceptibility to injury by inhaled environmental agents e.g. viral infection, pollen, cigarette smoke and HDM. HBEC injury induces release of DAMPs and inflammatory and repair mediators. This leads to increased recruitment, activation and survival of leucocytes such as eosinophils (Eos), neutrophils (N) and T cells (T). Remodelling also occurs, including basement membrane (BM) thickening, accumulation of ECM and increased fibroblast proliferation and differentiation into myofibroblasts (myoFB).

1.3.2 Modelling the EMTU

A growing body of evidence suggests that the EMTU is dysregulated in asthma. Therefore there is a need to understand in greater detail how inflammatory, repair and remodelling responses are co-ordinated within the EMTU. A variety of *in vivo*, *ex vivo* and *in vitro* models can be used to study cell-cell interactions and mechanisms of inflammation and repair within the EMTU. Each model has its merits and limitations and so it is important to choose the most appropriate model for the question to be asked. An overview of these different models is given below

1.3.2.1 *In vivo* models

In vivo studies are important for examining the EMTU in the context of the whole body system. However due to ethical reasons, studies in humans are limited to experimental challenge studies of healthy or mild asthmatic subjects (e.g. using HRV or allergen), with readouts constrained to the examination of clinical symptoms and samples collected by relatively non-invasive procedures [2, 177]. More detailed *in vivo* mechanistic studies can be carried out in animals [2] which can be genetically manipulated to examine specific signalling pathways and cellular responses. However, data generated from animal models need to be interpreted with care when translating to humans due to genetic, anatomical, physiological and immunological differences between the species. In addition, while mouse models have contributed substantially to our understanding of mechanisms of allergic airway inflammation and repair, they are not ideal for *in vivo* studies of HRV infection as they are not the natural hosts of the virus. For example, the major group HRVs are unable to bind mouse ICAM-1 for cell attachment and entry [178] and although minor group HRVs are able to bind and enter cells via the mouse LDL receptor [177, 179], minimal viral replication occurs and higher titres of viral inoculum are required for infection [177].

1.3.2.2 *In vitro* models

To eliminate the species-specific limitations of animal models, mechanistic studies can be performed using *ex-vivo* and *in vitro* human tissue-based models. The simplest human tissue-based models are *ex vivo* explants. Tissue

is resected from the lungs of patients, cultured *in vitro*, stimulated with relevant environmental stimuli and responses monitored. This allows the investigation of complex cell-cell interactions in tissue where the normal architecture is maintained. However, since the tissue is submerged direct apical stimulation is not achieved and the polarised release of mediators following challenge cannot be studied. In the EMTU, this may be important for controlling signalling to underlying fibroblasts and orchestrating responses to disruptions in tissue homeostasis. HBEC lines, such as 16HBE14o- cells, have therefore been developed that retain the ability to form a polarised epithelial barrier *in vitro* by the formation of TJs [180]. In addition, primary HBECs from bronchial brushings form a polarised barrier when differentiated *in vitro* at an air-liquid interface (ALI) and contain mucus-producing goblet and ciliated cells. These primary differentiated cultures also resemble the pseudostratified structure and transcriptional profile that is observed *in vivo* [181, 182]. However, by culturing HBECs separately, experiments using ALI cultures or HBEC lines do not reflect the integrated responses of the EMTU. While this can be partially overcome by incubating fibroblast monocultures with HBEC conditioned medium a more sophisticated EMTU model to examine cellular cross-talk is to polarise HBECs in the apical compartment of a Transwell® system with fibroblasts cultured basolaterally. This system allows bi-directional communication between cells of the EMTU, the apical delivery of environmental challenges and the assessment of epithelial barrier and fibroblast functions including vectorial mediator release.

1.4 Hypothesis and aims

Despite evidence suggesting that EMTU activation has a key role in asthma pathology only a limited number of *in vitro* studies have examined EMTU responses to common asthma triggers. HRV and eosinophil MBP have the potential to activate the EMTU via innate PRRs and cell cytotoxicity respectively. However, EMTU responses to HRV or MBP challenge are yet to be investigated in an epithelial-fibroblast co-culture model which allows bi-directional cross-talk and vectorial and/or localised signalling. Epithelial-mesenchymal interactions following challenge may have significant effects on the mileu of cytokines and growth factors, and be important for co-ordinating integrated

inflammatory and repair responses. I therefore developed a polarised, integrated epithelial-fibroblast co-culture model with which to test the following hypothesis:

Hypothesis:

HRV and MBP challenge of HBECs induces cellular cross-talk with the underlying fibroblasts, which is important for the co-ordination of proinflammatory and repair responses within the EMTU

Aims:

1. Develop polarised, integrated epithelial-fibroblast co-culture models of the EMTU using either cell lines or primary cells.
2. Use the polarised EMTU co-culture models to investigate proinflammatory responses following HRV challenge and identify mediators of cellular cross-talk.
3. Investigate induction of repair responses following HRV challenge and identify how these responses are co-ordinated within the EMTU co-culture models.
4. Investigate inflammatory and repair responses following challenge of the polarised EMTU model with a MBP-mimetic to allow comparison with responses to HRV.

2.Materials and methods

2.1 Materials

Reagent	Manufacturer	Product code
3,3',5,5'-Tetramethylbenzidin (TMB) ELISA substrate solution	eBioscience (Hatfield, UK)	00-4201-56
Alexa Fluor® 488 conjugated, mouse monoclonal anti-occludin antibody (clone OC-3F10, mIgG$_{1\kappa}$), targeted against glutathione S-transferase fusion protein consisting of the C-terminal region (~150aa) of human occludin (0.5mg/ml)	Life technologies (Paisley, UK)	331588
Bovine Serum Albumin (BSA)	Sigma-Aldrich (Gillingham, UK)	A3059
Click-iT® EdU Alexa Fluor® 647 Imaging Kit	Life technologies (Paisley, UK)	C10340
Crystal violet	Sigma-Aldrich (Gillingham, UK)	C3886
CytoTox 96® non-radioactive cytotoxic assay kit	Promega (Southampton, UK)	G1780
Diamidino-2-Phenylindole (DAPI) (1mg/ml)	Sigma-Aldrich (Gillingham, UK)	D9542
Dimethyl sulfoxide (DMSO)	Sigma-Aldrich (Gillingham, UK)	D2650
Dulbecco 'A' Phosphate Buffered Saline (PBS) Tablets (10 Tablets dissolved in 1 L of distilled water contains NaCl 8g/L, KCl 0.2g/ml, Na_2HPO_4 1.15g/L, H_2KO_4P, pH7.3)	OXOID Ltd (Basingstoke, UK)	BR0014
Dulbecco's Modified Eagle's Medium (DMEM), high glucose, no glutamine	Life technologies (Paisley, UK)	11960-044
Ethanol	Sigma-Aldrich (Gillingham, UK)	32221
Fetal Bovine Serum (FBS), qualified (endotoxin ≤10 EU/ml, haemoglobin ≤25mg/dl, heat inactivated)	Life technologies (Paisley, UK)	10500-064
FITC-conjugated monoclonal mouse anti-human α-SMA antibody (clone 1A4, mIgG$_{2a}$), targeted against the N-terminal synthetic decapeptide of α-SMA (2mg/ml)	Sigma-Aldrich (Gillingham, UK)	F3777
Fluorescein isothiocyanate (FITC)-4kDa dextran	Sigma-Aldrich (Gillingham, UK)	FD4

Fluticasone-propionate (FP)	Sigma-Aldrich (Gillingham, UK)	F9428
Formaldehyde solution	Sigma-Aldrich (Gillingham, UK)	F8775
Hank's Balanced Salt Solution (HBSS), no calcium, no magnesium	Life technologies (Paisley, UK)	14170-088
HBEC Basal Medium (BEBM)	Lonza (Slough, UK)	CC-3171
HBEC Growth Medium (BEGM) SingleQuot™ kit containing the following supplements: bovine pituitary extract, human EGF, insulin, hydrocortisone, transferrin, triiodothyronine and epinephrine.	Lonza (Slough, UK)	CC-4175
High molecular weight (Mw) polyinosinic-polycytidylic acid (poly(I:C)) (1.5-8 kb)	Invivogen (Toulouse, France)	tlrl-pic
Human CXCL10/IFN-γ induced protein 10 (IP-10) DuoSet™ ELISA kit	R&D Systems (Abingdon, UK)	DY266
Human CXCL8/IL-8 DuoSet™ ELISA kit	R&D Systems (Abingdon, UK)	DY208
Human GM-CSF ELISA Ready-SET-Go! (2nd Generation)	eBioscience Ltd (Hatfield, UK)	88-8337
Human IL-1 alpha/IL-1F1 DuoSet™ ELISA kit	R&D Systems (Abingdon, UK)	DY200
Human IL-29/IFN-lambda 1 DuoSet ELISA™ ELISA kit	R&D Systems (Abingdon, UK)	DY7246
Human IL-6 DuoSet™ ELISA kit	R&D Systems (Abingdon, UK)	DY206
Human Luminex® Screening Assay (for IL-1α, IL-1β, IL-1Ra MMP-2, MMP-9, VEGF and bFGF)	R&D Systems (Abingdon, UK)	LXSAH
Human TGF-beta 1 DuoSet ELISA™ ELISA kit	R&D Systems (Abingdon, UK)	DY240
Human TGF-beta 2 DuoSet ELISA™ ELISA kit	R&D Systems (Abingdon, UK)	DY302
Insulin-Transferrin-Selenium (ITS -G) (100X) (insulin 1g/L, transferrin 0.55g/L, sodium selenite $6.7x10^{-4}$g/L) (100X)	Life technologies (Paisley, UK)	41400-045
L-Glutamine (L-Glut) (200mM)	Life technologies (Paisley, UK)	25030-024
Meso Scale Discovery (MSD)® Human IFN-β Tissue Culture Kit	MSD (Rockville, MD, USA)	K151ADB-2
Minimum Essential Medium (MEM), GlutaMAX™ supplement	Life technologies (Paisley, UK)	41090

Monoclonal mouse anti- human IFN α/β receptor chain 2 (IFNAR2) antibody, (clone MMHAR-3, mIgG$_{2a}$) (0.5mg/ml)	Pbl assay science (Piscataway, NJ, USA)	21385-1
Monoclonal mouse anti-TGF-beta 1, 2, 3 antibody (Clone # 1D11, mIgG$_{1}$) (0.5mg/ml)	R&D Systems (Abingdon, UK)	MAB1835
Monoclonal mouse IgG$_{1}$ isotype control antibody (clone # 11711) (0.5mg/ml)	R&D Systems (Abingdon, UK)	MAB002
Monoclonal mouse IgG$_{2a}$ isotype control antibody (clone # 20102) (0.5mg/ml)	&D Systems (Abingdon, UK)	MAB003
Mowiol® 4-88	Harlow chemical company (Harco)	
N-(2-Hydroxyethyl)piperazine-N'-(2-ethanesulfonic acid) (HEPES) solution (1M, pH 7.0-7.6, sterile-filtered)	Sigma-Aldrich (Gillingham, UK)	H0887
Non-Essential Amino Acids (NEAA) solution (100X)	Life technologies (Paisley, UK)	11140-035
Paraformaldehyde (PFA)	TAAB (Aldermaston, UK)	P001/1
Penicillin-streptomycin (P/S) (5,000U/mL)	Life technologies (Paisley, UK)	15070-063
Poly-L-arginine (pLArg) hydrochloride (Mw 15,000-70,000, average 44,300)	Sigma-Aldrich (Gillingham, UK)	P7762
ProLong® gold antifade mountant containing 4',6-Diamidino-2-Phenylindole (DAPI)	Life technologies (Paisley, UK)	P36941
PureCol® collagen (Type I) solution, (3mg/ml)	Advanced BioMatrix (Tuscon, AZ, USA)	5005-B
Recombinant human IL-1Ra (sterile-filtered prior to lyophilisation, endotoxin <0.1 EU/µg (<1 EU/µg), purity >97%)	R&D Systems (Abingdon, UK)	280-RA
Recombinant human IL-1α, research grade (sterile-filtered prior to lyophilisation, endotoxin <0.1ng/µg (<1 EU/µg), purity >95%)	Miltenyi (Bergisch Gladbach, Germany)	130-093
Recombinant human TGF-β$_{1}$	PeproTech (London, UK)	100-21
Retinoic acid (RA)	Sigma-Aldrich (Gillingham, UK)	R2625

Roswell Park Memorial Institute (RPMI) 1640 Medium, no glutamine	Life technologies (Paisley, UK)	31870-025
Sodium azide	Sigma-Aldrich (Gillingham, UK)	S8032
Sodium bicarbonate solution ($NaHCO_3$)	Sigma-Aldrich (Gillingham, UK)	S8761
Sodium pyruvate (100mM)	Life technologies (Paisley, UK)	11360-039
Triton™ X-100 (TX-100)	Sigma-Aldrich (Gillingham, UK)	T8787
Trypan Blue Solution, 0.4%	Life technologies (Paisley, UK)	15250-061
Trypsin, 0.5% (10x) with ethylenediaminetetraacetic acid (EDTA) 4Na, no phenol red	Life technologies (Paisley, UK)	15400-054
Tryptose phosphate broth solution	Sigma-Aldrich (Gillingham, UK)	T8159
TWEEN® 20	Sigma-Aldrich (Gillingham, UK)	P1379
UltraCULTURE™ Serum-free medium without L-glut	Lonza (Slough, UK)	12-725F

2.2 Equipment

Equipment	Manufacturer
Bio-Plex® 200 suspension array system and software	Bio-Rad (Hemel Hempstead, UK)
CL-1000 Ultraviolet (UV) Crosslinker	Ultraviolet Products (UVP) Ltd. (Cambridge, UK)
Fluoroskan Ascent™ Microplate Fluorometer and software	Thermo Fisher Scientific (Loughborough, UK)
Improved Neubauer bright-light Haemocytometer	Marienfield (Lauda-Königshofen, Germany)
Labsystems Multiskan Ascent plate reader and software	Thermo Fisher Scientific (Loughborough, UK)
Leica AF6000 system fluorescent microscope and software	Leica Microsystems GmbH (Wetzlar, Germany)
Leica DMI6000B light microscope and software	Leica Microsystems GmbH (Wetzlar, Germany)
Leica True Confocal Scanner (TCS) SP5 and SP8 confocal microscope and software	Leica Microsystems GmbH (Wetzlar, Germany)
Millicell ERS-2 epithelial volt-ohm meter	Millipore UK Lts (Watford, UK)
Molecular Imager® Gel DocTM XR system	Bio-Rad (Hemel Hempstead, UK)
MSD® SECTOR Imager 6000 and software	MSD (Rockville, MD, USA)

2.3 Cell culture

2.3.1 Cell culture medium

Culture medium	Composition
16HBE reduced FBS medium	MEM plus GlutaMAX™ supplemented with FBS (2%) and P/S (1%)
16HBE14o$^-$ (16HBE) complete medium	MEM plus GlutaMAX™ supplemented with FBS (10%) & P/S (1%)
ALI medium	2X ALI BEGM supplemented with BSA (3μg/ml) and mixed with an equal volume of ALI DMEM (DMEM supplemented with FBS (10%), P/S (1%), L-glut (1%), NEAA (1%) & sodium pyruvate (1%)) and supplemented with RA (50nM)
ALI starvation medium	BEBM supplemented with ITS (1X), BSA (0.01%) and Pen/Strep (1%)).
BEGM	BEBM mixed with an equal volume of 2X BEGM and supplemented with RA and gentamicin (GA) singlequots)
Fibroblast complete medium	DMEM supplemented with FBS (10%), P/S (1%), L-glut (1%), NEAA (1%) & sodium pyruvate (1%))
H1-HeLa infection medium	MEM plus GlutaMAX™ supplemented with FBS (4%), NEAA (1%), P/S (1%), HEPES (15mM), NaHCO3 (0.12%), tryptose (0.118%) and $MgCl_2$ (0.3mM)
H1-HeLa medium	MEM plus GlutaMAX™ supplemented with FBS (10%) NEAA (1%) and P/S (1%)
Ohio-HeLa medium	DMEM supplemented with FBS (10%), L-glut (1%) and P/S (1%)
$TCID_{50}$ medium	DMEM supplemented with FBS (2%), L-glut (1%) and P/S (1%)

2.3.2 Cell culture techniques

2.3.2.1 Continuous cell culture and subculture

Cells were maintained in T75cm^2 flasks in a humidified atmosphere at 37°C, 5% CO_2 unless otherwise stated. Once 70-80% confluency was reached, cells were sub-cultured/ passaged. Briefly, the cell culture medium was removed and cells were rinsed with HBSS (minus Ca^{2+} and Mg^{2+}) (10ml) to remove any residual FBS. Cells were trypsinised by incubation at 37°C with 1X trypsin-EDTA solution (1ml). Once the cells were detached (after ~5min), trypsin was neutralised with cell culture medium containing FBS (10%) (10ml). Cells were transferred to a 15ml conical tube and harvested by centrifugation at 1200 revolutions per minute (rpm) (300 x g) for 5min at 20°C. The supernatant was removed and cells were resuspended in cell culture medium (1ml). Cells were counted as described in section 2.3.2.3 and re-seeded, typically at a density of 300,000 cells in relevant cell culture medium (10ml) per T75cm^2 flask for continuous culture. Note that for HBECs, T75cm^2 flasks were pre-coated with collagen I solution (30µg/ml) for 0.5h at 37°C, prior to seeding.

2.3.2.2 Cyropreservation of cells and establishment from frozen stocks

Once cells were 70-80% confluent and were in culture for 2 passages or more, they could be cryopreserved. Cells were trypsinised and harvested as described above (section 2.3.2.1) and resuspended in cryopreservation medium (cell medium supplemented with DMSO (10%)) at a density of 1x10^6 cells/ml. Cells were aliquoted into cryovials (1ml/vial), placed in Nalgene® cryocontainers containing isopropyl alcohol and placed in a -80°C freezer overnight. The next day cryovials were transferred to liquid nitrogen for storage.

To establish cells from frozen stocks, cryovials were removed from liquid nitrogen. Frozen cell suspensions were thawed by pipetting pre-warmed cell medium, up and down within the cryovial. As cells began to defrost, the thawed supernatant was transferred into a conical tube containing cell medium (9ml). Cells were harvested by centrifugation at 1200rpm (300 x g) for 5min at

20°C. The supernatant was removed and cells were resuspended in cell medium (~13ml) and cultured in a T75cm^2 flask.

2.3.2.3 Cell counting

Prior to counting, cell suspensions were diluted in HBSS (typically 1 in 5) and mixed with an equal volume of trypan blue solution (0.4%) (final dilution of 1 in 10). A microscope slide was placed onto the haemocytometer, which was filled with the diluted cell suspension and viewed under the light microscope. Viable cells, from which trypan blue dye was excluded, were typically counted in 4 of the 1 x 1 mm grid squares (Figure 2.3.2-1). Cells lying on the left or top grid lines of squares were included in the count, while cells lying on the right or lower grid lines were not counted as being in the square. The total cell count was then divided by 4, to determine the average count per 1 x 1mm grid square. Since the counting chamber of the haemocytometer has a depth of 0.1mm, to calculate the number of cells per cm^3 (ml) in the diluted cell suspension, the average count per 1 x 1mm grid square was multiplied by 10,000. Finally, to calculate the number of cells per ml of undiluted suspension, the number of cells per ml of diluted suspension was multiplied by the dilution factor. In summary, to calculate the number of cells per ml of cell suspension:

$$Cells\ per\ ml\ = cells\ per\ 1\ x\ 1\ mm\ grid\ square\ \times 10{,}000\ \times dilution\ factor$$

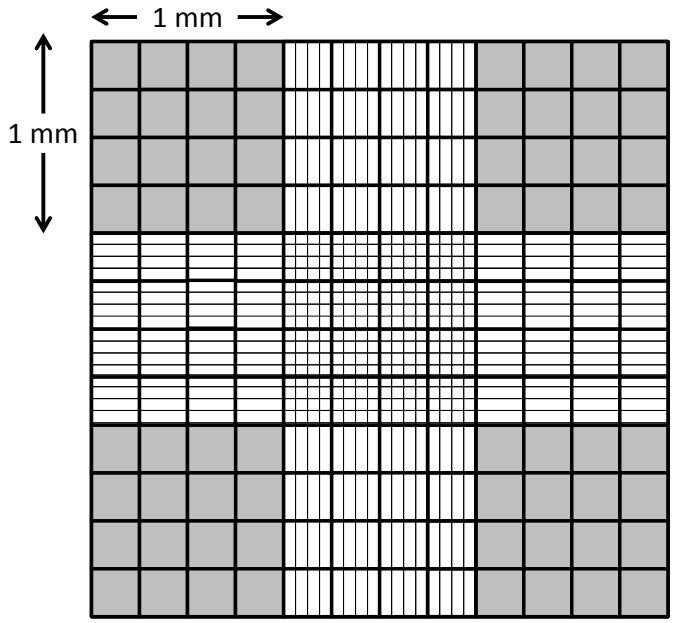

Figure 2.3.2-1 Counting grid of a haemocytometer.

The squares typically used for counting are shaded in grey.

2.3.3 Cell lines

2.3.3.1 HBEC (16HBE14o$^-$) culture

16HBE14o$^-$ (16HBE) cells (a gift from Professor D. C. Gruenert, San Francisco, USA) are a human BEC (HBEC) line that have been immortalised by transfection with replication-defective simian virus 40 (SV40) [180]. This cell line was chosen as 16HBE cells are able to form TJs, which are characteristic of the epithelial phenotype. 16HBE cells (passages 43-60) were maintained in 16HBE complete medium (section 2.3.1) and cultured as described above (section 2.3.2.1).

2.3.3.2 Fibroblasts (MRC-5)

MRC-5 cells are a fibroblast cell line (obtained from the European Collection of Authenticated Cell Cultures) derived from foetal lung tissue taken from a 14-week Caucasian male. These cells have been reported to attain up to 48 cell doublings before the onset of senescence [183]. MRC-5 cells (passage 23-30) were maintained in fibroblast culture medium (section 2.3.1) and cultured as described above (section 2.3.2.1).

2.3.3.3 HeLa cells

HeLa cells are an immortalised epithelial cell line derived from the cervical carcinoma of a 31 year old woman [184, 185]. High passage Ohio HeLa (Ohio HeLa cells of passage >50) and H1-HeLa cells are derivatives of the parent HeLa line that are susceptible to infection by HRVs. High passage Ohio HeLas were maintained in Ohio-HeLa medium (section 2.3.1) and were used to determine viral infectivity by tissue culture infective dose 50% ($TCID_{50}$) assay (see section 2.5.4.3). H1-HeLa cells were maintained in H1-HeLa medium (section 2.3.1) and used for amplification of virus stocks (see section 2.5.4.1) as they have been found to give higher titre stocks than Ohio HeLa cells.

2.3.4 Primary HBEC culture

Bronchial brushings were obtained by fibreoptic bronchoscopy with written and informed consent from healthy and severe asthmatic volunteers (see Appendix A, Table A4 for donor characteristics), as part of studies that were ethically

approved by the Southampton and South West Hampshire Research Ethics Committee (REC). These studies were entitled "Investigation of Pathophysiological Mechanisms in Airway Diseases such as Asthma and COPD" (REC no. 05/Q1702/165), "Investigation of gastro-oesophageal reflux disease (GORD) in asthma" (REC no. 13/SC/0182), "*Ex vivo* modelling of infection and therapeutics in airways disease" (REC no. 09/H0504/109) and "Cross sectional study IL-17 in asthma 10/H0504/2. Cells were kindly expanded from biopsies and brushings in cell culture by Dr. Natalie Smithers and Graham Berreen (Brooke Lab technicians) as described below.

Primary HBECs were isolated from bronchial brushings and grown at ALI as described previously [141]. Briefly, bronchial brushings were collected into PBS (typically 2 brushings per 10 ml), which was mixed with an equal volume of RPMI supplemented with FBS (20%) and P/S (1%). Cells were harvested by centrifugation at 1200rpm (300 x g), for 5min at room temperature (RT). Supernatants were removed and cells were re-suspended in 1 ml BEGM (section 2.3.1) per bronchial brushing. Clumps of cells were separated by passing through a sterile 23G needle and a 1 or 2ml syringe 3-5 times. Cells were then transferred to a T25cm^2 flask that had been pre-coated with collagen I solution (30µg/ml) for 0.5h at 37°C. Cells were then cultured for 24h in a total of 4 ml BEGM, after which they were checked for infection and the media was replaced with fresh BEGM to remove any non-adherent cells. Cultures were monitored and the media replaced every 2 days, until 70-80% confluency was reached, after which cells were passaged using standard cell culture techniques (see section 2.3.2.1).

At passage 2, primary HBECs were plated onto collagen I coated Transwells® (6.5mm with 0.4µm pore polyester membrane Insert) (Thermo Fisher Scientific, Loughborough, UK) at a density of 0.7x10^{5}cells/well. Cells were maintained in BEGM (200µl and 500µl in the apical and basolateral compartments of the Transwell® respectively) until a confluent monolayer was formed (typically after overnight culture). HBECs were then taken to ALI by removing the apical media and replacing the basolateral media with ALI medium (300µl) (section 2.3.1). ALI cultures were maintained over 21 days, during which time the basolateral medium was replaced daily with fresh ALI medium and any excess mucus was

removed with a fine-tip sterile Pasteur pipette. Differentiation of the epithelium was monitored visually using a light microscope and by monitoring formation of the epithelial barrier as determined by transepithelial resistance (TER) measurements (see section 2.7.1) on days 7, 14 and 21 after seeding.

2.4 Establishment of HBEC and fibroblast co-culture models

2.4.1 Polarised EMTU co-culture model

The apical and basolateral surfaces of Transwell® (6.5mm with 0.4µm pore polyester membrane Insert) membranes were coated with collagen I solution (100µl, 30µg/ml) for 0.5h at 37°C, inverted and seeded with a single cell suspension of the fibroblast cell line, MRC-5 (50,000 cells/50µl/well) (Figure 2.4.1-1A). For co-cultures where MRC-5 cells were seeded on the bottom of the well, 50,000 cells/500µl were seeded in each well of a 24-well Transwell® plate (Figure 2.4.1-1B). Cultures were then incubated for 2h to allow the MRC-5 cells to adhere, before the addition of 16HBE cells (150,000 cells/200µl/well) to the apical compartment of the Transwell®. Cultures were maintained in 16HBE complete medium (200µl apically and 500µl basolaterally) which was replaced with fresh medium on the 3rd and 5th day after seeding. Formation of the epithelial barrier was monitored by taking TER measurements (see section 2.7.1). On the 6th day after seeding, cultures were ready for stimulation with viral- or MBP mimetics (see section 2.5). Note that HBEC and fibroblast monocultures were established, maintained and challenged in the same way as the co-cultures but without the other cell type.

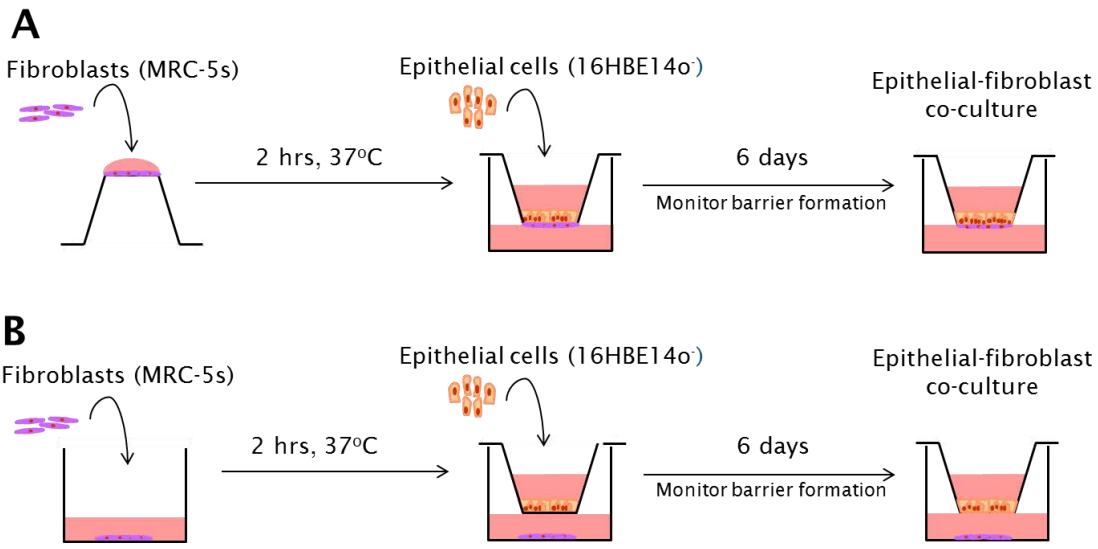

Figure 2.4.1-1 Establishment of cell line (polarised) HBEC and fibroblast co-culture models.

Fibroblasts (MRC-5 cells) were seeded onto the underside of the Transwell® (A) or the bottom of the well (B) and left to adhere for 2h at 37°C. HBECs (16HBE) were then seeded into the apical compartment and cells were co-cultured for 6 days to allow formation of TJs and the physical barrier.

2.4.2 Primary EMTU co-culture model

For the primary EMTU model, fully differentiated primary epithelial ALI cultures were inverted and MRC-5 cells (50,000 cells/50µl/well) were seeded onto the basolateral surface in MRC-5 culture medium and incubated for 2h at 37°C (Figure 2.4.2-1). Transwell® inserts were then turned upright and ALI starvation medium (see section 2.3.1) was added to the basolateral compartment (500µl). Cultures were ready for viral challenge (see section 2.5.4.2) after incubation overnight at 37°C.

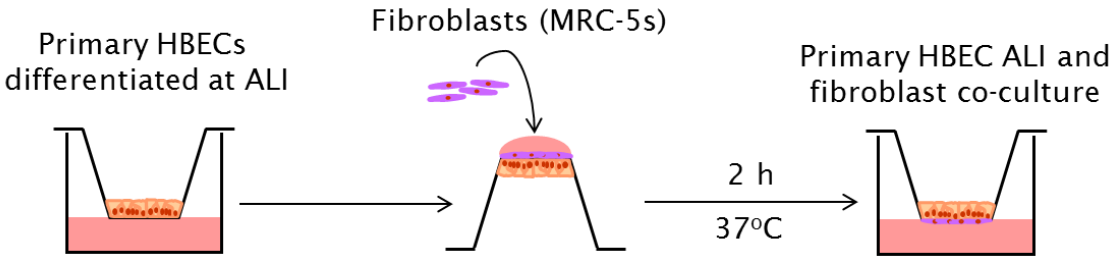

Figure 2.4.2-1 Establishment of the primary epithelial ALI and fibroblast co-culture model.
Fully differentiated primary epithelial ALI cultures were inverted and fibroblasts were seeded onto the basolateral surface of the Transwell®. After 2h incubation at 37°C, Transwell® inserts were turned upright.

2.5 Cell reagents & treatments

2.5.1 Poly(I:C)

Initially, the effects of viral infection were modelled using the viral mimetic, poly(I:C). Poly(I:C) is generated by annealing polymers of inosinic acid and cytidylic acid. This structure is an analogue of dsRNA; an intermediate produced during replication of the HRV genome. Poly(I:C) works as a mimetic of viral infection by binding PRRs (such as TLR-3, RIG-I and MDA-5) and inducing innate pro-inflammatory and anti-viral responses in a comparable way to HRV dsRNA [118]. Previously, recognition of dsRNA by RIG-1 and MDA-5 has been demonstrated to be length dependent, with RIG-1 and MDA-5 having specificity for short and long dsRNA respectively [186]. Since viruses of the picornaviridae family, such as HRV, are mainly recognised by MDA-5, high Mw poly(I:C) (1.5-8kb) was chosen as an HRV mimetic [118]. In addition high Mw poly(I:C) (1.5-8 kb) is closer to the length of the HRV genome (~7.2kb) than low Mw poly(I:C) (0.2-1kb) [187].

High Mw poly(I:C) was dissolved in ultrapure water to a stock concentration of 1mg/ml. To ensure proper annealing of polyinosinic acid and polycytidylic acid, the reconstituted mixture was mixed thoroughly, heated at 65-70°C for 10 mins and then allowed to cool for 1h at RT. Poly(I:C) stocks were stored at -20°C in 100µl aliquots, to prevent repeated freeze-thaw cycles and poly(I:C) degradation. On the 6th day after set up of the polarised co-culture model, an aliquot of poly(I:C) stock was thawed, pre-diluted in PBS and added to the apical compartment (10µl/200µl, 1 in 20 dilution) to reach the final test concentrations (Table 2.5.1-1). Cells and cell-free supernatants were harvested 24h after challenge as described in (section 2.6).

Table 2.5.1-1 Overview of poly(I:C) pre-dilutions and working concentrations

Pre-dilution of poly(I:C) stock (1mg/ml) required	**[Poly(I:C)] after pre-dilution (µg/ml)**	**Final dilution of pre-diluted poly(I:C) by addition to the apical compartment of the Transwell®.**	**Final [poly(I:C)] in the apical compartment of the Transwell® (µg/ml)**
1 in 5	200	1 in 20	10
1 in 50	20	1 in 20	1
1 in 500	2	1 in 20	0.1

2.5.2 pLArg

Rather than purifying MBP from eosinophils, its effects were modelled using the mimetic, pLArg. Similarly to MBP, pLArg is an arginine-rich polycation; properties which are responsible for some of the effects of MBP. For example, its positive charge allows MBP to bind avidly to negatively charged surfaces such as cell membranes, leading to damage, increased permeability and loss of cell-cell contacts [188-190].

pLArg was dissolved in ultrapure water to a stock concentration of 1mM, which was stored at -20°C in 25µl aliquots, to prevent repeated freeze-thaw cycles and pLArg degradation. On the 6th day after set up of the polarised co-culture model, an aliquot of pLArg stock was thawed, and pre-diluted in Ultrapure water to 500µM to reduce pLArg precipitation. Further dilutions were carried out in PBS and then added to the apical compartment (10µl/200µl, 1 in 20 dilutions) to reach the final test concentrations (Table 2.5.2-1). Barrier permeability was determined by TER measurements over 24h (section 2.7.1). Cells and cell-free supernatants were harvested 24h after challenge as described in (section 2.6).

Table 2.5.2-1 Overview of pLArg pre-dilutions and working concentrations

1st pre-dilution of pLArg stock (1mM) in water	**[pLArg] after 1st pre-dilution (µM)**	**2nd pre-dilution of pLArg (500µM) in PBS**	**[pLArg] after 2nd pre-dilution (µM)**	**Final dilution of pre-diluted pLArg by addition to the apical compartment of the Transwell®.**	**Final [pLArg] in the apical compartment of the Transwell® (µM)**
1 in 2	500	1 in 2.5	200	1 in 20	10
1 in 2	500	1 in 25	20	1 in 20	1
1 in 2	500	1 in 83.33 = 3 in 250	6	1 in 20	0.3
1 in 2	500	1 in 250	2	1 in 20	0.1

2.5.3 IL-1α

Human recombinant IL-1α was used to investigate the direct effects of IL-1α on HBEC and fibroblast monocultures. Binding of IL-1α to its receptor (IL-1R1), leads to recruitment of the IL-1 receptor accessory protein (IL-1RAcp) and formation of the IL-1R1 signalling complex. The signalling adaptor, myeloid differentiation primary response gene 88 (MyD88), is known to bind to the toll/IL-1 receptor (TIR) domain of IL-1R1, leading to activation of IKK, which causes degradation of the inhibitor of NF-κB (IκB) and the subsequent activation of NF-κB and a wide range of immune and inflammatory responses [191].

On the 6th day after seeding, 16HBE and MRC-5 monocultures were challenged apically and basolaterally, with concentrations of IL-1α that mimicked the levels induced by poly(I:C). Human recombinant IL-1α was reconstituted in PBS to a stock concentration of 1μg/ml, which was stored at -20°C in 10μl aliquots, to prevent repeated freeze-thaw cycles and IL-1α degradation. On the 6th day after set up of the polarised co-culture model, an aliquot of IL-1α stock was thawed, pre-diluted in PBS and added to the apical compartment (10μl/200μl, 1 in 20 dilution) to reach the final test concentrations (Table 2.5.3-1). Cells and cell-free supernatants were harvested 24h after challenge as described in (section 2.6).

Table 2.5.3-1 Overview of IL-1α pre-dilutions and test concentrations

Pre-dilution of IL-1α stock (1μg/ml) in PBS	**[IL-1α] after pre-dilution (ng/ml)**	**Final dilution of pre-diluted IL-1α by addition to the apical and/or the basolateral compartments of the Transwell®.**	**Final [IL-1α] in the apical and/or the basolateral compartment of the Transwell® (ng/ml)**
1 in 5	200	1 in 20	10
1 in 50	20	1 in 20	1

2.5.4 Human Rhinovirus-16 (HRV16)

2.5.4.1 Amplification of HRV16 using H1-HeLa cells and preparation of working stocks

The major group HRV, HRV16, was kindly amplified by Dr Emily Swindle (PhD supervisor) as previously described [192]. Briefly, H1-HeLA cells were cultured in a T75cm^2 flask until 80-90% confluent and washed with infection medium (5ml) (see section 2.3.1). Cells were then infected with HRV16 stocks at a 1:1 ratio with infection medium (total volume 4ml) and rocked on a plate shaker (0.35rpm) at RT for 1h. After which a further 4ml of infection medium was added to the flask and cells were incubated at 33°C, 5% CO_2, for 18h or until 80% cell death had occurred. Cells were then disrupted by 2X freeze-thaw cycles to -80°C, after which the cell supernatant was removed and the cell debris removed by centrifugation at 1200rpm (300 x g) for 5min at 4°C. Virus-containing supernatants were used for further amplification of viral stocks by repeating the above procedure until sufficient viral stock was generated. Note that after each round of amplification aliquots were taken to check virus activity by $TCID_{50}$ assay (see section 2.5.4.3) and for cryopreservation. Once sufficient viral stocks were generated, cellular debris was removed by passing the supernatant through a 0.22µM filter before aliquotting (2ml) and storing at -80°C. The final viral stock had a titre of $0.0056x10^6$ virions per µl.

2.5.4.2 HRV16 infection of the primary EMTU model

Ultra-violet (UV)-irradiated HRV16 stocks, as a control for inactive virus, were obtained by exposure of infective virus stocks to 120000µJ/cm^2 UV light for 50min, using a CL-1000 UV crosslinker (UVP, Cambridge, UK). Note that samples were irradiated on ice to prevent over-heating. Inactivation of the virus was confirmed by $TCID_{50}$ assay (see section 2.5.4.3).

Prior to HRV infection, ALI and ALI co-culture TERs were determined (see section 2.7.1), the apical surface was washed with HBSS (without Ca^{2+} or Mg^{2+}) (200µl), to remove excess mucus, and the basolateral media was replaced with fresh ALI starvation medium (500µl) (see section 2.3.1). The volume of HRV16 stock to add to each ALI culture for a multiplicity of infection (MOI) of 1 was then calculated by dividing the cell count of an equivalent (spare) ALI culture,

by the viral stock concentration. For an MOI of 2, double the volume of viral stock was used.

$$Virus\ stock\ required\ for\ an\ MOI\ of\ 1\ (\mu l) = \frac{cell\ number}{viral\ stock\ concentration\ (virions/\mu l)}$$

ALI mono- and co-cultures with fibroblasts were then infected apically with HRV16 or UV-HRV16 by incubation for 6h at 33°C in a humidified incubator. After which, apical washes (3X) with HBSS were performed to remove residual, virus particles and cultures were incubated at 37°C. After 24h, TERs were determined (see section 2.7.1), basolateral supernatants were harvested and apical supernatants were harvested by collection of 2 x 100µl apical washes with HBSS. Supernatants were clarified and cells were fixed as described in section 2.6.

2.5.4.3 $TCID_{50}$ assay

Virus infectivity was assessed by $TCID_{50}$ assay, which determines the highest dilution of virus suspension to produce a cytopathic effect (CPE) in 50% of the cultures inoculated. $TCID_{50}$ assays were performed as described previously [192]. Briefly, high passage Ohio HeLa cells (20,000 cells/100ul/well) were plated in 96-well plates and incubated at 37°C, 5% CO_2 until they had attached and were 80% confluent (typically 3h), after which, medium was removed and replaced with 180µl of $TCID_{50}$ medium (section 2.3.1). Virus-containing supernatants (20µl) were loaded onto the plate in quadruplicate and serially diluted (5X 10-fold serial dilutions) as shown in (Figure 2.5.4-1). Note that UV-HRV16 controls did not require serial dilution. Once the samples were loaded, plates were rocked on a plate shaker (0.35rpm) for 1h at RT. Plates were incubated for 96h (4 days) at 37°C, 5% CO_2 and then stained with 50µl of crystal violet staining solution (crystal violet (0.13%), formaldehyde (5%) and ethanol (5%) in PBS) at RT for 0.5h in the dark. Crystal violet staining solution was removed by inverting the plate and gentle submersion in water, after which the plate was left overnight to air dry and imaged using a Molecular Imager® Gel Doc™ XR system and Quantity One software (Bio-Rad, Hemel Hempstead, UK). Wells with a CPE (absence of crystal violet staining) >50 %

were counted and $TCID_{50}$ was calculated using the Spearman-Karber method [193]. For example:

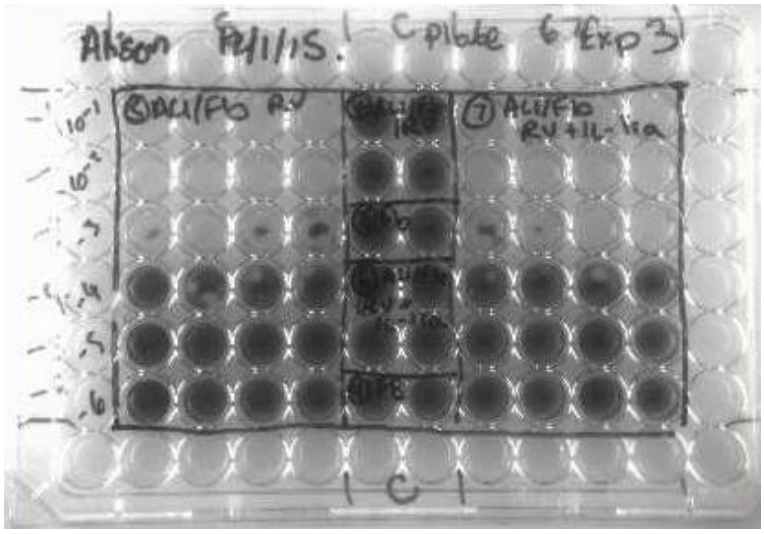

$$\boldsymbol{Log10\ TCID50 = L - [d(s - 0.5)]}$$

$L = Log10\ of\ the\ highest\ concentration\ (e.g. Log10\ of\ 10^{-1} = -1)$

$d = Log10\ of\ the\ difference\ between\ dilution\ steps\ (e.g. Log\ 10\ of\ 10X = 1)$

$s = sum\ of\ proportion\ of\ wells\ \ at\ each\ dilution\ with\ CPE\ > 50\%$

$(e.g. for\ samples\ in\ quadruplicate,\ s\ = no. of\ wells\ with\ CPE\ > 50\% \times \frac{1}{4})$

Both the ALI/Fb RV sample and ALI/Fb RV + IL-1ra sample above have 12 wells with CPE >50%. Therefore:

$$\boldsymbol{Log10\ TCID50 = -1 - [1(3 - 0.5)]}$$

$$\boldsymbol{Log10\ TCID50 = -3.5}$$

$$\boldsymbol{TCID50\ per\ well/180\mu l = 3162}$$

$$\boldsymbol{TCID50\ per\ ml = 17582}$$

	1	2	3	4	5	6	7	8	9	10	11	12
A	HBSS	HBSS	HBSS	HBSS	HBSS	HBSS	HBSS	HBSS	HBSS	HBSS	HBSS	HBSS
B	HBSS	Sample 1 (10^{-1})	Sample 1 (10^{-1})	Sample 1 (10^{-1})	Sample 1 (10^{-1})	Control (10^{-1})	Control (10^{-1})	Sample 2 (10^{-1})	Sample 2 (10^{-1})	Sample 2 (10^{-1})	Sample 2 (10^{-1})	HBSS
C	HBSS	Sample 1 (10^{-2})	Sample 1 (10^{-2})	Sample 1 (10^{-2})	Sample 1 (10^{-2})	Control (10^{-1})	Control (10^{-1})	Sample 2 (10^{-2})	Sample 2 (10^{-2})	Sample 2 (10^{-2})	Sample 2 (10^{-2})	HBSS
D	HBSS	Sample 1 (10^{-3})	Sample 1 (10^{-3})	Sample 1 (10^{-3})	Sample 1 (10^{-3})	Control (10^{-1})	Control (10^{-1})	Sample 2 (10^{-3})	Sample 2 (10^{-3})	Sample 2 (10^{-3})	Sample 2 (10^{-3})	HBSS
E	HBSS	Sample 1 (10^{-4})	Sample 1 (10^{-4})	Sample 1 (10^{-4})	Sample 1 (10^{-4})	Control (10^{-1})	Control (10^{-1})	Sample 2 (10^{-4})	Sample 2 (10^{-4})	Sample 2 (10^{-4})	Sample 2 (10^{-4})	HBSS
F	HBSS	Sample 1 (10^{-5})	Sample 1 (10^{-5})	Sample 1 (10^{-5})	Sample 1 (10^{-5})	Control (10^{-1})	Control (10^{-1})	Sample 2 (10^{-5})	Sample 2 (10^{-5})	Sample 2 (10^{-5})	Sample 2 (10^{-5})	HBSS
G	HBSS	Sample 1 (10^{-6})	Sample 1 (10^{-6})	Sample 1 (10^{-6})	Sample 1 (10^{-6})	Control (10^{-6})	Control (10^{-1})	Sample 2 (10^{-6})	Sample 2 (10^{-6})	Sample 2 (10^{-6})	Sample 2 (10^{-6})	HBSS
H	HBSS	HBSS	HBSS	HBSS	HBSS	HBSS	HBSS	HBSS	HBSS	HBSS	HBSS	HBSS

Figure 2.5.4-1 Typical plate layout of a $TCID_{50}$ assay.

The dilution factor of virus-containing sample in each well is indicated in brackets.

2.5.5 IL-1Ra

Human recombinant IL-1Ra was used as an inhibitor of IL-1 signalling. IL-1Ra works by binding to IL-1R1; preventing binding of IL-1α and IL-1β and the recruitment of IL-1RAcp, required for formation of the IL-1R1 signalling complex [194].

The effects of IL-1Ra in polarised EMTU model were investigated by the apical and/or basolateral incubation of IL-1Ra for 1h at 37°C prior to stimulation with poly(I:C) or pLArg (section 2.5.1 & 2.5.2). Human recombinant IL-1Ra was reconstituted in PBS to a stock concentration of 100µg/ml, which was stored at -20°C in 20µl aliquots, to prevent repeated freeze-thaw cycles and IL-1Ra degradation. On the 6th day after set up of the polarised co-culture model, an aliquot of IL-1Ra stock was thawed, pre-diluted in PBS (1 in 10 dilution) to give a working stock of 10µg/ml and added apically (10µl/200µl) and/or basolaterally (25µl/500µl) (1 in 20 dilutions) to give a final concentration of 500ng/ml within the apical and/or basolateral compartments of the Transwell® (Table 2.5.5-1).

The effects of IL-1Ra in the primary co-culture model were investigated by incubation with IL-1Ra in the basolateral compartment for 1h at 37°C prior to infection with HRV16 or UV-HRV16 as described in section (2.5.4.2). IL-1Ra stocks (100µg/ml) were diluted in ALI starvation medium (1 in 200 dilution) to a final concentration of 500ng/ml (Table 2.5.5-2), which was used to replace the basolateral medium in the primary co-culture model 1h before infection with HRV16 or UV-HRV16.

Table 2.5.5-1 Overview of IL-1Ra pre-dilutions and concentrations used in the cell line co-culture model

Pre-dilution of IL-1Ra stock (100 µg/ml) in PBS	**[IL-1Ra] after pre-dilution (µg/ml)**	**Final dilution of pre-diluted IL-1Ra by addition to the apical and/or the basolateral compartments of the Transwell®.**	**Final [IL-1Ra] in the apical and/or the basolateral compartment of the Transwell® (ng/ml)**
1 in 10	10	1 in 20	500

Table 2.5.5-2 Overview of IL-1Ra pre-dilutions and concentrations used in the cell line co-culture model

Dilution of IL-1Ra stock (100 µg/ml) in ALI starvation medium	**Final [IL-1Ra] in the basolateral compartment of the Transwell® (ng/ml)**
1 in 200	500

2.5.6 Anti-IFNAR2

The importance of IFN was examined by blocking type I IFN receptor signalling. The type I IFN receptor is a heterodimer consisting of IFNAR1 and IFNAR2. IFN-α and IFN-β bind to the IFNAR2 subunit, leading to dimerization with IFNAR1 and activation of STAT signalling [195].

Binding of type I IFNs to IFNAR2 was blocked using a neutralizing antibody to the extracellular domain of IFNAR2. The polarised EMTU model was incubated with mouse anti-human IFNAR2 (1μg/ml, clone MMHAR-3, $mIgG_{2a}$) or isotype control antibody (1μg/ml, $mIgG_{2a}$), by 1 in 500 dilution of 0.5mg/ml stocks into the apical (0.4μl/200μl) and basolateral compartments (1μl/500μl). After 1h the polarised EMTU model was stimulated with poly(I:C) (section 2.5.1). Cells and cell-free supernatants were harvested 24h after challenge as described in (section 2.6).

2.5.7 Fluticasone-propionate (FP)

FP is a second generation glucocorticoid, used to treat the inflammatory component of asthma. FP was reconstituted in DMSO to a stock concentration of 10mM, which was stored at -20°C in 10μl aliquots, to prevent repeated freeze-thaw cycles and FP degradation. On the 6th day after set up of the polarised co-culture model, an aliquot of FP stock was thawed, pre-diluted in 16HBE complete medium to a concentration of 10μM (1 in 1000 dilution). The 10μM solution was then diluted to a concentration of 200nM (1 in 50 dilution) and added apically (10μl/200μl, 1 in 20 dilution) and basolaterally (25μl/500μl, 1 in 20 dilution), to give a final concentration of 10nM (Table 2.5.7-1). Cultures were incubated with FP for 1h at 37°C before stimulation with poly(I:C) (section 2.5.1). Cells and cell-free supernatants were harvested 24h after challenge as described in (section 2.6).

Table 2.5.7-1 Overview of FP pre-dilutions and concentrations

1st pre-dilution of FP stock (10mM)	**[FP] after 1st pre-dilution (µM)**	**2nd pre-dilution of FP (10µM)**	**[FP] after 2nd pre-dilution (nM)**	**Final dilution by addition to the Transwell®.**	**Final [FP] (nM)**
1 in 1000	10	1 in 50	200	1 in 20	10

2.5.8 Pan-TGF-β Antibody

The importance of TGF-β was examined by blocking TGF-β signalling. The TGF-β receptor signalling complex is a hetero-tetrameric complex consisting of TGFBR1 and TGFBR2 dimers which forms following binding of TGF- β 1, 2, or 3 to TGFBR2 [196]. Formation of this complex leads to activation of SMAD signalling.

TGF-β signalling was blocked using a neutralizing antibody to TGF- β 1, 2, and 3. Anti-TGF-β antibody (Clone # 1D11, mIgG$_1$) was reconstituted in PBS to a stock concentration of 0.5mg/ml, which was stored at -20°C in 5µl aliquots, to prevent repeated freeze-thaw cycles and antibody degradation. On the 6th day after seeding, the polarised EMTU model was incubated with anti-TGF-β (1µg/ml) or isotype control antibody (1µg/ml, mIgG$_1$), by 1 in 500 dilution of 0.5mg/ml stocks into the apical (0.4µl/200µl) and basolateral compartments (1µl/500µl). After 1h the polarised EMTU model was stimulated with poly(I:C) (see section 2.5.1) or TGF-β$_1$ (5ng/ml basolaterally) as a positive control for myofibroblast differentiation. Cells and supernatants were harvested 24h after challenge as described in (section 2.6).

2.6 Harvest of cells and cell supernatants

Cell supernatants were removed and clarified by centrifugation at 1200rpm (300 x g), for 5min at 4°C. Cell-free supernatants were then stored at -20°C. Cells were either fixed (section 2.6.1) for analysis by immunofluorescent microscopy (section 2.8) or lysed by 3X freeze-thaw (2.6.2) for analysis of cell contents.

2.6.1 PFA fixation

Supernatants were harvested and cell cultures were washed with PBS (1ml) before fixing in PFA (4% in PBS) for 15min at RT. Fixed cells were stored in sodium azide (0.05% in PBS) at 4°C until required for immunofluorescent staining.

2.6.2 Cell lysis by freeze-thaw

Supernatants were harvested and cultures washed with PBS before adding another 200µl of cell culture medium to the apical compartment. Cells were then lysed with 3X freeze-thaw cycles (1h -80°C, 30 mins RT). After the final thaw cycle, lysates were clarified by centrifugation at 1200rpm (300 x g), for 5min at 4°C. Cell lysates were then stored at -20°C prior to analysis.

2.7 Assessment of epithelial barrier function

2.7.1 Assessment of ionic permeability of the epithelium

Ionic permeability of the epithelium was determined by TER measurements using chopstick electrodes and a Millicell® ERS-2 Volt-Ohm meter as indicated in Figure 2.7.1-1. TER measurements of epithelial ALI mono- and co-cultures with fibroblasts required the cultures to be submerged. Therefore, HBSS was pre-warmed to 37°C for 30min and 100µl was added to the apical compartment of the Transwell®. Cultures were then incubated for 15min at 37°C prior to reading the TER. Once TER measurements were acquired, cultures were returned to ALI by the removal of the apical HBSS. Note that TERs were corrected for the TER of an empty Transwell® (132Ω, n=4) and then expressed as Ω.cm^2 or normalised to control TERs at T=0 before challenge with poly(I:C) or infection with HRV16.

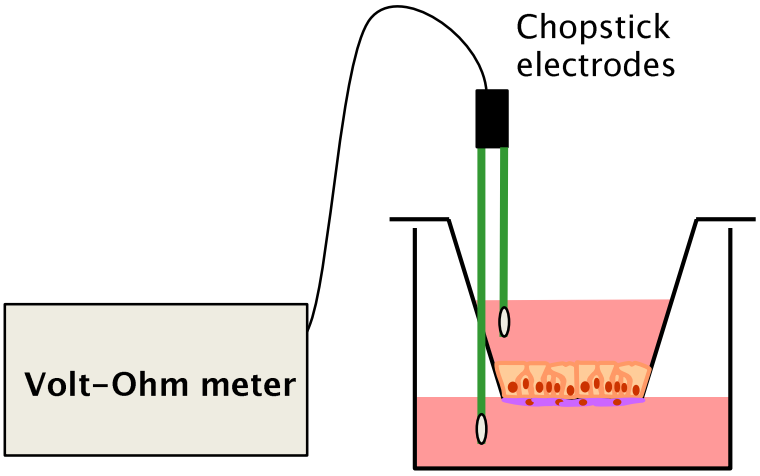

Figure 2.7.1-1 Measurement of TER using chopstick electrodes and a Volt-Ohm meter.

Chopstick electrodes were placed at a 90°C angle to the base of the plate, with the longest electrode submerged in the basolateral media on the outside of the Transwell® insert and the shortest electrode submerged in the apical media on the inside of the Transwell® insert.

2.7.2 Assessment of macromolecular permeability of the epithelium

At 3 or 21h after challenge with poly(I:C) or pLArg (sections 2.5.1 and 2.5.2), 4kDa FITC-labelled dextran was added to the apical compartment of each Transwell® (8µl of 50mg/ml stock to 200µl, 1 in 25 dilution) to a final concentration of 2mg/ml (Figure 2.7.2-1). After 3h incubation at 37°C, 5% CO_2, samples (50µl) were removed from the basolateral compartment and loaded onto a black 96-well plate in duplicate. Fluorescence was determined using a Fluoroskan Ascent FL 2.5 and accompanying software (excitation wavelength (ex) 485nm and emission wavelength (em) 530nm). FITC-dextran was quantified by comparison with a FITC-dextran standard curve (1-500µg/ml) and its diffusion was expressed as a percentage of diffusion through an empty Transwell®.

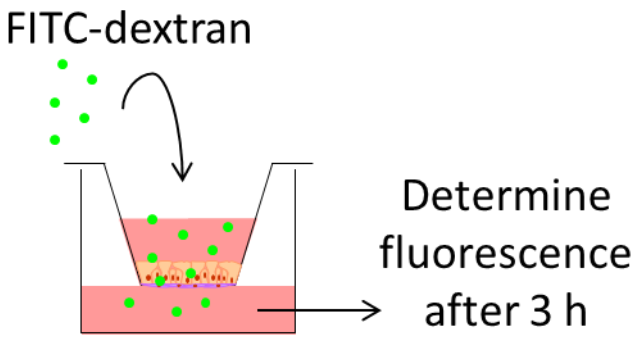

Figure 2.7.2-1 Measurement of macromolecular permeability of the epithelium.
FITC-labelled dextran was added to the apical compartment of the Transwell® and its diffusion into the basolateral compartment was determined 3h later.

2.8 Immunofluorescent staining and microscopy

Fixed cells obtained in section 2.6 were removed from storage, washed in PBS (3 x 5min) and permeabilised with TX-100 (0.1% in PBS) for 15min at RT. Transwells® were then blocked for 0.5h in PBS supplemented with BSA (1%) and Tween® 20 (0.1%) to reduce background staining due to non-specific antibody binding. Microscope slides were prepared by drawing a circle with a hydrophobic pen and adding a few drops of blocking buffer. The blocking buffer was then removed from the Transwells®, the membranes detached with a scalpel and transferred onto the microscope slide. Note that for fibroblast staining, the epithelial cells on the reverse side of the Transwell® were removed using a cotton bud to reduce background staining and vice versa. The blocking buffer was removed from the slide and replaced with 50µl immunofluorescent antibody/stain of interest diluted in blocking buffer (see Table 2.7.2-1 for dilutions). Slides were left to stain overnight in a humidified chamber at 4°C. After which, slides were washed (5 x 5min) in PBS supplemented with Tween® 20 (0.1%) for 5min. For initial experiments, slides were then mounted with ProLong® Gold Antifade Reagent containing DAPI. However, DAPI staining was clearer when the samples were stained prior to mounting. Subsequently, samples were stained with DAPI (1µg/ml for 6 mins) prior to mounting with mowiol. All slides were stored at 4°C until dry. Cells were imaged using a Leica AF6000 immunofluorescent microscope or a Leica true confocal scanner (TCS) (SP5 or SP8) confocal microscope as stated in the figure legends. See Table 2.7.2-1 for filters and excitation (ex) and emission (em) wavelengths used for each immunofluorescent stain/antibody. Note that for each Transwell® stained and imaged, at least 3 representative images were taken. These were generally taken in the centre, 12 o'clock and 6 o'clock positions of the Transwell®. Where serial optical sections were captured, these were projected to provide 2 dimensional (2D) maximum brightness images.

Table 2.7.2-1 Immunofluorescent staining: dilutions, final concentrations and ex/em wavelengths for each antibody and stain

Antibody/stain	**Dilution**	**Final concentration**	**Leica AF6000 filter cube**	**Wavelength (nm)**	
				Ex	**Em**
Alexa Fluor® 488 conjugated, mouse monoclonal anti-occludin antibody (clone OC-3F10, mIgG$_{1\kappa}$) (0.5mg/ml)	1 in 100	5µg/ml	FITC	485	530
FITC-conjugated monoclonal mouse anti-human α-SMA antibody (clone 1A4, mIgG2a) (2mg/ml)	1 in 250	8µg/ml	FITC	485	530
DAPI (1mg/ml)	1 in 1000	1µg/ml	DAPI	365	440

2.9 Fibroblast proliferation assay

2.9.1 Principles of the assay

Fibroblast proliferation was assessed using the Click-iT® EdU Alexa Fluor® 647 imaging kit, which uses deoxyribonucleic acid (DNA) synthesis as a surrogate marker of cell proliferation. DNA synthesis can be directly assessed by measuring incorporation of labelled nucleosides or nucleoside analogues into newly synthesised DNA, which occurs during the S-phase of the cell cycle (Figure 2.9.1-1).

Previous methods of DNA synthesis detection have included the use of radiolabelled nucleosides (e.g. ^{3}H-thymidine) and antibody-based detection of nucleoside analogues (e.g. bromo-deoxyuridine; BrdU). A relatively novel alternative which avoids the use of radiolabels and does not require DNA denaturation (as in antibody-based detection systems) is the Click-iT® EdU Assay. The Click-iT® Assay uses a thymidine analogue, 5-ethynyl-2´-deoxyuridine (EdU), which contains a terminal alkyne group (C≡C) instead of a methyl group (-CH_3) in the 5 position of the pyrimidine ring (see Figure 2.9.1-2). EdU detection is based on a copper-catalysed covalent reaction, between the EdU alkyne group and an azide group within a fluorescent Alexa Fluor® dye. Thus, EdU incorporation into newly synthesised DNA is fluorescently labelled and can be visualised by fluorescent microscopy.

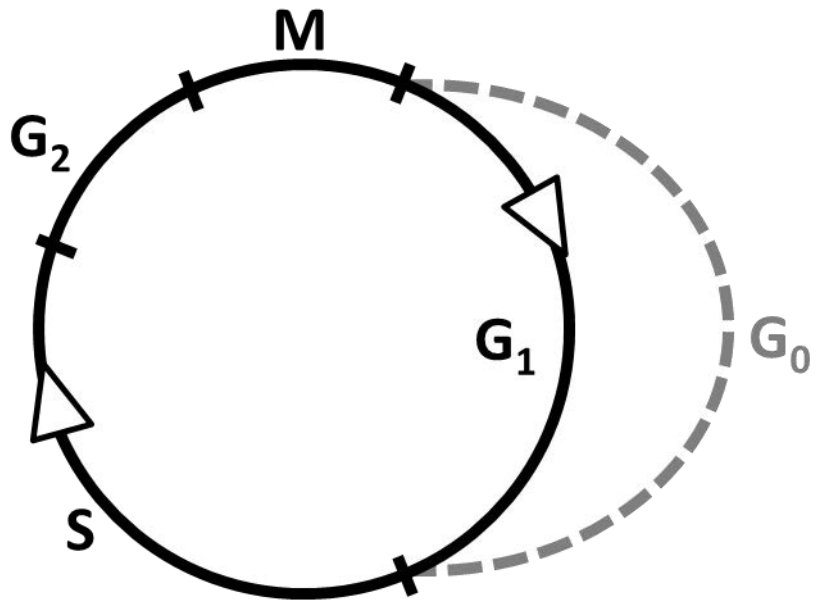

Figure 2.9.1-1 Phases of the cell cycle [197].

The cell cycle functions to accurately duplicate cellular DNA and segregate copies into two daughter cells. DNA synthesis occurs during S-phase. Chromosome segregation and cell division occur in M phase (M for mitosis). The G_1 and G_2 phases are gap or growth phases, during which time the cell is growing and doubling its proteins and organelles, ready for DNA synthesis and cell division. Gap phases also allow time to monitor the environment and ensure that conditions are suitable and preparations are complete before the cell commits itself to entering S or M-phase. If conditions are unsuitable, cells can delay progress through G_1 by exiting the cell cycle, and entering a specialised, quiescent resting state (G_0). Cells may remain in this state until stimulated (e.g. by growth factors) to resume proliferation and re-enter the cell cycle at S-phase.

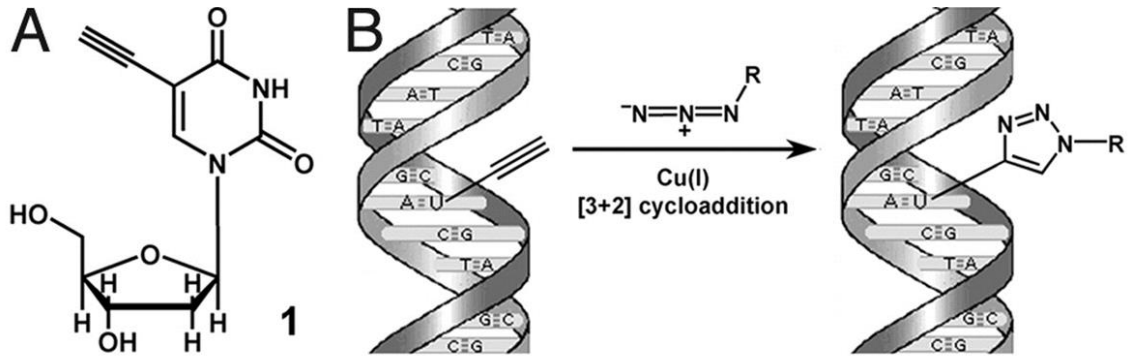

Figure 2.9.1-2 Overview of the Click-iT® EdU assay.

(A) 5-ethynyl-2′-deoxyuridine (EdU) is a thymidine analogue that carries a terminal alkyne group (C≡C) instead of a methyl group (-CH_3) in the 5 position of the pyrimidine ring. (B) Proliferating cells incorporate EdU into their DNA. When the Click-iT® reaction cocktail is added, copper Cu(I) readily catalyses a reaction where the EdU alkyne group is covalently linked to the Alexa Fluor®-azide (R-N_3). Thus, newly synthesised DNA is fluorescently labelled and can be visualised by fluorescent microscopy. Figure reproduced from reference [198] with permission from the National Academy of Sciences of the USA.

2.9.2 Assay optimisation

Changes in nucleoside incorporation and DNA synthesis can be difficult to detect in cultures where cells are at different stages of the cell cycle (Figure 2.9.1-1). In order to synchronize fibroblasts to the resting phase (G_0), cell proliferation was initially assessed in co-cultures that had been incubated overnight with 16HBE medium containing reduced FBS (2% and 1%) in the basolateral compartment. Serum starved cultures were stimulated basolaterally with 10% FBS as a positive control for activation of DNA synthesis. Increased EdU incorporation was detectable by 36h but not 24h post-stimulation, as demonstrated by increased EdU^+ nuclei (Figure 2.9.2-1). At this time point, there was no clear difference in the number of EdU^+ nuclei between cultures which were initially starved in 1 or 2% FBS (Figure 2.9.2-1). Therefore for all subsequent experiments, cells were cultured in 16HBE medium containing 2% FBS (basolateral only) and EdU incorporation determined after 36h.

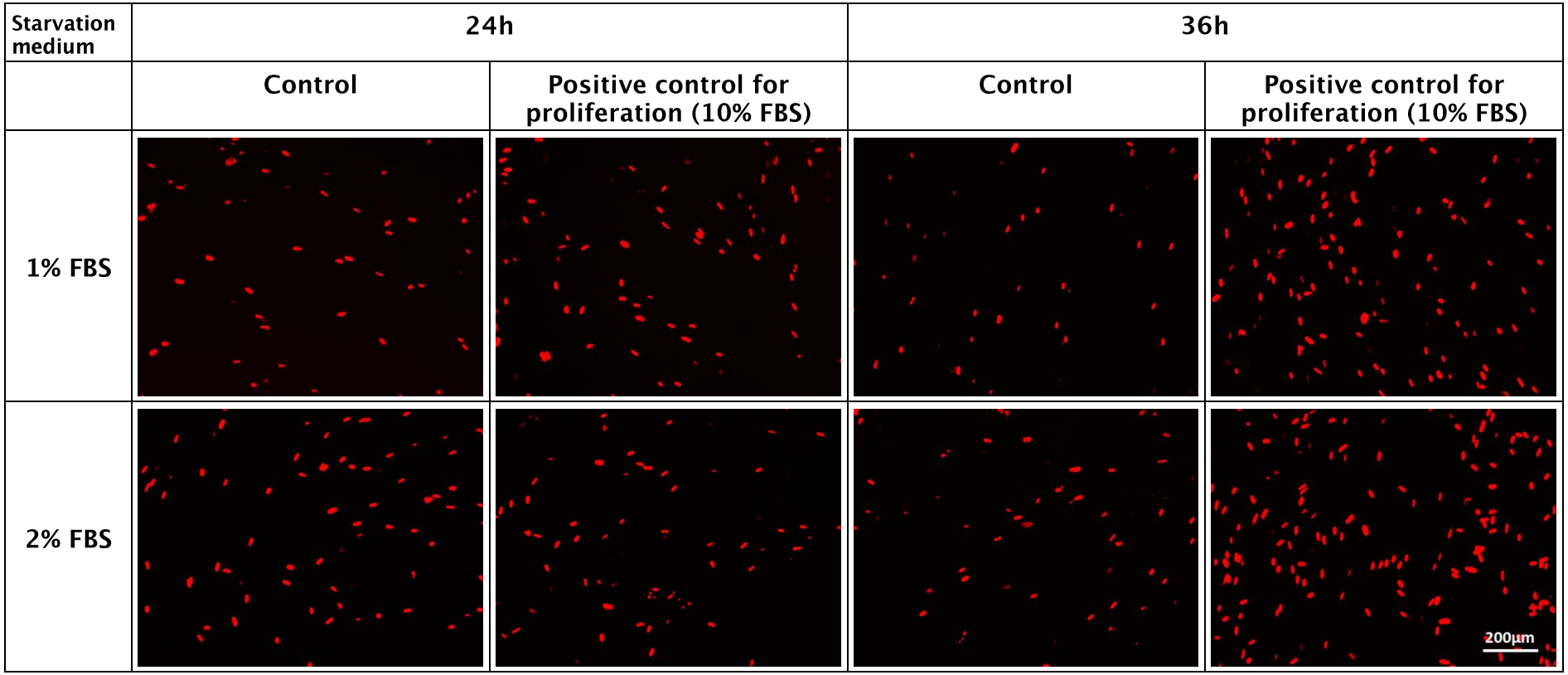

Figure 2.9.2-1 Optimisation of the Click-iT® EdU assay.

Co-cultures were established as described in section 2.4.1. To synchronise the fibroblast cell cycles prior to stimulation with the positive control for proliferation, cultures were starved overnight in 16HBE medium containing reduced FBS (2% or 1%). Co-cultures were fixed 24h and 36h post-stimulation and DNA synthesis assessed by detection of EdU incorporation into newly synthesised DNA by immunofluorescent microscopy. Red nuclei= EdU+ cells. Representative images were taken of each Transwell® at 10x magnification (n=1).

2.9.3 Click-iT® EdU assay protocol

Co-cultures of 16HBE cells and MRC-5 fibroblast cells were established on the apical and basolateral surfaces of a Transwell® nanoporous membrane respectively, as described in section 2.4.1. On the 5th day after seeding, the basolateral cell culture medium was replaced with reduced FBS (2%) 16HBE medium, while the apical medium was replaced with16HBE complete medium (10% FBS) (section 2.3.1).The next day, half the basolateral medium (250µl) was replaced with 2X EdU (20µM) in reduced FBS (2%) 16HBE medium (final EdU concentration of 10µM). Cultures were then stimulated with poly(I:C) or pLArg (as described in section 2.5) or with 10% FBS (50µl FBS added basolaterally) as a positive control for proliferation. Supernatants were harvested (as described in section 2.6) and cells fixed in PFA (as described in section 2.6.1) 36h hours post-stimulation. Fixed cells were stored in sodium azide (0.05% in PBS) at 4°C.

For detection of EdU incorporation, fixed cultures were washed with PBS supplemented with BSA (3%) (2 x 5min) and then permeabilised with TX-100 (0.5% in PBS) for 20min at RT. The wash step was repeated and Transwell® membranes were transferred onto a microscope slide (as described in section 2.8). Click-iT® reaction cocktail was prepared (Table 2.9.3-1) as described in the manufacturer's instructions [199], added to each slide (50µl/ Transwell®), and incubated at RT for 30min, protected from light. The Click-iT® reaction cocktail was then removed and slides were washed as before. To visualise all the cell nuclei, DNA staining was carried out using the Hoechst 33342 solution as described in the Click-iT® kit manufacturer's instructions [199]. Briefly, Hoechst 33342 solution was diluted in PBS (1 in 2000; final concentration 5µg/ml) and 50µl added to each slide. After 30min incubation at RT in the dark, the Hoechst 33342 was removed and slides were washed with PBS (2x 5min). Slides were mounted using mowiol and stored at 4°C until dry.

Table 2.9.3-1 Click-iT® reaction cocktail components [199].
Components were added in the order listed and used within 15 minutes of preparation. Reaction volumes were scaled up as required.

Reaction components	**Volume (µl)**
1X Click-iT® reaction buffer	430
$CuSO_4$	20
Alexa Fluor® azide	1.2
Reaction buffer additive	50
Total volume	**500**

2.9.4 EdU imaging and analysis

EdU was visualised using a Leica AF6000 immunofluorescent microscope and the 647/Cy5 filter cube (ex 645nm, em 660). Hoechst staining was visualised using the DAPI filter cube (ex 365nm, em 440). Initially I tried to quantify the total and EdU^+ nuclei in each field of view using the automated cell counting function in the image analysis software, ImageJ. However, the software had trouble distinguishing between separate nuclei in confluent cultures. I therefore assessed the suitability of images taken at x10, x20 and x40 magnifications to be used for manual cell counting. The lowest magnification that total nuclei could be counted accurately whilst still including a reasonable number of EdU^+ cells per field of view, was determined to be x20. I therefore counted total and EdU^+ nuclei in 3 representative fields of view for each Transwell® at x20 magnification. Images were generally taken in the centre, 12 o'clock and 6 o'clock positions of the Transwell®.

2.10 Assessment of cytotoxicity

Cytotoxicity of poly(I:C) and pLArg was assessed using a CytoTox 96® non-radioactive cytotoxic assay kit as described in the manufacturer's instructions [200]. The assay quantitatively measures lactate dehydrogenase (LDH), a stable cytosolic enzyme that is released upon cell lysis. Treatment of 1 control well of cells with 1% TX-100 in cell culture medium at 37°C for 45min, represented a positive control for 100% cell lysis. Standards were then created by 2-fold serial dilutions of the positive control. Clarified supernatants collected 24h after poly(I:C) or pLArg challenge and standards were loaded (2 x 25µl) onto a 96-well plate. The substrate mix provided in the kit (25µl) was added to each well and incubated at RT, for 0.5h. If LDH was present, tetrazolium salt (2-(4-iodophenyl)-3-(4-nitrophenyl)-5-phenyl-2H-tetrazolium chloride or INT) in the substrate mix was converted into a red formazan product. The reaction was stopped with the stop solution provided in the kit (1M acetic acid) and the plate was read using a Labsystems Multiskan Ascent plate reader set to 492nm. Background signal was corrected for by subtracting the signal from a blank control well (containing medium instead of culture supernatant).

Standard curves were created using the software accompanying the plate reader which was capable of generating a four parameter logistic curve fit.

2.11 Detection of mediator release

2.11.1 Enzyme linked immunosorbent assay (ELISA)

IL-29, IL-6, CXCL8, GM-CSF, CXCL10, IL-1α, TGF-β_1 and TGF-β_2 release was determined using commercially available sandwich ELISA kits, according to manufacturer's instructions except with the use of half volumes compared to those suggested [201]. Briefly, a 96-well plate was coated overnight with a capture antibody specific for the analyte of interest. Any unbound capture antibody was removed by washing the plate (3X) with wash buffer (typically 0.05% Tween® 20 in PBS). The plate was then treated with blocking buffer (5% Tween® 20 in PBS for TGF-β_1, 1% BSA in PBS for all other ELISAs) for 1h to reduce non-specific protein binding. After washing (3X) the samples and standards were added to the plate in duplicate. Note that the majority of the samples needed diluting in reagent (0.1% BSA and 0.05% Tween® 20 for CXCL8, 1% BSA in PBS for all other ELISAs) in order to give a signal that was within the range of the standard curve (Table 2.11.1-1). In addition, for detection of total TGF-β_1 and TGF-β_2, samples were acidified to activate latent TGF-β to the immunoreactive active form. One N HCl was added to each sample at a ratio of 1:5 and incubated for 10 mins at RT. Acidification reactions were neutralized using equal volumes of 1.2 N NaOH/0.5 M HEPES to HCl. Activated samples were diluted further with blocking buffer as required.

Once prepared and loaded onto the plate, samples and standards were incubated overnight at 4°C to allow any analytes in the sample to bind to the capture antibody. After which, any unbound protein was washed away (3X, wash buffer) prior to the addition of a second, biotinylated (detection) antibody that also binds the analyte. After 2h incubation with the detection antibody, the plate was washed again (3X) and streptavidin conjugated to horseradish-peroxidase (strep-HRP), which binds to the detection antibody, was added. After 20-30min, a final wash (3X) removed any unbound strep-HRP before addition of ELISA substrate solution, containing the hydrogen peroxide substrate (H_2O_2) and the chromogen 3,3-,5,5-tetramethylbenzidine (TMB). If

the analyte-antibody-strep-HRP complex is present, H_2O_2 is broken down into H_2O and oxygen free radicals which oxidise the TMB, leading to the production of a coloured (blue) product (Figure 2.11.2-1). After 15-20min the reaction was stopped by the addition of stop solution (1M H_2SO_4) to prevent the signal from surpassing the linear range of amplification and allow quantification using a standard curve. The absorbance of each well at 450nm was determined using a Labsystems Multiskan Ascent plate reader, with a reference wavelength of 570nm. Background signal was also corrected for by subtracting the signal from a blank control well (containing diluent instead of sample). Standard curves were created (Figure 2.11.1-2) and used to calculate analyte concentrations in the test samples, using the software accompanying the plate reader.

Table 2.11.1-1 Standard curve ranges of commercially available ELISA kits

ELISA kit	**Standard curve range (pg/ml)**
IL-6	9.38 – 600
CXCL8	31.2 – 2,000
GM-CSF	6 – 750
CXCL10	31.2 – 2,000
IL-1α	7.81 – 500
IL-29	62.5-4,000
TGF-β1	31.2-2,000
TGF-β2	31.2-2,000

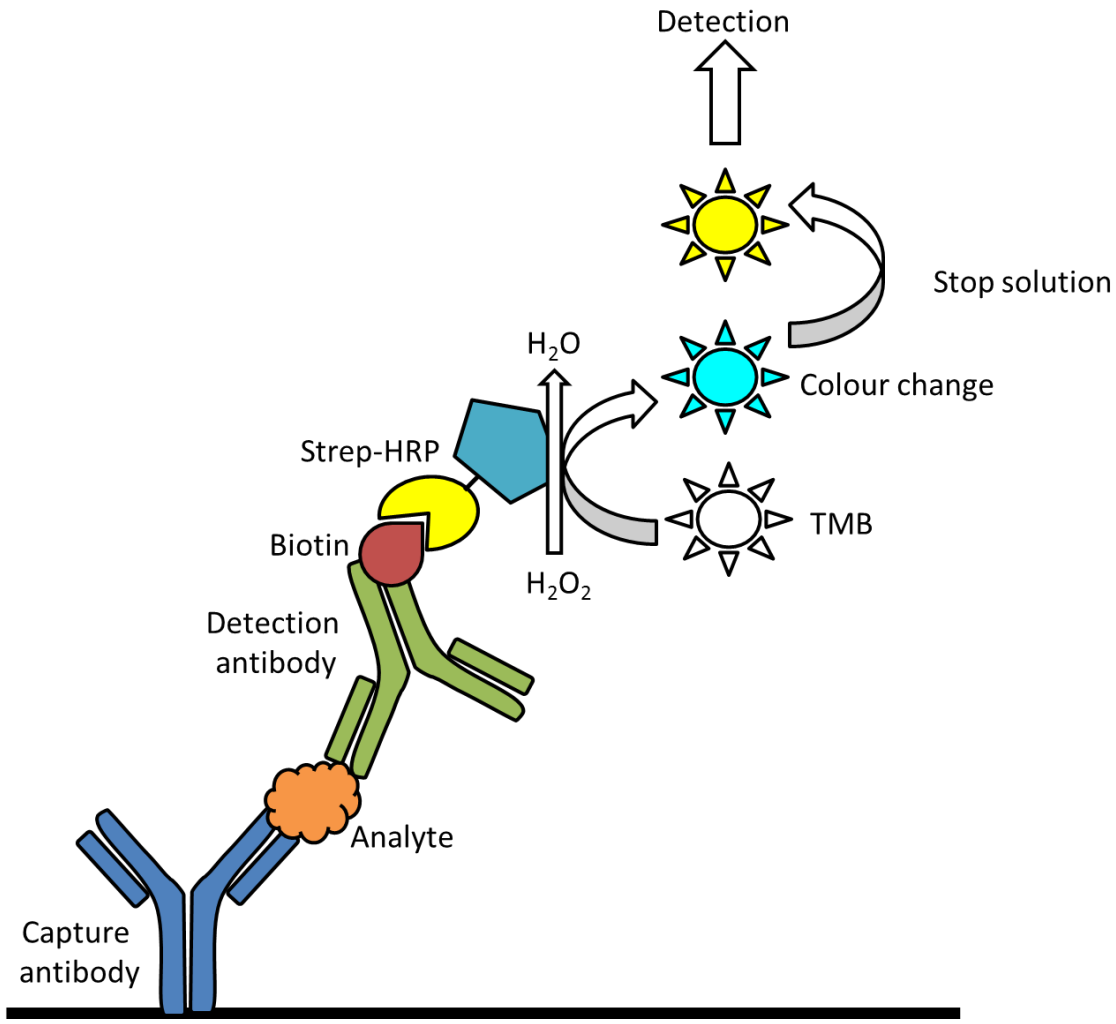

Figure 2.11.1-1 Overview of the sandwich ELISA for the detection of analytes. If antibody-analyte-antibody-strep-HRP complexes form, TMB is converted to a coloured product. Thus the colour change indicates the presence of the antigen of interest [201, 202].

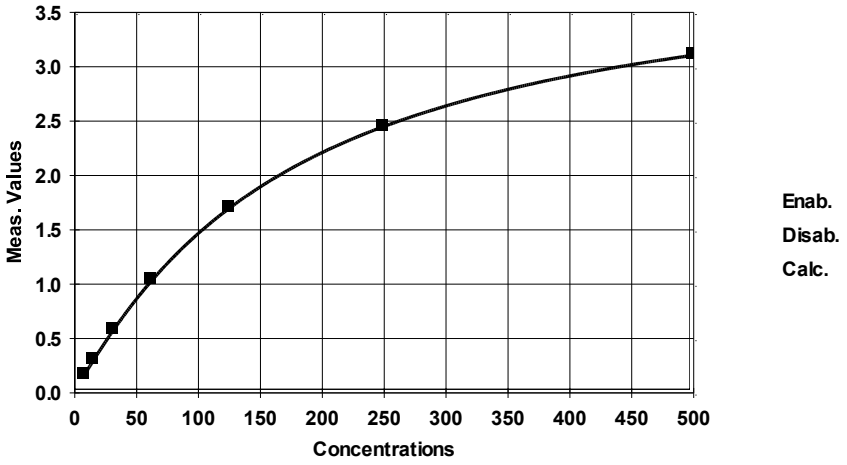

Figure 2.11.1-2 Typical IL-1α ELISA standard curve generated using the Labsystems Multiskan Ascent software.

Standard concentrations (x axis) were plotted against the background and blank corrected mean absorbance at 450nm (y-axis). Standard curves were generated using a 4-parameter logistic curve fit. Analyte concentrations in test samples were calculated by comparison to the standard curve generated for each assay.

2.11.2 Luminex® multiplex screening assay

MMP-2, MMP-9, VEGF, bFGF, IL-1α, IL-1β and IL-1Ra release into cell-free supernatants was determined using a commercially available Luminex® screening assay kit and the Bio-Plex® 200 suspension array system and accompanying software. The assay was carried out according to the manufacturer's instructions [203, 204]. Briefly, analyte-specific antibodies were pre-coated onto polystyrene bead microparticles that are colour coded with different intensities of red and infrared fluorophores specific for each analyte. Microparticles and standards or samples were loaded into a 96-well filter-bottomed plate in singlicate (due to the reliability and reproducibility observed using Luminex® assays and the fact that the read out is an average of the readings for each bead). Note that all samples were diluted (1 in 3) in the diluent provided in the kit, which gave a signal that was within the range of the standards for the majority of the samples (Table 2.11.2-1). Once loaded onto the plate, the samples and standards were incubated for 2h at RT on a shaking platform to allow analytes within the samples to bind to the antibodies immobilised on the beads. Unbound substances were washed away (3X washes using the wash buffer provided in the kit) and a vacuum manifold device. The microparticles were then incubated with a biotinylated (detection) antibody cocktail, specific to the analytes of interest, for 1h on a shaking platform. Another wash (3X) removed any unbound biotinylated antibody, before the addition of streptavidin conjugated to the fluorescent dye, phycoerythrin (PE). After 0.5h incubation on a shaking platform, a final wash (3X) removed unbound Strep-PE. The microparticles were then resuspended in wash buffer and read using the Bio-Plex analyser. Within the Bio-Plex analyser, microspheres were passed through a detection chamber in single file and excited with a red and green laser (Figure 2.11.2-1). The red laser excites the internal red and infrared dye of the microparticle and its spectral signature indicates which analyte is being detected. The green laser excites the PE and the magnitude of the signal indicates the amount of analyte bound. These signals were quantified by comparison to a standard curve, modelled by the Bio-Plex software and generated from the known standard concentrations (Figure 2.11.2-2). Note that background signal was corrected for by subtracting the signal from a blank control well (containing diluent instead of sample).

Table 2.11.2-1 Standard curve ranges for analytes in the Luminex® assay

Analyte	**Standard curve range (pg/ml)**
MMP-2	268 – 70627
MMP-9	19.8 – 50820
VEGF	1.3 – 3871
bFGF	2.9 – 5460
IL-1α	3.4 to 2303
IL-1β	3.9 – 2733
IL-1Ra	13 – 9000

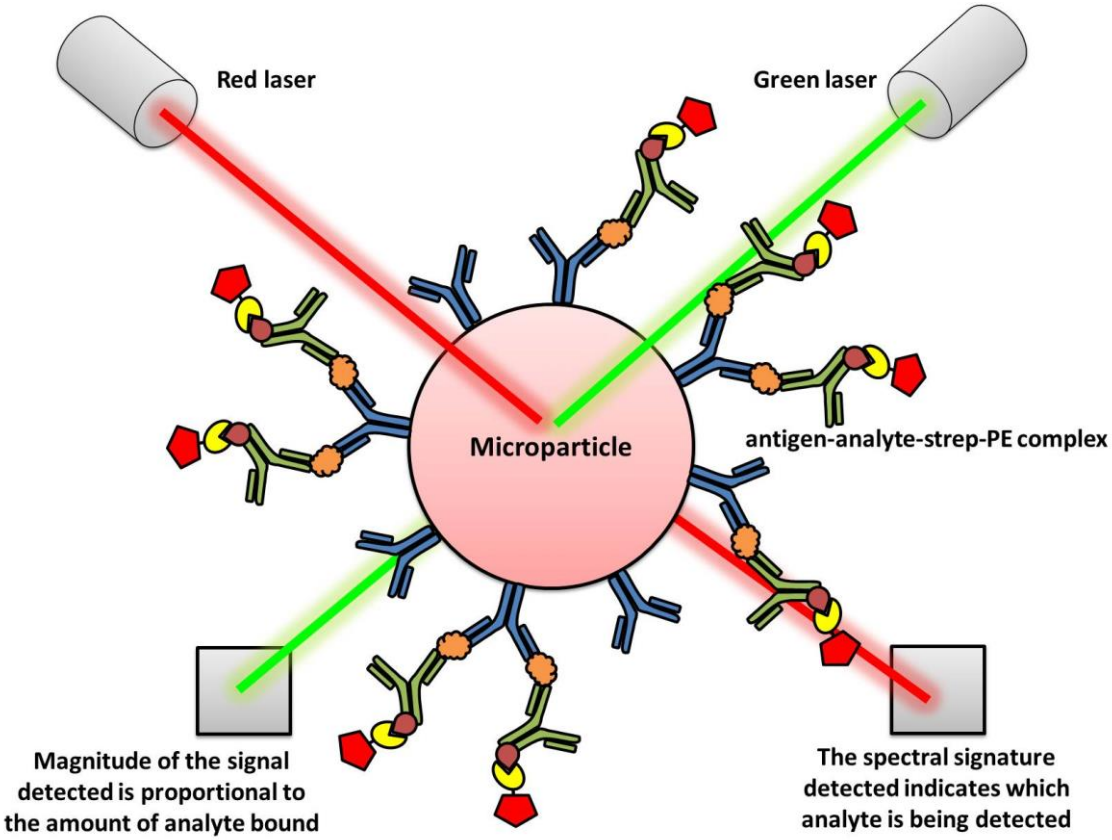

Figure 2.11.2-1 Overview of the Luminex® screening assay.

Colour-coded microparticles are coated in analyte-specific antibodies. If the analyte is present in the sample, antibody-analyte-antibody-strep-PE complexes form on the surface of the microparticle. Inside the Luminex analyser the internal dyes of the microparticle are excited by a red laser, which identifies the microsphere and which analyte is being detected. A green laser excites the reporter dye (PE) which indicates the amount of analyte detected [203, 204].

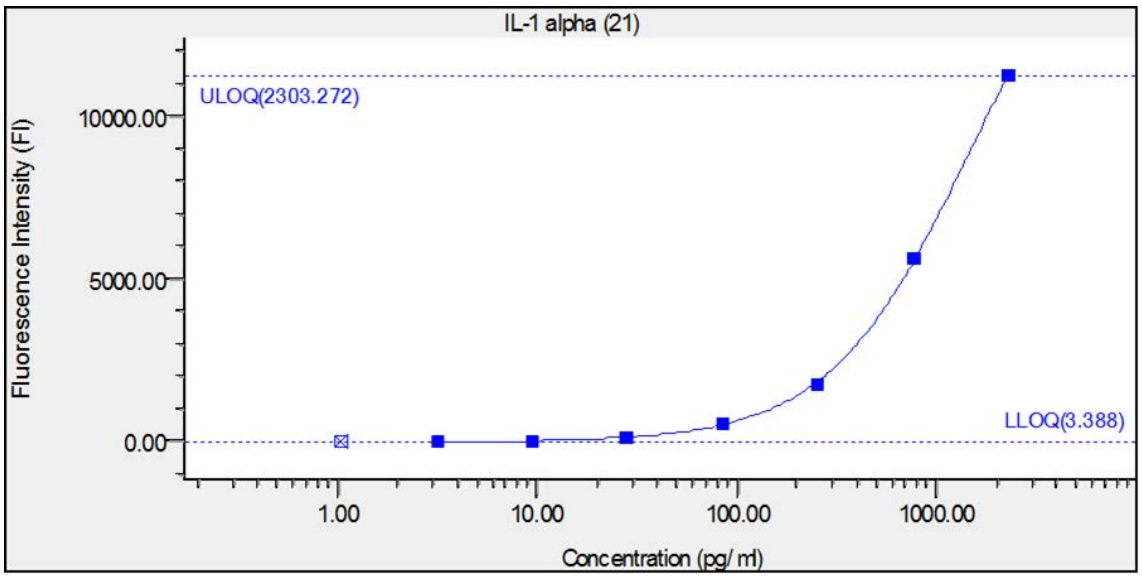

Figure 2.11.2-2 Typical Luminex® screening assay standard curve generated using the Bio-Plex software.

Standard concentrations (x axis) were plotted against the blank corrected mean absorbance at the emission wavelength for PE (580nm) (y-axis). Standard curves were generated using a 5-parameter logistic curve fit. Analyte concentrations in test samples were calculated by comparison to the standard curve generated for each assay.

2.11.3 MSD® human IFN-β assay

Clarified supernatants from the polarised EMTU model were kindly assayed for IFN-β release by Charlene Akoto (Brooke Lab PhD student) using a 96-well multi-array MSD® and a SECTOR® Imager 6000 instrument, according to the manufacturer's instructions [205, 206]. Briefly, plates were washed (3X PBS) and the MSD® plate coated with IFN-β capture antibody. After 1h, the plate was washed (3X PBS) and samples or standards were added along with electrochemiluminescently (SULFO)-tagged detection antibody. Note that samples were run undiluted and in singlicate (due to the reliability and reproducibility observed using MSD® assays), which gave a signal that was within the range of the standards for the majority of the samples (24-100,000 pg/ml).

The plate was then incubated for 1-2h at RT on a shaking platform to allow formation of antibody-analyte-antibody-SULFO-TAG™ complex. To remove any unbound substances, the plate was washed (3X PBS) before addition of the MSD® read buffer, which provides the appropriate chemical environment for electrochemiluminescence. The MSD® plate was analysed using the MSD® SECTOR Imager 6000, which applies a voltage to the electrodes in the base of the plate and induces the electrochemiluminescent (SULFO-TAG™) tags bound to the electrode surface to emit light (Figure 2.11.3-1). The intensity of the emitted light was measured and quantified by comparison to a standard curve, modelled by the software accompanying the plate reader and generated from the known standard concentrations (Figure 2.11.3-2). Note that background signal was corrected for by subtracting the signal from a blank control (well containing diluent instead of sample).

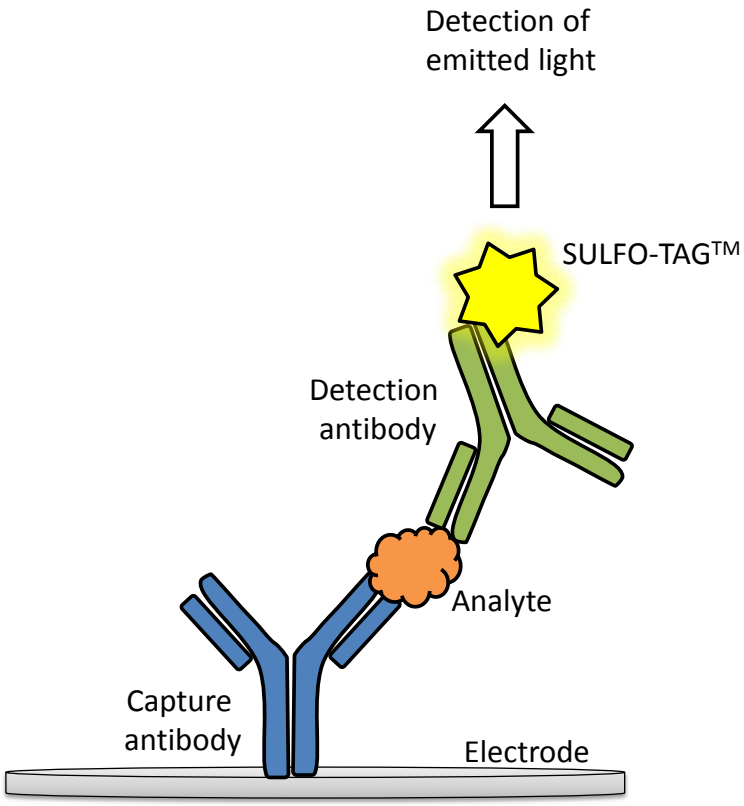

Figure 2.11.3-1 Overview of the MSD® assay.

The MSD® assay uses a sandwich immunoassay format in which the capture antibodies are coated onto electrodes in the base of a 96-well plate. The detection antibodies are tagged with the MSD SULFO-TAG™ which emits light when a voltage is applied to the plate electrodes. Thus, the detection of light indicates the presence of the analyte of interest [205].

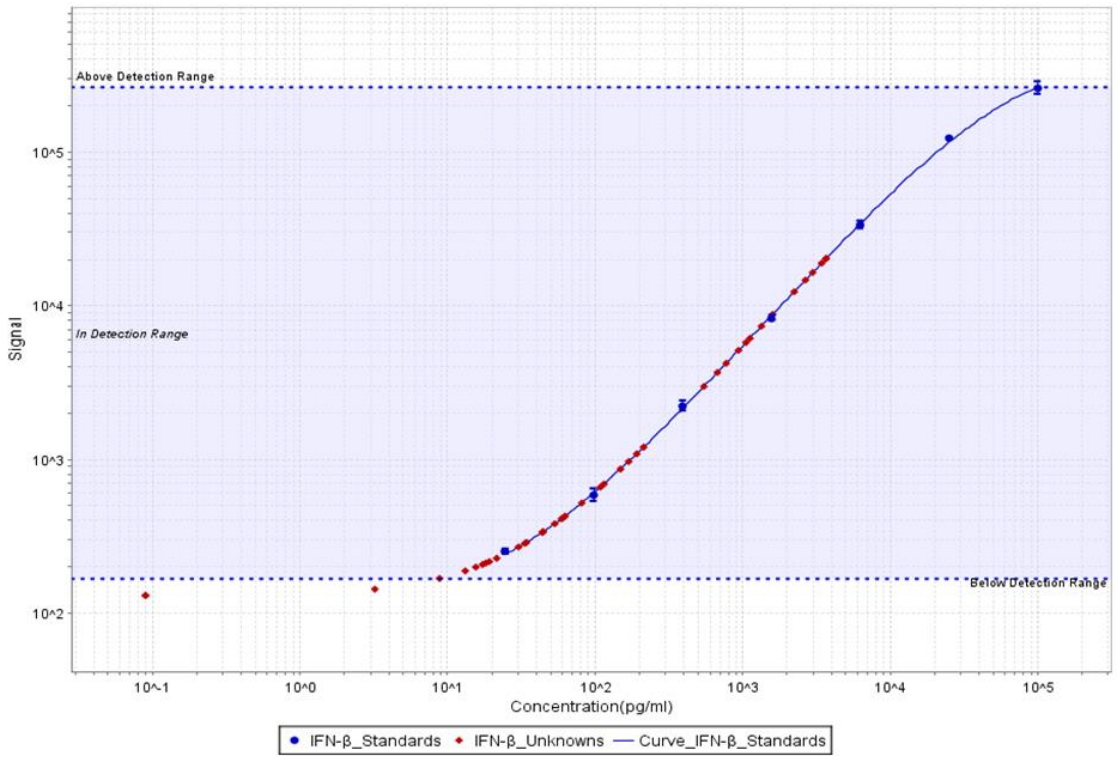

Figure 2.11.3-2 MSD® human IFN-β assay standard curve generated using the SECTOR Imager 6000 software.

Standard concentrations (x axis) were plotted against the blank corrected mean intensity of emitted light (at 640nm) (y-axis). Standard curves were generated using a 4-parameter logistic curve fit. Analyte concentrations in test samples were calculated by comparison to the standard curve generated for each assay.

2.12 Statistics

Data were analysed and graphed using GraphPad Prism version 6 (GraphPad Software, San Diego, CA, USA, www.graphpad.com) and SigmaPlot version 12.5 (Systat Software, Chicago, IL, USA).

Data were assessed for normality of distribution using the Shapiro-Wilk test. Parametric data were expressed as means ± standard deviation (SD). Differences between 2 groups were tested for statistical significance using the Student's t-test. Differences between more than 2 groups were tested for statistical significance by analysis of variance (ANOVA) with Bonferroni correction for multiple comparisons. Where there were 2 or more treatment groups (e.g. control, poly(I:C) and pLArg) in 2 or more categories (e.g. HBEC and fibroblast mono- and co-cultures) differences between groups were tested for statistical significance by two-way ANOVA with Bonferroni correction. Non-parametric data were expressed as medians with 25% and 75% interquartiles, and whiskers representing minimum and maximum values. Differences between groups were tested for statistical significance by the Kruskall-Wallis test with Dunn's correction for multiple comparisons. For all statistical tests $P<0.05$ was considered significant.

3. Modelling the airway EMTU and investigating proinflammatory responses to HRV infection

3.1 Introduction

The structural cells of the conducting airways control the tissue microenvironment and are critical in the maintenance of homeostasis. Central to this is the bronchial epithelium which forms a protective barrier against the external environment, with functions including secretion of a protective layer of mucus, control of paracellular permeability and production of immunomodulatory growth factors and cytokines [1]. Below the epithelium, the attenuated fibroblast sheath directs immune responses and it has been proposed that these cells work together as an EMTU to co-ordinate appropriate responses to environmental stimuli [153].

Evidence of cellular cross-talk has already been demonstrated in simple experiments using epithelial-derived conditioned media or in epithelial-fibroblast co-cultures where fibroblasts respond to epithelial-derived signals to drive inflammatory or remodelling responses. For example in a recent study, CXCL8 release was enhanced in co-cultures of HBECs and fibroblasts compared to equivalent monocultures [161]. This enhancement was due to constitutive IL-1α release from the epithelium, as demonstrated in experiments using epithelial-conditioned medium. In another study using conditioned medium experiments, epithelial-derived IL-1α release was increased following endoplasmic reticulum stress and demonstrated to drive proinflammatory mediator release from human lung fibroblasts (HLFs) [157]. In other studies, scrape-wounding of HBECs induced α-SMA expression in fibroblasts in a co-culture model via TGFβ [162]. While these studies have examined cellular cross-talk at baseline or in response to chemical or mechanical epithelial damage, none have examined the effects of HRV infection of the epithelium on the EMTU.

HRV infects the upper airways and causes symptoms of the common cold in healthy adults but in chronic respiratory diseases such as asthma it is a major cause of viral-induced exacerbations, causing increased lower respiratory tract symptoms [26, 29]. The bronchial epithelium is the major target for HRV

infection and replication [112]. Following *in vitro* stimulation of either monolayer or fully differentiated HBECs with HRV or PAMPs, such as dsRNA, increases in ionic permeability [112, 207] and release of proinflammatory mediators are observed [26, 112, 128, 208]. A critical role for some of these mediators on immune cell activation has been demonstrated following incubation of immune cells with epithelial conditioned medium from virus or dsRNA-treated cultures. For example, HRV-dependent epithelial IL-33 causes Th2 cytokine release from T cells and group 2 innate lymphoid cells [209], while dsRNA-dependent epithelial-derived TSLP promotes CCL17 production from monocyte-derived DCs [210] and Th2 cytokine release from MCs [211].

A key feature of the epithelial barrier is its polarised structure due to the expression of TJ proteins, leading to the vectorial release of mediators. This not only allows establishment of chemotactic gradients, required for immune cell recruitment and retention, but also controls signalling to underlying fibroblasts which orchestrate responses within the local tissue microenvironment. In this chapter I therefore developed polarised HBEC-fibroblast co-culture models of the EMTU using either cell lines or primary cells, that would allow the assessment of vectorial cytokine signalling following delivery of HRV (or dsRNA mimetic) to the apical surface of the epithelium, as occurs *in vivo*.

3.2 Characterisation of responses to dsRNA stimulation in the polarised EMTU model

3.2.1 Establishing the polarised EMTU model

Epithelial (16HBE) cells were seeded in the apical compartment of Transwell®s, while fibroblasts (MRC-5) were seeded on the underside of the Transwell® membrane. After 6 days in co-culture HBECs had formed TJ complexes in the apical compartment (Figure 3.2.1-1A), while a fibroblast network was evident on the underside of the nanoporous membrane in the basolateral compartment (Figure 3.2.1-1B). In addition, co-culture TERs had increased, indicating a reduction in ionic permeability and successful polarisation of the epithelial barrier (Figure 3.2.1-2). Compared to equivalent HBEC monocultures, ionic permeability was significantly lower in the co-culture model from the third day after cell seeding, as measured by an increase in TER (Figure 3.2.1-2). In comparison, in co-cultures where fibroblasts were seeded on to the bottom of the well, TERs were not significantly enhanced compared to HBEC monocultures until the 5th day after cell seeding (Figure 3.2.1-2). These enhancements in TER in co-culture were synergistic, rather than an additive effect of co-culturing the different cells types, as fibroblasts alone were unable to form a functional barrier (Figure 3.2.1-2).

Together these data indicate that the co-culture model is polarised and that fibroblasts support the polarised functions of HBECs with greatest effect when they are in close proximity to the epithelium, on the underside of the Transwell® membrane.

A B

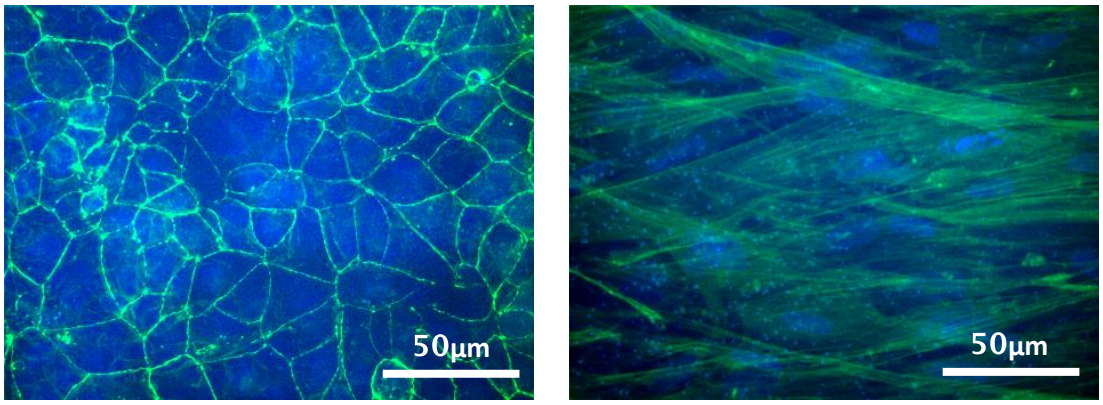

Figure 3.2.1-1 HBECs and fibroblasts in co-culture.

Seven days after cell seeding co-cultures were fixed and HBECs stained for the TJ protein, occludin (green) (A) and fibroblasts stained for α-SMA (green) (B). Cell nuclei were stained with DAPI (blue) (magnification x63, representative of 6 independent experiments).

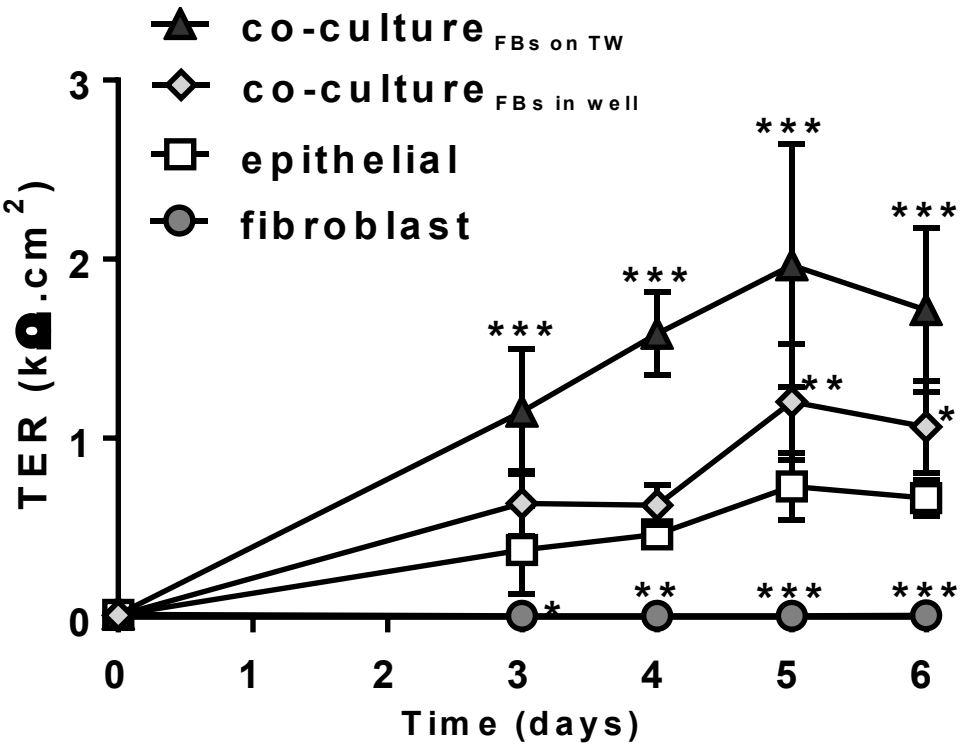

Figure 3.2.1-2 The EMTU co-culture model is polarised and has enhanced epithelial barrier properties compared to HBEC and fibroblast monocultures.

TERs were monitored from day 3-6 after initial cell seeding. = co-culture with fibroblasts (FBs) on the underside of the Transwell® (TW) membrane, = co-culture with FBs in the bottom of the well, = HBEC monoculture, = fibroblast monoculture Results are means ± SD, n=4-7 independent experiments. *$P \leq 0.05$, **$P \leq 0.01$ and ***$P \leq 0.001$ compared to HBEC monoculture (two-way ANOVA with Bonferroni correction).

3.2.2 Optimisation of dsRNA concentrations for stimulation of the polarised EMTU co-culture model

The effects of HRV infection were modelled using the synthetic dsRNA mimetic, poly(I:C). To determine the optimum dsRNA concentration with which to stimulate the EMTU model, concentration response experiments were initially carried out on HBEC monocultures.

Firstly, the effect of dsRNA on the ionic permeability of the epithelium was investigated. HBECs were challenged with increasing concentrations of dsRNA (0.1-10μg/ml) and TER was monitored over 24h (Figure 3.2.2-1A). After 6h there was a trend for reduced TERs in dsRNA-stimulated cultures, which was significant by 24h. In addition, the extent of the reduction in TER was concentration-dependent.

To determine the effects of dsRNA on mediator release, the apical and basolateral supernatants were harvested and assayed for the pleiotropic cytokine IL-6 by ELISA (Figure 3.2.2-1B). DsRNA significantly induced apical IL-6 release at concentrations ≥0.1μg/ml, whereas in the basolateral compartment IL-6 release was only induced at the highest dsRNA concentration tested of 10μg/ml.

To determine the effects of dsRNA on cell viability, HBEC monocultures were visualised by light microscopy 24h post-dsRNA stimulation and no signs of cell death were observed (Figure 3.2.2-2A). However, when the apical and basolateral cell-free supernatants were assayed for the cytosolic enzyme, LDH, a small but significant fold increase in its release was detected following stimulation with 10μg/ml dsRNA (Figure 3.2.2-2B). These data indicate that dsRNA has a small cytotoxic effect at high concentrations.

Therefore for the investigation of responses to dsRNA in the co-culture model, 1μg/ml dsRNA was chosen; a concentration that exhibited significant effects on ionic permeability and cytokine release, with minimal effects on cell viability.

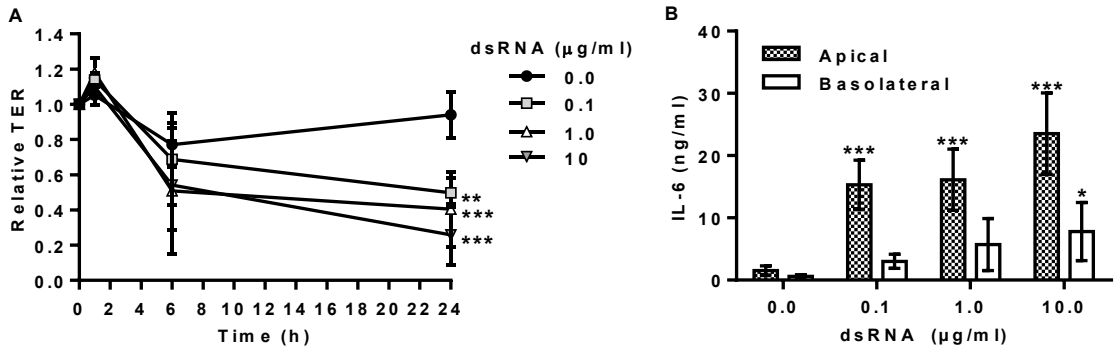

Figure 3.2.2-1 Concentration responses of polarised HBEC monocultures to dsRNA.

Polarised HBEC monocultures were apically challenged with dsRNA (poly(I:C); 0.1-10µg/ml) over 24h. TER was measured at 6 and 24h post-stimulation and expressed as TER relative to the TER value prior to challenge (A). After 24h, apical and basolateral cell-free supernatants were assayed for IL-6 (B). Results are means ± SD, n=3 independent experiments. *$P \leq 0.05$, **$P \leq 0.01$ and ***$P \leq 0.001$ compared to controls (two-way ANOVA with Bonferroni correction).

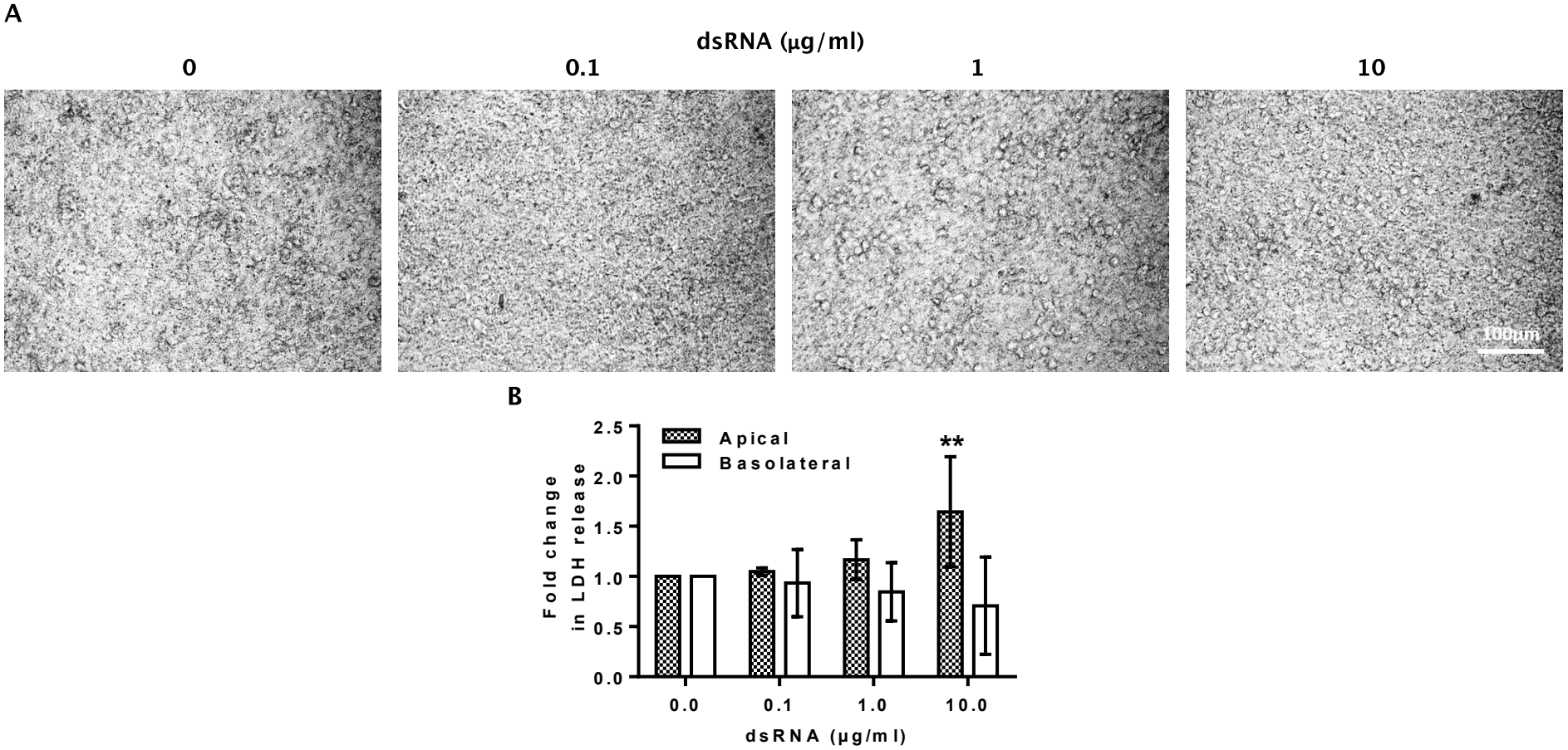

Figure 3.2.2-2 Cytotoxicity of dsRNA.
Polarised HBECs were apically challenged with dsRNA (poly(I:C); 0.1-10µg/ml) and imaged on a light microscope 24h after challenge (A) (magnification x20, representative of 3 independent experiments). Apical and basolateral supernatants were harvested and assayed for LDH release (B). Results are means ± SD, n=4 independent experiments. Differences between untreated controls and stimulated cultures were tested for statistical significance by two-way ANOVA with Bonferroni correction for multiple comparisons and are indicated by $^{**}P \leq 0.01$.

3.2.3 Effects of dsRNA on the epithelial barrier function of the EMTU model

To examine the effects of dsRNA on the EMTU model, dsRNA (1μg/ml) was applied apically following successful polarisation of the epithelium. Similarly to equivalent HBEC monocultures and previous findings in HBEC monocultures [207, 212] (Figure 3.2.3-1A), dsRNA increased the ionic permeability of the EMTU model with a significant decrease in TER by 6h (Figure 3.2.3-1B). However, in contrast with HBEC monocultures, by 24h ionic permeability of the EMTU model had partially recovered and was not significantly different from the control (Figure 3.2.3-1B).

To examine epithelial barrier function further, the macromolecular permeability of the epithelium was determined by measuring diffusion of FITC-dextran from the apical to the basolateral compartment between 21-24h after dsRNA challenge (Figure 3.2.3-2A). In fibroblast monocultures, which do not form TJs, 70-80% FITC-dextran diffusion was observed compared to an empty Transwell®. In contrast, FITC-dextran diffusion was less than 5% of an empty Transwell® in the EMTU co-culture model and was comparable with HBEC monocultures at baseline. In all culture types, dsRNA had no significant effect on macromolecular permeability between 21-24h (Figure 3.2.3-2A).

Macromolecular permeability of the EMTU co-culture model was also assessed between 3-6h following dsRNA challenge (Figure 3.2.3-2B), as ionic permeability was significantly increased at this time point (Figure 3.2.3-2B). Although there was a trend for increased FITC-dextran diffusion 3-6h after dsRNA challenge, this did not reach significance compared to the unstimulated control (Figure 3.2.3-2B). Together these data suggest that even after dsRNA treatment of the EMTU co-culture model, the movement of macromolecules (>4kDa) across the epithelial layer via the paracellular route is restricted, indicating maintenance of polarisation.

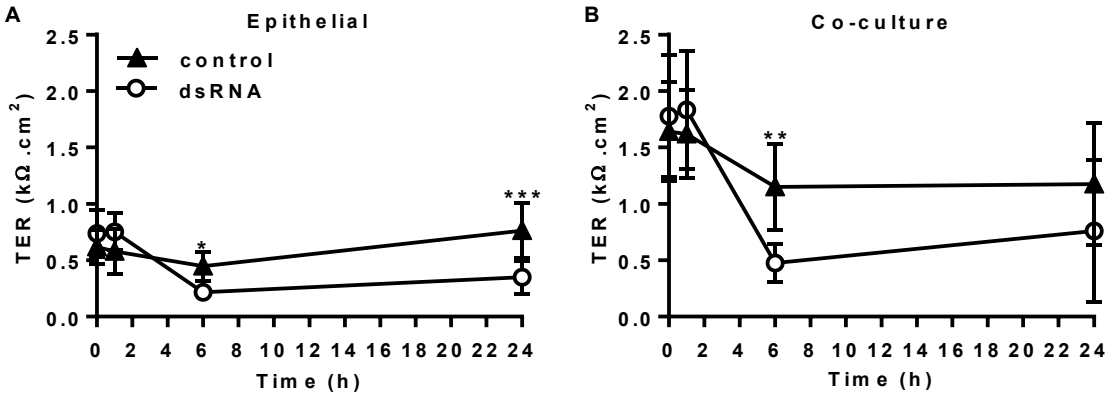

Figure 3.2.3-1 Effect of dsRNA on ionic permeability of the epithelium in HBEC monocultures (A) and the EMTU co-culture model (B).

Cultures were challenged with dsRNA (poly(I:C); 1µg/ml) and ionic permeability determined over 24h by TER measurements. Results are means ± SD, n=7 independent experiments. *$P \leq 0.05$, **$P \leq 0.01$ and ***$P \leq 0.001$ (two-way ANOVA with Bonferroni correction).

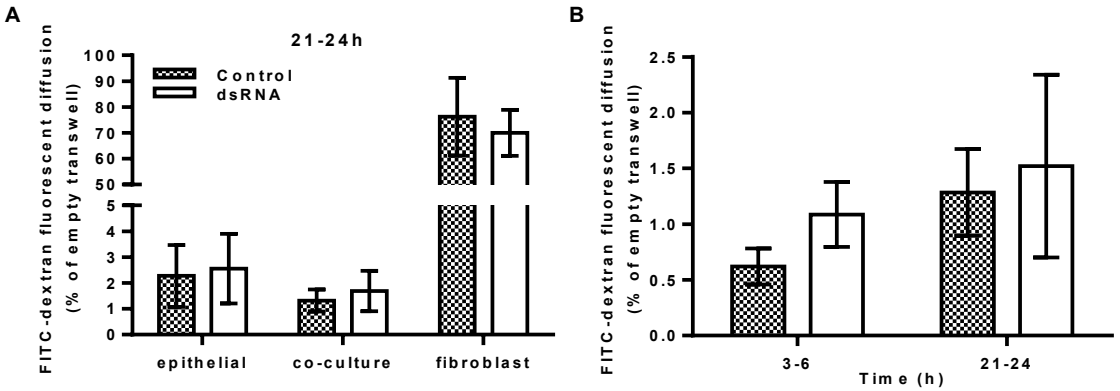

Figure 3.2.3-2 Effect of dsRNA on macromolecular permeability of the epithelium in the EMTU co-culture model.

Cultures were challenged with dsRNA (poly(I:C); 1µg/ml) and macromolecular permeability determined by FITC-dextran diffusion between 21-24h for HBEC and fibroblast mono- and co-cultures (A) and between 3-6h and 21-24h for the EMTU co-culture model. Results are means ± SD, n=3-5 independent experiments.

3.2.4 DsRNA stimulation of the polarised EMTU model activates innate anti-viral and proinflammatory responses

Innate immune responses to dsRNA were assessed within the polarised EMTU model by determining anti-viral and proinflammatory mediator release following apical stimulation with 1μg/ml of dsRNA. Consistent with the restricted movement of macromolecules across the epithelial barrier (section 3.2.3), dsRNA induced polarised mediator release. For example, dsRNA induced the anti-viral mediators IFN-β and IFN-λ (IL-29) in both the apical and basolateral compartments of the polarised EMTU model, with a greater response observed apically (Figure 3.2.4-1). Furthermore, these responses were comparable with HBEC monocultures suggesting that within the polarised EMTU model, IFN-β and IL-29 are predominantly epithelial derived and that their release was not modified by the presence of the underlying fibroblasts.

DsRNA also induced polarised release of proinflammatory mediators in the EMTU co-culture model. In the apical compartment, constitutive and dsRNA-induced levels of IL-6, CXCL8, and CXCL10 were comparable with HBEC monocultures (Figure 3.2.4-2A, B, D). However, in the basolateral compartment of the polarised EMTU model there was a trend for increased constitutive levels of IL-6 and CXCL8 compared to HBEC monocultures (Figure 3.2.4-2E-F). This is consistent with a recent publication using a similar experimental setup, except that fibroblasts were cultured in the bottom of the well rather than the underside of the Transwell® membrane [161]. Following dsRNA stimulation, basolateral IL-6, CXCL8, GM-CSF and CXCL10 release was significantly enhanced in the EMTU model compared to unstimulated controls and dsRNA-stimulated HBEC monocultures (Figure 3.2.4-2E-H). In the absence of HBECs, addition of dsRNA to the apical compartment did not stimulate significant mediator release from fibroblasts attached to the under surface of the Transwell® (Figure 3.2.4-2A-H). These data suggest that the enhanced proinflammatory response in the EMTU model is synergistic, rather than the cumulative effect of challenging the individual cell types and indicates that epithelial-fibroblast cross-talk is occurring within the EMTU model.

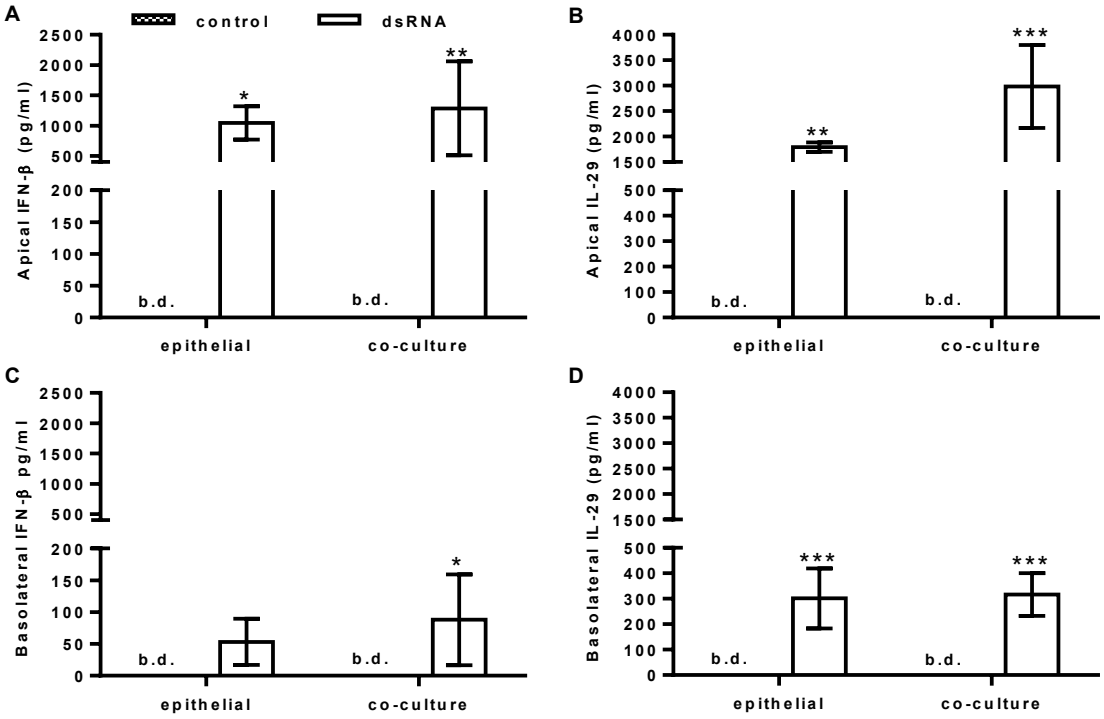

Figure 3.2.4-1 Effect of dsRNA on anti-viral mediator release in the polarised EMTU co-culture model.

Apical (A-B) and basolateral (C-D) cell-free supernatants were harvested from the EMTU co-culture model or HBEC monocultures 24h after challenge with dsRNA (poly(I:C); 1µg/ml) and assayed for IFN-β (A,C) and IL-29 (B,D) by MSD® multiplex assay and ELISA respectively. Results are means ± SD, n=3-5 independent experiments. *$P \leq 0.05$, *$P \leq 0.01$ and ***$P \leq 0.001$ for comparison between control and dsRNA stimulated cultures (two-way ANOVA with Bonferroni correction. b.d. indicates levels below the detection limit of the assay.

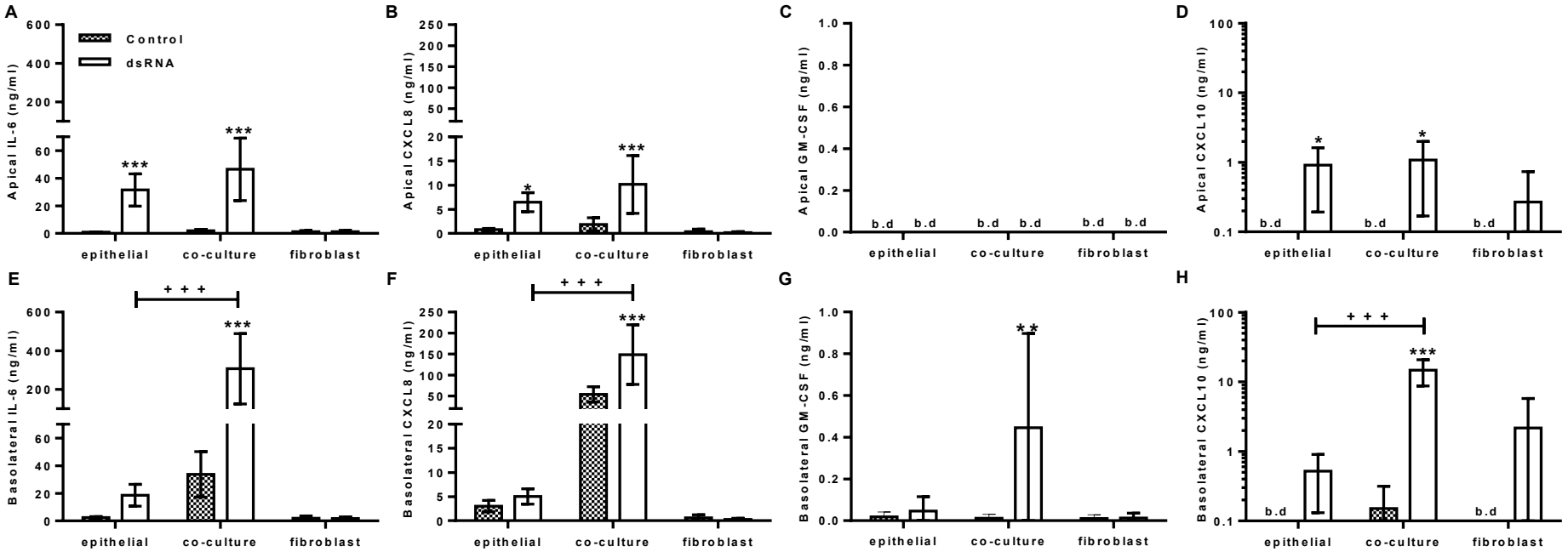

Figure 3.2.4-2 Effect of dsRNA on proinflammatory mediator release in the polarised EMTU co-culture model.
Apical (A-D) and basolateral (E-H) cell-free supernatants were harvested from the EMTU co-culture model or HBEC and fibroblast monocultures 24h after challenge with dsRNA (poly(I:C); 1µg/ml) and assayed for IL-6 (A,E), CXCL8 (BF), GM-CSF (C,G) and CXCL10 (D,H) by ELISA. Results are means ± SD, n=3-5 independent experiments. *$P \leq 0.05$, *$P \leq 0.01$ and ***$P \leq 0.001$ for comparison between control and dsRNA stimulated cultures and $^{+++}P \leq 0.001$ for comparison with HBEC monocultures and EMTU co-culture model (two-way ANOVA with Bonferroni correction). b.d. indicates levels below the detection limit of the assay.

3.3 Epithelial-fibroblast cross-talk in response to dsRNA stimulation of the polarised EMTU model

3.3.1 dsRNA stimulation of the polarised EMTU model induces IL-1α release

The synergistic enhancement in basolateral proinflammatory responses to dsRNA suggested that epithelial-fibroblast cross-talk was occurring within the EMTU model. IL-1 has previously been shown to drive autocrine proinflammatory mediator release in monocultures of non-polarised HBECs [208] or fibroblasts [157], as well as regulate constitutive proinflammatory mediator release in unstimulated HBEC-fibroblast co-cultures [161]. Therefore I hypothesised that IL-1 was an important mediator of cellular cross-talk and was responsible for augmenting dsRNA-induced proinflammatory responses within the EMTU model.

Release of IL-1α and IL-1β by dsRNA- and un-stimulated HBEC and fibroblast mono- and co-cultures was determined by Luminex® assay. The polarity of IL-1α release was mainly into the apical compartment, where it was significantly increased following dsRNA stimulation and comparable between HBEC monocultures and the polarised EMTU model (Figure 3.3.1-1A). Basolateral IL-1α concentrations were at least 10 times lower than those observed apically and there was a trend for its reduction in the polarised EMTU model compared to HBEC monocultures (Figure 3.3.1-1B). This is in contrast to the other proinflammatory cytokines measured, which were enhanced in the basolateral compartment of the polarised EMTU model (Figure 3.2.4-2E-H).

IL-1α was not detected in fibroblast monocultures, suggesting that HBECs are the primary source of IL-1α within the EMTU model (Figure 3.3.1-1). Consistent with these data, intracellular IL-1α could be detected in lysates from HBECs (Figure 3.3.1-2) but was below the limit of detection in lysates from fibroblast monocultures (data not shown, n=1). In addition, intracellular

IL-1α was significantly increased in HBEC monocultures following dsRNA stimulation (Figure 3.3.1-2). These intracellular levels of IL-1α were significantly higher than the total (apical and basolateral) levels of extracellular IL-1α ($P \leq 0.05$) (Figure 3.3.1-2).

In contrast to IL-1α, IL-1β levels were below or close to the detection limit of the assay in unstimulated and dsRNA-stimulated HBEC and fibroblast mono- and co-cultures. Together these data demonstrate that dsRNA-stimulation of the EMTU model induces polarised IL-1 release from the epithelium, of which IL-1α is the predominant isoform.

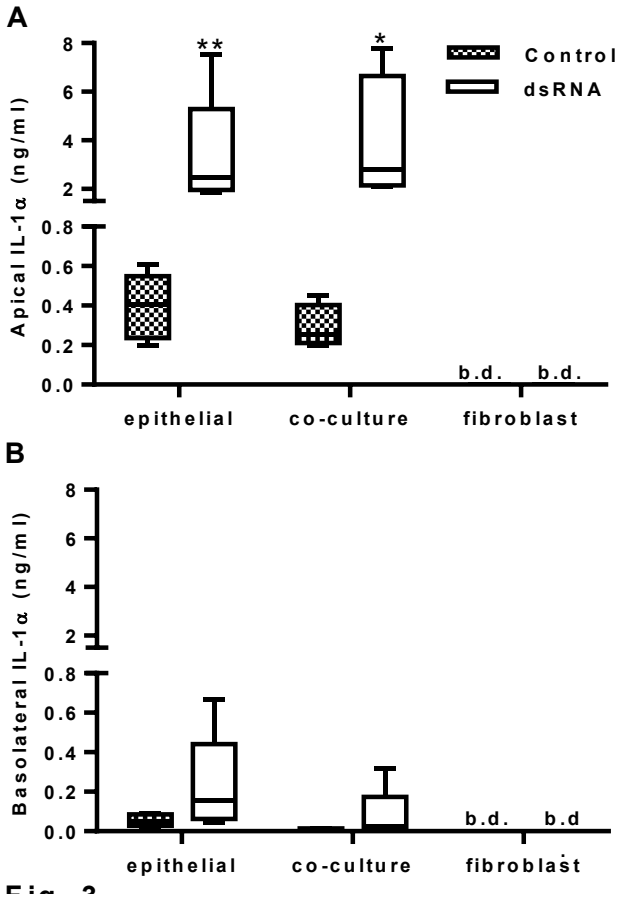

Figure 3.3.1-1 Comparison of IL-1α release from dsRNA-stimulated HBEC and fibroblast monocultures and the polarised EMTU co-culture model.

Apical (A) and basolateral (B) cell-free supernatants were harvested 24h after challenge with dsRNA (poly(I:C); 1µg/ml) and assayed for IL-1α and IL-1β by Luminex®. Results for IL-1α release are shown as box plots representing the median with 25% and 75% interquartiles, and whiskers representing minimum and maximum values, n=3-5 independent experiments. *$P \leq 0.05$, **$P \leq 0.01$ for comparison between control and dsRNA-stimulated cultures (Mann-Whitney U test). b.d. indicates levels below the detection limit of the assay. IL-1β was below the level of detection of the assay.

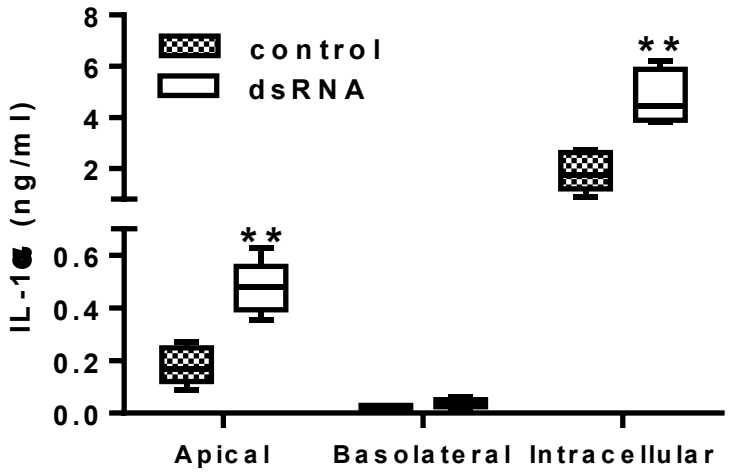

Figure 3.3.1-2 Effect of dsRNA on extracellular and intracellular IL-1α in HBEC monocultures.

Cell-free supernatants from HBEC monocultures and HBEC cell lysates (lysed by 3 cycles of freeze/thaw) were harvested 24h after challenge with dsRNA (poly(I:C);1µg/ml) and assayed for IL-1α by ELISA. Results are shown as box plots representing the median with 25% and 75% interquartiles, and whiskers representing minimum and maximum values, n=5 independent experiments. $^{**}P \leq 0.01$ for comparison between control and dsRNA stimulated cultures (Mann-Whitney U test).

3.3.2 Antagonism of IL-1 signalling inhibits a subset of dsRNA-induced proinflammatory mediator release

The importance of IL-1 signalling within the apical and basolateral compartments was examined by addition of IL-1Ra to either the apical, basolateral or both compartments of the polarised EMTU model. In unstimulated cultures, IL-1Ra caused a small decrease in constitutive proinflammatory mediator release which was significant for IL-6 and CXCL8 (Figure 3.3.2-1).

In dsRNA-stimulated co-cultures, pre-incubation with 500ng/ml of IL-1Ra significantly reduced dsRNA-induced IL-6, CXCL8 and GM-CSF release (Figure 3.3.2-2). For apical cytokine release, IL-1Ra only partially reduced dsRNA-dependent IL-6 and CXCL8 release and was most effective when added apically or to both compartments (Figure 3.3.2-2 A-B). For basolateral cytokine release, IL-1Ra had the greatest effect when added basolaterally or to both compartments with complete abrogation of dsRNA-dependent IL-6, CXCL8 and GM-CSF (Figure 3.3.2-2 E-G). The partial inhibitory effect of IL-1Ra in the opposing compartment could be explained by low levels of IL-1Ra diffusion since, in the basolateral compartment of the polarised EMTU model, a small but significant increase in IL-1Ra could be detected when exogenous IL-1Ra was added apically (Figure 3.3.2-3). While these levels were relatively low (*ca.* 1000X less than the 500ng/ml exogenous IL-1Ra added to the apical compartment), they would still be enough to compete with IL-1α secreted into the basolateral compartment. The effect of IL-1Ra on the opposing compartment is therefore mainly due to leakage of IL-1Ra between compartments, rather than cellular cross-talk.

In contrast to the other mediators measured, neither apical or basolateral dsRNA-induced CXCL10 release was significantly affected by IL-1Ra. Since IL-1β could not be detected, these data suggest that epithelial-derived IL-1α is absolutely required to drive a significant subset of dsRNA-induced proinflammatory responses within the polarised EMTU model.

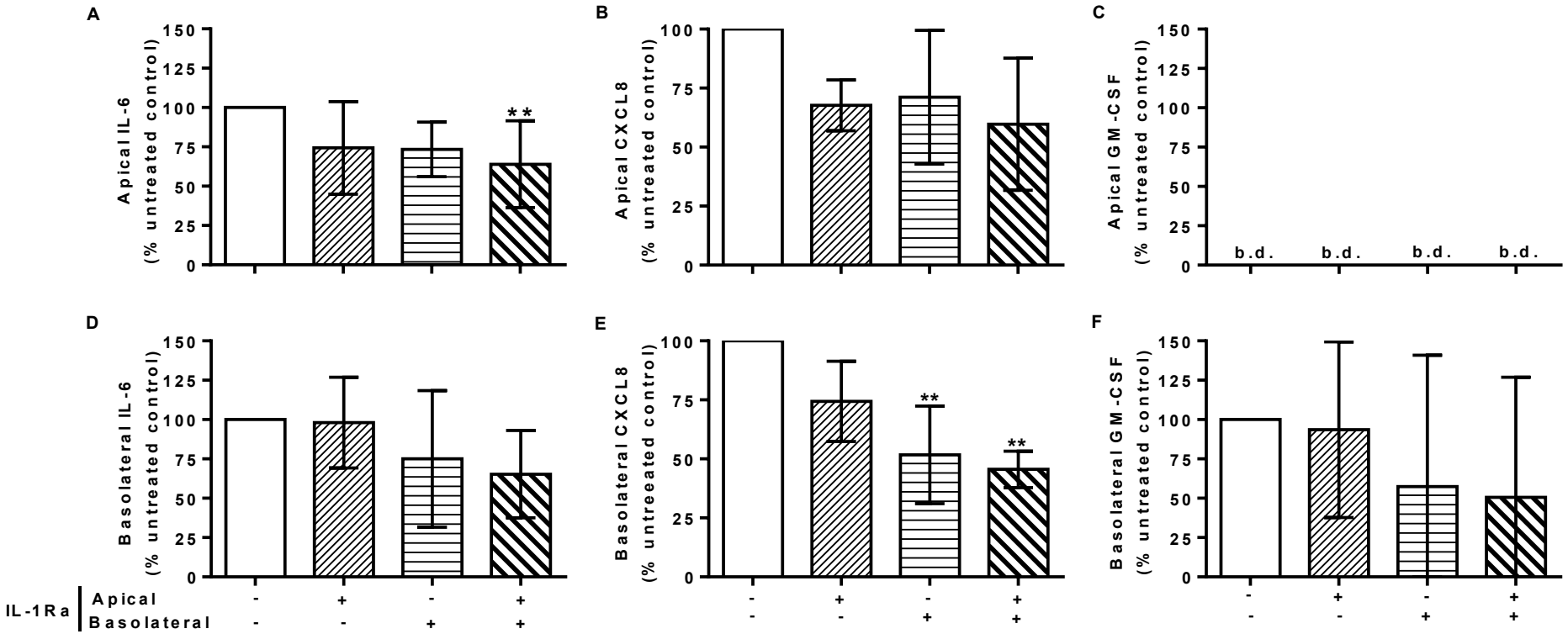

Figure 3.3.2-1 Effect of IL-1Ra on constitutive cytokine release in the polarised EMTU co-culture model.

HBEC and fibroblast co-cultures were treated with IL-1Ra (500ng/ml) either apically, basolaterally or in combination for 25h before harvesting apical (A-C) and basolateral (D-F) cell-free supernatants for detection of IL-6 (A, D), CXCL8 (B, E) and GM-CSF (C, F) by ELISA. The effects of IL-1Ra were expressed as a % of untreated control for each experiment (see Appendix A, Table A1 for raw data). Results are means ± SD, n=3-6 independent experiments. $^{**}P \leq 0.01$ compared to untreated controls (one-way ANOVA with Bonferroni correction).

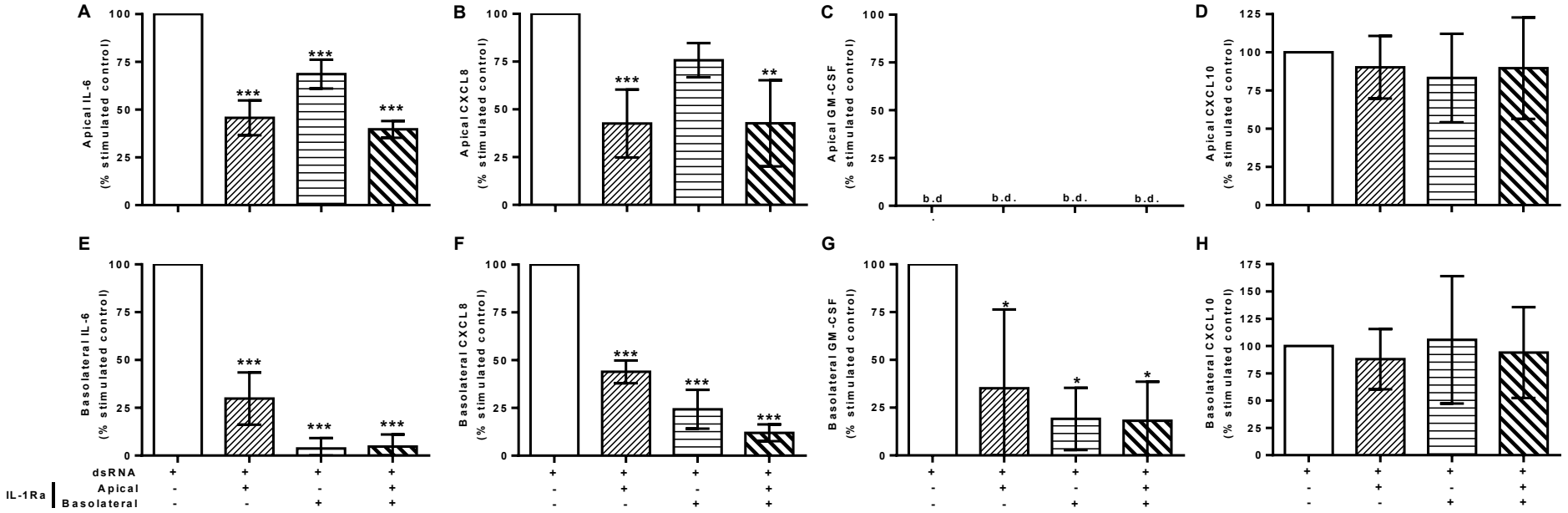

Figure 3.3.2-2 The effect of IL-1R antagonism on dsRNA-induced cytokine and chemokine release in the polarised EMTU co-culture model. The EMTU co-culture model was cultured in the absence or presence of IL-1Ra (500ng/ml) applied either apically, basolaterally or both for 1h prior to stimulation with dsRNA (poly(I:C); 1µg/ml). Apical (A-D) and basolateral (E-H) cell-free supernatants were harvested 24h after stimulation and assayed for IL-6 (A, E), CXCL8 (B, F), GM-CSF (C, G) and CXCL10 (D, H) by ELISA. To investigate the effects of IL-1Ra on dsRNA-dependent responses, control mediator levels were subtracted from stimulated levels and expressed as a percentage of the response to dsRNA (see Appendix A, Table A1 for raw data). Results are mean responses compared to the dsRNA-induced response in the absence of IL-1Ra (100%) ± SD, n=3-6 independent experiments. $^{**}P \leq 0.01$, $^{***}P \leq 0.001$ for comparison between dsRNA-stimulated cultures in the absence or presence of IL-1Ra (one-way ANOVA with Bonferroni correction).

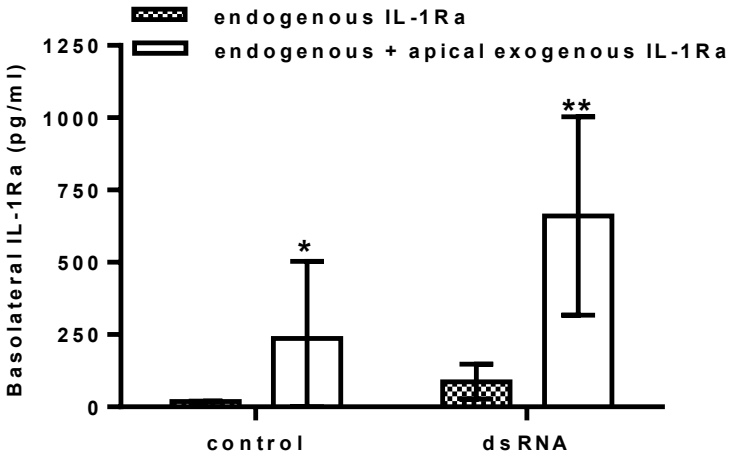

Figure 3.3.2-3 Macromolecular flux of exogenous IL-1Ra from the apical to basolateral compartments in unstimulated and dsRNA-stimulated co-cultures. Exogenous IL-1Ra (500ng/ml) was added to the apical compartment of the polarised EMTU model and incubated for 1h prior to stimulation with dsRNA (poly(I:C); 1µg/ml). Basolateral cell-free supernatants were harvested after 24h for detection of IL-1Ra by Luminex® assay. Results are means ± SD, n=3 independent experiments. *$P \leq 0.05$, **$P \leq 0.01$ comparing cultures with and without exogenous IL-1Ra in the apical compartment (two-way ANOVA with Bonferroni correction).

3.3.3 Fibroblasts are the main responders to IL-1α in the polarised EMTU model.

To investigate the direct effect of IL-1α on the different cell types, HBEC and fibroblast monocultures were seeded onto the upper or lower surface of Transwells® respectively, and then directly stimulated with IL-1α at concentrations similar to those measured apically or basolaterally following dsRNA challenge (See Figure 3.3.3-1). In fibroblast monocultures IL-1α significantly induced IL-6 (>100-fold) and CXCL8 (>200-fold) release (Figure 3.3.3-1 A-B). In contrast, HBECs were unresponsive to the concentrations of IL-1α used, but exhibited a typical response to dsRNA stimulation with IL-6 and CXCL8 release (Figure 3.3.3-1 A-B). These data suggest that within the polarised EMTU model, fibroblasts are the main responders to dsRNA-induced IL-1α.

In section 3.3.2, it was shown that blocking IL-1 signalling with IL-1Ra had no effect on dsRNA-induced CXCL10 within the EMTU co-culture model. It was therefore surprising that stimulation of fibroblast monocultures with IL-1α induced significant CXCL10 release (Figure 3.3.3-2). As observed in Figure 3.3.3-1, HBEC monocultures were unresponsive to IL-1α, but exhibited a typical CXCL10 response to dsRNA stimulation (3.3.2Figure 3.3.3-2B).

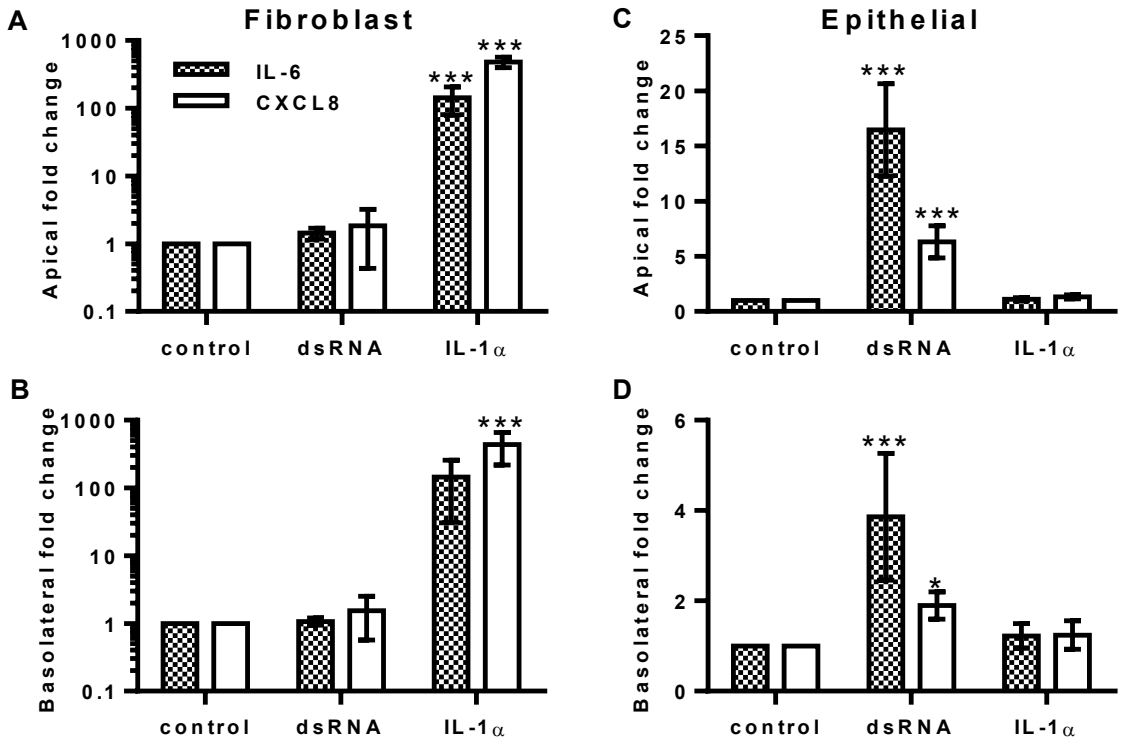

Figure 3.3.3-1 Effect of IL-1α stimulation on IL-6 and CXCL8 release from fibroblast and HBEC monocultures.

Fibroblast (A-B) and HBEC (C-D) monocultures were stimulated with IL-1α (10ng/ml apically, 1ng/ml basolaterally) or with dsRNA (poly(I:C); 1µg/ml) as a positive control. After 24h, cell-free supernatants were assayed for IL-6 and CXCL8 by ELISA. Fold change in mediator release compared to the unstimulated control was calculated for each experiment (See Appendix A, Table A2 for raw data). Results are mean fold changes ± SD, n=4-5 independent experiments. *$P \leq 0.05$, ***$P \leq 0.001$ compared to untreated control (two-way ANOVA with Bonferroni correction).

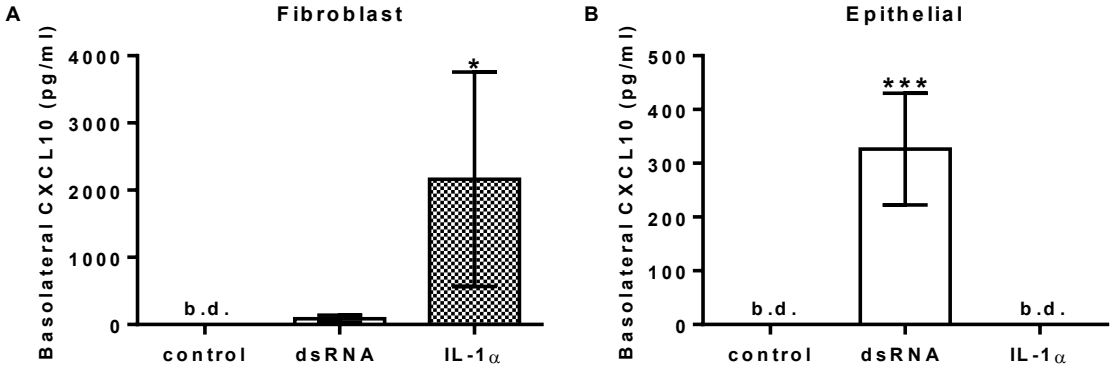

Figure 3.3.3-2 Effect of IL-1α stimulation on CXCL10 release from fibroblast and HBEC monocultures.

Fibroblast (A) and HBEC (B) monocultures were stimulated with IL-1α (10ng/ml apically, 1ng/ml basolaterally) or with dsRNA (poly(I:C); 1µg/ml) as a positive control. After 24h, basolateral cell-free supernatants were assayed for CXCL10 by ELISA. Results are means ± SD, n=4-5 independent experiments. *$P \leq 0.05$, ***$P \leq 0.001$ compared to untreated control (two-way ANOVA with Bonferroni correction). b.d. indicates levels below the detection limit of the assay.

3.3.4 DsRNA-induced IFNs mediate the CXCL10 response within the polarised EMTU model

In section 3.3.2, IL-1Ra was shown to have no effect on dsRNA-dependent CXCL10 responses within the polarised EMTU model. Previous publications have demonstrated that IFNs induce CXCL10 release in primary HBEC [213, 214] and fibroblast monocultures [215]. Since dsRNA-dependent IFN release was detected in the polarised EMTU model (section 3.2.4), I hypothesised that dsRNA-induced IFNs are important mediators of cellular cross-talk and are responsible for augmenting the CXCL10 response in the polarised EMTU model. The importance of IFN signalling was examined by pre-incubation of the polarised EMTU model with neutralising antibody to chain 2 of the IFNα/β (IFN type 1) receptor (IFNAR2). In anti-IFNAR2 antibody-treated cultures, a trend for a partial reduction in dsRNA-dependent CXCL10 release was observed (Figure 3.3.4-1). This reduction was most pronounced in the basolateral compartment. These data suggest that epithelial-derived type I IFNs are important mediators of dsRNA-induced CXCL10 responses within the polarised EMTU model.

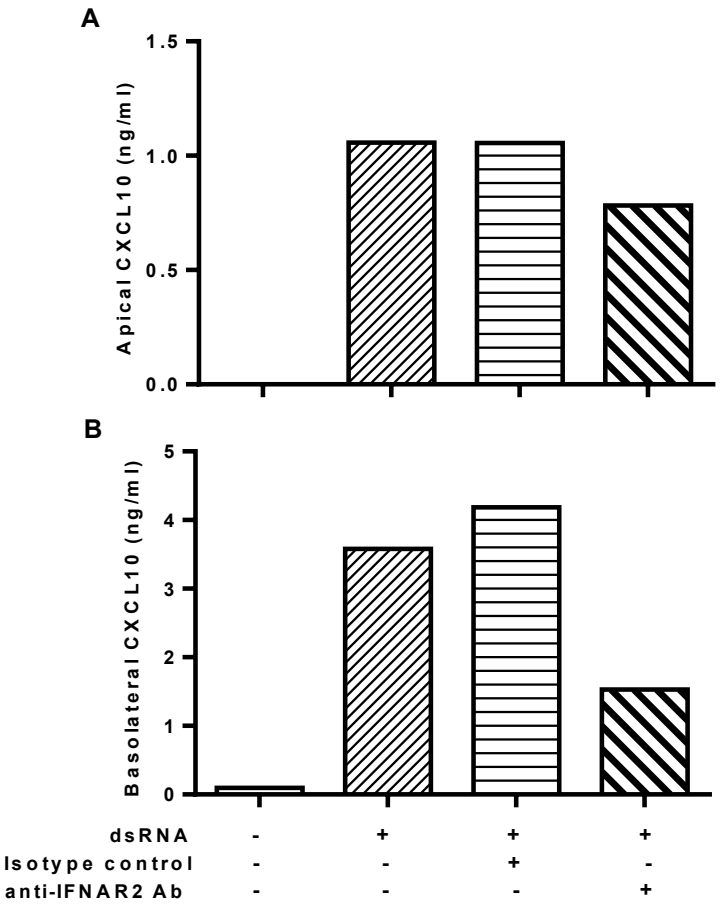

Figure 3.3.4-1 The effect of anti-IFNAR2 antibody on dsRNA-induced CXCL10 release in the polarised EMTU model.

The EMTU co-culture model was cultured in the absence or presence of anti-IFNAR2 antibody (1µg/ml), apically and basolaterally for 1h prior to stimulation with dsRNA (poly(I:C); 1µg/ml). Apical (A) and basolateral (B) cell-free supernatants were harvested 24h after stimulation and assayed for CXCL10 by ELISA. Results are means, n=2 independent experiments.

3.3.5 Fluticasone propionate inhibits dsRNA-induced IL-1α release in the polarised EMTU model

Corticosteroids are the most effective anti-inflammatory therapy for asthma and are the first-line treatment for adults and children with persistent asthma. However, they have limited benefit in treating acute asthma exacerbations induced by respiratory viruses [38, 39]. I was therefore interested to determine whether induction of IL-1 by dsRNA in the polarised EMTU model was steroid responsive. The polarised EMTU model was pre-incubated with 10nM of fluticasone-propionate (FP); a concentration previously shown to inhibit dsRNA-induced CXCL8 release in 16HBE monolayers [216]. In the apical compartment, FP reduced dsRNA-dependent IL-1α to control levels (Figure 3.3.5-1A). A similar effect was also observed in the basolateral compartment, where dsRNA-dependent IL-1α release was reduced to below the detection limit of the assay in the presence of FP (Figure 3.3.5-1B). Together these data suggest that dsRNA-dependent IL-1α is steroid responsive and that steroid treatments for asthma may inhibit IL-1 driven responses during viral-induced exacerbations.

The effect of FP on the antiviral response following dsRNA stimulation was also examined by detection of the IFN-inducible chemokine CXCL10. In contrast to IL-1α, FP had little effect on dsRNA-induced CXCL10 release in the apical compartment (Figure 3.3.5-1C). However, in the basolateral compartment dsRNA-induced CXCL10 release was reduced by approximately 50% in the presence of FP (Figure 3.3.5-1D). These data suggest that steroid treatments for asthma may also partially inhibit CXCL10 responses during viral-induced exacerbations.

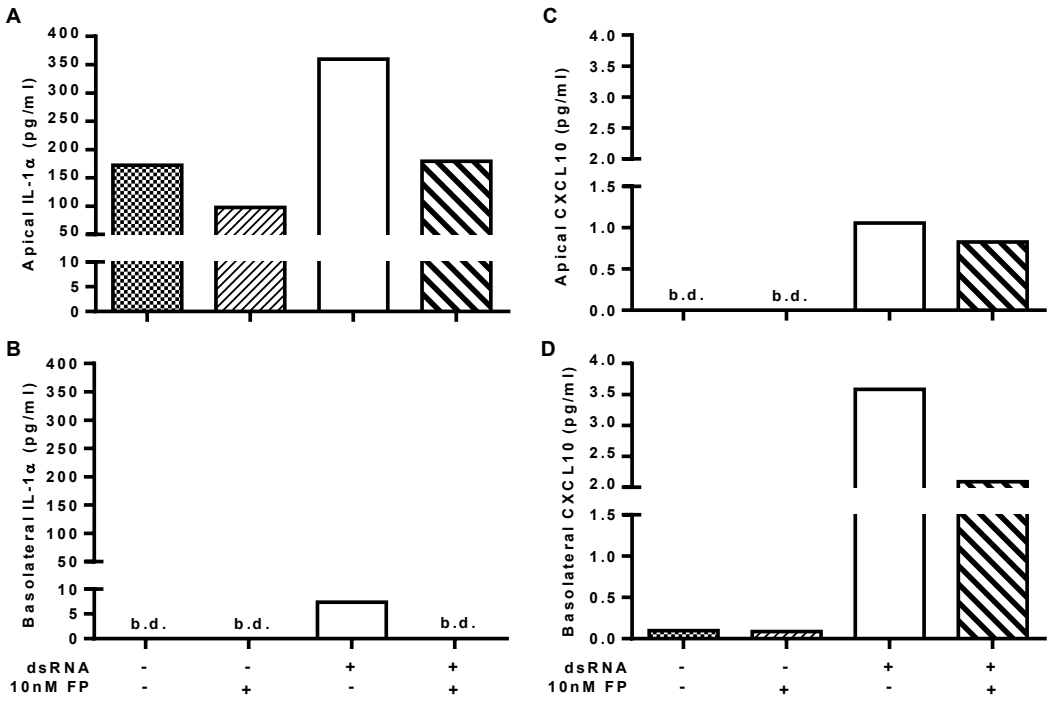

Figure 3.3.5-1 The effect of FP on dsRNA-induced IL-1α (A-B) and CXCL10 (C-D) release in the polarised EMTU co-culture model.

The EMTU co-culture model was cultured in the absence or presence of FP (10nM) applied apically and basolaterally for 1h prior to stimulation with dsRNA (poly(I:C); 1µg/ml). Apical and basolateral cell-free supernatants were harvested 24h after stimulation and assayed for IL-1α (A-B) and CXCL10 (C, D) by ELISA. Results are means (n=1 for IL-1α, n=2 independent experiments for CXCL10).

3.4 Role for IL-1α in mediating HRV16-induced inflammatory responses in a primary EMTU model

3.4.1 HRV16 infection induces IL-1α in primary HBECs differentiated at ALI

To determine whether observations using the polarised EMTU model could be translated to a more complex model, responses of fully differentiated primary HBEC monocultures to HRV16 infection were initially examined. Similarly to the dsRNA-challenged polarised EMTU model and HBEC monocultures, HRV16 infection induced IL-1α release from HBEC ALIs, which was higher in the apical compared to the basolateral compartment (Figure 3.4.1-1). IL-1α was also detected intracellularly and was significantly increased following HRV16 infection. Of note, the amount of intracellular IL-1α production was 50-100X greater than that detected extracellularly following HRV infection.

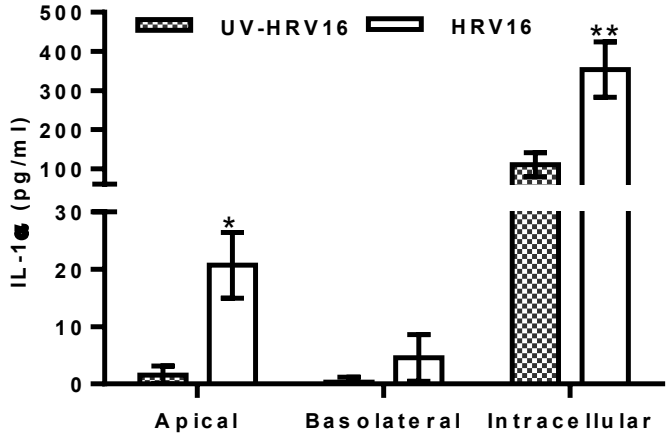

Figure 3.4.1-1 Increased extracellular and intracellular IL-1α release from primary HBEC ALI monocultures infected with HRV16.

ALI monocultures were infected apically with HRV16 (MOI=2) or UV-HRV16 as a negative control. After 24h, apical and basolateral supernatants were removed and the remaining cells went through 3 cycles of freeze/thaw before cell-free supernatants were assayed for IL-1α by ELISA. Results are means ± SD, n=5 different donors. *$P \leq 0.05$, **$P \leq 0.01$ compared to UV-HRV16 control (ANOVA with Bonferroni correction).

3.4.2 Effect of HRV16 infection on HBECs differentiated at ALI and cultured with fibroblasts

I next evaluated responses in the primary EMTU model where primary HBECs differentiated at ALI were cultured with fibroblasts and apically infected with HRV16. Similar to the dsRNA-stimulated polarised EMTU model and previous findings in ALI monocultures [112, 207, 217], HRV16 significantly reduced the ionic permeability of ALI monocultures (from 491±98 to 255±45Ω.cm^2) (Figure 3.4.2-1A) and the primary EMTU model (from 538±148 to 288±16Ω.cm^2) as measured by TER (Figure 3.4.2-1B).

Due to the limited availability of primary HBECs, paracellular permeability studies were not performed on the primary differentiated EMTU model. However, consistent with the maintenance of polarised functions, HRV16 induced polarised proinflammatory mediator release in the primary EMTU model and ALI monocultures. For example, while HRV16 induced basolateral IL-6 release (Figure 3.4.2-2A) in ALI monocultures and the primary EMTU model, it was below the limit of the detection in the apical compartment (data not shown). In addition, similar to the dsRNA-stimulated polarised EMTU model, HRV16-induced IL-6 release was synergistically enhanced in the basolateral compartment of the primary EMTU model compared to ALI monocultures (Figure 3.4.2-2A). HRV16 also induced CXCL8 and CXCL10 release in the primary EMTU model (Figure 3.4.2-2B-C). However, in contrast to the polarised EMTU model, these mediators were not synergistically enhanced compared to ALI monocultures. CXCL10 levels have previously been demonstrated to positively correlate with viral replication [218]. In accordance with this, an absence of replicating virus was confirmed in the UV-irradiated controls, by $TCID_{50}$ assay (Figure 3.4.2-3). In addition, viral replication and release did not differ significantly between ALI monocultures and the primary EMTU model. These data suggest that the HRV16-induced enhancement in IL-6 release in the primary EMTU model is not due to a difference in viral replication compared to ALI monocultures but could be due to epithelial-fibroblast cross-talk mediated by IL-1.

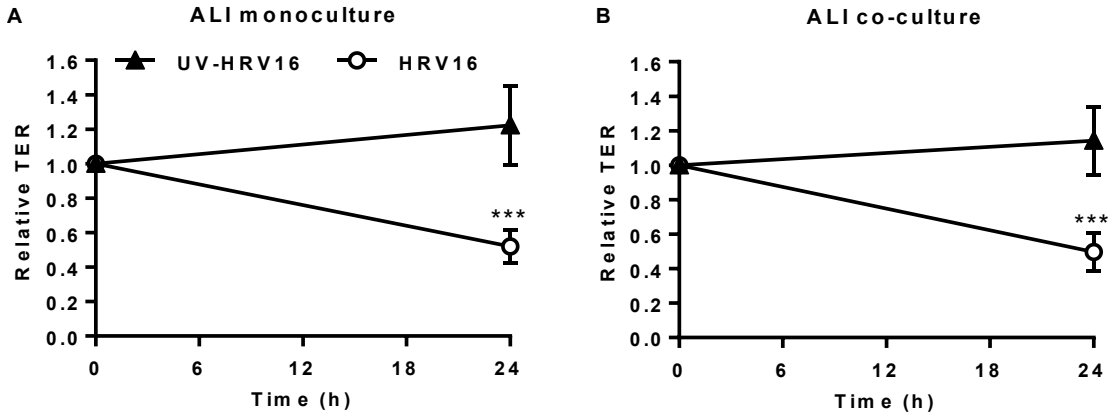

Figure 3.4.2-1 Effect of HRV16 on ionic permeability of the epithelium in primary differentiated ALI monocultures (A) and the primary EMTU co-culture model (B).

ALI mono- or co-cultures with fibroblasts were infected apically with HRV16 (MOI=2) or UV-HRV16 as a negative control and ionic permeability determined after 24h by TER measurements. Results are mean TERs relative to the TER value prior to infection ± SD, from 3 independent experiments using one epithelial cell donor. ***$P \leq 0.001$ compared to UV-HRV16 control (two-way ANOVA with Bonferroni correction).

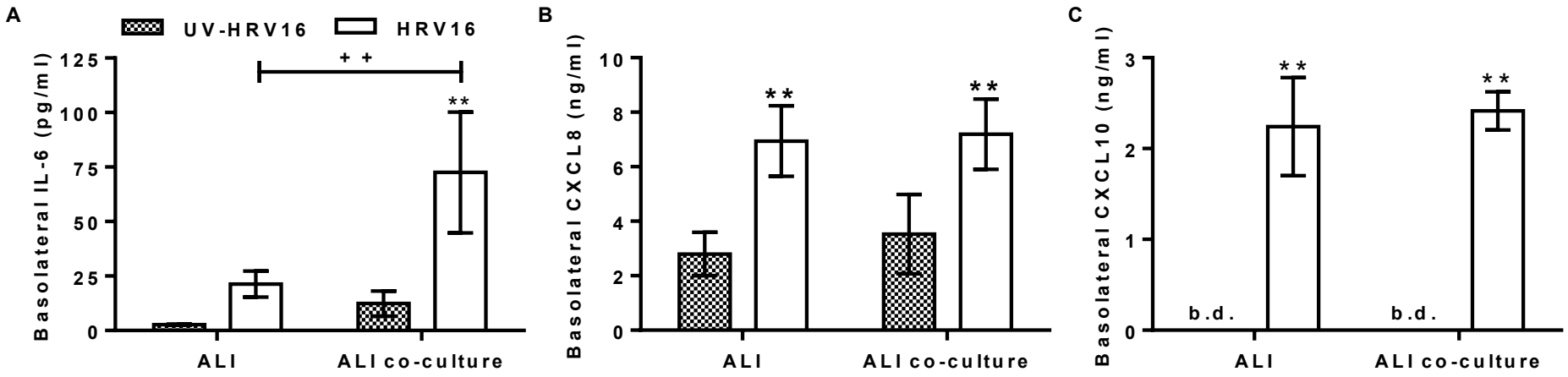

Figure 3.4.2-2 Cytokine and chemokine responses of primary HBEC ALI monocultures and the primary EMTU model to HRV16 infection.

ALI mono- or co-cultures with fibroblasts were infected apically with HRV16 (MOI=2) or UV-HRV16 as a negative control. After 24h, basolateral cell-free supernatants were assayed for IL-6 (A), CXCL8 (B) and CXCL10 (C) by ELISA. Results are means ± SD, 3 independent experiments from one epithelial cell donor and are representative of 3 donors. $^{**}P \leq 0.01$, compared to UV-HRV16 control and $^{++}P \leq 0.01$ comparing HRV16-treated mono- and co-cultures (two-way ANOVA with Bonferroni correction). b.d. indicates levels below the detection limit of the assay.

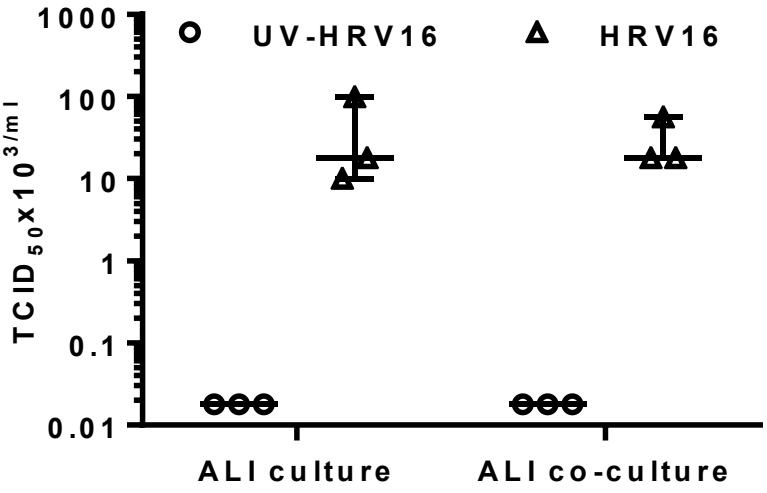

Figure 3.4.2-3 HRV16 virion release was not modified in the primary EMTU model compared to ALI monocultures.

ALI mono- or co-cultures with fibroblasts were infected apically with HRV16 (MOI=2) or UV-HRV16 as a negative control. After 24h, cell-free supernatants were assayed for virion release by $TCID_{50}$ assay. Results are medians ± range, 3 independent experiments from one epithelial cell donor.

3.4.3 Role for IL-1α in mediating inflammatory responses to HRV16 in the primary EMTU model

Similarly to the polarised EMTU model exposed to dsRNA and HRV16-infected ALI monocultures, HRV16 infection of the primary EMTU model induced polarised IL-1α release (Figure 3.4.3-1). While levels of IL-1α were lower than those detected in the dsRNA-stimulated polarised EMTU model, the polarity of IL-1α release followed a similar pattern with the majority of IL-1α released apically; IL-1β release was below the limit of detection.

The importance of IL-1 in driving proinflammatory responses was confirmed in the primary EMTU model by blocking IL-1 signalling using IL-1Ra. This significantly reduced basolateral HRV16-dependent IL-6 and CXCL8 release (Figure 3.4.3-2A-B) to levels comparable to the non-replicating UV-irradiated HRV control, while CXCL10 release was only modestly reduced (Figure 3.4.3-2C). These reductions were not due to an inhibitory effect of IL-1Ra on viral replication, as determined by $TCID_{50}$ assay (Figure 3.4.3-3) Together these data demonstrate an essential role for IL-1α in mediating proinflammatory signalling following viral infection of primary differentiated epithelium in co-culture with fibroblasts.

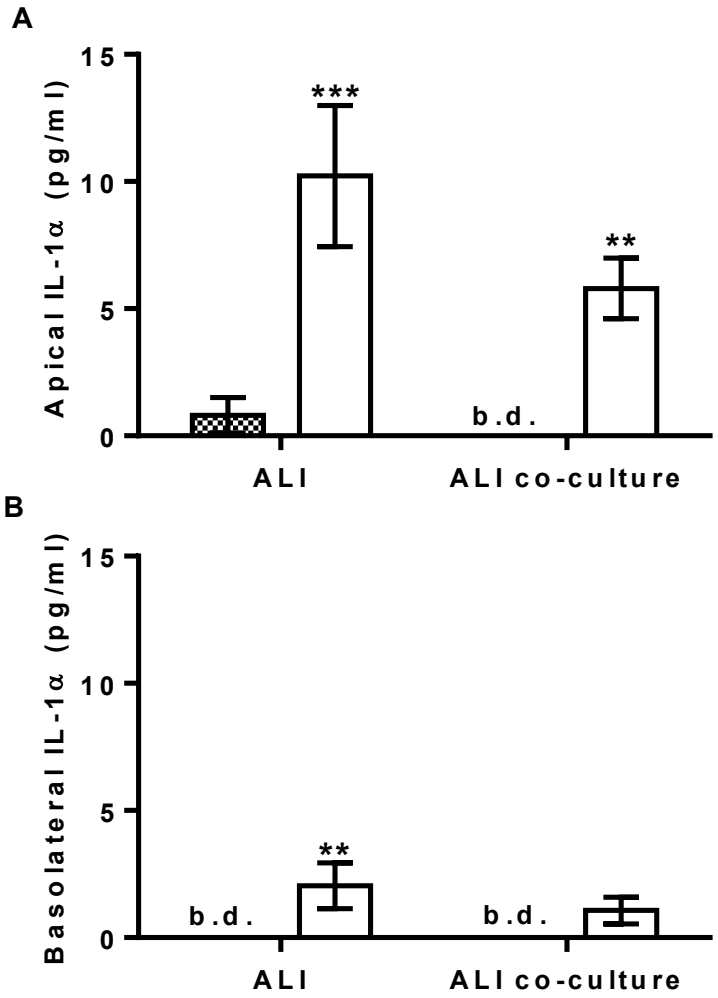

Figure 3.4.3-1 Increased IL-1α release from HRV16-infected epithelial ALI monocultures and the primary EMTU model.

ALI mono- and co-cultures with fibroblasts were infected apically with HRV16 (MOI=2) or UV-HRV16 as a negative control. After 24h, apical (A) and basolateral (B) cell-free supernatants were analysed for IL-1α by Luminex® assay. Results are means ± SD, 3 independent experiments from one epithelial cell donor. $^{**}P \leq 0.01$, $^{***}P \leq 0.01$ for comparison of UV-HRV16 and HRV16-infected cultures (two-way ANOVA with Bonferroni correction). b.d. indicates levels below the detection limit of the assay.

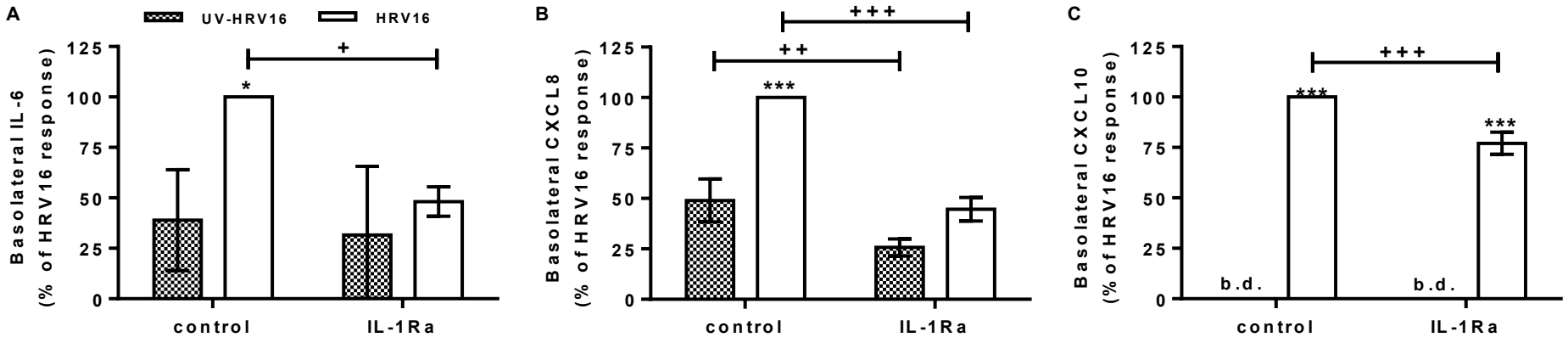

Figure 3.4.3-2 Effect of IL-1Ra on HRV16-induced proinflammatory responses in the primary EMTU co-culture model.

Co-cultures were treated with IL-1Ra (500ng/ml) basolaterally for 1h prior to HRV16 (MOI=2) or UV-HRV16 infection as a negative control. After 24h, cell-free supernatants were assayed for IL-6 (A), CXCL8 (B), and CXCL10 (C) by ELISA. To examine the effect of IL-1Ra on HRV16-induced cytokine release, cytokine levels are expressed as % of HRV16-induced control response (100%). Results are means ± SD, n=3 separate epithelial cell donors (see Appendix A, Table A3 for raw data for each donor). ***P≤0.001 compared to UV-HRV16 control and $^{+}P \leq 0.05$, $^{++}P \leq 0.01$ or $^{+++}P \leq 0.001$ comparing control and IL-1Ra-treated cultures (two-way ANOVA with Bonferroni correction). b.d. indicates levels below the detection limit of the assay.

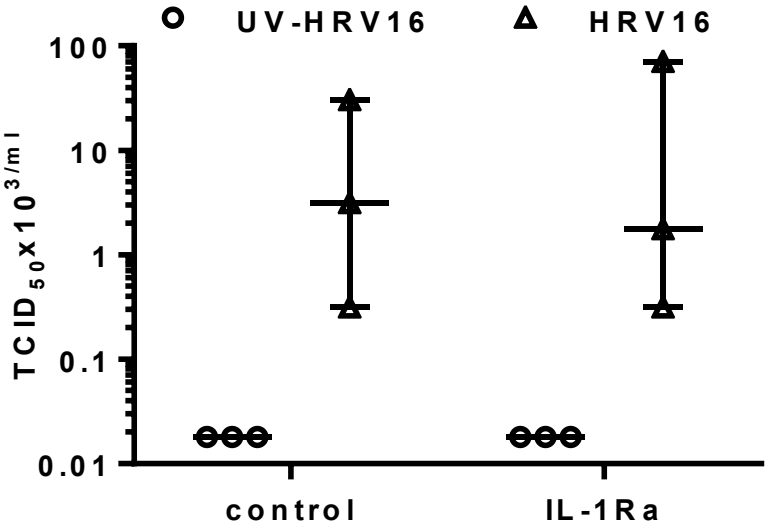

Figure 3.4.3-3 IL-1Ra had no effect on HRV16 virion release in the primary EMTU model.

ALI co-cultures with fibroblasts were infected apically with HRV16 (MOI=2) or UV-HRV16 as a negative control. After 24h, cell-free supernatants were assayed for virion release by $TCID_{50}$ assay. Results are medians ± range, n= 3 separate epithelial cell donors.

3.4.4 Comparison of HRV16-induced IL-1 between ALI monocultures from non-asthmatic and severe asthmatic donors

In chronic inflammatory diseases, such as asthma, viral-induced IL-1α release could potentially contribute to inflammation and disease exacerbation. To determine whether epithelial IL-1α release is altered in disease, intracellular and extracellular levels of IL-1α were compared between ALI cultures from non-asthmatic and severe asthmatic donors. In severe asthmatic donors, apical HRV16-induced IL-1α release did not reach statistical significance compared to UV-HRV16 controls, in contrast with non-asthmatic ALI cultures. In addition, apical HRV16-induced IL-1α release was more variable in ALIs from severe asthmatic donors compared to non-asthmatic donors (Figure 3.4.4-1A). For example, in severe asthmatic ALI cultures the HRV16-induced IL-1 response was enhanced for one donor while there was a trend for a reduced response in the remaining donors compared to non-asthmatic ALI cultures. A trend for a reduction in HRV16-induced IL-1α was also observed in the basolateral compartment (Figure 3.4.4-1B). Intracellularly, there was a trend for reduced HRV16-induced IL-1α in severe asthmatic donors which did not reach significance compared to UV-HRV16 controls, in contrast with non-asthmatic ALI cultures (Figure 3.4.3-2)..

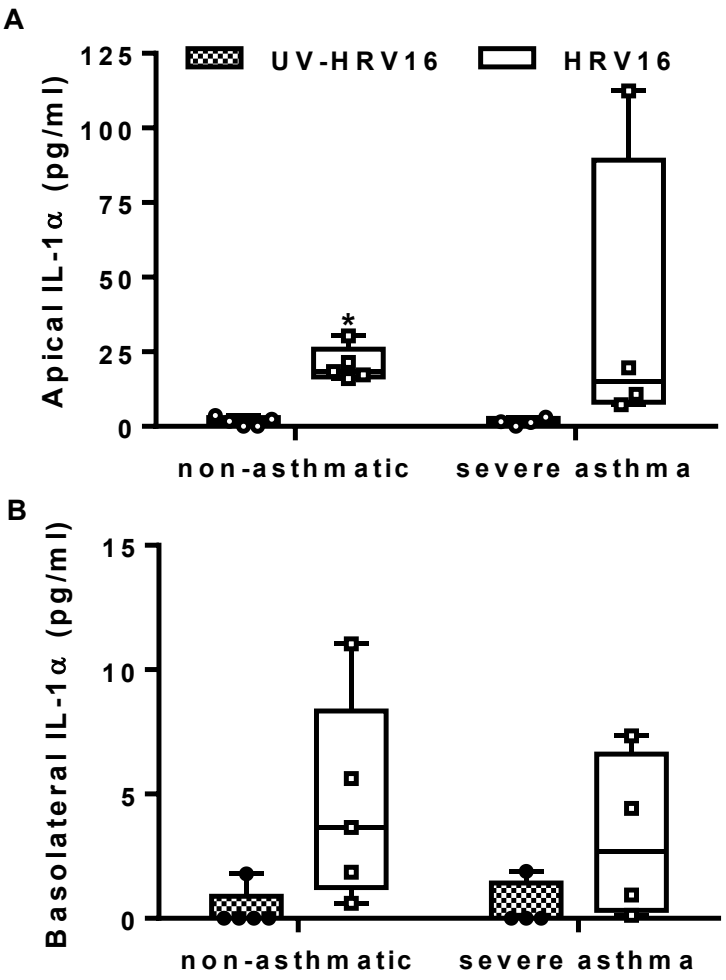

Figure 3.4.4-1 Comparison of IL-1α release from non-asthmatic and severe asthmatic primary HBEC ALI cultures infected with HRV16.

ALI monocultures were infected apically with HRV16 (MOI=2) or UV-HRV16 as a negative control. After 24h, apical and basolateral supernatants were removed and cell-free supernatants were assayed for IL-1α by ELISA. Results are shown as box plots representing the median with 25% and 75% interquartiles, and whiskers representing minimum and maximum values, n=4-5 different donors. *P≤0.05, compared to UV-HRV16 control (Kruskall-Wallis test with Dunn's correction).

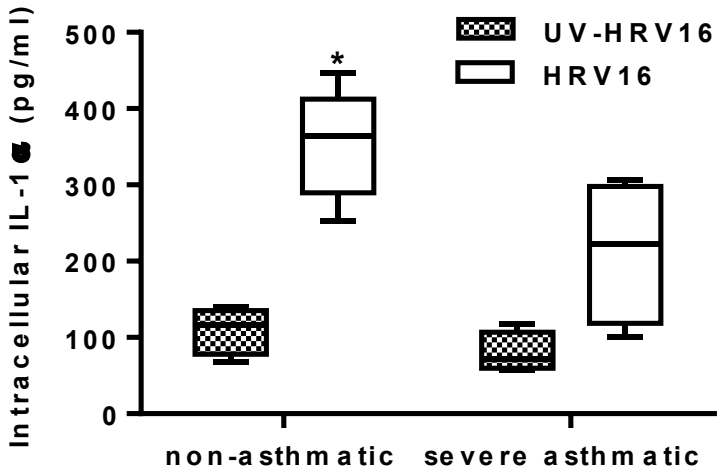

Figure 3.4.4-2 Comparison of intracellular IL-1α in non-asthmatic and severe asthmatic primary HBEC ALI cultures infected with HRV16.

ALI monocultures were infected apically with HRV16 (MOI=2) or UV-HRV16 as a negative control. After 24h, apical and basolateral supernatants were removed, fresh media added and cells lysed by 3 cycles of freeze/thaw before cell-free supernatants were assayed for IL-1α by ELISA. Results are shown as box plots representing the median with 25% and 75% interquartiles, and whiskers representing minimum and maximum values, n=4-5 different donors. *$P \leq 0.05$, compared to UV-HRV16 control and (Kruskall-Wallis test with Dunn's correction).

3.5 Discussion

3.5.1 Epithelial barrier function

Organisation of cells within the tissue architecture is vital for normal function, and this is particularly evident in the airway mucosa where epithelial cells form polarised sheets that cover the mucosal surface to provide a selective permeability barrier to the inhaled environment. The epithelial structure is supported by a basement membrane together with an attenuated sheath of flattened fibroblasts lying against the *lamina reticularis* of the basement membrane. Together these structures act as a coordinated unit, the EMTU, to control tissue homeostasis [153]. In this chapter, I modelled the EMTU using either polarised layers of immortalised 16HBE cells or fully differentiated primary HBECs grown on the upper surface of Transwell® membrane. To bring the fibroblasts into close proximity with the epithelium, they were seeded on the under surface of the Transwell® membrane. Evidence of cell-cell cross talk was immediately evident, as the presence of the fibroblasts decreased the ionic permeability of the epithelium compared with epithelial cells alone. A similar effect on ionic permeability was also observed in co-cultures where fibroblasts were seeded in the bottom of the well as opposed to the bottom of the Transwell®. This suggests that the enhancement in epithelial barrier function in the co-culture model is due to the release of soluble factors by the fibroblasts. These factors may reach higher localised concentrations when the cells are in closer proximity, explaining why the effect of co-culture on TER was more pronounced when fibroblasts were on the underside of the Transwell® as opposed to the bottom of the well. Similar enhancements in barrier function have previously been observed in co-cultures of MRC5 fibroblasts and the Calu-3 epithelial cell line on electrospun polymers [219, 220], and co-cultures of Wi-38 fibroblasts and HBECs [221]. Fibroblasts are also known to support other aspects of epithelial function; for example HLF feeder layers promote primary HBEC proliferation and differentiation [222, 223] through release of growth factors including HGF [154, 155].

Polarised epithelial functions are essential for development of chemotactic gradients for immune cell trafficking and/or retention during the immune

response to infection. The effect of viral stimulation on epithelial barrier function was therefore assessed in the polarised EMTU model. While dsRNA transiently increased ionic permeability of the polarised EMTU co-culture model, paracellular permeability was not significantly affected, contrasting with previous publications which demonstrated both increased ionic and macromolecular permeability following viral stimulation of 16HBE monocultures [112, 207, 212, 217]. This discrepancy may be due to methodological differences in terms of the stimulus and the way in which macromolecular permeability was assessed. For example Sajjan *et al*. used replicating HRV as opposed to dsRNA [112], while in another study a higher dsRNA concentration (5μg/ml) was used to assess FITC-dextran diffusion [212]. In other studies using HRV and dsRNA, macromolecular permeability was assessed by bacterial transmigration assay [207, 217] or by diffusion of sodium fluorescein [212]. Furthermore, none of these studies examined the effect of dsRNA in co-culture. My data using the co-culture model suggests that diffusion of macromolecules such as cytokines and chemokines is restricted, even following challenge. This ensures maintenance of polarised functions which are essential for development of chemotactic gradients and may be important for immune cell retention or trafficking into the airway lumen in response to infection.

3.5.2 Synergistic responses within the EMTU model

Consistent with the absence of any effects of viral stimulation on paracellular permeability, apical challenge of the epithelium with HRV or dsRNA resulted in polarised inflammatory mediator release.

While dsRNA-induced mediator release was mainly apical in HBEC monocultures, in the EMTU model the polarisation of release was altered due to an enhancement in basolateral mediator release. This enhancement was synergistic as it was greater than the combined response of epithelial and fibroblast monocultures, the latter of which did not respond to dsRNA treatment. The lack of fibroblast response is in line with a previous publication in which dsRNA did not induce IL-6 release from fibroblasts [224], but contrasts to a previous study by Bedke *et al*., where fibroblast monocultures were responsive to HRV and UV-irradiated virus in terms of IL-6 and CXCL8 release [225]. This suggests that the mechanism of viral-induced

proinflammatory mediator release in fibroblasts does not require viral dsRNA and could explain the lack of fibroblast response to dsRNA in my study. Alternatively the lack of fibroblast response may be due to the relatively low concentrations of dsRNA used, which also had restricted access to the fibroblasts due to the presence of the Transwell® membrane.

The synergistic enhancement in the basolateral compartment of the EMTU models suggests a co-ordinated response to viral infection. This enhancement was observed for dsRNA-induced IL-6, CXCL8 and CXCL10 in the polarised EMTU model, while only IL-6 was enhanced in the HRV16-infected primary EMTU models (the reasons for which will be discussed in section 3.5.3). In addition, the magnitude of the viral-induced IL-6 response was less robust in the primary EMTU model compared to the polarised model. This may be due to the use of HRV instead of dsRNA. For a response to HRV, the virus first needs to infect HBECs and replicate to generate dsRNA, in contrast with the bolus treatment with exogenously added dsRNA. Furthermore, the fully differentiated HBEC cultures have a protective mucus layer which may reduce accessibility of the epithelial surface to the virus and, even if HRV reaches the cell surface, differentiated HBECs are less susceptible to infection than basal cells [146]. Irrespective of the differences in the magnitude of response, synergistic enhancements in basolateral mediator release in both models suggest cross-talk between HBECs and fibroblasts following viral infection. This is consistent with a recent study, where influenza virus infection enhanced mediator release in alveolar epithelial cell and fibroblast co-cultures, however polarised responses were not examined [226]. My data adds to this study and is the first to demonstrate a synergistic enhancement in basolateral responses to virus in a co-culture model of the EMTU. As discussed in section 3.5.1 polarised responses are important for developing chemotactic gradients which may be required for activation fibroblast responses. The ability of fibroblasts to respond to and amplify signals from a virally-infected epithelium reflects their role as sentinels of the immune system [153, 227, 228]. For example, fibroblast chemokine release has been demonstrated to regulate DC trafficking in the lung [228] and may be important for retaining immune cells at the site of injury or infection.

3.5.3 Role for IL-1α in the viral-induced proinflammatory response

In the EMTU models I determined a key role for epithelial-derived IL-1α in mediating cellular cross-talk and amplifying innate immune responses following viral stimulation. IL-1α is constitutively expressed in the cytoplasm of cells as a 31kDa precursor (pro-IL-1α) which is cleaved via membrane-bound calpain [229] to release mature IL-1α (17kDa) following necrotic cell death where it is fully active and acts as an alarmin [230, 231]. In this context, IL-1 amplifies local innate and adaptive immunity by rapidly initiating a cascade of inflammatory cytokines and chemokines that promote sterile inflammation. Active IL-1 secretion can also occur in the absence of necrotic cell death [157, 161] and has been shown to contribute to host defences against pathogens [208, 232]. While there was no evidence of dsRNA-induced epithelial cell death in the co-culture model, approximately 10% cell death was observed in HRV-infected ALI cultures (data not shown) [233]. However an upregulation of intracellular IL-1α in HBECs following exposure to HRV or dsRNA was observed, suggesting intracellular IL-1α protein is induced by viral challenge and may be actively released, as reported previously [208]. It was concluded that the viral-induced IL-1α was epithelial-derived since it was detected equivalently in HBEC mono- and co-cultures but not in fibroblast monocultures or fibroblast cell lysates. This is consistent with immunohistochemical staining of bronchial tissue showing that the epithelium is a major site of IL-1α expression [157], with localization towards the apical surface of the epithelium.

The polarised nature of the models allowed the investigation of apical and basolateral IL-1 signalling by the addition of IL-1Ra. Although both IL-1α and IL-1β can be inhibited by the use of IL-1Ra [194], in my system it is likely that IL-1Ra primarily blocks IL-1α signalling as I could not detect IL-1β in the EMTU co-culture models. In HBECs, other stimuli also induce high levels of IL-1α compared to IL-1β [157, 234] and IL-1α is the predominant epithelial-derived IL-1 isoform to activate fibroblasts [157, 161]. However following viral infection, IL-1β has previously been detected from primary HBECs [208, 235, 236]. While relative levels of IL-1α and IL-1β were not compared in the majority of these studies, Piper *et al.* detected more IL-1β release than IL-1α in

HRV-infected primary HBEC cultures [208]. This discrepancy could be due to differences in responses between the fully differentiated or polarised HBECs, used in my study, compared to undifferentiated monolayers used previously.

In the apical compartment, IL-1Ra partially inhibited a subset of dsRNA-dependent proinflammatory responses. This suggests that epithelial-derived IL-1α is partly responsible for autocrine activation of the epithelium following dsRNA challenge, and that other dsRNA-dependent mediators may also contribute to the response within this compartment. Alternatively, the partial reduction may be due to the effects of intracellular IL-1α, which would not be affected by exogenous IL-1Ra and were increased following dsRNA challenge of the epithelium. Intracellular IL-1α, in its pro-form has previously been detected in the nucleus and a nuclear localisation sequence has been identified in the N-terminal pro-domain [237]. A role for nuclear-localised IL-1α has been demonstrated for a variety of biological functions, notably as an intracrine proinflammatory activator of transcription [238].

In contrast to the apical compartment, IL-1Ra completely suppressed a subset of dsRNA- and HRV-dependent proinflammatory responses in the basolateral compartment. This suggests that in response to dsRNA or HRV, epithelial cells release IL-1α basolaterally, and that this is required to drive proinflammatory mediator release from fibroblasts, leading to the synergistic enhancement of basolateral responses. Consistent with this, I showed that fibroblasts are highly sensitive to direct stimulation with concentrations of IL-1α similar to that induced by dsRNA. These results are in line with previous findings that IL-1α present in conditioned medium from unstimulated [161] or damaged epithelial cells [157, 160] induces production of proinflammatory mediators from fibroblasts [157, 160]. In the primary EMTU model, HRV-induced IL-1α release was much lower than dsRNA-induced IL-1α release in the polarised EMTU model. However, the synergistic enhancement in HRV-induced IL-6 release in the primary EMTU model, suggests that fibroblasts are responsive to these low IL-1α concentrations. In contrast to IL-6, no enhancement was observed in the HRV-induced CXCL8 response in the primary EMTU model. This difference between IL-6 and CXCL8 could potentially be due to the autocrine effects of

IL-6 on its own release, leading to the amplification of even small IL-1 induced responses [239].

Given the relatively high levels of apically released IL-1α, it was surprising that the low levels of basolateral IL-1α measured in the EMTU co-culture models were not only sufficient, but essential, for dsRNA-induced proinflammatory mediator release in this compartment. This may be explained by the close proximity of the fibroblasts to the basolateral surface of the epithelium resulting in high localised concentrations of IL-1α. Alternatively, the trend for reduced basolateral IL-1α in the polarised and primary EMTU models 24h post-viral stimulation may be a consequence of IL-1α utilisation by the fibroblasts over this time period. Also IL-1R1 is highly expressed by fibroblasts [157] suggesting that they are highly sensitive to activation, even at low concentrations of IL-1α. Furthermore IL-6 is known to act as an autocrine factor that can drive its own release [239], thus IL-1α may be a trigger for this effect.

In contrast to the marked sensitivity of fibroblasts to exogenous or paracrine IL-1α, HBECs were relatively unresponsive to direct IL-1α stimulation. This was unexpected as dsRNA-dependent cytokine release was inhibited by IL-1Ra in HBEC monocultures (see Appendix A, Figure A1), similar to findings with HRV-infected primary HBECs [208]. In addition, another publication showed that HBEC ALI cultures were responsive to direct stimulation with exogenous IL-1α, using concentrations much higher than in my experiments and those induced by dsRNA or HRV [234]. High concentrations of IL-1α may be required to overcome the blocking effect of natural inhibitors present in HBEC cultures at baseline. For example, although IL-1R2 (decoy receptor), is reported to be below the level of detection in HBEC monocultures [240], IL-1Ra is secreted constitutively [241]. Overcoming the blocking effect of this inhibitor may require high IL-1α concentrations, or other factors (such as those induced during anti-viral responses) to synergise with IL-1α.

Although out of the scope of the current study, the high levels of IL-1α in the apical compartment are of considerable interest as they have the potential to amplify local innate and adaptive immunity through direct activation or enhancement of luminal immune cell functions. Macrophages are the first line of cellular defence against invading pathogens and the IL-1α-IL-1RI pathway

has been identified as a key driver of inflammatory cytokine and chemokine activation after adenovirus infection [242]. However, direct evidence for IL-1α-mediated cross-talk with infected epithelium has not been investigated. The human monocytic cell line, THP-1, expresses IL-1R1 and alveolar macrophages have reduced lipopolysaccharide (LPS)-dependent CXCL8 release in the presence of IL-1Ra [157, 243]. MCs also respond to IL-1α with enhanced Th2 cytokine production [244, 245].

Together these data demonstrate the importance of viral-induced IL-1α in driving proinflammatory responses within the EMTU model. However, in section 3.3.2, a subset of the response (CXCL10) was identified that appeared to be IL-1α independent. On further investigation, dsRNA-induced CXCL10 responses were shown to be partially mediated by type I IFNs, adding to previous studies where CXCL10 release was mediated by IFNs in primary HBEC [213, 214] and fibroblast monocultures [215]. The data also suggests a dichotomy between IL-1 signalling and other anti-viral (IFN) responses, previously demonstrated in primary HBEC monolayers [208]. It was therefore surprising that direct stimulation of fibroblasts with exogenous IL-1α induced low levels of CXCL10 release. These levels were much lower than dsRNA-dependent CXCL10 release in the polarised EMTU model. In addition, it is likely that IL-1-induced CXCL10 release from fibroblasts would be even lower in dsRNA-stimulated co-cultures, where the epithelial barrier prevents diffusion of apical IL-1α into the basolateral compartment. In addition the pro-form of IL-1α is 31KDa, while the mature form is 17KDa [229]; larger than the 4KDa FITC-dextran used for macromolecular permeability studies, and therefore potentially less able to flux across the epithelial barrier. Together these data suggest that in the co-culture model, IL-1-induced CXCL10 from fibroblasts only accounts for a very small proportion of the response. In addition, it could explain why I failed to observe a significant effect of IL-1Ra on dsRNA-induced CXCL10 in the polarised EMTU model, but observed a partial inhibitory effect on HRV-induced CXCL10 in the primary EMTU model. In conclusion, the relationship between IL-1 and anti-viral signalling is more complex than first thought and requires further investigation. For example, IL-1 induced CXCL10 could be one reason why the IFN-blocking antibody does not completely abrogate the dsRNA-induced CXCL0 response in co-culture.

3.5.4 Consequences of viral-induced IL-1 in asthma

In this chapter, IL-1α has been demonstrated to be a potent mediator of cellular cross-talk and viral-induced proinflammatory responses within the EMTU. Dysregulated release of such a mediator could potentially have important consequences on viral-induced proinflammatory responses *in vivo*. Asthma is a chronic inflammatory disease that is commonly exacerbated by HRV infection. When HRV-induced IL-1 release was compared between ALIs from non-asthmatic and severe asthmatic donors, there was a trend for reduced IL-1α in severe asthmatic ALI cultures. This was unexpected, due to the chronic inflammatory nature of the disease. In addition, Willart *et al.* previously observed increased HDM-induced IL-1α release from primary HBECs from asthmatic compared to non-asthmatic donors [234]. This discrepancy may be due to differences between the HDM and viral stimuli or differences in the asthma phenotypes. Furthermore, the medications taken by the severe asthmatic donors in my study e.g. ICSs could potentially affect IL-1 levels.

The reduced viral-induced IL-1α release in my study does not necessarily correspond to reduced IL-1 signalling, as it depends on the ratio of IL-1 compared to its inhibitors and within the EMTU model may also depend on fibroblast responsiveness. Notably, polymorphisms in the IL-1Ra gene have been associated with asthma risk [76] and in one study, patients with the A2 allele of *IL1RN* had significantly lower serum IL-1Ra levels [83]. In addition in the asthmatic airway, subepithelial fibrosis [17] and increased numbers of inflammatory cells [132, 246-248] could lead to increased numbers of cells becoming activated and augmentation of inflammatory responses. Furthermore, IL-1α has the potential to influence the polarisation of inflammatory responses and promote allergic asthma as demonstrated by Willart *et al* [234], who showed that IL-1α controls allergic sensitisation to HDM in mice. In chronic respiratory diseases, such as asthma, where respiratory viral infections are a major cause of acute exacerbations (6) targeting viral-induced IL-1α may therefore be of potential therapeutic benefit. In section 3.3.5, I showed preliminary data to demonstrate that FP, a first-line asthma glucocorticosteroid therapeutic, blocks viral-induced IL-1 release in the polarised EMTU co-culture model. This data suggests that inhibition of IL-1 release could be one mechanism by which ICS reduce inflammation and are

of therapeutic benefit in asthma. However, ICS may have a number of other effects, since binding of ICS to the intracellular glucocorticoid receptor, leads to translocation to the nucleus where the ICS-receptor complex regulates transcription of a number of target genes, which are yet to be fully characterised [249]. In contrast to ICS, IL-1Ra is a specific inhibitor of IL-1 signalling and clinical trials have demonstrated minimal adverse effects for the treatment of inflammatory diseases [250-252]. In addition, our data suggests that IL-1Ra may suppress airway inflammation while leaving anti-viral (IFN) responses relatively intact, thus allowing effective clearance of viral infections. This is in contrast to FP, which has been shown to suppress inflammatory as well as viral-induced CXCL10 responses in fibroblast [253] and HBEC monocultures [254]. Consistent with these studies, there was a trend for reduced viral-induced CXCL10 in co-cultures treated with FP.

The IL-1R1 antagonist anakinra is already FDA-approved [250] and clinical trials have shown its effectiveness in inflammatory diseases [251] and LPS-induced airway inflammation in healthy volunteers without adverse effects [252]. A characteristic of these trials is the report that anakinra benefits patients who are unresponsive to other treatments such as corticosteroids. In asthma, where corticosteroids have little benefit in treating acute asthma exacerbations induced by respiratory viruses [38, 39], targeting IL-1 signalling may have therapeutic benefit.

3.5.5 Summary and conclusions

Although cell-cell communication is essential for normal function of all tissues, the relationship between structural organization and function is not addressed in most *in vitro* studies. Here I examined this relationship using an integrated co-culture system in which fully differentiated (or polarised HBECs) were apically challenged with HRV (or dsRNA) and demonstrated clear evidence of a synergistic interaction between the infected bronchial epithelium and fibroblasts. This interaction was mediated by epithelial-derived IL-1α and IFN which mediated differential subsets of the proinflammatory response by activation of the underlying fibroblasts. To my knowledge this is the first study to demonstrate direct epithelial-fibroblast cross-talk in response to HRV

infection or dsRNA and it highlights the importance of epithelial barrier function and integrity. In addition the dichotomy between IL-1α- and IFN –induced responses suggests that IL-1 signalling could be a potential therapeutic target for chronic respiratory diseases. For example in asthma, where respiratory viral infections are a major cause of acute exacerbations, targeting IL-1α may suppress airway inflammation while having minimal effects on anti-viral signalling.

4. Viral stimulation of HBECs activates repair responses in a co-culture model of the airway EMTU

4.1 Introduction

Local exchange of information between cells of the EMTU is important for promotion of co-ordinated responses to tissue injury. These include inflammatory responses, as investigated in chapter 3, and also repair responses, which may be induced by epithelial activation following inhalation of environmental agents e.g. viruses, cigarette smoke, pollution, pollen, dust. This activates the release of mediators, including growth factors, MMPs and ECM components that have autocrine and paracrine effects within the EMTU [17, 166]. Autocrine effects include growth factors which promote epithelial cell migration and proliferation to re-seal the barrier. Paracrine factors activate fibroblasts inducing their proliferation and differentiation to a myofibroblastic (repair) phenotype, which promotes epithelial barrier repair by the secretion of growth factors and ECM components, and by α-SMA expression required for wound contraction. Once epithelial barrier functions are restored myofibroblasts start to apoptose.

Evidence suggests that these wound healing mechanisms are dysregulated in the asthmatic airway, where distinct structural changes, termed airway remodelling can be observed (see section 1.1.3.2). For example, epithelial basement membrane thickening, subepithelial fibrosis and ECM deposition [17]. This is hypothesised to occur as a consequence of increased activation of repair responses and a lack of resolution due to ongoing inflammation, i.e. a chronic wound response [17]. Consistent with this, the levels of factors involved in remodelling are altered in the asthmatic airway. For example, MMP-2, MMP-9 and TIMP-1 are increased in the BALF of asthmatics, although the overall MMP/TIMP ratio is decreased [167-169]. Growth factors such as TGF-β and bFGF are also increased in the BALF of asthmatics [170, 171] and increased bFGF and VEGF expression has been detected in biopsies from asthmatic

compared to healthy subjects and was associated with increased vascularity of the bronchial mucosa [172, 173]. Some of these remodelling factors are further increased during asthma exacerbations, including MMP-9 [255], VEGF [256, 257] and bFGF [116] in nasal aspirates.

Mediators associated with repair and remodelling in asthma have also been detected in HBEC monocultures following HRV infection *in vitro*. These include ECM components (e.g. perlecan and collagen V), MMPs (e.g. MMP-9) and growth factors (e.g. VEGF, TGF) [113, 115, 258, 259]. These factors may have important paracrine effects within the EMTU. For example, bFGF release by HRV-infected HBECs induces fibroblast proliferation [116]. However, this study used conditioned medium from epithelial monolayers which does not allow bi-directional communication between the epithelium and fibroblasts. In addition, vectorial mediator release, which is important for accumulation of factors at the apical or basolateral epithelial surface *in vivo,* was not examined. This may be crucial in the control of signalling to underlying fibroblasts and orchestrating repair responses within the EMTU. In view of this literature and the demonstration that cellular cross-talk is important in mediating proinflammatory responses to viral infection (see chapter 3), within this chapter I will investigate the effect of viral infection on repair responses within the EMTU co-culture models.

.

4.2 Effect of dsRNA on repair responses in the polarised EMTU model

4.2.1 DsRNA stimulation of the polarised EMTU model induces vectorial release of mediators involved in repair

Repair responses to dsRNA stimulation were initially assessed by detection of MMPs and growth factors in cell-free supernatants obtained in chapter 3. In the apical compartment of the EMTU model, dsRNA (1µg/ml) induced a significant increase in MMP-9 and MMP-2 release, which was comparable with HBEC monocultures (Figure 4.2.1-1A-B). In the basolateral compartment, dsRNA did not induce MMP-9 or MMP-2 release (Figure 4.2.1-1C-D) but constitutive levels of these MMPs were altered between cultures. Basolateral MMP-9 release was significantly reduced in EMTU co-cultures compared to HBEC monocultures (Figure 4.2.1-1C) suggesting the presence of fibroblasts suppresses constitutive MMP-9 release by HBECs. In contrast, there was a trend for increased basolateral MMP-2 release in the polarised EMTU model compared to HBEC monocultures (Figure 4.2.1-1D suggesting a cumulative effect of co-culturing both cell types together. These data suggest that HBECs are the main source of dsRNA-induced MMP-9 and MMP-2 since these MMPS were only induced in the apical compartment by dsRNA where HBECs were located.

The release of growth factors, VEGF and bFGF, was next investigated in dsRNA-stimulated EMTU co-cultures. Similar to MMP release, the polarity of dsRNA-induced VEGF and bFGF release was apical and was comparable between the EMTU model and HBEC monocultures (Figure 4.2.1-2A-B). In the basolateral compartment, dsRNA did not induce VEGF or bFGF release (Figure 4.2.1-2C-D). In contrast to MMP release, the presence of fibroblasts had no effect on VEGF or bFGF levels within the basolateral compartment when compared with HBEC monocultures. These data suggest that HBECs are the main source of VEGF and bFGF in both unstimulated and dsRNA-stimulated

cultures since fibroblast monocultures did not release these factors and increased levels were detected in the apical compartment where HBECs were located.

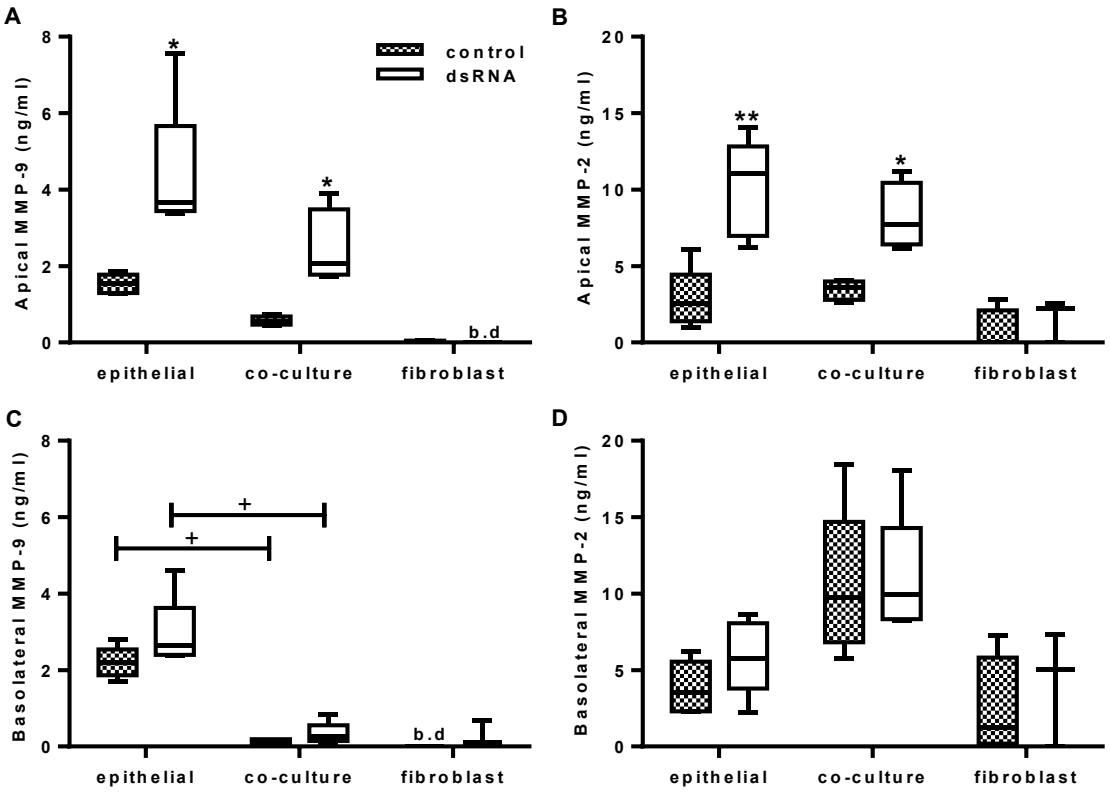

Figure 4.2.1-1 Effect of dsRNA on MMP release in the polarised EMTU co-culture model.

Apical (A-B) and basolateral (C-D) cell-free supernatants were harvested from the EMTU co-culture model or HBEC and fibroblast monocultures 24h after challenge with dsRNA (poly(I:C); 1µg/ml), and assayed for MMP-9 (A,C), and MMP-2 (B,D) by Luminex® assay. Results were corrected for growth factor levels in the culture medium (b. d. for MMP-9 and 0.08ng/ml MMP-2) and are shown as box plots representing the median with 25% and 75% interquartiles, and whiskers representing minimum and maximum values, n=3-5 independent experiments. *$P \leq 0.05$, and **$P \leq 0.01$ for comparison between control and dsRNA stimulated cultures and $^{+}P \leq 0.05$ for comparison between HBEC monocultures and the EMTU co-culture model (Kruskall-Wallis test with Dunn's correction). b.d. indicates levels below the detection limit of the assay.

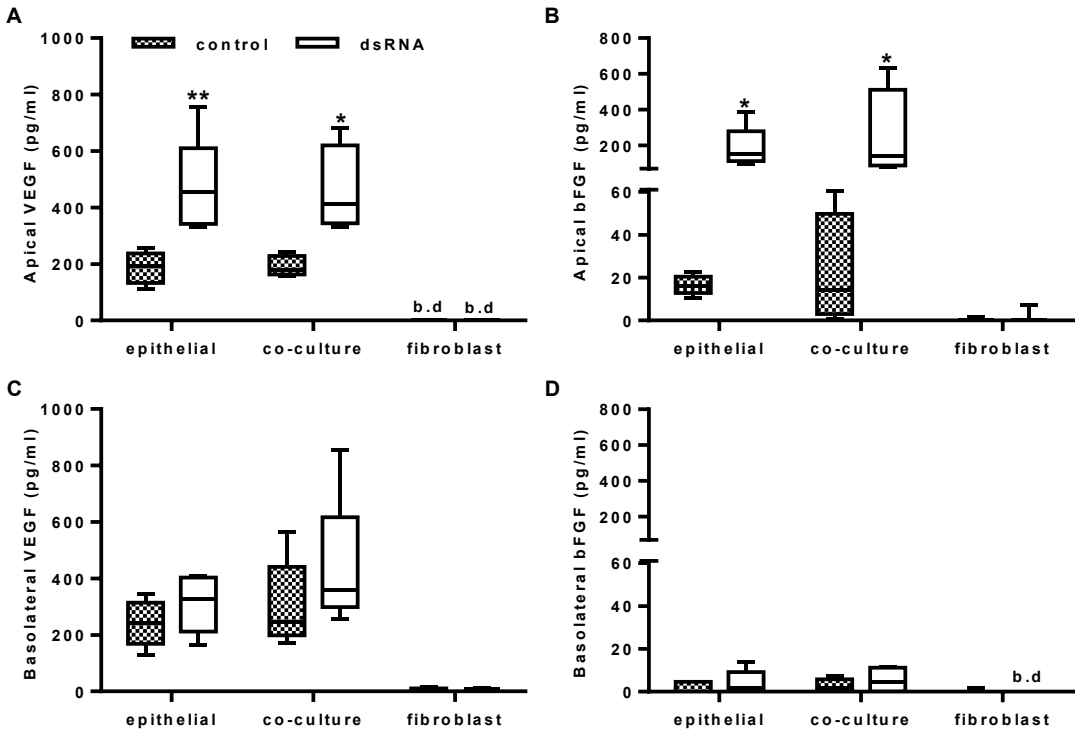

Figure 4.2.1-2 Effect of dsRNA on growth factor release in the polarised EMTU co-culture model.

Apical (A-B) and basolateral (C-D) cell-free supernatants were harvested from the EMTU co-culture model or HBEC and fibroblast monocultures 24h after challenge with dsRNA (poly(I:C); 1µg/ml) and assayed for VEGF (A,C), and bFGF (B,D) by Luminex® assay. Results were corrected for growth factor levels in the culture medium (1.4pg/ml VEGF and 21pg/ml bFGF) and shown as box plots representing the median with 25% and 75% interquartiles, and whiskers representing minimum and maximum values, n=3-5 independent experiments. *$P \leq 0.05$, and **$P \leq 0.01$ for comparison between control and dsRNA stimulated cultures (Kruskall-Wallis test with Dunn's correction). b.d. indicates levels below the detection limit of the assay.

4.2.2 Effect of IL-1 signalling on dsRNA-induced MMP and growth factor release in the polarised EMTU model

In chapter 3, IL-1 signalling was demonstrated to drive a subset of viral-induced proinflammatory responses. I therefore hypothesised that IL-1α was an essential mediator of cellular cross-talk and was responsible for inducing dsRNA-dependent mediators involved in repair responses. MMP and growth factor release was compared between IL-1Ra-treated and untreated cultures following dsRNA stimulation. However, dsRNA-induced MMP and growth factor responses were small and in some cases did not reach significance (Figure 4.2.2-1 and Figure 4.2.2-2). This was in contrast to the initial experiments, which demonstrated a significant increase in MMPs and growth factors (Figure 4.2.1-1 and Figure 4.2.1-2). It was therefore difficult to interpret whether IL-1Ra had an effect on MMP and growth factor release due to the low signal to noise ratio. This was in contrast to IL-6 release, which was synergistically enhanced by dsRNA in the same samples as those used in this chapter (chapter 3 section 3.2.4) demonstrating that the cultures where still responsive to dsRNA stimulation.

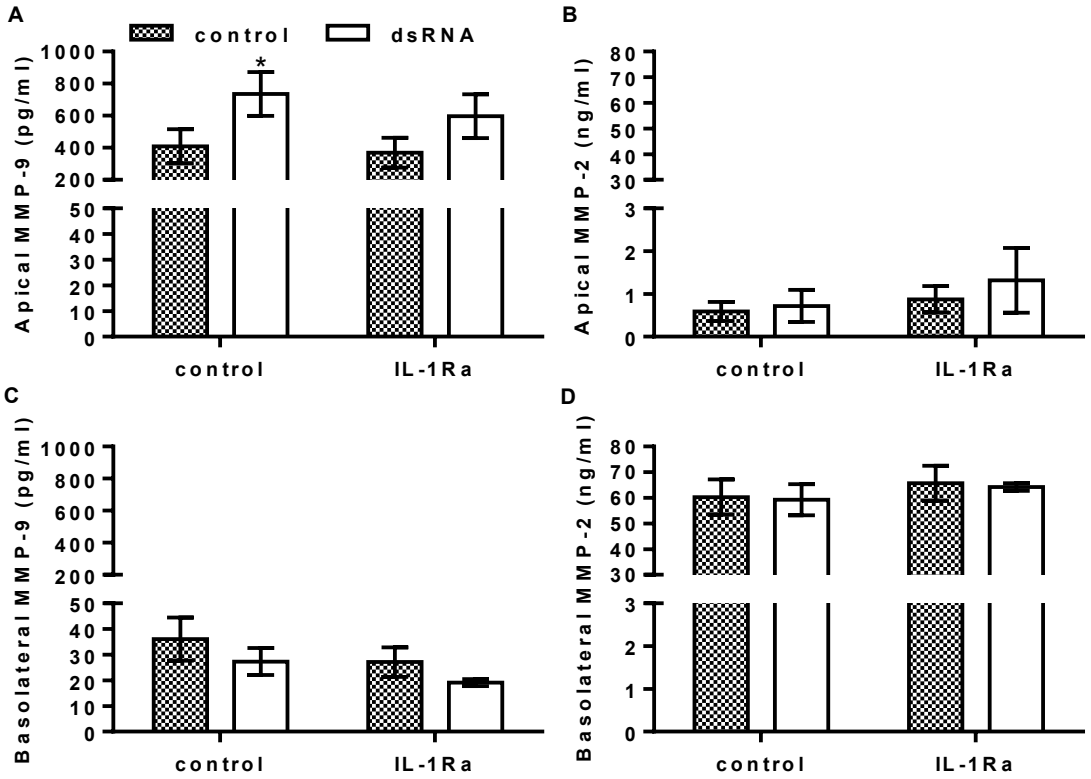

Figure 4.2.2-1 The effect of IL-1R antagonism on dsRNA-induced MMP release in the polarised EMTU co-culture model.

The EMTU co-culture model was cultured in the absence or presence of IL-1Ra (500ng/ml) applied apically and basolaterally for 1h prior to stimulation with dsRNA (poly(I:C); 1µg/ml). Apical (A-B) and basolateral (C-D) cell-free supernatants were harvested 24h after stimulation and assayed for MMP-9 (A,C), and MMP-2 (B,D) by Luminex® assay. Results were corrected for growth factor levels in the culture medium (b.d for MMP-9 and 0.08ng/ml MMP-2) and shown as means ± SD, n=3 independent experiments. *$P \leq 0.05$, for comparison between control and dsRNA stimulated cultures (two-way ANOVA with Bonferroni correction).

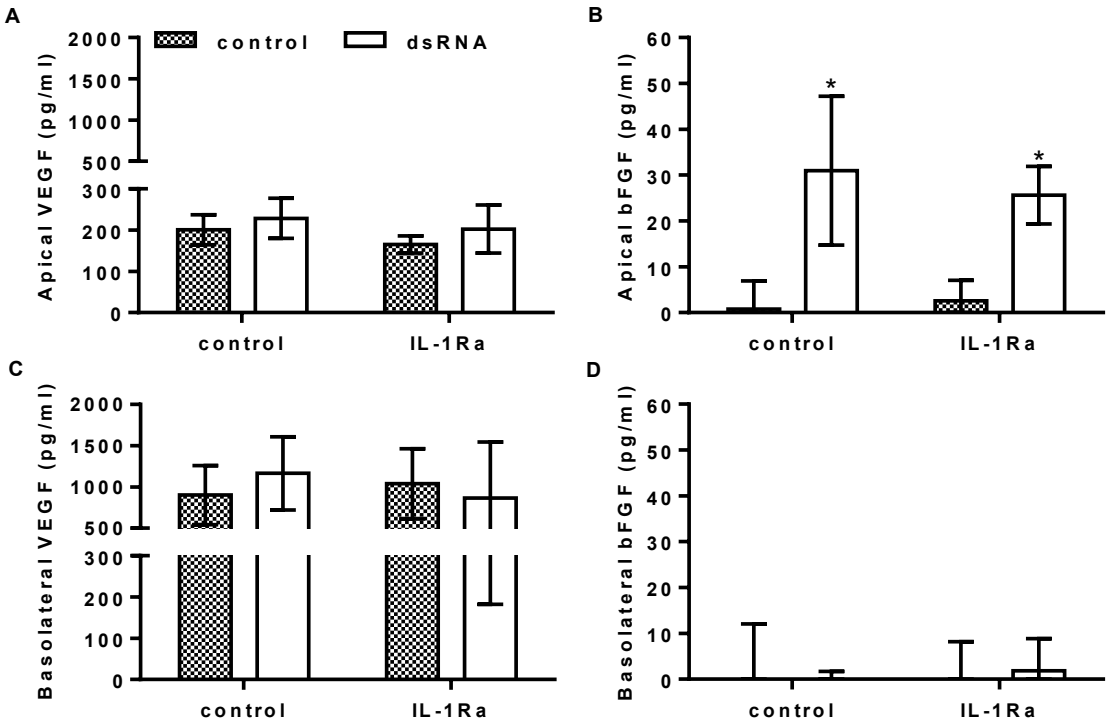

Figure 4.2.2-2 The effect of IL-1R antagonism on dsRNA-induced growth factor release in the polarised EMTU co-culture model.

The EMTU co-culture model was cultured in the absence or presence of IL-1Ra (500ng/ml) applied apically and basolaterally for 1h prior to stimulation with dsRNA (poly(I:C); 1µg/ml). Apical (A-B) and basolateral (C-D) cell-free supernatants were harvested 24h after stimulation and assayed for VEGF (A,C), and bFGF (B,D) by Luminex® assay. Results were corrected for growth factor levels in the culture medium (1.4pg/ml VEGF and 21pg/ml bFGF)) and shown as means ± SD, n=3 independent experiments. *$P \leq 0.05$, for comparison between control and dsRNA stimulated cultures (two-way ANOVA with Bonferroni correction).

4.2.3 Effect of dsRNA on fibroblast proliferation in the polarised EMTU model.

In the previous section dsRNA stimulation of the polarised EMTU model resulted in the release of MMPs and growth factors. Of those detected, MMP-2 [260] and bFGF [116] have been shown to induce fibroblast proliferation with the latter induced by HRV1B-infected BECs. Therefore I next investigated the effect of dsRNA on fibroblast proliferation within the polarised EMTU model, using a Click-iT® EdU assay kit. This assay uses fluorescent labelling of a thymidine analogue, EdU, to detect newly synthesised DNA and was optimised for use in co-culture (as described chapter 2 section 2.9.2) by reducing FBS in the medium (from 10% to 2%) and increasing the assay endpoint (from 24h to 36h).

Prior to investigating fibroblast proliferation using 2% FBS medium, control experiments were performed to compare epithelial barrier functions and mediator release between cells cultured in 2% or 10% FBS medium. In unstimulated cultures, barrier functions and proinflammatory mediator release were not much altered between the conditions (Figure 4.2.3-1 and Figure 4.2.3-2), demonstrating that reduced FBS levels had no adverse effect on the EMTU model. In contrast, dsRNA stimulation had more pronounced effects on ionic permeability and proinflammatory mediator release when FBS was reduced; with a greater reduction in TER and enhanced CXCL8 release (Figure 4.2.3-1 and Figure 4.2.3-2). These responses were little modified with time (Figure 4.2.3-1 and Figure 4.2.3-2). The enhanced responses in low FBS may be beneficial for the detection of dsRNA-induced effects. I therefore proceeded using 2% FBS medium to investigate the effect of dsRNA on fibroblast incorporation of EdU in the EMTU co-culture model. While increased EdU incorporation was detected in the positive control of 10% FBS, dsRNA stimulation had no effect on fibroblast proliferation in the EMTU co-culture model (Figure 4.2.3-3). This was confirmed in 3 separate experiments and quantified by cell count (Table 4.2.3-1) and is consistent with the polarity of dsRNA-induced growth factor release, which was apical rather than

basolaterally onto the fibroblasts. These data suggest that dsRNA stimulation of the EMTU model has no effect on fibroblast proliferation.

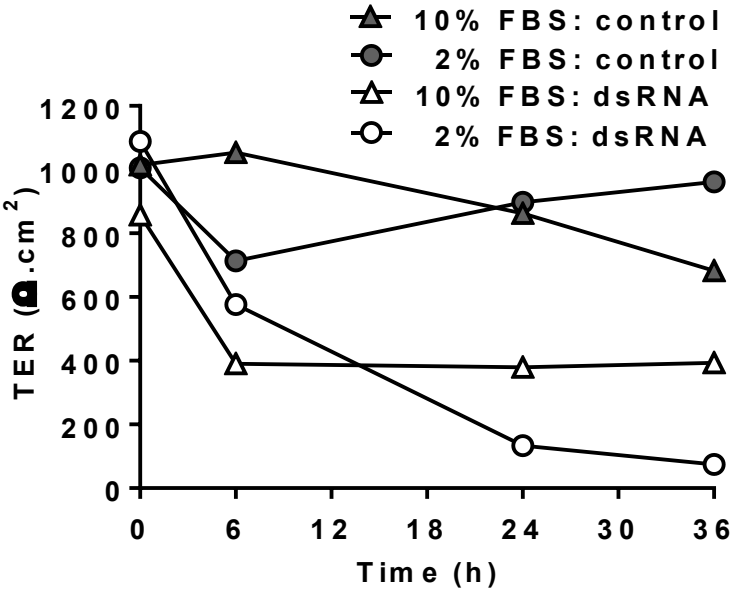

Figure 4.2.3-1 Effect of altering FBS percentage on ionic permeability of unstimulated and dsRNA-stimulated polarised EMTU co-cultures over time.
On day 5 after initial co-culture set up, the apical medium was replaced with standard cell culture medium (10% FBS), while the basolateral medium was replaced with either standard medium (10% FBS) or low FBS (2%) medium. The next day cultures were challenged with dsRNA (poly(I:C); 1µg/ml) and ionic permeability determined over 36h by TER measurements (n=1).

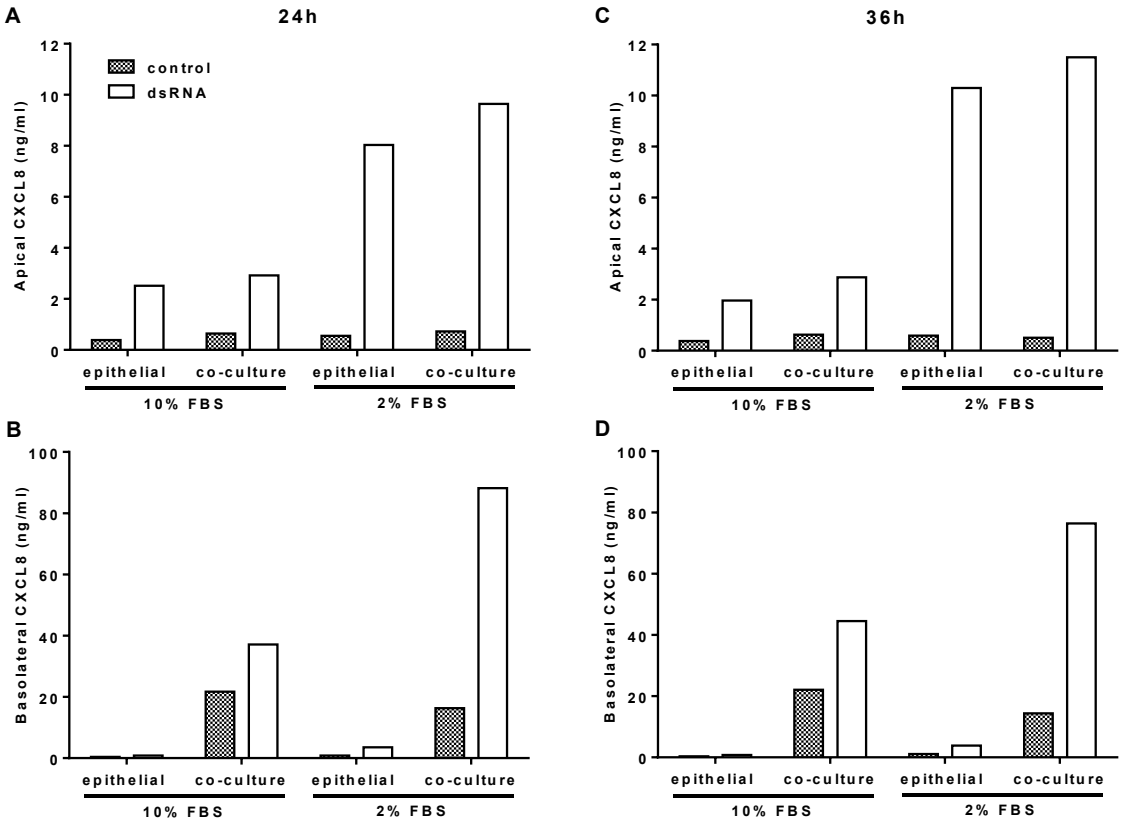

Figure 4.2.3-2 Effect of altering FBS percentage on CXCL8 release in unstimulated and dsRNA-stimulated HBEC mono- and co-cultures with fibroblasts over time.

On day 5 after initial co-culture set up, the apical medium was replaced with standard cell culture medium (10% FBS), while the basolateral was replaced with either standard medium (10% FBS) or low FBS (2%) medium. The next day cultures were challenged with dsRNA (poly(I:C); 1µg/ml). After 24h (A-B) and 36h (C-D) apical and basolateral cell-free supernatants were harvested and assayed for CXCL8 release by ELISA (n=1).

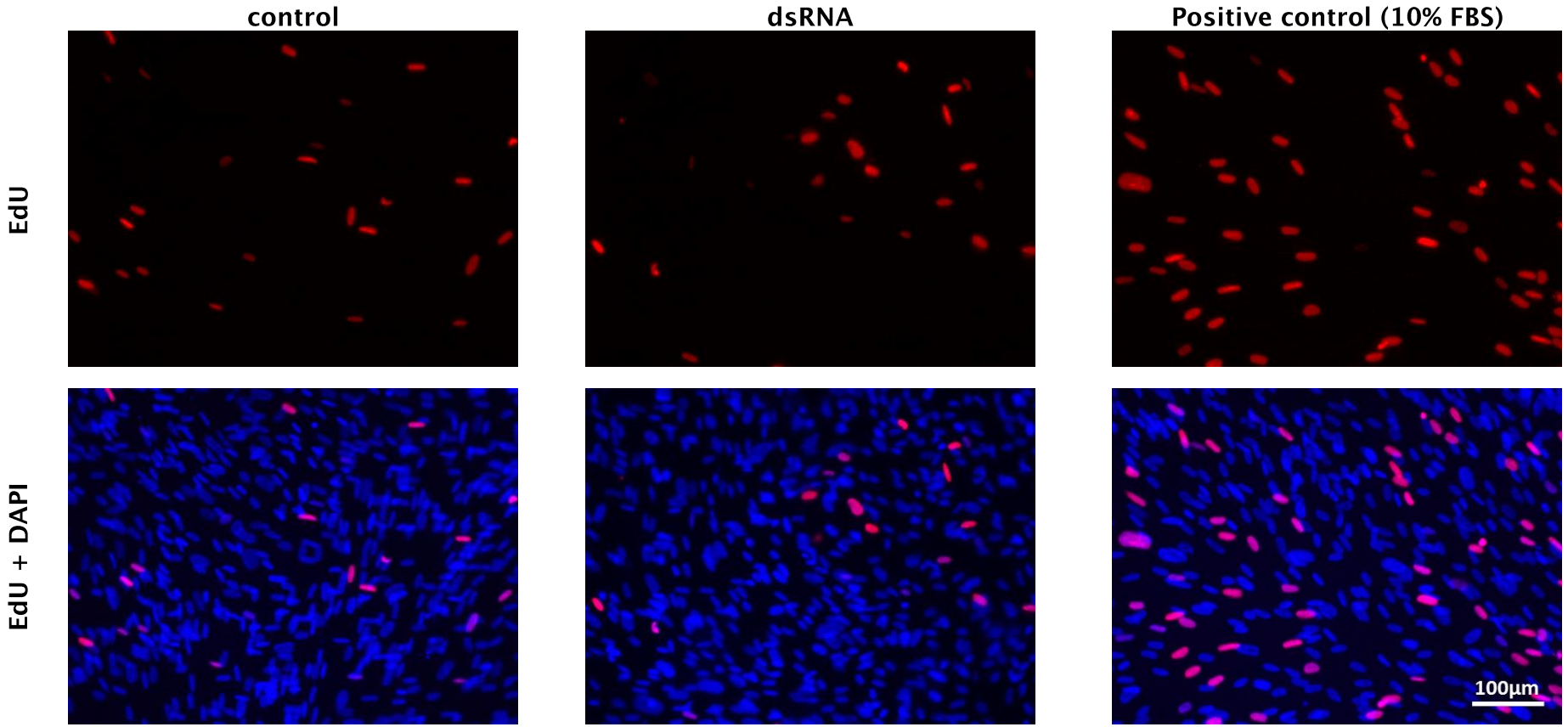

Figure 4.2.3-3 Effect of dsRNA stimulation on fibroblast proliferation within the polarised EMTU model.
Co-cultures were fixed 36h after challenge with dsRNA (poly(I:C); 1µg/ml) and proliferation assessed by detection of the fluorescently labelled thymidine analogue, EdU, into newly synthesised DNA using the immunofluorescent microscope. Red nuclei= EdU^+ cells, blue nuclei= DAPI stain. Images were taken at a magnification of x20 and are representative of 3 independent experiments.

Table 4.2.3-1 Quantification of fibroblast proliferation in the dsRNA-stimulated polarised EMTU model.

Co-cultures were fixed 36h after challenge with dsRNA (poly(I:C); 1µg/ml) and proliferation assessed by detection of the fluorescently labelled thymidine analogue, EdU, into newly synthesised DNA by immunofluorescent microscopy. Cell counts for each experiment are the mean count from 3 fields of view at x20 magnification. Results are means ± SD, from 3 separate experiments. *P≤0.05 compared to control

	control	**dsRNA**	**FBS (positive control)**
Edu$^+$ cells/field of view	28±9	25±6	50±6*
Total cells/field of view	428±95	444±203	371±51
% EdU$^+$ cells	7.0±0.7	6.3±1.8	13.6±0.5*

4.2.4 Effect of dsRNA on myofibroblast differentiation in the polarised EMTU model

To examine the effect of dsRNA stimulation of the polarised EMTU model on other aspects of the fibroblast repair responses, myofibroblast differentiation was next investigated by assessing α-SMA staining by immunofluorescent microscopy (Figure 4.2.4-1). At low magnifications (x10) dsRNA induced a small increase in the intensity of staining for α-SMA (Figure 4.2.4-1A), while at higher magnifications (63X), increased α-SMA stress fibres were also observed (Figure 4.2.4-1B). This result was consistent over replicate experiments.

Among the many factors released by HBECs following activation, TGF-β is a potent inducer of α-SMA expression in fibroblasts [164]. I therefore investigated whether TGF-β release could be detected from dsRNA-stimulated polarised EMTU cultures by ELISA. However, I could not detect an increase in total TGF-β_1 or TGF-β_2 or the active form of these cytokines following dsRNA stimulation of co-cultures (data not shown). TGF-β is notoriously difficult to detect in cell culture supernatants and can be obscured by the presence of TGF-β within 10% FBS-containing cell culture medium (384pg/ml TGF-β_1 and 83pg/ml TGF-β_2 (n=1)). However, even when FBS content was reduced to 2% and 1%, a substantial amount of TGF-β_1 was detected in the culture media (130pg/ml and 82pg/ml TGF-β_1 respectively; TGF-β_2 was b.d (n=1)), and there was no effect of dsRNA on release or activity of either isoform. I therefore investigated the effect of TGF-β on dsRNA-dependent α-SMA expression by addition of a pan-TGFβ neutralising antibody to the basolateral compartment of the polarised EMTU model. In initial control experiments, the pan-TGF-β antibody reduced TGF-β-dependent α-SMA expression, demonstrating that the effects of TGF-β could be successfully neutralised by the antibody (Figure 4.2.4-2). In the EMTU co-culture model, the pan-TGF-β neutralising antibody inhibited dsRNA-dependent α-SMA expression, which was confirmed over replicate experiments (Figure 4.2.4-2). These data suggest that TGF-β is required to drive myofibroblast differentiation following activation of the polarised EMTU model by dsRNA.

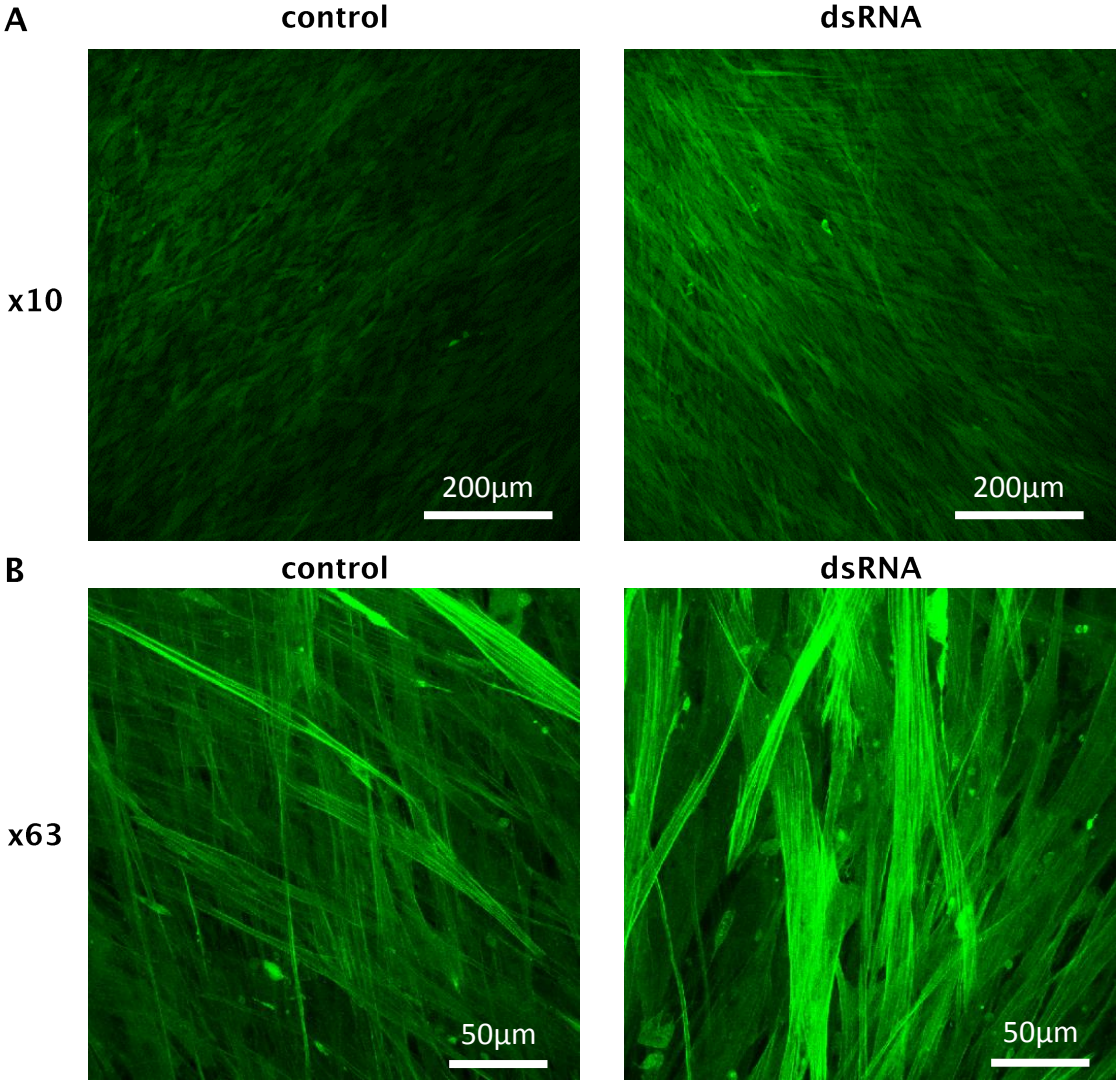

Figure 4.2.4-1 Effect of dsRNA stimulation of the polarised EMTU model on myofibroblast differentiation.
Co-cultures were fixed 24h after challenge with dsRNA (poly(I:C); 1µg/ml) and assessed for α-SMA (green) by immunofluorescent microscopy using x10 (A) and x63 (B) magnifications on the confocal microscope. Images are representative of 6 independent experiments.

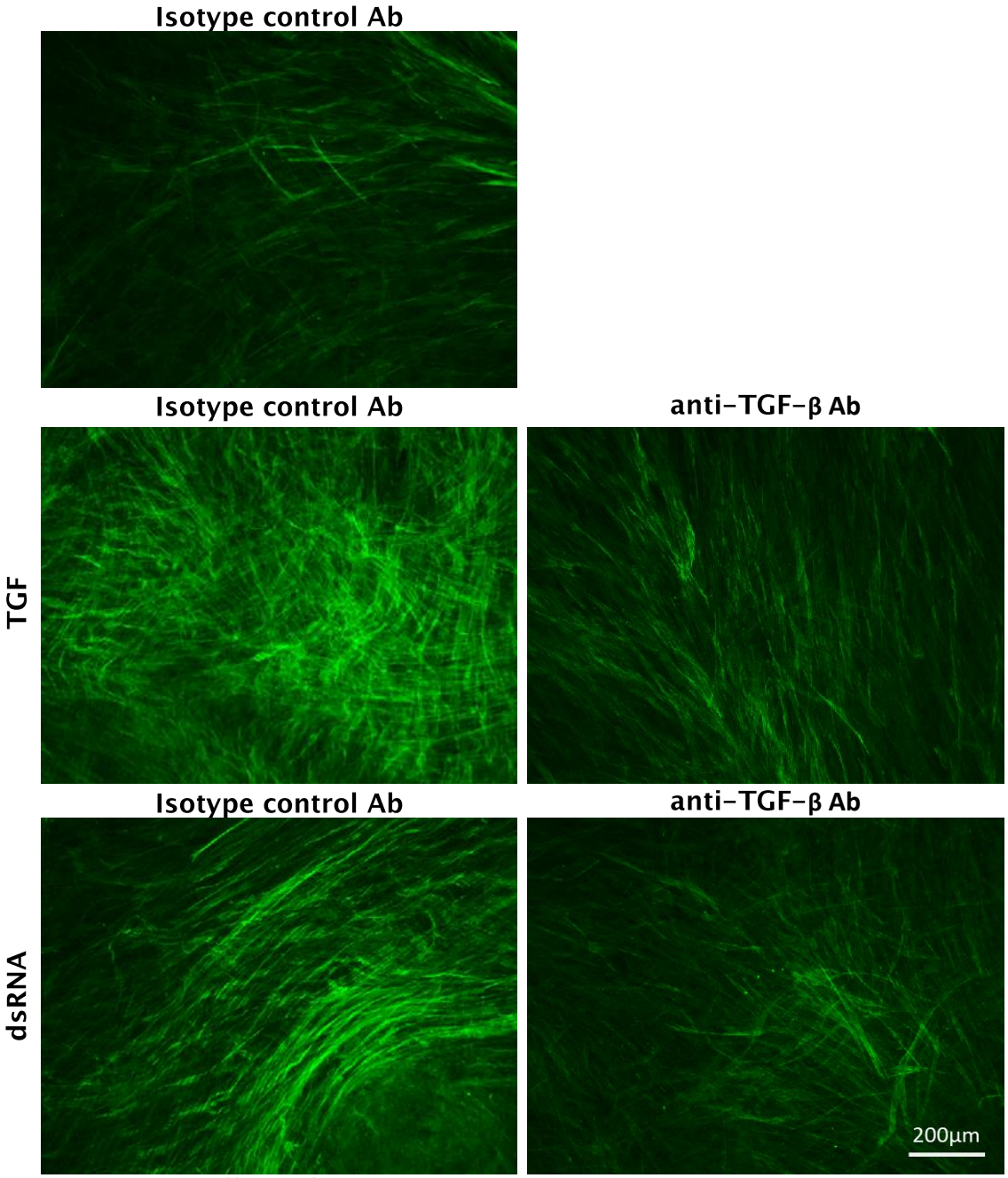

Figure 4.2.4-2 Effect of the pan-TGF-β neutralising antibody on TGF-β-and dsRNA-dependent α-SMA expression in the polarised EMTU co-culture model. The pan-TGF-β neutralising antibody (1µg/ml) or isotype control antibody (1µg/ml, mIgG$_1$) were applied to the basolateral compartment of the polarised EMTU model for 1h prior to basolateral stimulation with exogenous TGF-β$_1$ (5ng/ml) or apical stimulation with dsRNA (poly(I:C); 1µg/ml).. Co-cultures were fixed in 4% PFA 24h after challenge and assessed for α-SMA protein expression (green) using immunofluorescent microscopy. Images are representative of 3 independent experiments at x10 magnification.

4.3 Effect of HRV16 on repair responses in the primary EMTU model

4.3.1 HRV16 infection of the primary EMTU model induces vectorial release of mediators involved in repair

I next evaluated repair responses in a primary EMTU model where primary HBECs differentiated at ALI were cultured with fibroblasts and apically infected with HRV16. Similar to the dsRNA-stimulated polarised EMTU model, infection of the primary EMTU model with HRV16 induced the apical release of MMP-9 and MMP-2 and was comparable with ALI monocultures (Figure 4.3.1-1A-B). However, constitutive levels of apical MMP-9 and MMP-2 were lower in the primary EMTU model compared to ALI monocultures (Figure 4.3.1-1A-B). While HRV16 had no effect on basolateral MMP-9 or MMP-2 release, constitutive levels of basolateral MMP-2 were enhanced in the primary EMTU model compared to ALI monocultures (Figure 4.3.1-1C-D). This was consistent with the polarised EMTU model where a trend for increased basolateral MMP-2 levels were observed compared to HBEC monocultures (Figure 4.2.1-1D).

The release of growth factors was next investigated in the primary EMTU model following HRV16 infection. Similar to the dsRNA-stimulated polarised EMTU model, infection of the primary EMTU model with HRV induced the apical release of VEGF (Figure 4.3.1-2) which was not observed in ALI monocultures. In the basolateral compartment, HRV did not induce VEGF release in the primary EMTU model or ALI monocultures. However, in contrast to the dsRNA-stimulated polarised EMTU model, bFGF release could not be detected in HRV16-stimulated primary mono- or co-cultures with fibroblast. These data demonstrate that HRV16 infection of the primary EMTU model induces the apical release of MMP-9 and MMP-2 and the growth factor, VEGF.

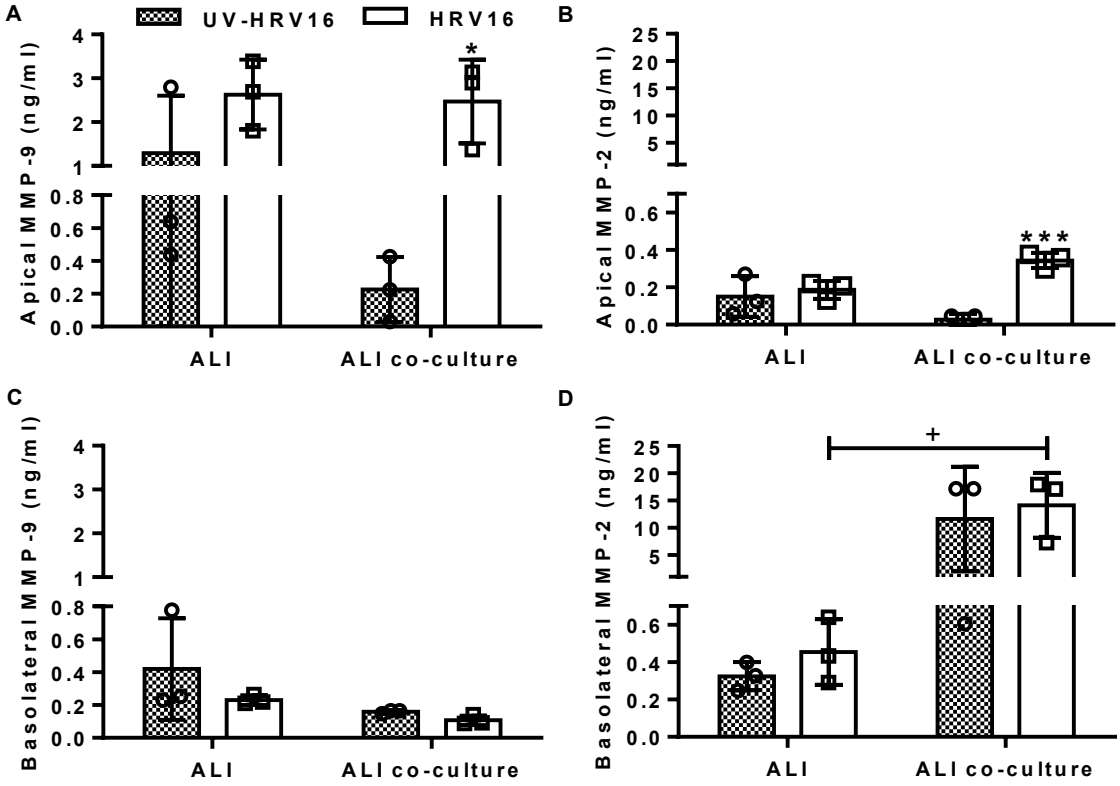

Figure 4.3.1-1 Effect of HRV16 on MMP release in the primary EMTU co-culture model.

ALI mono- or co-cultures with fibroblasts were infected apically with HRV16 (MOI=2) or UV-HRV16 as a negative control. After 24h, apical (A-B) and basolateral (C-D) cell-free supernatants were assayed for MMP-9 (A, C) and MMP-2 (B, D) by Luminex® assay. Results were corrected for growth factor levels in the culture medium (b. d. for MMP-9 and 0.07ng/ml MMP-2) and shown as means ± SD, 3 separate experiments from one epithelial cell donor. $^{*}P \leq 0.05$ $^{***}P \leq 0.001$, compared to UV-HRV16 control and $^{+}P \leq 0.05$ comparing ALI mono- and co-cultures (two-way ANOVA with Bonferroni correction).

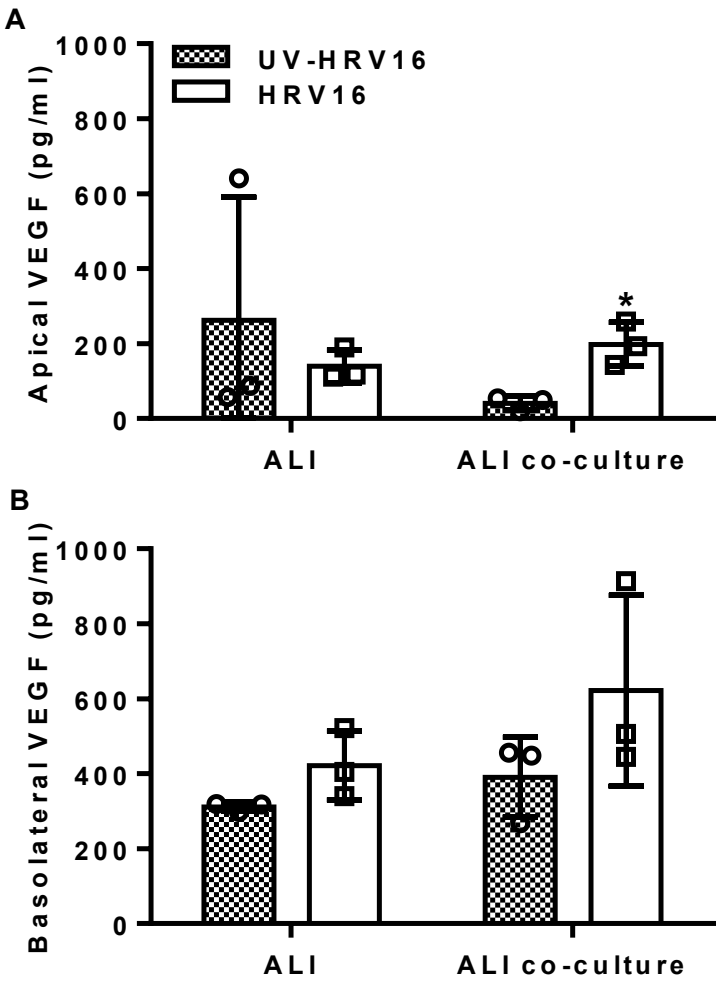

Figure 4.3.1-2 Effect of HRV16 on VEGF release in the primary EMTU co-culture model.

ALI mono- or co-cultures with fibroblasts were infected apically with HRV16 (MOI=2) or UV-HRV16 as a negative control. After 24h, apical (A) and basolateral (B) cell-free supernatants were assayed for VEGF by Luminex® assay. Results were corrected for growth factor levels in the culture medium (2pg/ml) and shown as means ± SD, 3 separate experiments from one epithelial cell donor. *$P \leq 0.05$ compared to UV-HRV16 control (two-way ANOVA with Bonferroni correction).

4.3.2 Effect of IL-1 signalling on MMPs and growth factors in the primary EMTU model

In the dsRNA-stimulated polarised EMTU model, IL-1 signalling was essential in driving the release of proinflammatory mediators but the effect on mediators involved in repair could not be established due to low levels of induction. Since IL-1 signalling was also confirmed to be essential in driving a subset of proinflammatory mediators following HRV challenge of the primary EMTU model I therefore hypothesised that IL-1α was an essential mediator of cellular cross-talk and was responsible for HRV-dependent release of mediators involved in repair responses. HRV16-induced MMP and VEGF release were compared in the absence or presence of 500ng/ml of IL-1Ra. In the apical compartment, HRV16-dependent MMP-9, MMP-2 and VEGF release was not inhibited by IL-1Ra in the primary EMTU model (Figure ⁋4.3.2-1A-B and Figure ⁋4.3.2-2A). In the basolateral compartment, neither HRV16 nor IL-1Ra had an effect on MMP-9, MMP-2 or VEGF release (Figure ⁋4.3.2-1C-D and Figure ⁋4.3.2-2). These data suggest that IL-1α is not involved in HRV-dependent MMP or growth factor release in a primary model of the EMTU. However, as mentioned in results section ⁋4.2.2, the signal to noise ratio is low and the large variability between data points makes the results difficult to interpret.

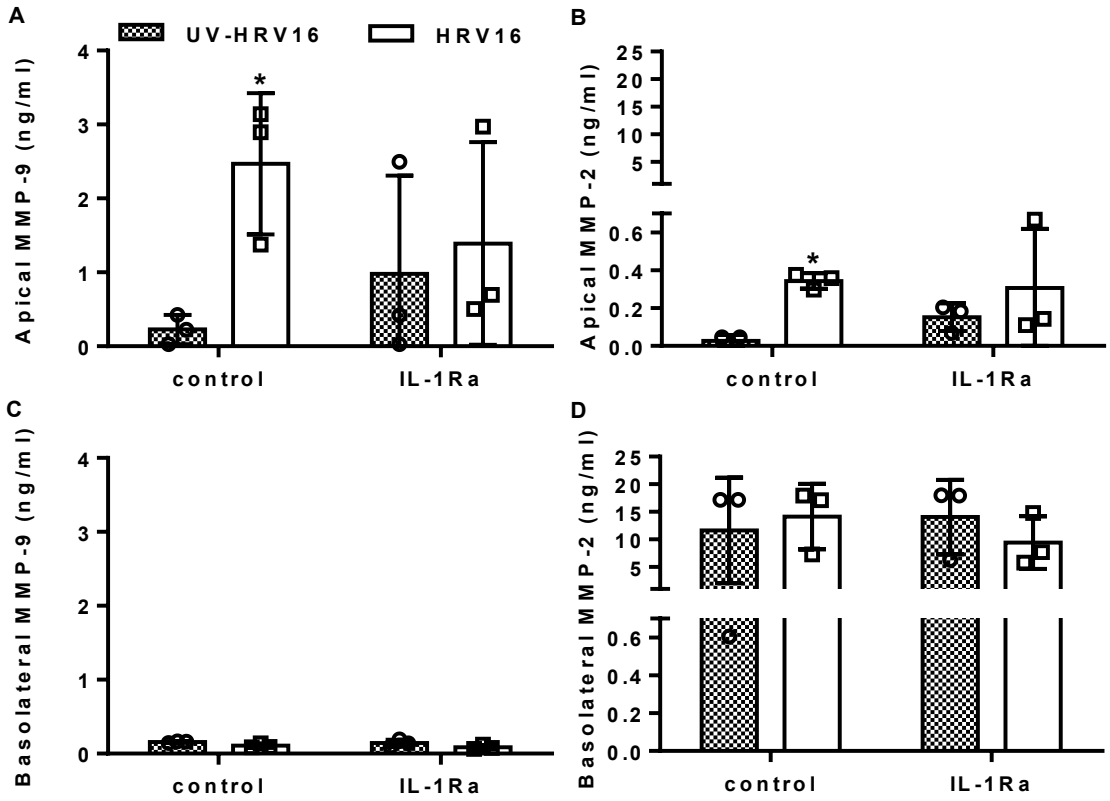

Figure 4.3.2-1 The effect of IL-1R antagonism on HRV16-induced MMP release in the primary EMTU co-culture model.

The primary EMTU co-culture model was cultured in the absence or presence of IL-1Ra (500ng/ml) applied basolaterally for 1h prior to HRV16 (MOI=2) or UV-HRV16 infection as a negative control. After 24h, apical (A-B) and basolateral (C-D) cell-free supernatants were harvested and assayed for MMP-9 (A, C) and MMP-2 (B,D) by Luminex® assay. Results were corrected for growth factor levels in the culture medium (b. d. for MMP-9 & 0.07ng/ml MMP-2) and shown as means ± SD, 3 separate experiments from one epithelial cell donor. *$P \leq 0.05$ compared to UV-HRV16 control (two-way ANOVA with Bonferroni correction).

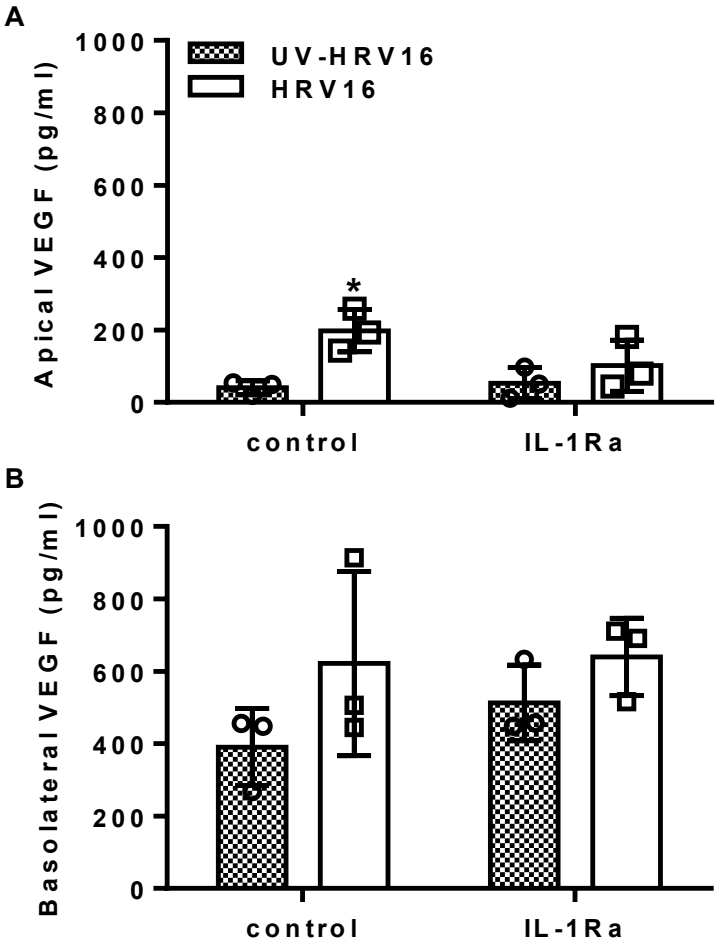

Figure 4.3.2-2 The effect of IL-1R antagonism on HRV16-induced VEGF release in the primary EMTU co-culture model.

The primary EMTU co-culture model was cultured in the absence or presence of IL-1Ra (500ng/ml) applied basolaterally for 1h prior to HRV16 (MOI=2) or UV-HRV16 infection as a negative control. After 24h, apical (A) and basolateral (B) cell-free supernatants were harvested and assayed for VEGF by Luminex® assay. Results were corrected for growth factor levels in the culture medium (2pg/ml) and shown as means ± SD, 3 separate experiments from one epithelial cell donor. *$P \leq 0.05$ compared to UV-HRV16 control (two-way ANOVA with Bonferroni correction).

4.3.3 Effect of HRV16 infection of the primary EMTU model on myofibroblast differentiation

In the polarised EMTU model, dsRNA stimulation of the epithelium resulted in increased α-SMA staining within fibroblasts suggesting differentiation to myofibroblasts. To determine whether these observations could be confirmed in a more complex model, fully differentiated primary HBECs were infected with HRV16 and α-SMA staining was quantified in the underlying fibroblasts within the primary EMTU model. However, no differences were observed in fibroblast α-SMA staining between primary co-cultures infected with HRV16 and UV-HRV16 controls (Figure 4.3.3-1).

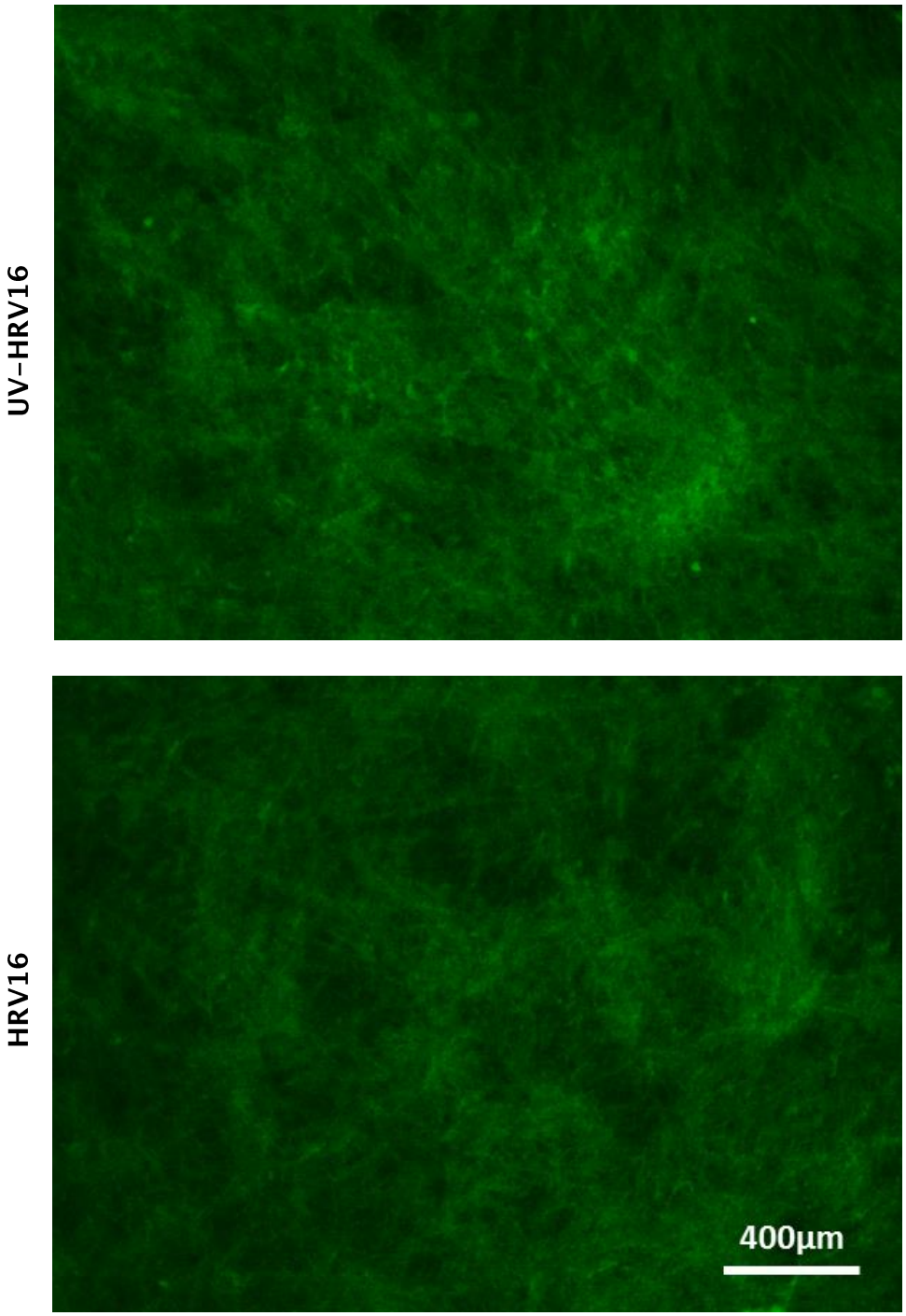

Figure 4.3.3-1 Effect of HRV16 infection on fibroblast α-SMA expression in the primary EMTU model.

ALI mono- or co-cultures with fibroblasts were infected apically with HRV16 (MOI=2) or UV-HRV16 as a negative control. After 24h co-cultures were fixed and assessed for α-SMA expression (green) by immunofluorescent microscopy (x5 magnification). Images are representative of 3 experiments from one epithelial cell donor.

4.4 Discussion

4.4.1 Viral stimulation of the EMTU models induces polarised release of mediators involved in repair

MMPs and growth factors are key mediators of tissue homeostasis and have important roles in repair responses at the epithelial surface following epithelial activation. For example, MMPs are proteases whose main substrates include ECM components and are key regulators of ECM accumulation/degradation within the basement membrane and lamina propria of the airways. MMP substrates also include cell-associated factors and other pro-MMPs, which can be released or activated following proteolytic cleavage. These cell-associated factors may include growth factors which are important for stimulating cell proliferation, migration, and differentiation. MMP and growth factor release was therefore assessed in the EMTU models following viral stimulation.

Viral stimulation induced polarised release of MMP-2, MMP-9 and VEGF in the EMTU co-culture models, which confirms previous studies using non-polarised HBEC monolayers [113, 114, 116, 256]. Notably, the polarity of viral-induced mediator release was mainly apical suggesting that viral-induced MMP and growth factor release in the polarised EMTU model is epithelial derived. Furthermore, in the apical compartment, viral-induced responses in the EMTU model did not differ significantly to equivalent HBEC monocultures suggesting that fibroblasts do not modulate the epithelial response. However, constitutive basolateral MMP-9 release was significantly suppressed in the polarised EMTU model compared to HBEC monocultures. These data are consistent with a recent study by Iskandar *et al.,* where constitutive basolateral MMP-9 release was reduced in co-cultures of ALIs and fibroblasts compared to ALI monocultures [261]. However, this suppression was not significant in the primary EMTU model. This could be due to the short time the cells are in co-culture compared with the polarised EMTU model of 7 days and in the Iskandar *et al* study of 45 days [261]. In contrast to MMP-9, there was a trend for increased basolateral MMP-2 release in the polarised EMTU model compared to HBEC and fibroblast monocultures, which was significant in the primary EMTU model. This increase is probably the cumulative effect of co-culturing both cell

types rather than a synergistic enhancement in the response, as considerable MMP-2 levels were detected in both HBEC and fibroblast monocultures. These data suggest that the presence of fibroblasts has no effect on the apical release of viral-induced MMPs and growth factors but suppresses constitutive MMP-9 release.

Consistent with the apical polarity of MMP and growth factor release, dsRNA-stimulation of the epithelium had no effect on fibroblast proliferation within the EMTU model. This is in contrast to a previous studies which showed that epithelial-derived bFGF from non-polarised virally-infected HBECs have paracrine effects on fibroblast proliferation [116]. These differences could be partly explained by differences in cell type, stimuli (HRV *cf.* dsRNA), cell confluency or timing of the DNA synthesis assays. Another major difference is that previous studies used conditioned medium from non-polarised epithelial cells (BEAS-2B or primary HBECs), as opposed to my study using polarised, integrated co-cultures, which more closely reflects the structural organisation of the EMTU.

The apical polarity of viral-induced release of mediators involved in repair was unexpected, as *in vivo* the main substrates of MMP-9 and MMP-2 (e.g. collagen IV, elastin, vitronectin and aggrecan) are subepithelial [262]. However, MMP-9 [168], MMP-2 [169], bFGF [171] and VEGF [263] are increased in the BALF of asthmatic subjects. In addition bFGF [116] and VEGF [256] are increased in nasal aspirates during HRV-associated asthma exacerbations. I acknowledge that the source of these mediators in the BALF and nasal aspirates may include multiple cell types. Nevertheless, their detection in the airways could suggest that apical MMP and growth factor release occurs *in vivo.* It is therefore interesting to speculate about the role of these factors at the apical epithelial surface. Basic FGF has been shown to enhance cell-associated and soluble collagen and intra- and extracellular fibronectin in 16HBE cells [264]. These matrix components can influence cell behaviour including chemotaxis, proliferation, cell migration and attachment, important functions in repair responses. In a study by Brown *et al.*, treatment of fetal lung explants with exogenous VEGF induced airway epithelial cell proliferation [265]. In another study, faster growth rates were observed in nasal airway epithelial cells from patients with chronic rhinosinusitis and could be inhibited by blocking VEGF signalling [266]. Together these studies suggest that apical dsRNA-dependent

VEGF and bFGF release has the potential to induce epithelial proliferation. This could be investigated as part of future work, using the Click-iT EdU assay, although some additional assay optimisation may be required. Activation of epithelial proliferation may be particularly important during viral infection, where infected cells are shed as part of the innate response and the remaining cells need to proliferate to maintain the epithelial barrier.

The apical release of MMP-2 and MMP-9 may also co-ordinate epithelial responses to viral infection. While the main substrates for MMP-2 and MMP-9 are ECM and basement membrane components such as gelatinous collagens [262], other substrates include cell- or ECM-associated growth factors [262]. These growth factors (bFGF, VEGF, TGF and EGF) may be released at the apical epithelial surface by MMP activity [262, 267, 268] and contribute to the proliferative effects of MMPs [260, 262]. MMP activity is regulated by two key mechanisms; (1) secreted MMPs need to be activated by removal of their pro-domain by extracellular proteases and (2) the ratio of MMPs to TIMPs needs to be reduced for MMPs to be active [262]. While MMP activity and TIMP levels were not assessed in the EMTU co-culture model, previous studies have demonstrated increased MMP-9 activity in supernatants from HRV1B-infected HBECs [116] while having no effect on TIMP-1 activity [114]. In contrast, viral-mediated MMP-2 expression and activity was unaffected [114, 269]. However, these studies were carried out in monolayer cultures and may not reflect what is occurring within the integrated, polarised EMTU model. Therefore, MMP activity should be assessed as part of future work for example, using zymography or a commercially available fluorometric assay kit.

4.4.2 Lack of a role for IL-1 in the release of mediators involved in repair

Given the importance of epithelial-derived IL-1α in driving inflammatory responses within the EMTU, I investigated whether this mediator also had effects on repair responses. However, results presented in this chapter suggested that IL-1α had no effect on viral-induced MMP-2, MMP-9, VEGF and bFGF release in both the polarised and primary EMTU model. This contrasts with previous studies which demonstrated a role for IL-1α in regulating MMP

[270-273] and growth factor release [274-276] in a range of fibroblast cultures derived from non-lung tissues. Only recently (July 2016) the effect of epithelial-derived IL-1α on fibroblast responses within the airway EMTU was investigated and demonstrated a reduction in TGF-β_1 and ECM components including collagen Iα, decorin and fibulin in fibroblasts [161]. However this study did not investigate the effect of an activated epithelium. As mentioned in results section 4.2.2, my experiments using IL-1Ra were difficult to interpret due to the low signal to noise ratio observed in viral-induced MMP and growth factor release which was less robust than dsRNA-induced proinflammatory mediator release. This could be improved by increasing the power of the study. Future work could also examine the effect of IL-1 signalling on other mediators and aspects of the repair response (e.g. ECM production, myofibroblast differentiation). Finally it is important to consider that IL-1α may have indirect effects on repair responses *in vivo* due to its effects in mediating proinflammatory mediator release. For example, IL-1α induces IL-6 which is a pro-fibrotic cytokine affecting fibroblast differentiation and survival [277, 278]. Also IL-1α induces CXCL8 which is chemotactic for fibroblasts [279] and may promote subepithelial fibrosis by increasing fibroblast migration to the subepithelial fibroblast sheath.

4.4.3 Effect of viral-stimulation of the epithelium on fibroblast activation within the EMTU co-culture models

Within the EMTU, fibroblasts not only have important inflammatory functions (as observed in chapter 3), but also have functions in tissue repair. Following epithelial activation, mediator release from the epithelium (e.g. TGF-β) and changes in ECM deposition, composition, structure and stiffness lead to activation of fibroblast proliferation and differentiation to a myofibroblast phenotype with expression of α-SMA stress fibres [165].

Fibroblast proliferation in the polarised EMTU model was assessed using (low FBS) conditions optimised for detection of DNA synthesis. Under these conditions dsRNA-induced effects on TER and proinflammatory mediator release were enhanced compared to standard culture conditions suggesting that the EMTU model was more sensitive to dsRNA stimulation. This may be, in

part, explained by the reduced levels of growth factors and anti-inflammatory mediators including TGF-β present in FBS, which would help maintain epithelial barrier function and reduce cytokine responses. Despite this, I was unable to detect an effect of dsRNA stimulation on fibroblast proliferation which contrasts a previous study where conditioned medium from HRV-infected primary HBEC monolayers stimulated HLF proliferation [116]. This difference can be explained by the polarity of release of growth factors in my study, which was not considered in the study by Skevaki *et al.* [116], as discussed in section 4.4.1.

In addition to proliferative responses, the effect of dsRNA stimulation on fibroblast differentiation was investigated in the EMTU models by staining for the myofibroblast marker, α-SMA. Previously, constitutive primary HLF α-SMA expression was reduced in co-cultures with 16HBEs, when compared to fibroblast monocultures [161]. Consistent with this study, we observed a similar effect on α-SMA staining in the polarised EMTU co-culture model at baseline, when compared to equivalent fibroblast monocultures (see Appendix A, Figure A2). In another study, constitutive fibroblast α-SMA expression was increased in co-cultures with primary HBECs from asthmatic donors compared to HBECs from non-asthmatic donors [175]. Together these studies suggest that epithelial cells are important modulators of fibroblast α-SMA expression in co-culture. However, my results are the first study to investigate the effect of a virally infected epithelium on fibroblast differentiation. In this chapter, I demonstrate an increase in α-SMA staining intensity and fibres in the polarised EMTU model following dsRNA-stimulation. These increases could not be replicated in the primary EMTU model infected with HRV. However, this could be explained by differences in the magnitude of responses between the models, which as discussed for inflammatory responses in (chapter 3 section 3.5.2), are less robust in the HRV-stimulated primary EMTU model compared to the dsRNA-stimulated polarised EMTU model. Another explanation could be the timing of when the response occurs. Both models were fixed and stained at the 24h time point, but for a response to HRV the virus first needs to infect the epithelial cells and replicate to generate dsRNA. This is in contrast with the bolus treatment with exogenously added dsRNA. The response to HRV may therefore be observable at a later time point.

Alternately, an earlier time point could be examined as the viral-induced increase in α-SMA expression may be a transient effect and resolve, as would be expected in an acute wound response. Another difference between the polarised and primary EMTU models is the cell culture media. Different supplements in these media may lead to high levels of α-SMA at baseline, saturating the assay and making dsRNA-induced effects difficult to detect. For example, ALI starvation medium contains insulin which activates the same receptor as IGF-1; a mediator previously shown to activate myofibroblast differentiation [280]. Whether the presence of insulin in ALI starvation medium affects the detection of HRV-induced α-SMA is yet to be investigated and would be important for future assay optimisation as well as determining the optimum time point for detection.

Following the finding that dsRNA induces increased fibroblast α-SMA staining in the polarised EMTU co-culture model; I was interested to investigate the mechanism behind this response. TGF-β is a well-documented stimulus of myofibroblast proliferation and persistence [165]. In addition, respiratory viruses (respiratory syncytial virus (RSV) [281] and influenza [282]), have previously been shown to induce TGF-β expression and release [281] or increased TGF-β activity [282] in epithelial cell cultures. However, reports on the effect of HRV on TGF-β have been conflicting. For example, TGF-β_1 expression and release was significantly increased in cultures of HRV16-infected BET-1A HBECs, compared to uninfected controls [258]. A similar trend was also observed in another study, using BEAS2B cells [259]. In contrast, changes in TGF-β levels could not be detected in RV1B-infected primary HBEC monolayers [144], or in the EMTU model following dsRNA-stimulation. Although this discrepancy between studies could be due to differences in culture type and/or viral stimuli, the differences could also be due to difficulties with the detection of TGF-β. For example, one difficulty with TGF-β detection in the EMTU co-culture model is the presence of FBS in the cell culture medium. FBS is important for maintenance of the epithelial barrier but is also a source of TGF-β. Its presence in the culture medium could therefore obscure any dsRNA-dependent effects on TGF-β release from the epithelium or fibroblasts. In addition TGF-β is notoriously difficult to detect due to its expression in a cell or ECM-associated latent form. This form may be locally activated, released at low concentrations and quickly cleared from solution by

binding to cell-surface receptors, ECM or serum proteins such as α-2-macroglobulin (α_2M) [283-285]. Therefore, although TGF-β could not be detected, it does not rule out a role for TGF-β in mediating dsRNA-induced increases in α-SMA staining in the polarised EMTU model. Similarly, in a study by Bedke *et al.,* although active TGF-β could not be detected, a pan-TGF-β neutralising antibody had a suppressive effect on viral replication [144]. I therefore investigated the effect of a pan-TGF-β neutralising antibody within the EMTU model and observed a reduction in dsRNA-induced α-SMA staining. This suggests that TGF-β has a role in mediating the increase in α-SMA staining by dsRNA, despite being below the detection limit of the ELISA.

One disadvantage of using the pan-TGF-β antibody in my experiments was that the TGF-β isoform responsible for dsRNA-induced increases in α-SMA staining could not be identified. In previous studies, the main isoform detected following viral infection of epithelial cells was TGF-β_1 [258, 259]. However, TGF-β_2 may also be involved in dsRNA-induced increases in α-SMA as it is reported to be the predominant isoform constitutively expressed by the epithelium [143, 286] and could become activated following dsRNA-stimulation. While TGF-β may be epithelial-derived, a substantial amount of latent TGF-β was also detected in the cell culture medium and could potentially become activated following dsRNA-stimulation of the polarised EMTU model. Future work could use PCR to investigate the cellular source and isoforms of TGF-β involved or immunofluorescence to detect cell-surface associated TGF-β.

A diverse group of mechanisms have been reported to activate the latent TGF-β complex. These include activation by interacting with integrins at the cell surface. The first integrin to be identified as a TGF-β activator was $\alpha_v\beta_6$, which is normally expressed at low levels by epithelial cells and upregulated in response to wounding or inflammation [285, 287]. The integrin $\alpha_v\beta_6$ may therefore be upregulated following dsRNA-stimulation leading to increased TGF-β activation. Binding of latent TGF-β to $\alpha_v\beta_6$ induces a conformational change, which liberates TGF-β from its latent complex. In addition, integrin binding may also bring latent TGF-β into close proximity with MMPs localised to the cell surface which can remove the latent complex by proteolysis [287,

288]. MMPs are also reported to activate TGF-β independently of integrin binding. Interestingly, these include MMP-2 and MMP-9 [267, 289], which were both detected in the polarised EMTU model. Therefore another avenue of future investigation could be to investigate the effects of inhibiting MMP activity on TGF-β-induced increases in α-SMA. In summary, dsRNA stimulation of the polarised EMTU model potentially activates a variety of TGF-β activation mechanisms.

In addition, to inducing fibroblast α-SMA expression, TGF-β is also known to induce expression of growth factors and ECM components [290-292]. Furthermore, previous *in vitro* studies have shown that HRV induces ECM component expression (Collagen V) by HBEC and fibroblast monocultures [115] and that HBECs can modulate ECM component expression (e.g. collagen I, collagen III) by fibroblasts in co-culture [174]. Future work could therefore investigate the effect of viral stimulation on growth factors and ECM components in the absence or presence of pan-TGF-β antibody.

4.4.4 Consequences of viral-induced repair and remodelling in asthma

In this chapter I have demonstrated that viral-stimulation of the epithelium activates a variety of repair responses within the EMTU. These include the polarised release of MMPs and growth factors, as well as myofibroblast differentiation via TGF-β. These viral-induced repair responses could potentially have important consequences *in vivo.* For example, when the airways are still growing and developing during childhood, they may be more vulnerable to the effects of HRV-induced repair and remodelling factors [26]. Thus, HRV infection may reveal a pre-existing tendency for airway remodelling and asthma development [26].

HRV infection may also promote repair and remodelling in established asthma. In line with this MMP-2, MMP-9, VEGF and bFGF, which were all induced by viral stimulation of the EMTU model, are also elevated in the BALF and/or biopsies of asthmatic compared to healthy subjects [167, 169, 171-173]. In addition, a study by Oshita *et al.* showed that circulating MMP-9 was elevated in patients with asthma exacerbations compared to patients with stable asthma

[255]. However, it was not investigated whether the exacerbations in the Oshita *et al.* study were associated with HRV infection [255].

The effects of HRV-induced growth factors may be further augmented in the asthmatic airway, where the EMTU is dysregulated. For example, impaired IFN responses by the asthmatic epithelium lead to reduced virus-induced apoptosis and increased viral replication [148], which may lead to a greater magnitude of viral-induced MMP and growth factor release. In addition, while viral-induced MMP and growth factor release was mainly apical in the EMTU model, in the asthmatic airway epithelial barrier functions are disrupted [121]. This may allow the flux of HRV-induced MMPs and growth factors to the basolateral epithelial surface, leading to increased activation of fibroblast proliferation and differentiation. HRV infection of the EMTU may also stimulate fibroblast differentiation via TGF-β and as discussed in section 4.4.3., viral stimulation has the potential to upregulate mechanisms of TGF-β activation [287]. This may have important consequences in asthma where TGF-β_2 expression and release is increased in bronchial biopsies [143] and primary HBEC monolayers respectively [144]. For example, HRV-infection in asthma may further increase active TGF-β_2 levels in the EMTU and promote increased myofibroblast differentiation.

Despite increasing evidence of a role for HRV in airway repair using *in vitro* models, only a limited number of studies have investigated its effects *in vivo.* For example, in subjects with confirmed HRV infections, MMP-9 was elevated in nasal lavage samples [114]. In another study, epithelial expression of remodelling genes (e.g. tenascin C and MMP-12) was significantly induced following experimental HRV infection of healthy volunteers [293]. Although these studies provide insight into the effects of HRV *in vivo*, it is unknown whether single or repeated bouts of infection affect lung structure and function in asthma and asthma development due to ethical reasons.

4.4.5 Summary

Cellular cross-talk is essential for the activation and co-ordination of tissue repair responses within the EMTU. While several *in vitro* studies have investigated EMTU repair mechanisms in response to chemical and mechanical

injury, studies examining EMTU repair responses to HRV have not fully addressed the relationship between structural organisation and function. Here I used integrated co-culture models of the EMTU to examine responses to viral stimulation and demonstrated for the first time the apical polarity of viral-induced MMPs and growth factor release. My study highlights the importance of the epithelial barrier and vectorial mediator release in modelling EMTU responses, as viral-induced release of growth factors into the apical compartment failed to activate fibroblast proliferation in the basolateral compartment. Although fibroblast proliferation was unaffected by viral stimulation of the polarised EMTU model, an increase in myofibroblast differentiation was observed which was mediated by TGF-β. Together these data suggest that HRV infection has the potential to activate repair and remodelling responses within the EMTU.

5. Inflammatory and repair responses to pLArg in a co-culture model of the airway EMTU

5.1 Introduction

Inhaled environmental agents such as viruses, cigarette smoke, pollution, dust or pollen can cause notable disruptions in tissue homeostasis, leading to activation of proinflammatory and repair responses within the EMTU. However, in chronic inflammatory diseases such as asthma, host derived factors can also cause significant disruptions in tissue homeostasis. For example eosinophils, may disrupt homeostasis by release of their granule contents following activation. The predominant constituent of the eosinophil granule is MBP [133]; an arginine rich polycation. In the asthmatic airway, increased numbers of degranulated eosinophils are localised to the bronchial epithelium [132, 133] and MBP is elevated in the sputum and BALF [134, 294]. Furthermore, MBP has been detected in mucus plugs and on damaged epithelial surfaces in lung tissue from patients who died from asthma [131]. MBP has therefore been associated with the pathogenesis of epithelial damage in asthma [133].

MBP is highly cytotoxic and has previously been shown to damage guinea pig tracheal epithelium *in vitro* [135] and reduce ciliary activity in rabbit tracheal explants [136]. While these studies used MBP purified from eosinophils, the majority of studies have used a mimetic; pLArg. Similarly to MBP, pLArg is positively charged. It is this property that allows MBP and pLArg to bind to negatively charged cell membranes, where they exhibit their cytotoxic effects [190]. For example, following treatment of HBECs with pLArg, cell membranes appeared damaged with pores and leakage of cell ions was increased [189]. In addition there was evidence of apoptosis and necrosis including mitochondrial and nuclear damage [189]. pLArg also increased penetration of lanthanum cations (electron microscopic stain) into intracellular spaces, indicating TJ damage [189]. Furthermore, decreased plakoglobin immunoreactivity following pLArg challenge indicated desmosomal damage [189]. Polycationic proteins,

such as MBP, are therefore host-derived factors that have the potential to disrupt tissue homeostasis and activate the EMTU.

Only a limited number of studies have examined the effects of MBP or pLArg on inflammatory and repair responses *in vitro*. The majority of these studies were carried out using HBEC monocultures. For example, pLArg has been shown to induce release of proinflammatory mediators from 16HBE cell monocultures, including IL-6, CXCL8 and IL-1α [137]. In another study, MBP isolated from eosinophils stimulated epithelial expression of mediators associated with repair including ET-1, TGF-α, TGF-β1, PDGF-β, EGFR, MMP-9, fibronectin, and tenascin [139]. These epithelial-derived mediators could potentially have paracrine effects and only a limited number of studies have investigated this. For example, in epithelial-fibroblast co-cultures, pLArg stimulation of the epithelium activated HLF proliferation and was partly mediated by bFGF, PDGF and ET-1 [138]. However, no other studies have investigated cellular cross-talk or the integrated responses to pLArg in a polarised, co-culture model of the EMTU. The importance of epithelial-mesenchymal cross-talk and polarised mediator release were demonstrated in chapters 3 and 4, where responses to an environmental stimulus (virus) were investigated. In this chapter, I will investigate the effect of pLArg stimulation on inflammatory and repair responses within the polarised EMTU co-culture model.

5.2 Characterisation of proinflammatory responses to pLArg stimulation

5.2.1 Optimisation of pLArg concentrations for stimulation of the polarised EMTU co-culture model

The effects of eosinophilic MBP were modelled using the synthetic mimic, pLArg. Initial concentration response experiments were carried out using polarised HBEC monocultures to determine the optimum pLArg concentration with which to stimulate the EMTU co-culture model.

Firstly, the effect of pLArg on ionic permeability was investigated. HBECs were challenged with increasing concentrations of pLArg (0.1-10μM) and TER was monitored over 24h (Figure 5.2.1-1A). After 1h, pLArg (≥0.3μM) induced significant reductions in TER. These reductions in TER were maintained at 6h and 24h in HBEC monocultures stimulated with 1-10μM but not 0.3μM.

The effects of pLArg on proinflammatory mediator release in HBEC monocultures was next determined following the collection of apical and basolateral supernatants 24h after challenge and assayed for IL-6 (Figure 5.2.1-1B). pLArg significantly induced apical IL-6 release at concentrations of ≥1μM, whereas in the basolateral compartment IL-6 release was only induced at the highest pLArg concentration tested of 10μM (Figure 5.2.1-1B).

To determine the effects of pLArg on cell viability, HBEC monocultures were visualised by light microscopy 24h post-pLArg stimulation. pLArg-induced cell death was observable at concentrations of 1-10μM (Figure 5.2.1-2A). This was confirmed for cultures stimulated with 10μM pLArg, which showed a significant fold increase in the apical release of the cytosolic enzyme LDH (Figure 5.2.1-2B). These data indicate that pLArg is cytotoxic at higher concentrations.

Therefore for the investigation of responses to pLArg in the co-culture model, 1μM pLArg was chosen; a concentration that exhibited minimal effects on cell viability and significant effects on ionic permeability and cytokine release.

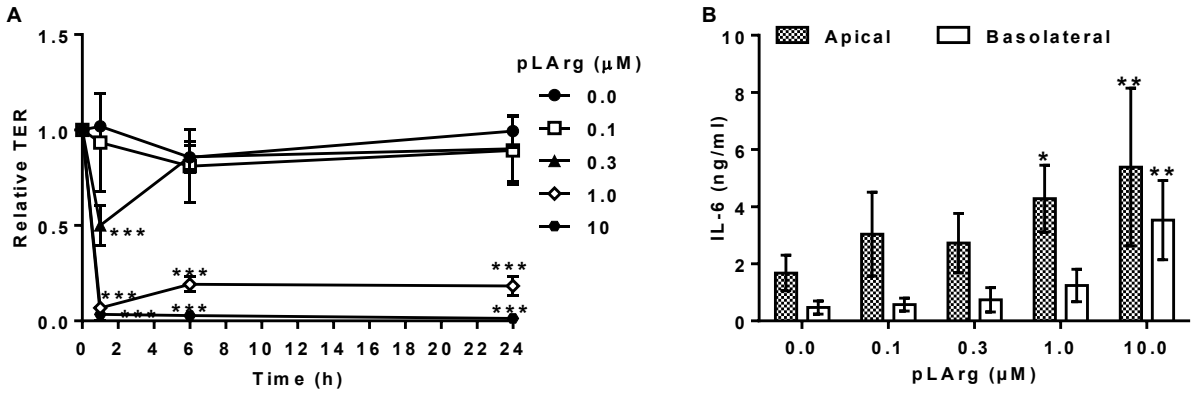

Figure 5.2.1-1 Responses of HBEC monocultures to pLArg stimulation.

Polarised HBECs were apically challenged with pLArg (0.1-10µM). TER was measured at 1, 6 and 24h post-stimulation and expressed as TER relative to the TER value of the Transwell® prior to challenge (A). After 24h, apical and basolateral cell-free supernatants were harvested and assayed for IL-6 (B). Results are means ± SD, n=4 independent experiments for all treatments except 0.3µM PLA where n=3 independent experiments. Differences between untreated controls and stimulated cultures were tested for statistical significance by two-way ANOVA with Bonferroni correction for multiple comparisons and are indicated by *$P \leq 0.05$, **$P \leq 0.01$ and ***$P \leq 0.001$.

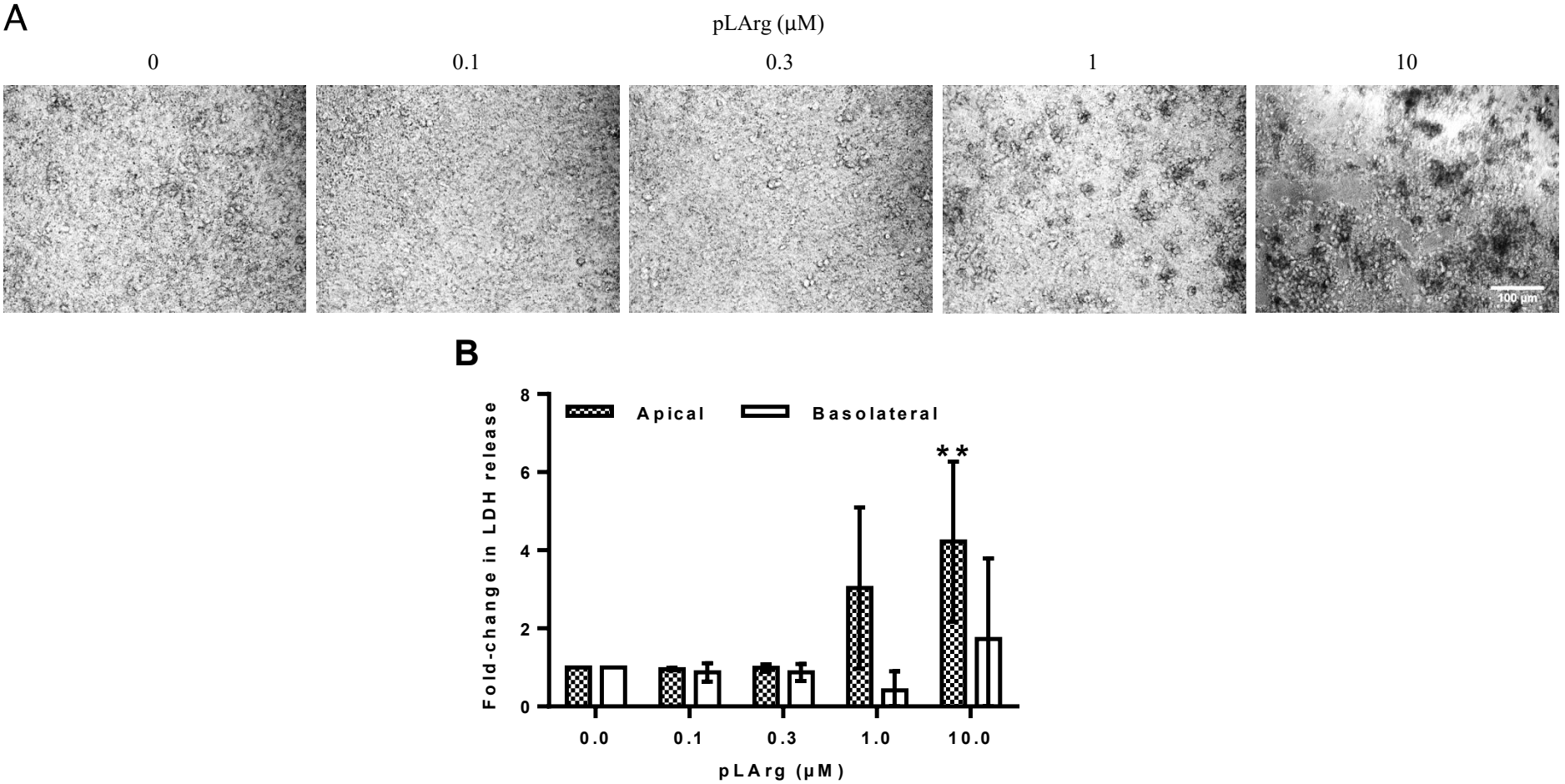

Figure 5.2.1-2 Cytotoxicity of pLArg.
Polarised HBECs were apically challenged with pLArg (0.1-10μM) and imaged on a light microscope 24h after challenge (A) (magnification x20, representative of 3 experiments). Apical and basolateral supernatants were harvested and assayed for LDH release (B) (results are means ±SD, n=3-4 independent experiments. Differences between untreated controls and stimulated cultures were tested for statistical significance by two-way ANOVA with Bonferroni correction for multiple comparisons and are indicated by $^{**}P \leq 0.01$.

5.2.2 Effect of pLArg on epithelial barrier functions of the EMTU model

To examine the effects of pLArg on epithelial barrier functions of the EMTU model, pLArg (1μM) was applied apically and ionic and macromolecular permeability were determined 24h post-stimulation by monitoring TER and FITC-dextran fluorescent diffusion respectively (Figure 5.2.2-1).

PLArg increased ionic permeability of the EMTU model with a significant decrease in TER 1h after challenge, which was comparable to HBEC monocultures (Figure 5.2.2-1A). While this reduction in TER was maintained at 6 and 24h in both cultures, there was a significant partial recovery in TER in the EMTU co-culture model compared to the initial pLArg-induced drop at 1h ($P \leq 0.05$).

To examine epithelial barrier function further, the macromolecular permeability of the epithelium was determined by measuring diffusion of FITC-dextran from the apical to the basolateral compartment between 21-24h after pLArg challenge (Figure 5.2.2-1B). In fibroblast monocultures, which do not form TJs, 70-80% FITC-dextran diffusion was observed compared to an empty Transwell®. In contrast, in unstimulated HBEC mono- and co-cultures with fibroblasts, FITC-dextran diffusion was less than 5% of an empty Transwell® (Figure 5.2.2-1B). Following pLArg stimulation there was a trend for increased FITC-dextran diffusion in HBEC monocultures, which was not observed in the EMTU co-culture model (Figure 5.2.2-1B). This is consistent with the TER data in which there was some recovery of barrier functions in the EMTU model compared to HBEC monocultures. Taken together these data suggest that although pLArg disrupts the ionic permeability of the epithelium, the movement of macromolecules (>4kDa) across the epithelial layer via the paracellular route is restricted, indicating maintenance of polarised functions in the EMTU model.

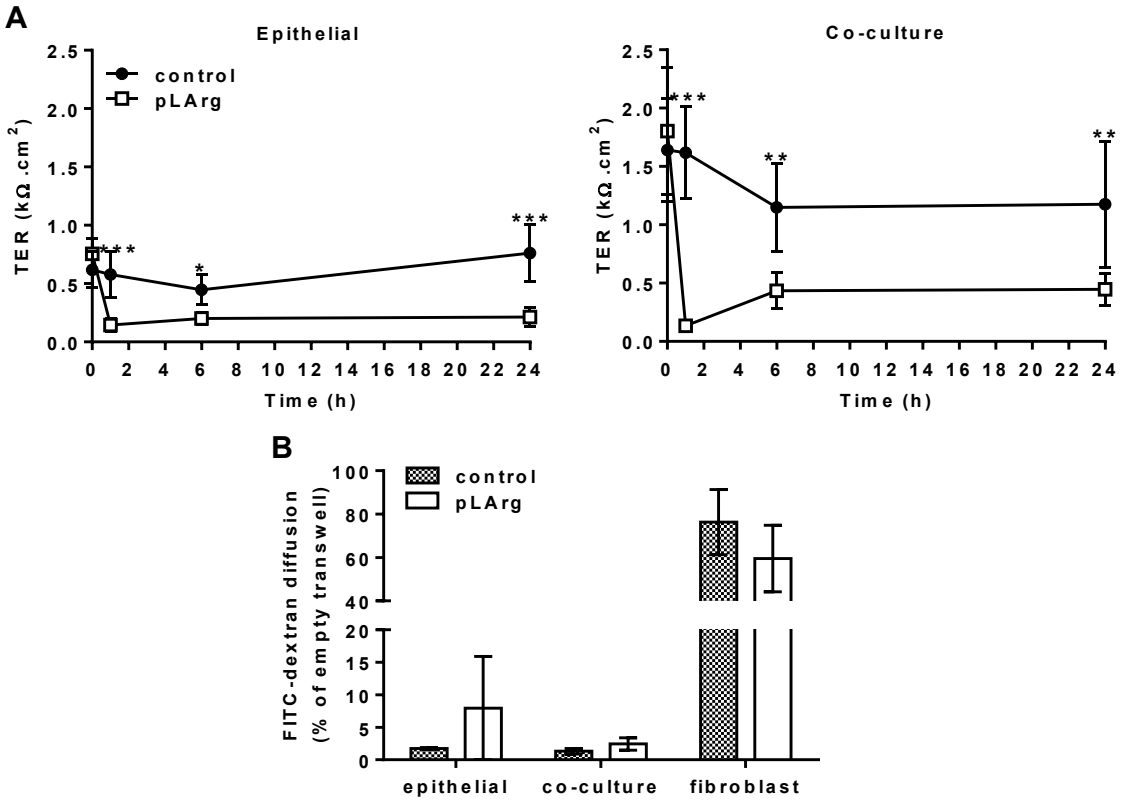

Figure 5.2.2-1 Effect of pLArg on epithelial barrier function in HBEC mono and co-cultures with fibroblasts.

Following successful polarisation of the epithelium, mono- and co-cultures were stimulated with pLArg (1μM). TER was measured at 1, 6 and 24h post-stimulation (A) while diffusion of FITC-labelled dextran was determined between 21-24h (B). Results are means ± SD, n=7 independent experiments for TER measurements, n=4-5 independent experiments for FITC-dextran measurements. Differences between stimulated and unstimulated cultures were tested for statistical significance by two-way ANOVA with Bonferroni correction for multiple comparisons and are indicated by *$P \leq 0.05$, **$P \leq 0.01$ and ***$P \leq 0.01$.

5.2.3 pLArg-induced proinflammatory responses are enhanced in the basolateral compartment of the EMTU model

The effects of pLArg on innate immune responses in the EMTU model were investigated following apical stimulation of the epithelium with pLArg. After 24h apical and basolateral supernatants were harvested and assayed for proinflammatory mediators (IL-6, CXCL8, GM-CSF and CXCL10) by ELISA. Similar to dsRNA stimulated cultures (Chapter 3 section 3.2.4), pLArg significantly induced apical IL-6 and CXCL8 release in HBEC monocultures and the polarised EMTU model (Figure 5.2.3-1A, B). However, apical secretion of GM-CSF in pLArg- stimulated and unstimulated cultures was below the detection limit of the assay (Figure 5.2.3-1C).

In the basolateral compartment of the polarised EMTU model, constitutive IL-6 and CXCL8 release was significantly enhanced compared to HBEC monocultures (Figure 5.2.3-1D, E). Following pLArg challenge release of these mediators was significantly enhanced compared to the unstimulated control and HBEC monocultures (Figure 5.2.3-1D, E). There was also a trend for increased basolateral GM-CSF release following pLArg stimulation of the EMTU model, which reached significance compared to pLArg-stimulated HBEC monocultures but not the unstimulated control (Figure 5.2.3-1F). As expected the IFN-inducible chemokine, CXCL10, was not detected in the apical or basolateral compartment of unstimulated and pLArg-stimulated HBEC mono- and co-cultures with fibroblasts (data not shown). In the absence of HBECs, addition of pLArg to the apical compartment did not stimulate significant mediator release from fibroblasts attached to the under surface of the Transwell® (Figure 5.2.3-1). These data suggest that the enhanced proinflammatory mediator release in the basolateral compartment of the EMTU model is synergistic and indicates that epithelial-fibroblast cross-talk is occurring within the EMTU model at baseline and following pLArg challenge.

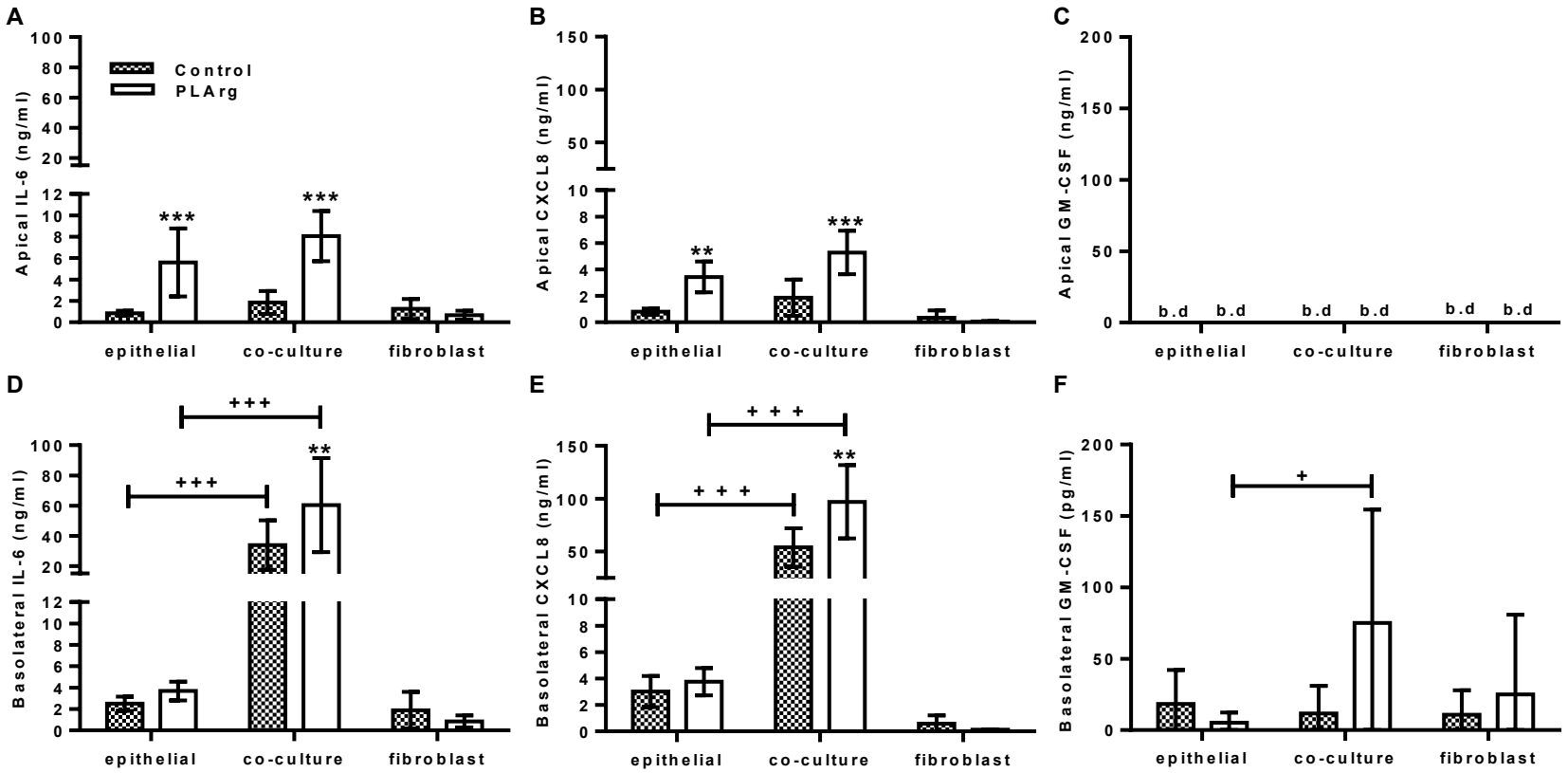

Figure 5.2.3-1 Cytokine and chemokine responses of HBEC and fibroblast mono- and co-cultures to pLArg stimulation.
Apical (A-C) and basolateral (D-F) cell-free supernatants were harvested 24h after stimulation with pLArg (1µM) and were assayed for IL-6 (A, D), CXCL8 (B , E) and GM-CSF (C, F) by ELISA. Results are means ± SD, n=3-5 independent experiments. Differences between groups were tested for statistical significance by two-way ANOVA with Bonferroni correction (control vs stimulated are indicated by $^{**}P \leq 0.01$ $^{***}P \leq 0.001$ and differences between cultures are indicated by $^{+}P \leq 0.05$, $^{++}$, $^{+++}P \leq 0.001$. b.d. indicates levels below the detection limit of the assay.

5.2.4 IL-1α is induced by pLArg stimulation of the EMTU model

The synergistic enhancement in pLArg-induced proinflammatory responses suggested that epithelial-fibroblast cross-talk was occurring within the EMTU model. IL-1α has previously been shown to be an important inflammatory mediator of cellular cross-talk [157, 160, 161], as demonstrated in Chapter 3. I therefore hypothesised that pLArg-induced basolateral proinflammatory responses in the polarised EMTU model were mediated by epithelial-derived IL-1α.

pLArg induced IL-1α release into the apical compartment of the EMTU model, which was comparable to HBEC monocultures (Figure 5.2.4-1A). While there was no induction of IL-1α in the basolateral compartment following pLArg stimulation there was a significant reduction in constitutive IL-1α levels in the polarised EMTU model compared to HBEC monocultures (Figure 5.2.4-1B). IL-1α was not detected in fibroblast monocultures, suggesting that pLArg-induced IL-1α is predominantly epithelial-derived (Figure 5.2.4-1). In contrast to IL-1α, IL-1β levels were below or close to the detection limit of the assay in all conditions tested. These data were consistent with dsRNA-stimulated cultures where IL-1α release was mainly apical and was not synergistically enhanced in the EMTU model.

IL-1α is constitutively expressed in the cytoplasm of cells and can be released actively or passively as an alarmin following necrotic cell death [231, 232]. Since pLArg can induce cell death I was interested to determine the extra- and intracellular levels of IL-1α following stimulation of HBECs with relatively low (1μM) and high (10μM) cytotoxic concentrations of pLArg. Low pLArg concentrations (1μM) resulted in a small increase in extracellular release of IL-1α into the apical but not the basolateral compartment and a significant upregulation of IL-1α intracellularly (Figure 5.2.4-2). In contrast, higher pLArg concentrations (10μM) resulted in a greater increase in extracellular release of IL-1α in both the apical and basolateral compartments than 1μM. This increase

extracellularly, corresponded with a significant reduction in intracellular IL-1α (Figure 5.2.4-2). Together these data suggest that at highly cytotoxic pLArg concentrations (10μM), intracellular IL-1α is released passively from necrotic cells while at lower pLArg concentrations (1μM) it is induced intracellularly, suggesting active induction.

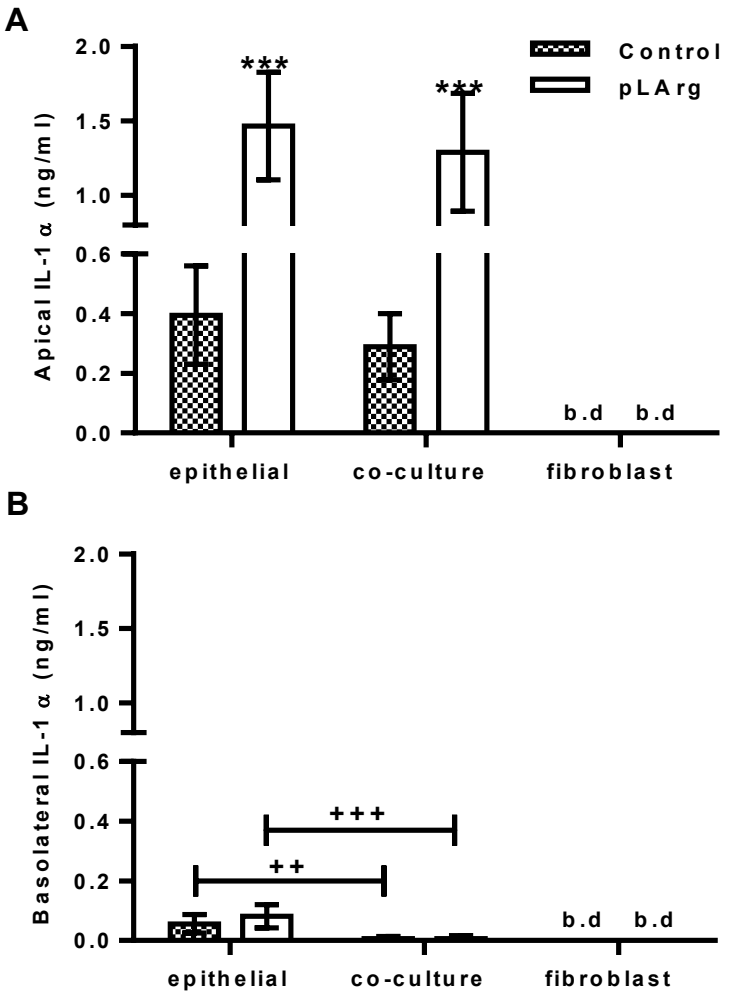

Figure 5.2.4-1 Comparison of IL-1α release from pLArg-stimulated HBEC and fibroblast monocultures with the polarised EMTU co-culture model.

Apical (A) and basolateral (B) cell-free supernatants were harvested 24h after challenge with pLArg (1μM) and assayed for IL-1α by Luminex®. Results are means ± SD, n=3-5 independent experiments. Differences between groups were tested for statistical significance by two-way ANOVA with Bonferroni correction (control vs stimulated are indicated by $^{***}P \leq 0.001$ and differences between cultures are indicated by $^{++}P \leq 0.01$ and $^{+++}P \leq 0.001$. b.d. indicates levels below the detection limit of the assay).

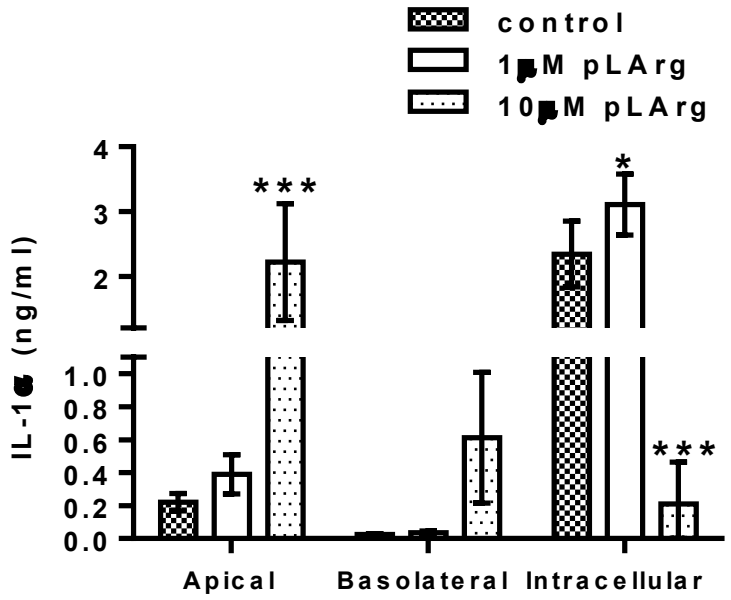

Figure 5.2.4-2 Effect of pLArg on extracellular and intracellular IL-1α in HBEC monocultures.

Cell-free supernatants from HBEC monocultures and HBEC cell lysates (lysed by 3 cycles of freeze/thaw) were harvested 24h after challenge with pLArg (1 and 10µM) and assayed for IL-1α by ELISA. Results are means ± SD, n=5 independent experiments. *$P \leq 0.05$ ***$P \leq 0.001$ for comparison between control and pLArg stimulated cultures (two-way ANOVA with Bonferroni correction).

5.2.5 Antagonism of IL-1 signalling inhibits pLArg-induced proinflammatory mediator release

To determine whether epithelial-derived IL-1α was an important mediator of pLArg-induced responses, IL-1Ra was added to either the apical, basolateral or both compartments of the polarised EMTU model prior to stimulation with pLArg. In the apical compartment, IL-1Ra partially reduced pLArg-dependent IL-6 and CXCL8 (Figure 5.2.5-1A-B) release and was most effective when added apically or to both compartments. In the basolateral compartment, IL-1Ra had the greatest effect when added basolaterally or to both compartments with complete abrogation of pLArg-dependent IL-6 and CXCL8 release (Figure 5.2.5-1C-D). Since IL-1β could not be detected, these data suggest that epithelial-derived IL-1α has an important role in driving proinflammatory responses to pLArg within the polarised EMTU model.

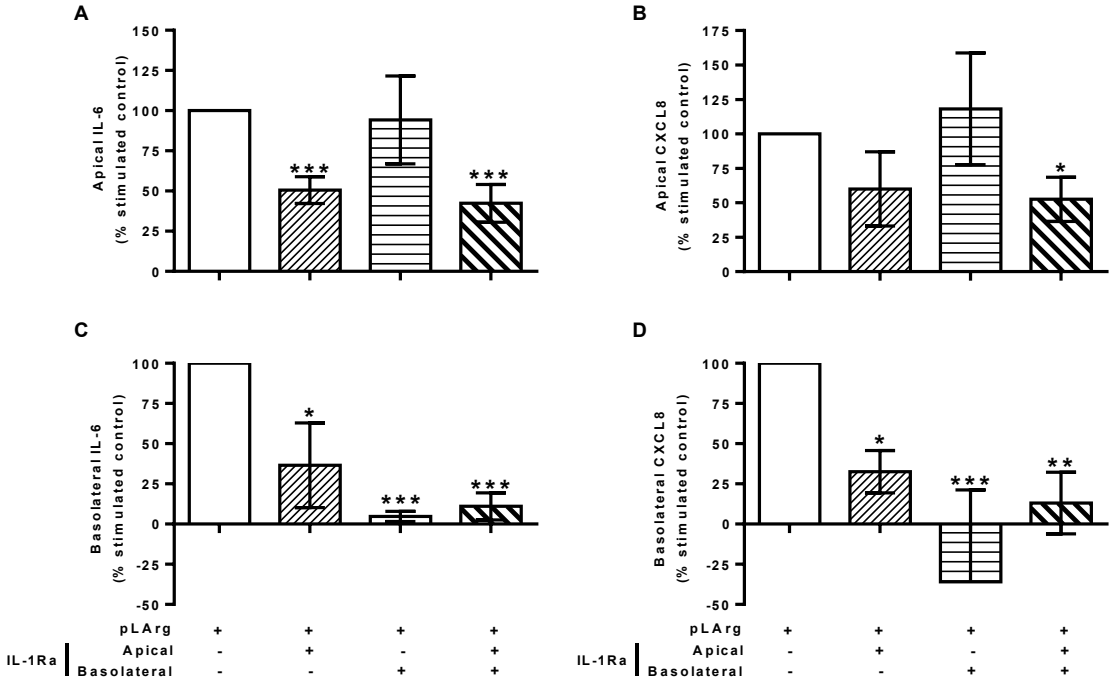

Figure 5.2.5-1 The effect of IL-1R antagonism on pLArg-induced cytokine and chemokine release in the polarised EMTU co-culture model.

The EMTU co-culture model was cultured in the absence or presence of IL-1Ra (500ng/ml) applied either apically, basolaterally or both for 1h prior to stimulation with pLArg (1μM). Apical (A-B) and basolateral (C-D) cell-free supernatants were harvested 24h after stimulation and assayed for IL-6 (A, C) and CXCL8 (B, D) by ELISA. To investigate the effects of IL-1Ra on pLArg-dependent responses, control mediator levels were subtracted from stimulated levels and expressed as a percentage of the response to pLArg. Results are mean responses compared to the pLArg-induced response in the absence of IL-1Ra (100%) ± SD, n=4-6 independent experiments. *$P \leq 0.05$, **$P \leq 0.01$, ***$P \leq 0.001$ for comparison between pLArg-stimulated cultures in the absence or presence of IL-1Ra (one-way ANOVA with Bonferroni correction).

5.3 Characterisation of repair responses to pLArg stimulation

5.3.1 PLArg stimulation of the EMTU model induces vectorial release of mediators involved in repair

Repair responses to pLArg stimulation were initially assessed by determining MMP and growth factor release following apical stimulation of the polarised EMTU model with 1μM pLArg. In the apical compartment, pLArg induced a small but not significant increase in MMP-9 and MMP-2 release from the EMTU co-culture model (Figure 5.3.1-1A-B). This was in contrast to HBEC monocultures where a significant increase in apical MMP-9 and MMP-2 was observed. Apical MMP-9 release was significantly reduced and MMP-2 release unchanged in pLArg-stimulated co-cultures compared to HBEC monocultures (Figure 5.3.1-1A-B). In the basolateral compartment, pLArg had no effect on MMP-9 and MMP-2 release (Figure 5.3.1-1C-D). However, basolateral MMP levels were modified between the culture types. For example, basolateral MMP-9 release was significantly reduced in both unstimulated and pLArg-stimulated co-cultures compared to HBEC monocultures (Figure 5.3.1-1C). These data suggest that cellular cross-talk is occurring and that fibroblasts have a suppressive effect on epithelial MMP-9 release. In contrast, there was a trend for increased basolateral MMP-2 release in the polarised EMTU model compared to HBEC monocultures (Figure 5.3.1-1D); due to the cumulative effect of co-culturing both cell types.

It should also be noted that in both the apical and basolateral compartments of fibroblast monocultures, pLArg had no effect on MMP-9 or MMP-2 release (Figure 5.3.1-1). These data, along with the apical polarity of pLArg-induced MMP release, suggest that within the EMTU co-culture model, HBECs are the main source of pLArg-induced MMP-9 and MMP-2.

The release of the growth factors, VEGF and bFGF, was next investigated in pLArg-stimulated EMTU co-cultures (Figure 5.3.1-2). In the apical

compartment, pLArg induced VEGF release, which was comparable with HBEC monocultures (Figure 5.3.1-2A). In contrast, pLArg had no effect on apical bFGF release (Figure 5.3.1-2B). In the basolateral compartment of the EMTU model, neither pLArg nor the presence of fibroblasts induced VEGF or bFGF release (Figure 5.3.1-2C-D). In fibroblast monocultures VEGF and bFGF were close to or below the detection limit of the assay. These data, along with the apical polarity of pLArg-induced release, suggest that within the EMTU co-culture model, HBECs are the main source of pLArg-induced VEGF.

Together these data demonstrate that following pLArg challenge of the EMTU model, there is a trend for increased apical MMP release and increased apical VEGF release, suggesting that cationic proteins activate EMTU repair responses.

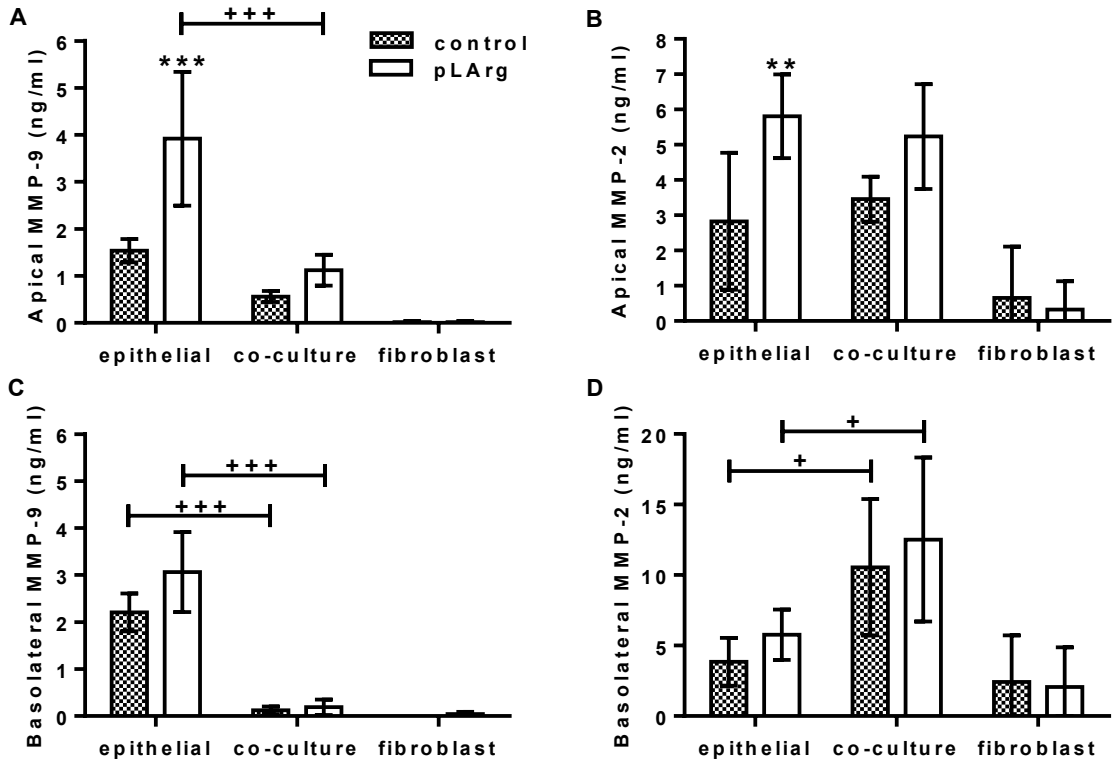

Figure 5.3.1-1 Effect of pLArg on MMP release in the polarised EMTU co-culture model.

Apical (A-B) and basolateral (C-D) cell-free supernatants were harvested from the EMTU co-culture model or HBEC and fibroblast monocultures 24h after challenge with pLArg (1μM), and assayed for MMP-9 (A,C), and MMP-2 (B,D) by Luminex® assay. Results were corrected for growth factor levels in the culture medium (below detection for MMP-9 & 0.08ng/ml MMP-2) and shown as means ± SD, n=3-5. $^{**}P \leq 0.01$, and $^{***}P \leq 0.001$ for comparison between control and pLArg stimulated cultures and $^{+}P \leq 0.05$ and $^{+++}P \leq 0.001$ for comparison between HBEC monocultures and the EMTU co-culture model (two-way ANOVA with Bonferroni correction).

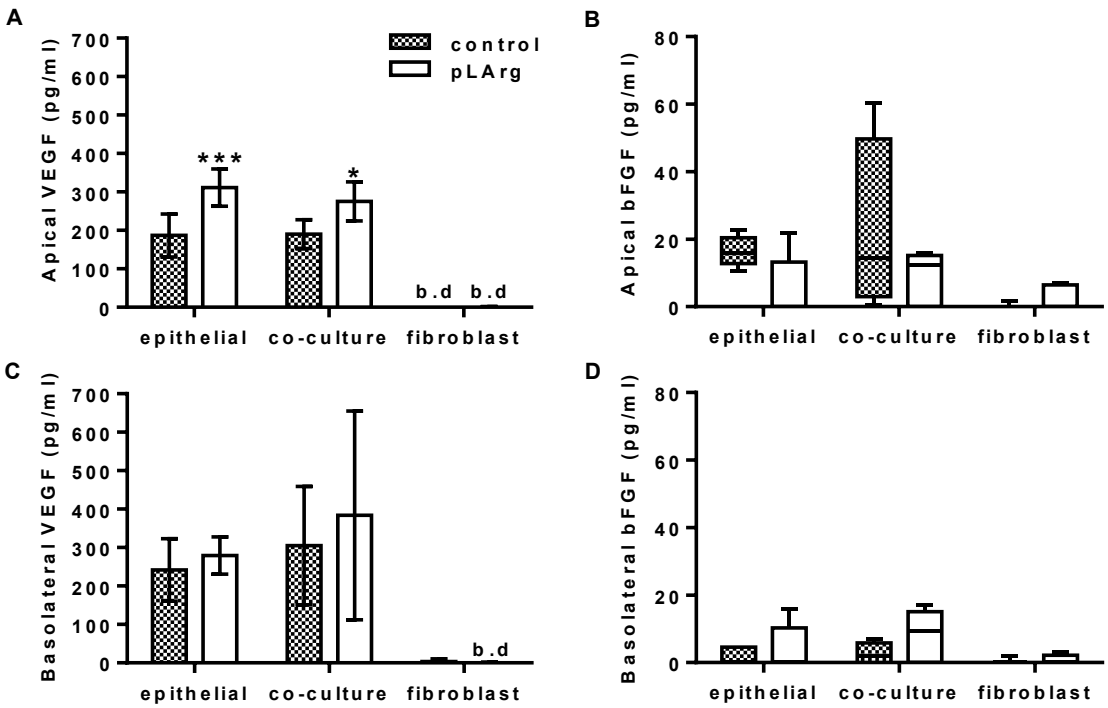

Figure 5.3.1-2 Effect of pLArg on growth factor release in the polarised EMTU co-culture model.

Apical (A-C) and basolateral (C-D) cell-free supernatants were harvested from the EMTU co-culture model or HBEC and fibroblast monocultures 24h after challenge with pLArg (1μM) and assayed for VEGF (A,C), and bFGF (B,D) by Luminex® assay. Results were corrected for growth factor levels in the culture medium (1.4pg/ml VEGF & 21pg/ml bFGF) and shown as means ± SD or box plots representing the median with 25% & 75% interquartile, and whiskers representing minimum & maximum values as appropriate, n=3-5 independent experiments. *$P \leq 0.05$, and ***$P \leq 0.001$ for comparison between control and pLArg stimulated cultures (two-way ANOVA with Bonferroni correction). b.d. indicates levels below the detection limit of the assay.

5.3.2 Effect of pLArg on fibroblast activation in the polarised EMTU model

To investigate the effect of pLArg on fibroblast repair responses within the polarised EMTU model, fibroblast proliferation was assessed using a Click-iT® EdU assay kit as described in Chapter 2 section 2.9. Consistent with the lack of bFGF induction and apical induction of VEGF, pLArg had no effect on fibroblast proliferation (Figure 5.3.2-1& Table 5.3.2-1). This was in contrast to a positive control of 10% FBS which induced an increase in EdU positive cells.

The effect of pLArg on differentiation of fibroblasts to myofibroblasts in the EMTU model was next investigated by assessing α-SMA staining by immunofluorescent microscopy. pLArg stimulation of the epithelium increased α-SMA staining intensity in the underlying fibroblasts (Figure 5.3.2-2A). At higher magnifications, increased α-SMA stress fibres were observed in pLArg-stimulated co-cultures (Figure 5.3.2-2B). These data suggest that pLArg stimulation of the epithelium promotes fibroblast differentiation to a myofibroblast phenotype, whilst having no effect on fibroblast proliferation in the EMTU model.

TGF-β is a strong inducer of α-SMA and myofibroblast differentiation [164] therefore the role of TGF-β signalling in the pLArg-induced response was investigated in the EMTU co-culture model. Initially, I determined the release of TGF-β isoforms in EMTU culture supernatants. However, pLArg had no effect on total TGF-β_1 and TGF-β_2 release, while the active forms were below the detection limit of the assay (data not shown). However, as discussed in Chapter 4, a role for TGF in α-SMA responses should not be discounted as this growth factor is notoriously difficult to measure. Therefore the effects of TGF-β neutralisation were investigated by addition of a pan-TGF-β neutralising antibody to the basolateral compartment of the polarised EMTU model and pLArg-mediated α-SMA expression determined. In a preliminary experiment, anti-TGFβ neutralising antibody inhibited the pLArg-induced increase in α-

SMA (Figure 5.3.2-3), suggesting that TGF-β has a role in pLArg-induced myofibroblast activation in the polarised EMTU model.

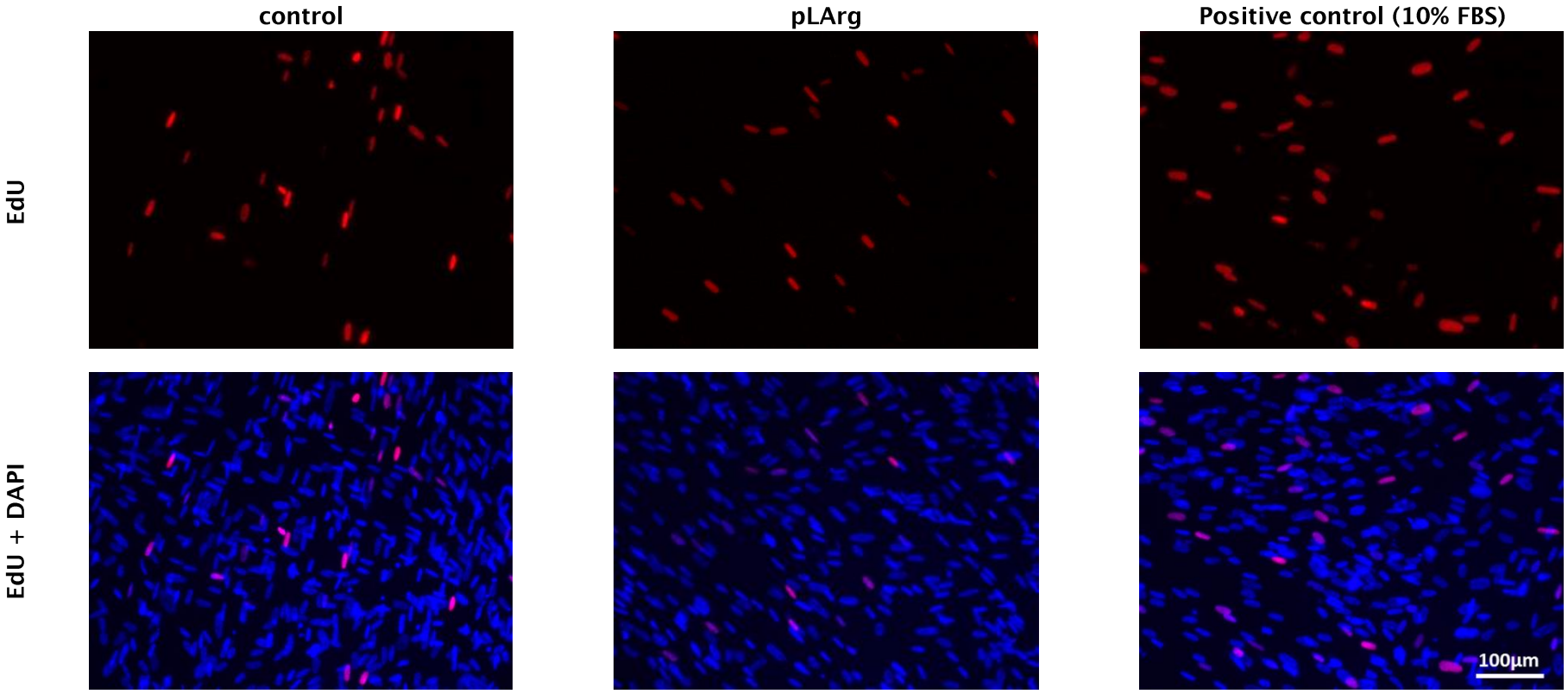

Figure 5.3.2-1 Effect of pLArg stimulation of the polarised EMTU model on fibroblast proliferation.
Co-cultures were fixed 36h after challenge with 1µM pLArg and proliferation assessed by detection of the fluorescently labelled thymidine analogue, EdU, into newly synthesised DNA using the immunofluorescent microscope. Red nuclei= EdU^+ cells, blue nuclei= DAPI stain. Images were taken at a magnification of x20 and are representative of 2 independent experiments.

Table 5.3.2-1 Effect of pLArg stimulation of the polarised EMTU model on fibroblast proliferation.

Co-cultures were fixed 36h after challenge with pLArg (1μM) and proliferation assessed using the Click-iT® EdU assay kit to detect incorporation of the fluorescently labelled thymidine analogue, EdU, into newly synthesised DNA. EdU incorporation was quantified by immunofluorescent microscopy. Cell counts for each experiment are the mean count from 3 fields of view at x20 magnification. Results are means from 2 separate experiments.

	control	**pLArg**	**positive control (10% FBS)**
Edu^+ cells/field of view	32	27	52
Total cells/field of view	477	426	392
% EdU^+ cells	7.1	6.4	13.3

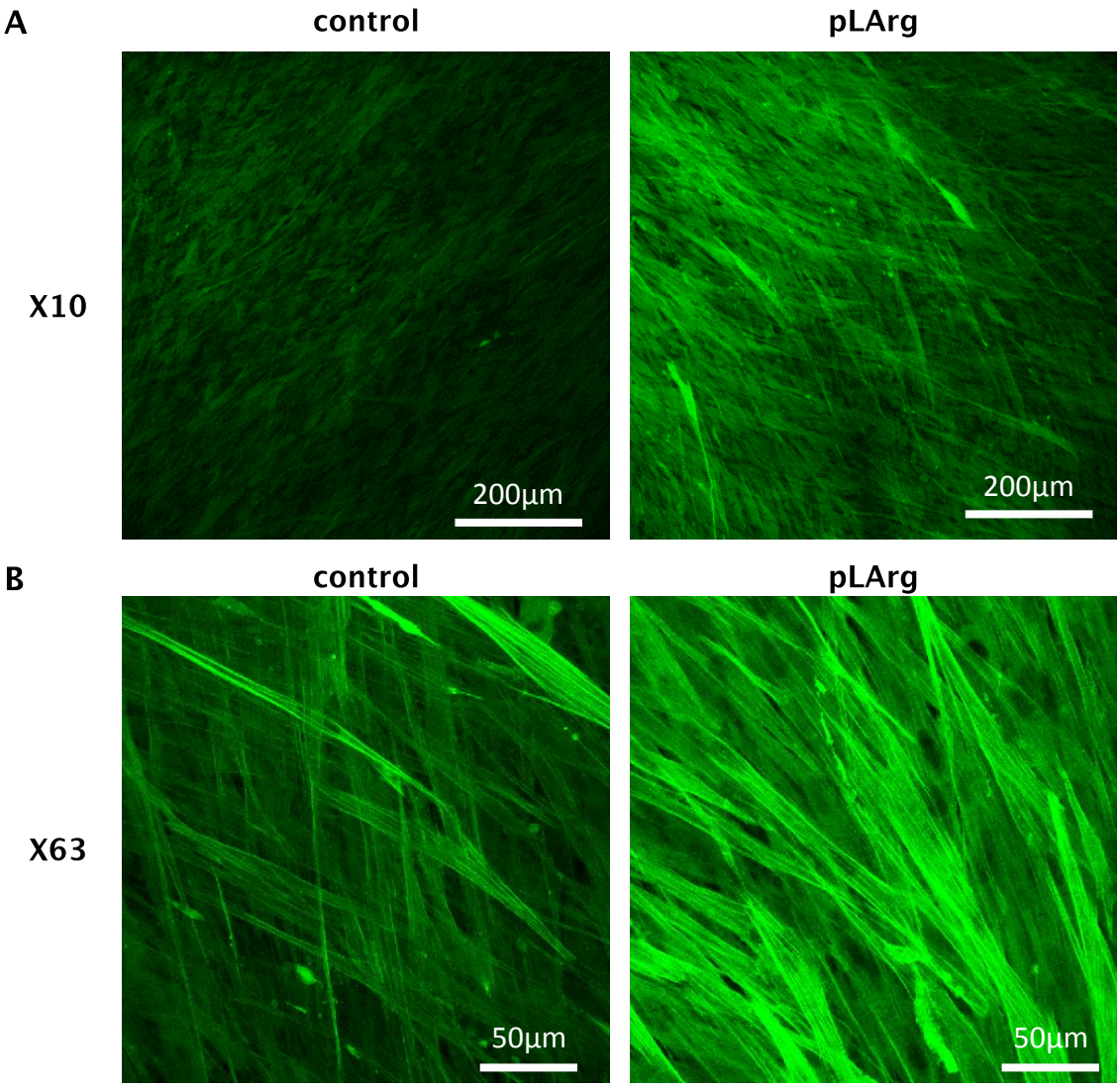

Figure 5.3.2-2 Effect of pLArg stimulation of the polarised EMTU model on fibroblast α-SMA.

Co-cultures were fixed 24h after challenge with pLArg (1µM) and assessed for α-SMA (green) by immunofluorescent microscopy using x10 (A) and x63 (B) magnifications on the confocal microscope. Images are representative of 3 independent experiments. Note that control images are shared with dsRNA controls, as experiments were performed in parallel.

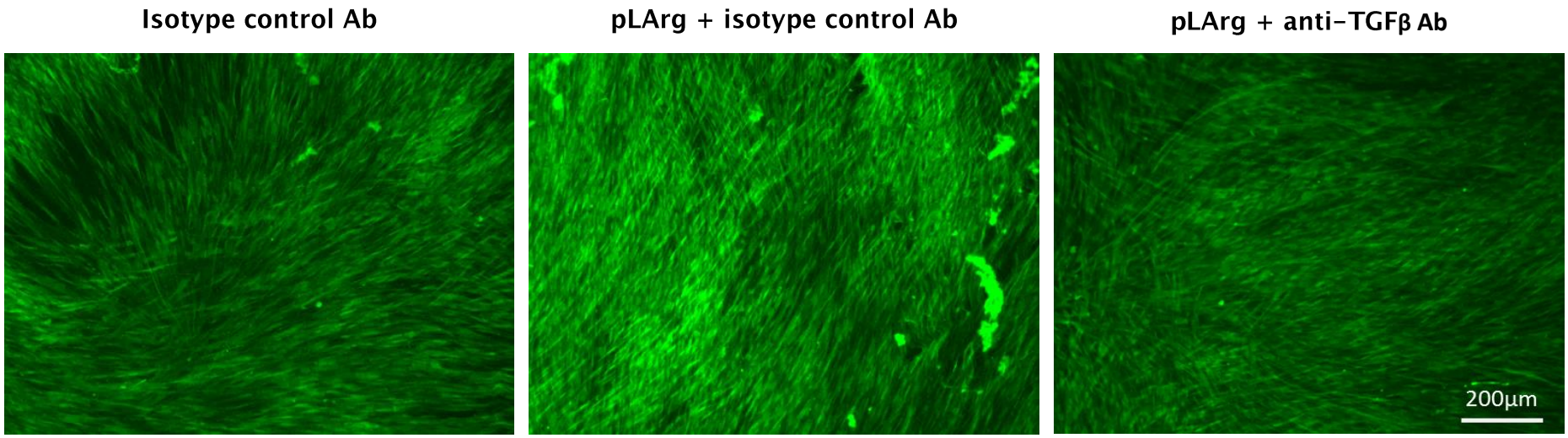

Figure 5.3.2-3 The effect of TGF-β neutralisation on pLArg-induced α-SMA in the polarised EMTU co-culture model.

The polarised EMTU co-culture model was cultured in the absence or presence of pan-TGF-β neutralising antibody (1µg/ml) applied basolaterally for 1h prior to stimulation with pLArg (1µM). Co-cultures were fixed 24h after challenge and assessed for α-SMA using immunofluorescent microscopy. Green= α-SMA. Images are representative of 1 experiment at x10 magnification.

5.4 Discussion

5.4.1 Effects of pLArg on epithelial barrier functions

Within the airway EMTU, the polarised structure of the epithelium forms a selective permeability barrier to the external environment which protects the body from inhaled pathogens. The polarised nature of the epithelium also results in differential concentrations of cytokines and chemokines at the apical and basolateral surface. This allows the establishment of chemotactic gradients, required for immune cell recruitment and retention and signalling to the underlying fibroblasts. In this chapter, I examined for the first time the effect of pLArg, a mimetic of eosinophil-derived MBP, on epithelial barrier functions within a co-culture model of the EMTU. The effects of pLArg on barrier function, mediator release and cell viability were initially investigated in HBEC monocultures to determine the optimum pLArg concentration for use in the EMTU co-culture model. pLArg concentrations between 1-10μM showed effects on cell viability, TER and cytokine release which confirmed previous studies [137, 189]. While the magnitude of these responses was greater than observed in previous studies (potentially due to differences in experimental set up), the induction of the effect was similar [137, 295-297].

The effect of pLArg on ionic permeability was quicker than that observed for dsRNA which showed a slower reduction in ionic permeability of 6-12h. This may be explained by differences in the mechanism of action of the different stimuli. DsRNA must first be taken up into the cell, bind to PRRs and activate intracellular signalling which ultimately causes disruption in TJ assembly. For example, Rezaee *et al*. demonstrated that dsRNA-induced reductions in 16HBE culture TERs were dependent on recognition by TLR3 and activation of PKD signalling, which induced TJ disassembly and remodelling of the cytoskeleton [212]. In contrast, cationic proteins interact with the cell surface via relatively non-specific electrostatic interactions [190]. For example, experiments using poly-L-lysine suggest that cationic-proteins may displace Ca^{2+} ions from

intracellular junctions [297]. In another study, pLArg altered the phosphorylation of key TJ proteins including ZO-1 and occludin [296]. However, the effect of pLArg on ionic permeability may also be due to cytotoxicity. In this chapter, I observed increasing reductions in TER and cell death with increasing concentrations of pLArg (0.3-10μM). While the disruptions in TER were completely or partially recoverable at pLArg concentrations of 0.3 or 1μM respectively, at 10μM they were not, suggesting that not enough viable cells remained to repair the epithelial barrier. Despite having minimal effects on cell viability, 0.3μM pLArg was not chosen for use in co-culture experiments as it had no significant effect on proinflammatory mediator release. Instead 1μM pLArg was used, as this was the least cytotoxic concentration that disrupted ionic permeability and induced cytokine production.

In the EMTU model pLArg disrupted ionic permeability 1h post-stimulation, which partially recovered by 6-24h, in contrast to HBEC monocultures in which no significant recovery of TER was observed. In addition, while pLArg significantly increased macromolecular permeability of HBEC monocultures, consistent with previous studies using rabbit airway epithelial cells [295-297], macromolecular permeability of co-cultures was unaffected. Together these data suggest that recovery of barrier function following pLArg stimulation is enhanced in co-culture compared to HBEC monocultures. This is in accordance with previous studies where recovery of barrier functions was enhanced in epithelial-fibroblast co-cultures following mechanical [220] or enzymatic damage [154]. My data also demonstrates that, although 1μM pLArg has potent effects on ionic permeability, the movement of macromolecules across the epithelial barrier is restricted following challenge of the EMTU model. Thus polarised functions are maintained following pLArg stimulation, which may be important for the activation and co-ordination of integrated inflammatory and repair responses.

5.4.2 pLArg activates proinflammatory responses in the EMTU model

Studies suggest that pLArg has the potential to activate proinflammatory responses within the EMTU. For example, pLArg induces a range of proinflammatory mediators (including IL-6 and CXCL8) in polarised HBEC monocultures which are mainly released apically [137]. The same polarity of pLArg-induced IL-6 and CXCL8 release was also observed in my experiments using HBEC monocultures. This indicates that polarised functions are still relatively intact following pLArg stimulation of HBEC monocultures, despite the trend for increased macromolecular permeability, which was very small compared to an empty Transwell®.

In comparison to HBEC and fibroblast monocultures, constitutive basolateral release of proinflammatory mediators was enhanced in the EMTU model, in accordance with a similar trend observed in Chapter 3, and in a previous study using HBEC and fibroblast co-cultures [161]. Following pLArg stimulation of the EMTU model, IL-6, CXCL8 and GM-CSF release was increased compared to unstimulated controls and was enhanced in the basolateral compared to the apical compartment. These data are similar to the synergistic enhancement in mediator release by dsRNA stimulation (shown in chapter 3) and suggest a common mechanism of mediator release irrespective of stimuli. Fibroblast monocultures produced low levels of inflammatory mediators at baseline and did not respond to pLArg stimulation, consistent with a previous study [298]. In contrast to dsRNA, pLArg did not induce CXCL10 release. This was expected as CXCL10 is inducible by IFN responses which are specifically activated following viral recognition by PRRs.

The synergistic enhancement in pLArg-induced proinflammatory responses suggested that epithelial-fibroblast cross-talk was occurring within the EMTU model. IL-1α has previously been demonstrated to be an important inflammatory mediator of cellular cross-talk at baseline and in response to other stimuli [157, 160, 161] such as HRV, as demonstrated in chapter 3. In addition, increased IL-1α secretion has been detected in nonpolarised HBEC

monocultures stimulated with pLArg [137]. In this chapter I added to previous studies by demonstrating the apical polarity of pLArg-induced IL-1α release in HBEC monocultures and in the EMTU model. The magnitude of this response did not differ significantly between the culture types. However, in the basolateral compartment, IL-1α levels in pLArg- and unstimulated cultures were reduced compared to HBEC monocultures. This is in line with a similar trend observed in chapter 3, which could be due to IL-1α utilisation by the fibroblasts.

In addition to examining the effects of pLArg on extracellular IL-1α, this is the first study to examine pLArg-induced effects on intracellular IL-1α in HBEC monocultures. Using highly cytotoxic (10μM) concentrations of pLArg, intracellular IL-1α was greatly reduced and corresponded to a large increase in extracellular IL-1α. This response may be due to passive release of IL-1α as an alarmin following pLArg-induced cell death. In contrast, at less cytotoxic (1μM) concentrations of pLArg, intracellular IL-1α was increased, suggesting that IL-1α protein may be actively induced, as observed for dsRNA in chapter 3. Together these data demonstrate that pLArg has differential effects on intracellular IL-1α levels, depending on its concentration and cytotoxicity.

PLArg concentration and cytotoxicity also affected extracellular IL-1α levels, which were much lower following stimulation with 1μM compared to 10μM pLArg. Despite the lower magnitude of response, IL-1α induced by 1μM of pLArg had an important role within the EMTU co-culture model, as demonstrated by blocking IL-1 signalling with IL-1Ra. This led to a similar pattern of inhibition of proinflammatory mediator release as was observed for viral-induced responses in chapter 3. This suggests a similar mechanism by which IL-1α induces proinflammatory mediator release irrespective of stimuli. IL-1Ra partially inhibited pLArg-induced responses in the apical compartment. This partial inhibitory effect may be explained by the contribution of other pLArg-dependent mediators or intracellular IL-1α acting as a proinflammatory activator of transcription [237, 238]. In addition to autocrine effects at the apical surface, IL-1α may also have paracrine effects *in vivo*, on luminal immune cells. While out of the scope of the current study, previous publications have demonstrated that macrophages [157, 242, 243] and MCs

are responsive to IL-1α [244, 245] in terms of cytokine production. In the basolateral compartment of the EMTU model, pLArg-induced proinflammatory responses were completely suppressed by IL-1Ra, which was surprising considering the apical polarity of release. However, IL-1α may be present at high localised concentrations between the cells and evidence suggests that fibroblasts are highly sensitive to IL-1α activation [157]. *In vivo*, activation of fibroblast inflammatory responses by epithelial-derived IL-1α may be required to amplify signals from the epithelium following damage with MBP and be important for recruiting and retaining immune cells at the site of injury.

5.4.3 PLArg activates repair responses in the EMTU model

Polycationic proteins such as MBP and pLArg have previously been shown to induce mediators of repair in HBEC monocultures, suggesting that they have the potential to activate the EMTU. For example, MBP stimulates expression of ET-1, TGF-α, TGF-β_1, PDGF-β, EGFR, MMP-9, fibronectin, and tenascin by BEAS-2B cells [139]. Similarly, pLArg stimulates bFGF, PDGF and ET-1 release by 16HBE cells [138]. In this chapter I added to these studies by investigating the effects of pLArg on polarised release of mediators involved in repair and remodelling that are associated with asthma. These included MMP-9 [168], MMP-2 [169], bFGF [171] and VEGF [263], which are increased in the BALF of asthmatic compared to non-asthmatic patients.

In contrast to dsRNA, pLArg had no effect on bFGF release in HBEC monocultures or the EMTU model. This also contrasts with a study by Zhang *et al.* which used a much higher concentration of pLArg (400μM) but shorter exposure time (10 mins) [138]. In addition, although Zhang *et al.* detected pLArg-induced bFGF release 24h post-stimulation, peak release occurred at 4h. This could explain why I did not detect increased bFGF release at 24h, using a lower pLArg concentration. Furthermore, a substantial amount of bFGF was detected in the cell culture medium used in my experiments, which could potentially obscure any pLArg-dependent effects. Finally the lack of pLArg-

induced bFGF release in my experiments could simply be due to the differences between polarised and non-polarised 16HBE cells.

In contrast to bFGF, pLArg induced MMP-9, MMP-2 and VEGF release in polarised HBEC monocultures. This is consistent with the effects of MBP on MMP-9 in BEAS-2B epithelial monolayers [139] but is the first time MMP-2 and VEGF release have been investigated following stimulation of HBECs with polycationic protein. In addition, this is the first study to demonstrate the apical polarity of pLArg-induced MMP-9, MMP-2 and VEGF release in HBEC monocultures. In the EMTU model, a similar pattern of release was also observed in the apical compartment, with a trend for increased pLArg-induced MMP-2 and VEGF, which was significant for VEGF. However, MMP-9 levels were significantly reduced in the apical and basolateral compartments of the co-culture model compared to HBEC monocultures. This in accordance with chapter 4 and a similar study using ALI-fibroblast co-cultures [261], and suggests that fibroblasts are important regulators of epithelial MMP-9. In contrast to MMP-9, VEGF levels did not differ significantly between the culture types, while basolateral MMP-2 was enhanced in co-culture. This is probably the cumulative effect of co-culturing both cell types as discussed in chapter 4, where a similar effect was observed.

The polarity of pLArg-induced MMP and VEGF release was the same as observed for viral-induced responses in chapter 4, where the role of these factors at the apical surface was discussed in depth. For example, VEGF may have autocrine effects on epithelial proliferation [265], while MMPs may release cell-associated growth factors at the apical surface [262]. In a previous study, pLArg had no effect on MMP-9 and MMP-2 activity in HBEC monolayers [138]. However, the effect of pLArg on MMP activity is yet to be investigated in polarised HBEC monocultures and within the EMTU model.

Consistent with the apical polarity of pLArg-induced VEGF and the lack of induction of bFGF, pLArg-stimulation of the EMTU model had no effect on fibroblast proliferation. This is in contrast to a study by Zhang *et al.*, which showed increased HLF proliferation following pLArg-stimulation of HBECs in co-culture and using epithelial-conditioned medium [138]. As discussed earlier, this difference compared to my data may be due to the higher

concentration of pLArg used (400μM) by Zhang *et al.*, which damaged approximately 70% of epithelial cells in co-culture [138]. This higher concentration may therefore be a stronger activator of growth factor release than the concentration of pLArg used in my experiments. In addition, at this high concentration, the large amount of pLArg-induced epithelial damage may lead to increased exposure of the underlying fibroblasts to growth factors and enhance proliferation.

In addition to proliferation, fibroblast differentiation was investigated following pLArg stimulation of the EMTU model, by staining for the myofibroblast marker, α-SMA. As discussed in chapter 4 studies have shown that epithelial cells are important modulators of fibroblast α-SMA expression in co-culture [161, 175]. In this chapter I demonstrated for the first time that epithelial stimulation with pLArg increases fibroblast α-SMA in co-culture, suggesting increased myofibroblast differentiation. Preliminary experiments using a pan-TGF-β neutralising antibody suggested that this may be mediated by TGF-β, despite being unable to detect a pLArg-induced increase in total and active TGF-β_1 and TGF-β_2. However, as discussed in chapter 4 this may be due to difficulties with TGF-β detection which include FBS-derived TGF-β in cell culture medium and the highly localised nature of TGF-β release and activation. Consistent with my data, a study using HBEC monocultures was also unable to detect an effect of pLArg on TGF-β_2 protein release while TGF-β_1 was not examined. In another study by Pegorier *et al.*, TGF-β gene expression was examined rather than protein release and showed that MBP but not pLArg induces TGF-β_1 expression by HBECs [139]. However, TGF-β_2 was not examined. This highlights that there are differences between MBP and its mimetic pLArg, which only mimics the cationic properties of MBP. Alternatively TGF-β may not be released from the epithelium at all; instead latent TGF-β in the cell medium may become activated. For example, as discussed in chapter 4, mechanisms of TGF activation, such as $\alpha_v\beta_6$, integrin [285, 287] and MMPs [287, 288], can be upregulated following wounding or inflammation.

5.4.4 Consequences of cationic protein activation of the EMTU in asthma

In this chapter I demonstrated that pLArg activates inflammatory and repair responses within the EMTU model. Whether polycationic proteins, such as MBP, activate these responses *in vivo* is yet to be determined. However using guinea pigs, intratracheal and intravenous administration of pLArg has been shown to increase the number of eosinophils and neutrophils in the BALF, suggesting activation of inflammatory responses [299]. In addition, while responses of primary epithelial cells to pLArg were not investigated in this study, others have shown that that they exhibit similar responses to epithelial cell lines [139, 189]. For example, BEAS-2B cells and primary HBECs exhibit similar responses to MBP in terms of increased ET-1, TGF-α TGF-β_1, PDGF-β, MMP-9, tenascin and fibronectin expression [139]. In addition, pLArg has cytotoxic effects on 16HBEs and primary HBECs, although primary HBECs were more sensitive [189]. Importantly the concentrations of pLArg and MBP used in these studies, and also in my experiments, are lower than that measured in the asthmatic airway [134, 139]. Together these data suggest that cationic proteins, such as MBP, may have important consequences *in vivo* and activate EMTU inflammatory, repair and remodelling responses. In allergic asthma, where MBP levels are increased [131, 133, 134], and the airway epithelium is more sensitive to disruption [121, 140] there may be increased activation of these responses.

Activation of proinflammatory responses by MBP may have important consequences in asthma. For example, I showed that pLArg induces epithelial IL-1α; a mediator of cellular cross-talk and activator of proinflammatory responses. In established asthma, increased numbers of cells may be activated by IL-1α due to subepithelial fibrosis [17] and increased localisation of inflammatory cells to the airway mucosa [132, 246-248]. Furthermore, IL-1α has the potential to influence the polarisation (Th1 vs Th2) of inflammatory responses and has been shown to control allergic sensitisation to HDM in mice [234]. In addition, HDM-induced lung eosinophilia was strongly reduced in *Il1r1*$^{-/-}$ mice [234]. This suggests that IL-1 induced by eosinophil polycationic

proteins such as MBP, may have a positive feedback effect on lung eosinophilia.

Activation of repair responses by MBP may also have important consequences in the asthmatic airway. For example, epithelial barrier functions are disrupted in the asthma [121, 140] and may be disrupted further by MBP. This could allow increased flux of polycation-induced MMPs and growth factors to the basolateral epithelial surface, leading to increased fibroblast activation. In childhood, when the airways are still growing and developing, activation of these responses by polycationic proteins may have important effects on airway structure. In adulthood, they may contribute to established airway remodelling.

In addition to the inflammatory and repair responses observed in this study, MBP may also have other effects on the EMTU *in vivo*. This is because pLArg only mimics MBP's cationic properties, which do not fully explain all of its activities [300]. For example, in a previous study where the effects of MBP and pLArg on epithelial monocultures were directly compared, MBP induced significant expression of more mediators of repair than pLArg [139]. Another possible limitation of the model was that pLArg was only added apically due to the localisation of eosinophils and their cationic proteins to the epithelium and airway lumen in asthma [131-133]. However, degranulated eosinophils and MBP have also been detected beneath the basement membrane [132]. Whether basolateral stimulation would affect pLArg induced responses is yet to be investigated within the EMTU model. However, my data suggests that basolateral pLArg would have minimal effects on fibroblast responses within the EMTU, as pLArg had no effect on inflammatory or repair mediators in fibroblast monocultures. This is consistent with studies, where MBP and pLArg had no direct effect on fibroblast proinflammatory cytokine release [298], collagen production [298] and proliferation [138, 298]. In contrast, cationic proteins have been shown to augment contraction of fibroblasts in collagen gels [301] and enhance the effects of growth factors and inflammatory mediators [188, 298]. For example, MBP and pLArg synergistically enhance IL-1α- and TGF-β_1-induced IL-6 release in fibroblast monocultures [298]. Together these studies suggest that subepithelial MBP may augment fibroblast

contraction and enhance responses to epithelial-derived mediators induced by agents such as MBP.

EMTU inflammatory and repair responses may also be further enhanced in *vivo* by other eosinophil granule contents, released at the same time as MBP. These include a variety of other cationic proteins such as eosinophil peroxidase (EPO) which induces epithelial expression of repair factors including ET-1, TGF-α, TGF-β_1, EGFR and PDGF-β. [139]. In addition to its cationic properties, EPO also has enzymatic activity and produces free radicals which may cause additional epithelial damage and activate repair responses [133]. Furthermore, eosinophils may also release eosinophil collagenase which remodels connective tissue [133]. Finally, eosinophil granules also contain cytokines and lipid mediators which may attract and activate immune cells [13] including eosinophils, which are a source of the pro-fibrotic cytokine TGF-β [21, 302].

Together these data suggest that therapeutics targeting eosinophils and their cationic proteins may be successful in reducing EMTU inflammation, repair and remodelling in allergic asthma. Corticosteroids reduce the number of inflammatory cells in the airway, including eosinophils, and improve symptoms in the majority of patients [43]. However in some patients with severe asthma, corticosteroid therapy has no effect on eosinophilic inflammation or symptom control. In addition, as discussed in chapter 3, the effects of corticosteroids are very broad. An IL-1 receptor antagonist could therefore be used to target inflammatory responses within the EMTU more specifically, and potentially control allergic inflammation. Other therapies that directly target eosinophils, rather than EMTU signalling include monoclonal antibodies. For example, mepolizumab neutralises IL-5, preventing IL-5-dependent eosinophilic inflammation. Anti-IL-5 treatment has also been shown to reduce some aspects of airway remodelling in asthma [303] with a significant reduction in expression of tenascin, lumican, and procollagen III in the basement membrane of bronchial biopsies [303]. In addition, TGF-β_1 expression by eosinophils and TGF-β_1 detected in the BALF were also reduced following anti-IL-5 treatment [303]. However, despite these effects on inflammation and repair anti-IL-5 is not a front line treatment for asthma. This is because only some patients respond to anti-IL-5 in terms of symptom control. These tend

to be patients with severe asthma and persistent airway eosinophilia [58, 59]. Another potential novel therapeutic is heparin; a positively charged polysaccharide that can bind cationic proteins and has been shown to limit their effects *in vitro* [139, 189, 297, 298]. *In vivo*, heparin has anti-inflammatory effects and has been shown to reduce eosinophil influx and cationic protein levels in nasal washes following allergen challenge [304]. However, more studies are needed to support its use in a clinical setting [305].

5.4.5 Summary

Polarised mediator release and bi-directional cellular cross-talk is essential for co-ordination of inflammatory and repair responses within the EMTU following epithelial activation. Here I examined the integrated responses of a polarised EMTU co-culture model where HBECs were apically challenged with the cationic protein pLArg, a mimetic of eosinophil MBP. A synergistic interaction between the activated epithelium and fibroblasts in terms of proinflammatory mediator release was demonstrated following pLArg challenge. This interaction was mediated by epithelial-derived IL-1α and showed for the first time that, as well as inducing extracellular IL-1α release from the epithelium, subcytotoxic concentrations of pLArg induce IL-1α intracellularly suggesting active induction rather than passive release as an alarmin. In contrast to proinflammatory mediator release, the polarity of pLArg-induced repair mediators were apical and while pLArg stimulation of the EMTU model had no effect on fibroblast proliferation it induced myofibroblast differentiation which may be mediated by TGF-β. The induction of inflammatory and repair responses within the EMTU by pLArg may have important consequences in allergic asthma where MBP levels are increased and the airway epithelium is more sensitive to disruption. While therapies that reduce eosinophilic inflammation and neutralise cationic proteins have been relatively successful in a subset of asthmatic patients they do not alter the natural course of the disease. It is therefore important to continue improving our understanding of mechanisms of cationic protein-induced inflammation, repair and remodelling within the EMTU.

6. Final Discussion

6.1 Overview

Asthma is a burden on society, affecting over 334 million people world-wide [5] While treatments alleviate symptoms, they do not alter the natural course of the disease. Thus there is a need to better understand asthma disease mechanisms. However, the disease is complex, involving multiple gene-environment interactions, resulting in a range of endotypes and phenotypes. The epithelium is in a key position to mediate these interactions and has important functions in sensing and responding to environmental challenges and host-derived factors, and signalling to underlying immune and structural cells. These structural cells include fibroblasts, whose close proximity to the epithelium allows local exchange of information, and the cells to work together as an EMTU, that maintains tissue homeostasis and co-ordinates inflammatory and repair responses to stimuli. In the asthmatic airway chronic inflammation and structural remodelling indicate that tissue homeostasis is disrupted and that the EMTU is dysregulated. It has therefore been hypothesised that there is dysregulation in the communication between epithelial cells and fibroblasts in the EMTU which contributes to disease pathogenesis.

Although cell-cell communication is essential for normal function of all tissues, the relationship between structural organisation and function is not addressed in most *in vitro* studies. In addition only a limited number of studies have examined EMTU responses to common asthma triggers such as HRV and MBP, which have the potential to activate cellular cross-talk leading to co-ordination of EMTU inflammatory and repair responses. Considering the important role of HRV infections in asthma development and exacerbations, and the association of activated eosinophils in Th2-type asthma, I developed a co-culture model of the EMTU with which to investigate inflammatory and repair responses to these agents. An important characteristic of the model was that the epithelial cells formed a functional polarised barrier, an important role of HBECs within the EMTU. In addition, fibroblasts were located in close proximity to HBECs, beneath the Transwell® membrane, allowing bi-directional communication between the cell types. This cross-talk was immediately

evident at baseline, where fibroblasts enhanced epithelial barrier functions (Chapter 3), enhanced constitutive basolateral IL-6 and CXCL8 release (Chapter 5) and suppressed MMP-9 release (chapter 4 and 5). I also demonstrated that cellular cross-talk is important for the co-ordination of inflammatory and repair responses within the EMTU model following challenge with viral or MBP mimetics (Figure 5.4.5-1). For example, viral- or pLArg- induced inflammatory responses were enhanced in the basolateral compartment of the EMTU model, a subset of which were mediated by epithelial-derived IL-1α. The remaining subset (dsRNA-dependent CXCL10) was partly mediated by IFN. These IL-1α- and IFN-dependent responses may have important effects within the EMTU. For example, IL-6 has autocrine effects on its own release and has also been shown to stimulate CXCL8 release from HBECs [239, 306]. IL-6 also promotes fibroblast differentiation and survival [277, 278]. Furthermore, CXCL8 and CXCL10 are chemotactic factors for fibroblasts [279].

In contrast to the inflammatory mediators, viral- and pLArg-induced release of growth factors and MMPs was mainly at the apical epithelial surface where they may have effects on epithelial proliferation [260, 262, 265, 266] and production or release of ECM components and growth factors [262, 264, 267, 268]. In the basolateral compartment, TGF-β activated fibroblast differentiation following challenge with viral- or MBP-mimetics (Figure 5.4.5-1). *In vivo,* this may lead to increased numbers of myofibroblasts which secrete matrix components, important for repair responses. The presence of active TGF-β within the EMTU, along with other growth factors such as bFGF may also promote epithelial-mesenchymal transition (EMT) [307]. EMT is a process where epithelial cells transition into fibroblastoid cells via molecular reprogramming and the downregulation of cell-cell adhesions. In this way the epithelium may become a source of mesenchymal cells following epithelial stress or injury [307].

In summary, this thesis highlights the importance of the epithelial barrier for generating concentration gradients within the EMTU, as well as the importance of bi-directional cellular cross-talk at baseline and in the co-ordination of inflammatory and repair responses to stimuli such as HRV and MBP.

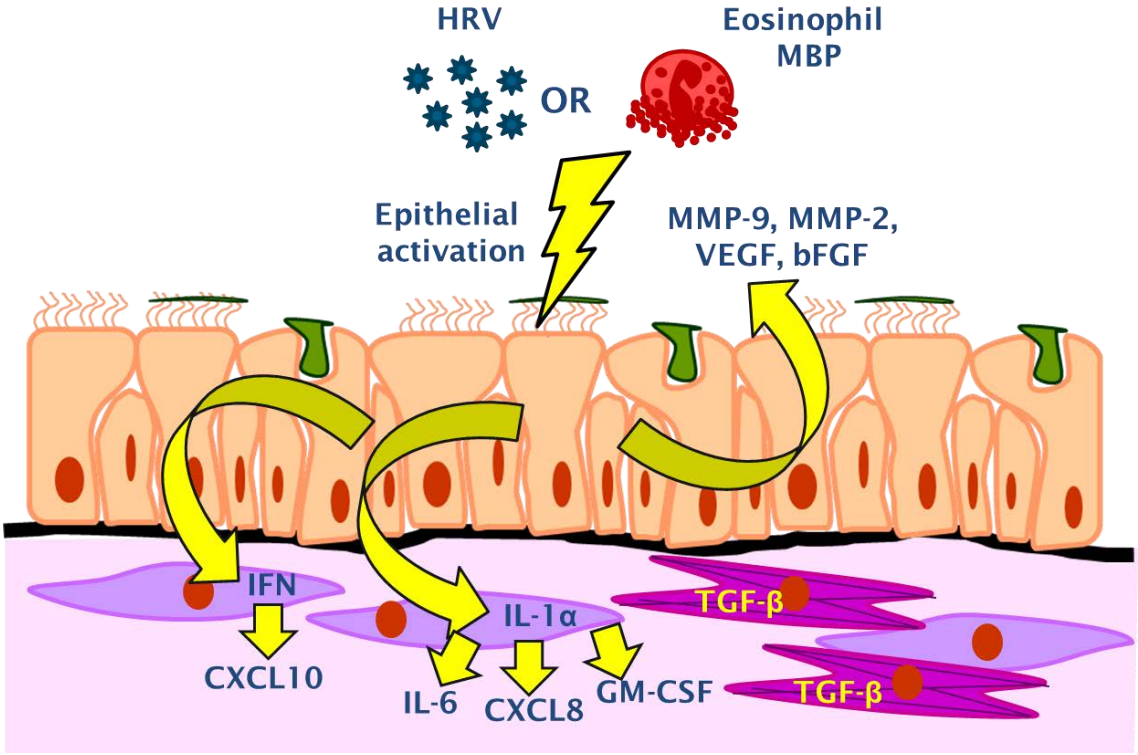

Figure 5.4.5-1 Overview of inflammatory and repair responses to HRV or MBP within the polarised EMTU model.

Epithelial activation stimulates the release of IL-1α and IFN from the epithelium which activates inflammatory mediator release by the underlying fibroblasts. Epithelial activation also stimulates the apical release of MMPs and growth factors, as well as fibroblast differentiation which is mediated by TGF-β.

.

6.2 Beyond the EMTU

Activation of cellular cross-talk and the accumulation of inflammatory and repair mediators following viral- or MBP-stimulation of the EMTU model demonstrates that the EMTU has an important influence over the local microenvironment. Therefore *in vivo*, following apical stimulation, the EMTU may transmit signals and have important effects on other cells that reside within, or are in close proximity to, the airway mucosa. Furthermore, through the differential release of mediators at the apical and basolateral surface and the establishment of chemotactic gradients, the EMTU may influence migration of immune cells within the airway mucosa as well as recruitment from the circulation.

6.2.1 EMTU interactions with tissue resident cells

6.2.1.1 Immune cells

Cells that reside within the EMTU *in vivo* include a number of immune cells, the activation, survival and migration of which is highly influenced by cellular interactions and the local microenvironment. In asthma, these cells include DCs, Th2 cells, MCs and eosinophils. Activation of the EMTU by asthma triggers may influence the function of these cells. For example, using an *in vitro* model containing polarised epithelial cells, DCs and fibroblasts, DCs were shown to migrate to the apical epithelial surface in response to HDM and LPS, suggesting that the EMTU has an important role in regulating DC migration [220]. Co-culture studies have also shown that HBECs and fibroblasts regulate DC activation, differentiation and cytokine responses [104, 308]. For example, signals from an activated epithelium, such as TSLP and IL-33, are particularly important in driving DC-mediated allergic inflammation [77, 79, 309]. In contrast, fibroblasts have recently been shown to suppress DC activation [308]. However, these experiments with fibroblasts were carried out in the absence of an activated epithelium, which as demonstrated in this thesis, can greatly

influence fibroblast cytokine production and could potentially amplify Th2-promoting epithelial signals.

In addition to driving Th2 inflammation via DC-activation, the EMTU may also directly affect the recruitment and survival of T cells. For example, both HBECs and fibroblasts are sources of the T cell chemotactic agent, CCL17, which is produced in response to a combination of cytokines (e.g. TNF-α, IL-4, IL-13, IFN-γ) or stimuli (e.g. poly(I:C), LPS) [125, 310, 311]. EMTU activation by HRV or MBP and activation of inflammatory mediator release may therefore promote T cell recruitment. In a triple culture of HBECs, fibroblasts and T cells, the cells of the EMTU were also demonstrated to modulate T cell survival, which was speculated to be mediated by TGF-β [312]. Thus viral- and MBP-induced TGF-β within the EMTU could potentially increase T cell survival *in vivo*.

Evidence suggests that the EMTU may also affect MC differentiation and survival. For example, the epithelium is a source of SCF; a MC-specific chemotactic and prosurvival factor that also promotes differentiation [108, 109, 313]. However, perhaps more relevant to this thesis is that IL-6 also promotes MC differentiation [313, 314]. The activation and amplification of IL-6 release following HRV or MBP challenge of the EMTU may therefore increase the number of mature (tryptase positive) MCs within the airway mucosa. Similarly, activation and amplification of GM-CSF release (a chemotactic and pro-survival factors for eosinophils [315, 316]) following HRV or MBP challenge of the EMTU, may promote eosinophilic inflammation.

Immune cells are an important source of inflammatory mediators which may also be involved in cellular-cross-talk and influence EMTU responses following HRV or MBP challenge. For example, Th1 cells characteristically produce IL-2 and IFN-γ [13], Th2 cells produce IL-4, [13, 14] and Th17 cell produce IL-17 [317, 318]. In co-culture with HBECs, these T cell subsets stimulate HBEC expression of IL-6 and IL-β, with the Th17 subset having the greatest effect [319]. In addition, IL-17 stimulates neutrophil chemoattractant secretion (e.g. CXCL8 and CXCL1) from HBECs and fibroblasts [317, 318]. Together this suggests that T cells and the cells of the EMTU influence each other's functions to regulate inflammation. Activated MCs and eosinophils may also amplify inflammation within the EMTU following activation. For example, these cells are

both sources of IL-3, IL-5 and GM-CSF [13], and may consequently augment eosinophilic inflammation. Activated MCs and eosinophils may also contribute to airway remodelling. For example, MC tryptase and chymase and eosinophil collagenase are enzymes which remodel connective tissue [13]. Eosinophils are also a source of the pro-fibrotic growth factor TGF-β [21]. Finally, activated eosinophils release MBP as well as other cationic proteins such as ECP, EDM and EPO, the latter of which is also an enzyme which produces reactive oxygen species (ROS) [13]. Together these agents may cause tissue damage, and as demonstrated for MBP, activate EMTU inflammatory and repair responses. Thus activation of the EMTU by MBP may lead to a positive feedback loop between the EMTU and eosinophils.

In summary, activation of the EMTU by HRV or MBP may have important consequences in terms of immune cell migration, survival and differentiation. Furthermore, activation of these cells within the EMTU may lead to increased inflammation and activation of repair/remodelling responses. To examine this, future work could involve investigating immune cell functions in EMTU-conditioned medium experiments or in experiments where immune cells are incorporated into the EMTU model.

6.2.1.2 Structural cells

Beneath the EMTU and within the deeper layers of the submucosa are structural cells including smooth muscle cells and endothelial cells. These cells are responsive to cytokines, chemokines and growth factors and may therefore be influenced by the EMTU. In support of this, in co-cultures of HBECs and human airway smooth muscle cells (HASM), the number of HASM cells is increased compared to HASM monocultures and further increased following epithelial scrape injury, the latter of which was partially mediated by IL-6 and CXCL8 [320]. Amplification of IL-6 and CXCL8 responses by fibroblasts following HRV or MBP challenge of HBECs may therefore promote proliferation of smooth muscle cells. Matrix components secreted by fibroblasts may also influence smooth muscle cell proliferation as well as the contractile phenotype of smooth muscle cells [17, 321]. In addition, it has been suggested that

fibroblasts contribute directly to smooth muscle mass, due to their phenotypic plasticity and ability to differentiate into myofibroblasts, which share similar contractile characteristics to smooth muscle cells [17]. Increased myofiboblast differentiation following viral or MBP challenge of the EMTU, may therefore increase the number of potential HASM precursors in the airway.

The EMTU may also influence endothelial cell repair and remodelling responses. For example, VEGF in conditioned medium from HRV-infected epithelial monolayers induces endothelial cell proliferation and angiogenesis *in vitro* [256]. However, in this thesis I show that that the polarity of epithelial VEGF release following HRV or MBP challenge is apical. This suggests that when the epithelial barrier is intact, HRV or MBP-induced VEGF from the epithelium may not reach the underlying endothelial cells *in vivo*. However, this does not rule out an effect of other basolateral epithelial or fibroblast-derived mediators on the endothelium.

Endothelial cells may also contribute to airway inflammation following HRV or MBP challenge of the EMTU. For example, epithelial inflammatory responses to dsRNA were synergistically enhanced in co-culture with endothelial cells compared to epithelial and endothelial cell monocultures [322]. Whether endothelial cells within the lamina propria are in close enough proximity to the epithelium *in vivo* to enhance these epithelial signals is unknown. However, given the ability of fibroblasts to participate in cellular-cross-talk they could potentially have a role in relaying signals between the epithelium and endothelium. Endothelial cells may not only enhance epithelial inflammatory responses but are also involved in leukocyte recruitment by the expression of adhesion molecules (e.g. E-selectin, vascular cell adhesion molecule-1 (VCAM-1)) required for immune cell attachment and extravasation into the tissue [322]. Expression of these molecules may be modulated by the epithelium. For example, in co-cultures of alveolar epithelial cells and endothelial cells, TNF-α stimulation of the epithelium increased endothelial cell expression of ICAM-1 [323]. In another co-culture study, dsRNA challenge of HBECs increased endothelial cell expression of VCAM-1 and E-selectin [322]. While the exact mechanisms of epithelial-endothelial cellular cross-talk were not investigated, addition of an inhibitor of NFκB signalling reduced endothelial expression of E-selectin, VCAM-1 and ICAM-1 [322]. This suggests that epithelial-derived inflammatory mediators are involved in epithelial-endothelial cell cross-talk.

However as discussed above, it is unclear whether the epithelium and endothelium are in close enough proximity for direct cell-cell cross-talk and fibroblasts may therefore have a role in relaying the epithelial signals between the epithelium and endothelium.
Given the potential for the EMTU to activate smooth muscle and endothelial cell inflammatory and repair responses, future work could involve examining their activation either in EMTU-conditioned medium experiments or by their incorporation into the EMTU model.

6.2.2 EMTU interactions with circulating immune cells

In addition to influencing tissue resident cells, cytokine and chemokine gradients along with activation of endothelial cell expression of adhesion molecules by the EMTU, may have important effects on immune cell recruitment from the circulation. In order to study immune cells *in vitro*, models have been developed where cells are introduced to the basolateral culture medium using microfluidics [322, 323]. For example, neutrophil recruitment has been examined within microfluidic epithelial and endothelial cell co-cultures [322, 323]. In these studies, activation of the epithelium increased neutrophil adhesion and recruitment to the endothelium, suggesting that cross-talk between these cells is important for immune cell recruitment [322, 323]. However as discussed above *in vivo* the bronchial epithelium and endothelial cells are separated by the fibroblast sheath. The effect of this fibroblast sheath could be investigated in the future by incorporating fibroblasts into microfluidic models.

6.3 Potential role for EMTU activation in airways disease.

6.3.1 Asthma

The effects of epithelial-mesenchymal cross-talk on the local microenvironment as well as the potential effects on other cells beyond the EMTU, suggest that EMTU activation or dyresgulation may have important consequences on airway inflammation and remodelling. In addition, I have shown that HRV and MBP, agents associated with asthma exacerbations and Th2-type asthma respectively, are able to activate EMTU inflammatory and repair responses. This may have important consequences in childhood, where the airways are not yet fully developed and more vulnerable to the effects of cytokines and growth factors. Furthermore, evidence suggests that the EMTU is dysregulated in asthma. For example, a number of asthma susceptibility genes have been identified within the cells of the EMTU and several HBEC and fibroblast functions are impaired. However, whether HRV- and MBP-induced EMTU activation and co-ordination of responses is dysregulated in asthma is yet to be investigated and could be the subject of future work.

Investigating mechanisms of cellular cross-talk in the asthmatic EMTU would ideally involve the use of donor-matched primary HBECs and fibroblasts from asthmatic donors. However, the limited availability of primary cells means that this may not always be possible, and donor variability may require a large power and potentially stratification of the data into the different asthmatic phenotypes in order to observe anything of significance. An alternative model of the asthmatic EMTU would be to mimic some of the pathological features of the disease. For example, in the majority of asthma cases, inflammation is Th2 driven and therefore cultures could be treated with exogenous IL-4 and IL-13. Culture of primary HBECs with IL-13 induces hallmarks of asthma including goblet cell metaplasia and hypersecretion, and disruption of epithelial barrier functions [130, 324, 325]. This has been shown to alter constitutive cytokine release and inflammatory responses to HRV. For example, IL-4 and IL-13 enhance constitutive CXCL8 release and HRV-induced CXCL8, GM-CSF and CXC10 release in primary HBEC monocultures [150].

In addition to Th2 inflammation, asthma is characterised by BHR, which exerts compressive forces on the cells. These forces can be modelled *in vitro* using apparatus which increases the air pressure at the apical epithelial surface [152, 326, 327] or introduces lateral compressive strain [328]. Compressive stress shrinks the lateral epithelial space, leading to increased localised concentrations of cytokines and growth factors and enhanced signalling [327]. Compressive stress may therefore augment EMTU inflammatory and repair responses by enhancing HRV or MBP-dependent signalling. Compressive stress also directly induces release of inflammatory and repair mediators in epithelial monocultures and co-cultures with fibroblasts [152, 326, 328]. These mediators could potentially interact or have cumulative effects with mediators induced by HRV and MBP. However, these interactions are yet to be investigated in epithelial mono- or co-cultures with fibroblasts.

Finally, while I have investigated the effects of HRV or pLArg as a single stimulation, these agents are likely to be present at the same time in allergic asthma. Therefore it would be important to study the effects of HRV and MBP in combination. Both HRV and pLArg activated similar inflammatory and repair responses in the EMTU model. In combination, the magnitude of these responses may be enhanced in an additive or even a synergistic manner. In support of this, a previous study showed that epithelial cell death and cytokine release was significantly enhanced when epithelial cells were treated with virus (RSV) and MBP in combination, compared to either treatment alone [329]. Notably, the cytokines that were enhanced included IL-17, which has been implicated in the pathogenesis of non-Th2 asthma [317], and GM-CSF, which activates and enhances eosinophil effector functions [13]. However, the epithelial cells used in these experiments were A549 cells, which are a cancer-derived alveolar type II cell line. Whether HBECs in co-culture with fibroblasts exhibit similar responses to combined viral and MBP stimulation is yet to be investigated.

6.3.2 Other chronic respiratory diseases

6.3.2.1 Chronic obstructive pulmonary disease (COPD)

While the main focus of this thesis investigated cellular cross-talk within the EMTU in response to agents associated with asthma, viral agents such as HRV may also exacerbate symptoms of other chronic airway diseases such as COPD.

COPD is a chronic respiratory disease defined by airflow limitation that is not reversible by treatment [330]. The condition is preventable in many incidences as development is highly associated with oxidative stress, such as that caused by cigarette smoke [330]. Despite these differences compared to asthma, airway inflammation and remodelling is characteristic of both diseases. For example, similarly to asthma, airway remodelling in COPD includes goblet cell hyperplasia leading to increased mucus production, and increased airway fibrosis and smooth muscle mass [330, 331]. However in contrast to asthma it is mainly the small, rather than the large airways that are affected [331]. In addition, there is enlargement and destruction of the alveoli, leading to a type of COPD called emphysema. Inflammation in COPD is also distinct compared to asthma in that it is neutrophilic rather than eosinophilic [332]. An extensive body of evidence implicates neutrophils as key mediators of tissue damage and lung function decline in COPD [332]. For example, neutrophil activation and degranulation leads to release of neutrophil elastase which damages the epithelium, increases vascular permeability and induces mucus hypersecretion, metaplasia of mucus glands, bronchoconstriction and BHR [248, 333, 334]. Other key mediators of neutrophil-induced damage and remodelling in COPD include myeloperoxidase, which causes oxidative stress, and MMP-9 [332].

Inhaled environmental agents associated with the COPD pathogenesis and disease exacerbation, e.g. cigarette smoke, pollutants and HRV, have been shown to trigger neutrophil chemoattractant release from pulmonary epithelial cells [332]. This suggests that activation of EMTU inflammatory responses by HRV and other environmental agents may not only be important in the context of asthma, but also in the context of COPD. In addition, evidence indicates that epithelial and fibroblast cell functions are dysregulated in COPD. For example, epithelial mucociliary functions are impaired, due to increased mucus secretion

and goblet cell metaplasia [335]. In addition, evidence suggests that there are abnormalities in TJ formation in COPD [336]. This may increase epithelial susceptibility to disruption, leading to increased activation of inflammatory and repair responses. In support of this, cigarette smoke extract-induced IL-1α release is enhanced in epithelial cultures from COPD compared to healthy donors [161]. As a mediator of cellular cross-talk, increased IL-1α release may have important consequences within the EMTU [161]. Evidence also suggests that fibroblast functions are dysregulated in COPD. For example, increased numbers of senescent fibroblasts have been detected in cultures from patients with emphysema compared to HLFs from healthy smokers [337]. This increase in senescent cells may lead to dysregulation of tissue repair. In addition, senescence may favour viral replication as it suppresses apoptosis, which is required for viral-clearance.

6.3.2.2 Cystic fibrosis

In addition to asthma and COPD, activation of the EMTU may also be important in the context of cystic fibrosis (CF). CF is an autosomal recessive disorder arising from functional deficiency of the cystic fibrosis conductance regulator (CFTR) [338]. CFTR is an ion channel, primarily responsible for facilitating conductance of chloride ions across membranes. This leads to dysregulation of epithelial functions. For example, the imbalance in chloride secretion and ion uptake by epithelial cells leads to resorption of airway surface liquid and increases mucus viscosity [338, 339]. This also causes a build-up of mucus as its removal by the mucocilliary escalator is more difficult. The microenvironment of the airway lumen is therefore more static and favours colonisation of the airways with opportunistic pathogens [338]. For example, *Pseudomonas aeruginosa* is the most common bacterial pathogen associated with CF [339]. Development of *P. aeruginosa* infection in CF is associated with viral infections, which also account for 40-50% of CF exacerbations [339]. HRV is the predominant cause of viral exacerbation and is detected in 20-60% of cases [338]. Together these viral and bacterial infections are thought to drive the sustained neutrophilic inflammation and airway remodelling (e.g. deposition of fibrous tissue, thickening of the basement membrane and

increased smooth muscle mass) which are observed in the airways of CF patients [340, 341]. For example, infectious agents may increase activation of EMTU and promote inflammation and remodelling in CF. Mechanisms of cellular cross-talk in response to HRV and other pathogens are therefore important in the context of CF as well as asthma and COPD.

6.3.3 Other respiratory infections

In addition to HRV, a number of other infectious agents can exacerbate chronic respiratory diseases such as asthma, COPD and CF. These agents interact with HBECs and have the potential to activate the EMTU. For example, coronavirus, parainfluenza, influenza and RSV all have similar genomic structures to HRV, in that they are single-stranded RNA (ssRNA) viruses. These viruses may therefore activate a similar repertoire of PRRs and innate EMTU responses as HRV. For example, in a previous study CXCL8 and CXCL10 responses to influenza virus were synergistically enhanced in alveolar epithelial cell and fibroblast co-cultures compared to monocultures. However, the mechanism of the enhancement was linked to C-met rather that IL-1α signalling, and polarised responses were not examined [226]. Another ssRNA virus of particular interest is RSV, which is the most common pathogen to cause severe airway disease in infants. In addition, similarly to HRV, RSV is associated with asthma development and exacerbation [342]. Previous studies have shown that RSV induces IL-1α release from A549 cells, which has an autocrine effect on CXCL8 release and ICAM-1 expression [343, 344]. In experiments using conditioned medium from RSV-infected A549 cells, IL-1α also induced ICAM-1 expression by endothelial cells [345]. Studies using primary HBECs to examine the effect of RSV on IL-1α are limited to experiments by Oshansky *et al.* which showed that purified RSV G protein significantly induces IL-1α release from primary HBECs [346]. In other studies, RSV infection of primary HBECs has been found to induce a similar repertoire of cytokines as observed in this thesis following HRV infection. For example, these include IL-6, CXCL8, GM-CSF and CXCL10 [129, 347]. In contrast, there have been limited studies investigating repair responses to RSV infection. However, Wang *et al.* recently showed that RSV infection of 16HBEs increases fibroblast α-SMA expression in co-culture [348]. This response is similar to that observed in my thesis with HRV,

although the mechanism of the RSV-induced response was not investigated by Wang *et al.*. Together these studies suggest that BECs may exhibit similar responses to HRV and RSV and that RSV may activate EMTU inflammatory and repair responses via similar mechanisms of cellular cross-talk as HRV.

Evidence also suggests that viruses with different genomic structures can activate similar EMTU responses, despite being recognised by different PRRs. For example, adenoviruses are dsDNA viruses, which are recognised by TLR7 or TLR9 [118, 119]. In experiments using conditioned medium from adenovirus-infected A549 cells, IL-1α induced ICAM-1 expression by endothelial cells [349]. However, studies of adenovirus infection in primary HBECs are mainly limited to experiments using genetically engineered adenovirus as viral vectors for gene transfection, and do not assess responses to wild type virus. Therefore it is still unclear whether primary HBECs exhibit similar responses to adenovirus as A549s and whether adenovirus-infected HBECs can activate fibroblast inflammatory and repair responses.

Finally, bacteria are also important agents of infectious respiratory diseases with the potential to activate innate EMTU responses. Bacterial PAMPs include cell wall components such as LPS and proteoglycans which are recognised by host TLR-4 and TLR-2 respectively [13]. Interestingly, TLR-4 also recognises RSV fusion protein and TLR-9 is able to recognise both viral and bacterial dsDNA, suggesting that bacteria and viruses may share some mechanisms of innate immune activation [13, 350]. In addition, evidence suggests that bacteria can activate inflammatory responses within the EMTU via IL-1α. For example, conditioned medium from *P. aeruginosa*-infected epithelial cells induces fibroblast proinflammatory responses via IL-1α [351]. In contrast, it has been suggested that *P. aeruginosa* inhibits repair responses. For example, the *P. aeruginosa* secretome inhibits cell migration [352, 353]. However, fibroblast differentiation may still be activated as *P. aeruginosa* flagellin induces TGF-β_1 release from epithelial cells [354].

In summary, different types of respiratory infectious agents have the potential to activate the EMTU and evidence suggests that these agents may trigger some of the same mechanisms of cellular cross-talk as HRV.

6.4 Identification of novel therapeutic targets

As discussed above, EMTU activation and dysregulation may have an important role in the pathology of a variety of respiratory diseases. Therefore improving understanding of epithelial-mesenchymal cross-talk and integrated EMTU responses may be of vital importance for the identification of novel therapeutic targets. For example, here I have identified IL-1α as a mediator of cellular cross-talk, which is important for the activation of EMTU inflammatory responses. IL-1α signalling may therefore be a potential therapeutic target for the treatment of inflammation in chronic respiratory diseases. While a potential adverse effect of targeting IL-1-dependent inflammation is a reduction in the ability of the immune system to clear infection, my data suggests that anti-viral (IFN) responses would be left relatively intact, thus allowing effective clearance of viral infections. The IL-1R1 antagonist has already been shown to be effective in the treatment of other inflammatory diseases [251] and LPS-induced airway inflammation in healthy volunteers without adverse effects [252]. I also identified TGF-β as an important mediator of fibroblast differentiation following activation of HBECs, suggesting that therapies targeting TGF signalling may be useful in the treatment of airway diseases such as asthma. TGF-β has already been identified as a therapeutic target for the treatment of fibrotic lung diseases such as idiopathic pulmonary fibrosis (IPF) [355, 356]. In addition, treatment strategies that interfere with TGF-β-induced cellular responses have shown promise in mouse models of fibrosis [355, 357]. These strategies include TGF-β neutralisation, inhibition of receptor signalling and blockade of latent TGF-β activation [355, 356]. Notably, monoclonal antibodies targeting TGF-β and the activator of TGF-β, αvβ6, have demonstrated acceptable safety in phase I clinical trials [355, 358],

In this thesis, mediators of cellular cross-talk were identified using an integrated and polarised co-culture model of the EMTU, demonstrating the potential of these models for the identification of novel mechanisms and

therapeutic targets. Improved, disease relevant, *in vitro* models also have potential to replace and reduce animal testing at the early stages of drug development. Not only is this important in terms of animal welfare, but avoiding the use of animal models (which only examine the inflammatory component of chronic human respiratory disease), may improve the success of drug discovery strategies. The success of these strategies is extremely important for patients with chronic respiratory disease who do not achieve symptom control with current treatments. In asthma, this represents approximately 5-10% of patients [7, 11, 12, 42].

6.4.1 Summary/ conclusions

This thesis demonstrates the importance of the polarised epithelial barrier and epithelial-mesenchymal cross-talk in regulating the local microenvironment, and co-ordinating responses to the common asthma triggers, HRV and MBP. One of the mediators involved in co-ordinating these responses is IL-1α, which was released by the epithelium in response to viral- or MBP-stimulation and activated fibroblasts, leading to an enhancement in basolateral proinflammatory responses. Viral- and MBP-stimulation of the epithelium also activated repair responses. For example, growth factor and MMP release was induced at the apical epithelial surface and fibroblast differentiation was increased, which was mediated by TGF-β. Activation of these inflammatory and repair responses may have important effects on immune cell recruitment and other cells that reside within, or are in close proximity to the EMTU. Therefore, in chronic respiratory diseases such as asthma, where epithelial and mesenchymal cell functions are dysregulated, EMTU activation may have important consequences on airway inflammation and remodelling. Thus there is a continuing need to better understand how inflammatory and repair mechanisms are co-ordinated within the EMTU and to investigate whether mechanisms of cellular cross-talk are dysregulated in asthma. Improving understanding of these mechanisms may allow the identification of novel therapeutic targets and strategies for patients who are unresponsive to current treatments.

References

1. Swindle, E.J., J.E. Collins, and D.E. Davies, *Breakdown in epithelial barrier function in patients with asthma: identification of novel therapeutic approaches.* J Allergy Clin Immunol, 2009. **124**(1): p. 23-34; quiz 35-6.
2. Blume, C. and D.E. Davies, *In vitro and ex vivo models of human asthma.* Eur J Pharm Biopharm, 2013. **84**(2): p. 394-400.
3. NHS. *NHS choices - Asthma*. 2012 [cited 2014 21st March]; Available from: http://www.nhs.uk/conditions/Asthma/Pages/Introduction.aspx.
4. AsthmaUK. *Asthma basics*. [cited 2014 21st March]; Available from: http://www.asthma.org.uk/knowledge-basics.
5. GlobalAsthmaNetwork. *The Global Asthma Report 2014*. 2014 [cited 2015 23rd March]; Available from: http://www.globalasthmareport.org/burden/burden.php.
6. WorldHealthOrganization. *Asthma Fact Sheet*. 2013 [cited 2015 23rd March]; Available from: http://www.who.int/mediacentre/factsheets/fs307/en/.
7. ERS. *ERS white book*. 2015 [cited 2015 23rd March]; Available from: http://www.erswhitebook.org/chapters/adult-asthma/.
8. AsthmaUK. *Asthma facts and FAQs*. 2014 [cited 2016 15th September]; Available from: https://www.asthma.org.uk/about/media/facts-and-statistics/.
9. RoyalCollegeOfPhysicians. *National Review of Asthma Deaths (NRAD)*. 2014.
10. AsthmaUK. *Asthma UK Data Portal*. 2014 [cited 2016 15th September]; Available from: https://data.asthma.org.uk/SASVisualAnalyticsViewer/VisualAnalyticsViewer_guest.jsp?reportName=Asthma+UK+data+portal&reportPath=/Shared+Data/Guest/&reportViewOnly&_ga=1.83456789.2031348650.1381490862.
11. Holgate, S.T. and R. Polosa, *The mechanisms, diagnosis, and management of severe asthma in adults.* Lancet, 2006. **368**(9537): p. 780-93.
12. Cottini, M. and R. Asero, *Asthma phenotypes today.* Eur Ann Allergy Clin Immunol, 2013. **45**(1): p. 17-24.
13. Janeway, C.A., P. Travers, and M. Walport, *Immunobiology: The Immune System in Health and Disease*. 5th Edition ed. 2001, New York: Garland Science.
14. Holgate, S.T., M.K. Church, and L.M. Lichtenstein, *Allergy*. 3rd Edition ed. 2012.
15. Valenta, R., *The future of antigen-specific immunotherapy of allergy.* Nat Rev Immunol, 2002. **2**(6): p. 446-53.
16. Al-Muhsen, S., J.R. Johnson, and Q. Hamid, *Remodeling in asthma.* J Allergy Clin Immunol, 2011. **128**(3): p. 451-62; quiz 463-4.
17. Davies, D.E., et al., *Airway remodeling in asthma: new insights.* J Allergy Clin Immunol, 2003. **111**(2): p. 215-25; quiz 226.
18. Jeffery, P.K., *Remodeling and inflammation of bronchi in asthma and chronic obstructive pulmonary disease.* Proc Am Thorac Soc, 2004. **1**(3): p. 176-83.

19. Fedorov, I.A., et al., *Epithelial stress and structural remodelling in childhood asthma.* Thorax, 2005. **60**(5): p. 389-94.
20. Pascual, R.M. and S.P. Peters, *Airway remodeling contributes to the progressive loss of lung function in asthma: an overview.* J Allergy Clin Immunol, 2005. **116**(3): p. 477-86; quiz 487.
21. Wong, D.T., et al., *Eosinophils from patients with blood eosinophilia express transforming growth factor beta 1.* Blood, 1991. **78**(10): p. 2702-7.
22. Manuyakorn, W., *Airway remodelling in asthma: role for mechanical forces.* Asia Pac Allergy, 2014. **4**(1): p. 19-24.
23. Grainge, C.L., et al., *Effect of bronchoconstriction on airway remodeling in asthma.* N Engl J Med, 2011. **364**(21): p. 2006-15.
24. Wadsworth, S.J., D.D. Sin, and D.R. Dorscheid, *Clinical update on the use of biomarkers of airway inflammation in the management of asthma.* Journal of Asthma and Allergy, 2011. **4**: p. 77-86.
25. Jacobs, S.E., et al., *Human rhinoviruses.* Clin Microbiol Rev, 2013. **26**(1): p. 135-62.
26. Gavala, M.L., P.J. Bertics, and J.E. Gern, *Rhinoviruses, allergic inflammation, and asthma.* Immunol Rev, 2011. **242**(1): p. 69-90.
27. Palmenberg, A.C., J.A. Rathe, and S.B. Liggett, *Analysis of the complete genome sequences of human rhinovirus.* J Allergy Clin Immunol, 2010. **125**(6): p. 1190-9; quiz 1200-1.
28. Bella, J. and M.G. Rossmann, *ICAM-1 receptors and cold viruses.* Pharm Acta Helv, 2000. **74**(2-3): p. 291-7.
29. Kennedy, J.L., et al., *Pathogenesis of rhinovirus infection.* Curr Opin Virol, 2012. **2**(3): p. 287-93.
30. Bochkov, Y.A., et al., *Cadherin-related family member 3, a childhood asthma susceptibility gene product, mediates rhinovirus C binding and replication.* Proc Natl Acad Sci U S A, 2015. **112**(17): p. 5485-90.
31. Jackson, D.J., J.E. Gern, and R.F. Lemanske, Jr., *The contributions of allergic sensitization and respiratory pathogens to asthma inception.* J Allergy Clin Immunol, 2016. **137**(3): p. 659-65; quiz 666.
32. Corne, J.M., et al., *Frequency, severity, and duration of rhinovirus infections in asthmatic and non-asthmatic individuals: a longitudinal cohort study.* Lancet, 2002. **359**(9309): p. 831-4.
33. Hyvarinen, M.K., et al., *Teenage asthma after severe early childhood wheezing: an 11-year prospective follow-up.* Pediatr Pulmonol, 2005. **40**(4): p. 316-23.
34. Kusel, M.M., et al., *Early-life respiratory viral infections, atopic sensitization, and risk of subsequent development of persistent asthma.* J Allergy Clin Immunol, 2007. **119**(5): p. 1105-10.
35. Nicholson, K.G., J. Kent, and D.C. Ireland, *Respiratory viruses and exacerbations of asthma in adults.* BMJ, 1993. **307**(6910): p. 982-6.
36. Johnston, S.L., et al., *The relationship between upper respiratory infections and hospital admissions for asthma: a time-trend analysis.* Am J Respir Crit Care Med, 1996. **154**(3 Pt 1): p. 654-60.
37. Fleming, H.E., et al., *Rhinovirus-16 colds in healthy and in asthmatic subjects: similar changes in upper and lower airways.* Am J Respir Crit Care Med, 1999. **160**(1): p. 100-8.

38. Grunberg, K., et al., *Rhinovirus-induced airway inflammation in asthma: effect of treatment with inhaled corticosteroids before and during experimental infection.* Am J Respir Crit Care Med, 2001. **164**(10 Pt 1): p. 1816-22.
39. Hansbro, N.G., et al., *Understanding the mechanisms of viral induced asthma: new therapeutic directions.* Pharmacol Ther, 2008. **117**(3): p. 313-53.
40. Ricciardolo, F.L., et al., *Therapeutic novelties of inhaled corticosteroids and bronchodilators in asthma.* Pulm Pharmacol Ther, 2015. **33**: p. 1-10.
41. Cazzola, M., et al., *beta2-agonist therapy in lung disease.* Am J Respir Crit Care Med, 2013. **187**(7): p. 690-6.
42. GINA, *Global strategy for asthma management and prevention*, 2016.
43. Barnes, P.J., *Corticosteroids: the drugs to beat.* Eur J Pharmacol, 2006. **533**(1-3): p. 2-14.
44. Matsuse, H. and S. Kohno, *Leukotriene receptor antagonists pranlukast and montelukast for treating asthma.* Expert Opin Pharmacother, 2014. **15**(3): p. 353-63.
45. BTS/SIGN, *British guideline on the management of asthma*, 2014.
46. Manuyakorn, W., P.H. Howarth, and S.T. Holgate, *Airway remodelling in asthma and novel therapy.* Asian Pac J Allergy Immunol, 2013. **31**(1): p. 3-10.
47. Haldar, P., et al., *Cluster analysis and clinical asthma phenotypes.* Am J Respir Crit Care Med, 2008. **178**(3): p. 218-24.
48. Moore, W.C., et al., *Identification of asthma phenotypes using cluster analysis in the Severe Asthma Research Program.* Am J Respir Crit Care Med, 2010. **181**(4): p. 315-23.
49. Wenzel, S.E., *Asthma phenotypes: the evolution from clinical to molecular approaches.* Nat Med, 2012. **18**(5): p. 716-25.
50. Desai, M. and J. Oppenheimer, *Elucidating asthma phenotypes and endotypes: progress towards personalized medicine.* Ann Allergy Asthma Immunol, 2016. **116**(5): p. 394-401.
51. Bel, E.H., *Clinical phenotypes of asthma.* Curr Opin Pulm Med, 2004. **10**(1): p. 44-50.
52. Miranda, C., et al., *Distinguishing severe asthma phenotypes: role of age at onset and eosinophilic inflammation.* J Allergy Clin Immunol, 2004. **113**(1): p. 101-8.
53. Wenzel, S.E., *Asthma: defining of the persistent adult phenotypes.* Lancet, 2006. **368**(9537): p. 804-13.
54. de Marco, R., et al., *Inhaled steroids are associated with reduced lung function decline in subjects with asthma with elevated total IgE.* J Allergy Clin Immunol, 2007. **119**(3): p. 611-7.
55. Berry, M., et al., *Pathological features and inhaled corticosteroid response of eosinophilic and non-eosinophilic asthma.* Thorax, 2007. **62**(12): p. 1043-9.
56. Holgate, S.T., *New strategies with anti-IgE in allergic diseases.* World Allergy Organ J, 2014. **7**(1): p. 17.
57. Normansell, R., et al., *Omalizumab for asthma in adults and children.* Cochrane Database Syst Rev, 2014. **1**: p. CD003559.

58. Busse, W.W., et al., *A review of treatment with mepolizumab, an anti-IL-5 mAb, in hypereosinophilic syndromes and asthma.* J Allergy Clin Immunol, 2010. **125**(4): p. 803-13.
59. Menzella, F., et al., *Clinical usefulness of mepolizumab in severe eosinophilic asthma.* Ther Clin Risk Manag, 2016. **12**: p. 907-16.
60. Green, R.H., et al., *Analysis of induced sputum in adults with asthma: identification of subgroup with isolated sputum neutrophilia and poor response to inhaled corticosteroids.* Thorax, 2002. **57**(10): p. 875-9.
61. Douwes, J., et al., *Non-eosinophilic asthma: importance and possible mechanisms.* Thorax, 2002. **57**(7): p. 643-8.
62. Van Den Berge, M., et al., *The role of female sex hormones in the development and severity of allergic and non-allergic asthma.* Clinical & Experimental Allergy, 2009. **39**(10): p. 1477-1481.
63. Pavord, I.D., et al., *Non-eosinophilic corticosteroid unresponsive asthma.* Lancet, 1999. **353**(9171): p. 2213-4.
64. Cox, G., *Glucocorticoid treatment inhibits apoptosis in human neutrophils. Separation of survival and activation outcomes.* J Immunol, 1995. **154**(9): p. 4719-25.
65. Schleimer, R.P., et al., *An assessment of the effects of glucocorticoids on degranulation, chemotaxis, binding to vascular endothelium and formation of leukotriene B4 by purified human neutrophils.* J Pharmacol Exp Ther, 1989. **250**(2): p. 598-605.
66. Kato, T., et al., *Inhibition by dexamethasone of human neutrophil apoptosis in vitro.* Nat Immun, 1995. **14**(4): p. 198-208.
67. Woolley, K.L., et al., *Eosinophil apoptosis and the resolution of airway inflammation in asthma.* Am J Respir Crit Care Med, 1996. **154**(1): p. 237-43.
68. Woodruff, P.G., et al., *T-helper type 2-driven inflammation defines major subphenotypes of asthma.* Am J Respir Crit Care Med, 2009. **180**(5): p. 388-95.
69. Dougherty, R.H., et al., *Accumulation of intraepithelial mast cells with a unique protease phenotype in T(H)2-high asthma.* J Allergy Clin Immunol, 2010. **125**(5): p. 1046-1053 e8.
70. Walsh, G.M., *Anti-IL-4/-13 based therapy in asthma.* Expert Opin Emerg Drugs, 2015. **20**(3): p. 349-52.
71. Agache, I.O., *From phenotypes to endotypes to asthma treatment.* Curr Opin Allergy Clin Immunol, 2013. **13**(3): p. 249-56.
72. Wjst, M., M. Sargurupremraj, and M. Arnold, *Genome-wide association studies in asthma: what they really told us about pathogenesis.* Curr Opin Allergy Clin Immunol, 2013. **13**(1): p. 112-8.
73. Tamari, M., S. Tanaka, and T. Hirota, *Genome-wide association studies of allergic diseases.* Allergol Int, 2013. **62**(1): p. 21-8.
74. Harada, M., et al., *Thymic stromal lymphopoietin gene promoter polymorphisms are associated with susceptibility to bronchial asthma.* Am J Respir Cell Mol Biol, 2011. **44**(6): p. 787-93.
75. Moffatt, M.F., et al., *A large-scale, consortium-based genomewide association study of asthma.* N Engl J Med, 2010. **363**(13): p. 1211-21.

76. He, Y., et al., *Association between Polymorphism of Interleukin-1beta and Interleukin-1 Receptor Antagonist Gene and Asthma Risk: A Meta-Analysis.* ScientificWorldJournal, 2015. **2015**: p. 685684.
77. Soumelis, V., et al., *Human epithelial cells trigger dendritic cell mediated allergic inflammation by producing TSLP.* Nat Immunol, 2002. **3**(7): p. 673-80.
78. Wang, Y.H. and Y.J. Liu, *Thymic stromal lymphopoietin, OX40-ligand, and interleukin-25 in allergic responses.* Clin Exp Allergy, 2009. **39**(6): p. 798-806.
79. Liew, F.Y., N.I. Pitman, and I.B. McInnes, *Disease-associated functions of IL-33: the new kid in the IL-1 family.* Nat Rev Immunol, 2010. **10**(2): p. 103-10.
80. Prefontaine, D., et al., *Increased IL-33 expression by epithelial cells in bronchial asthma.* J Allergy Clin Immunol, 2010. **125**(3): p. 752-4.
81. Ying, S., et al., *Thymic stromal lymphopoietin expression is increased in asthmatic airways and correlates with expression of Th2-attracting chemokines and disease severity.* J Immunol, 2005. **174**(12): p. 8183-90.
82. Ying, S., et al., *Expression and cellular provenance of thymic stromal lymphopoietin and chemokines in patients with severe asthma and chronic obstructive pulmonary disease.* J Immunol, 2008. **181**(4): p. 2790-8.
83. Mao, X.Q., et al., *Imbalance production between interleukin-1beta (IL-1beta) and IL-1 receptor antagonist (IL-1Ra) in bronchial asthma.* Biochem Biophys Res Commun, 2000. **276**(2): p. 607-12.
84. Miller, M., et al., *ORMDL3 is an inducible lung epithelial gene regulating metalloproteases, chemokines, OAS, and ATF6.* Proc Natl Acad Sci U S A, 2012. **109**(41): p. 16648-53.
85. Miller, M., et al., *ORMDL3 Transgenic Mice Have Increased Airway Remodeling and Airway Responsiveness Characteristic of Asthma.* J Immunol, 2014.
86. Bonnelykke, K., et al., *A genome-wide association study identifies CDHR3 as a susceptibility locus for early childhood asthma with severe exacerbations.* Nat Genet, 2014. **46**(1): p. 51-5.
87. Van Eerdewegh, P., et al., *Association of the ADAM33 gene with asthma and bronchial hyperresponsiveness.* Nature, 2002. **418**(6896): p. 426-30.
88. Ober, C., et al., *Effect of variation in CHI3L1 on serum YKL-40 level, risk of asthma, and lung function.* N Engl J Med, 2008. **358**(16): p. 1682-91.
89. Barton, S.J., et al., *PLAUR polymorphisms are associated with asthma, PLAUR levels, and lung function decline.* J Allergy Clin Immunol, 2009. **123**(6): p. 1391-400 e17.
90. Himes, B.E., et al., *Genome-wide association analysis identifies PDE4D as an asthma-susceptibility gene.* Am J Hum Genet, 2009. **84**(5): p. 581-93.
91. Davies, E.R., et al., *Soluble ADAM33 initiates airway remodeling to promote susceptibility for allergic asthma in early life.* JCI Insight, 2016. **1**(11).
92. Komi, D.E., T. Kazemi, and A.P. Bussink, *New Insights Into the Relationship Between Chitinase-3-Like-1 and Asthma.* Curr Allergy Asthma Rep, 2016. **16**(8): p. 57.

93. Lodish, H., et al., *Molecular Cell Biology*. 2007.
94. Loxham, M., D.E. Davies, and C. Blume, *Epithelial function and dysfunction in asthma.* Clin Exp Allergy, 2014. **44**(11): p. 1299-313.
95. Tsukita, S., et al., *Tight junction-based epithelial microenvironment and cell proliferation.* Oncogene, 2008. **27**(55): p. 6930-8.
96. Gonzalez-Mariscal, L., R. Tapia, and D. Chamorro, *Crosstalk of tight junction components with signaling pathways.* Biochim Biophys Acta, 2008. **1778**(3): p. 729-56.
97. Ganesan, S., A.T. Comstock, and U.S. Sajjan, *Barrier function of airway tract epithelium.* Tissue Barriers, 2013. **1**(4): p. e24997.
98. Garrod, D. and M. Chidgey, *Desmosome structure, composition and function.* Biochim Biophys Acta, 2008. **1778**(3): p. 572-87.
99. Thornton, D.J., K. Rousseau, and M.A. McGuckin, *Structure and function of the polymeric mucins in airways mucus.* Annu Rev Physiol, 2008. **70**: p. 459-86.
100. Ballard, S.T. and S.K. Inglis, *Liquid secretion properties of airway submucosal glands.* J Physiol, 2004. **556**(Pt 1): p. 1-10.
101. Kelly, F.J., *Vitamins and respiratory disease: antioxidant micronutrients in pulmonary health and disease.* Proc Nutr Soc, 2005. **64**(4): p. 510-26.
102. Bonfield, T.L., et al., *Normal bronchial epithelial cells constitutively produce the anti-inflammatory cytokine interleukin-10, which is downregulated in cystic fibrosis.* Am J Respir Cell Mol Biol, 1995. **13**(3): p. 257-61.
103. Schmidt, L.M., et al., *Bronchial epithelial cell-derived prostaglandin E2 dampens the reactivity of dendritic cells.* J Immunol, 2011. **186**(4): p. 2095-105.
104. Papazian, D., S. Hansen, and P.A. Wurtzen, *Airway responses towards allergens - from the airway epithelium to T cells.* Clin Exp Allergy, 2015. **45**(8): p. 1268-87.
105. Abdelaziz, M.M., et al., *The effect of conditioned medium from cultured human bronchial epithelial cells on eosinophil and neutrophil chemotaxis and adherence in vitro.* Am J Respir Cell Mol Biol, 1995. **13**(6): p. 728-37.
106. Cox, G., et al., *Promotion of eosinophil survival by human bronchial epithelial cells and its modulation by steroids.* Am J Respir Cell Mol Biol, 1991. **4**(6): p. 525-31.
107. Kato, Y., et al., *Airway epithelial cells promote transmigration of eosinophils in a new three-dimensional chemotaxis model.* Clin Exp Allergy, 2002. **32**(6): p. 889-97.
108. Otsuka, H., et al., *Stem cell factor mRNA expression and production in human nasal epithelial cells: contribution to the accumulation of mast cells in the nasal epithelium of allergy.* J Allergy Clin Immunol, 1998. **102**(5): p. 757-64.
109. Hsieh, F.H., et al., *Human airway epithelial cell determinants of survival and functional phenotype for primary human mast cells.* Proc Natl Acad Sci U S A, 2005. **102**(40): p. 14380-5.

110. Kim, J., et al., *Constitutive and inducible expression of b7 family of ligands by human airway epithelial cells.* Am J Respir Cell Mol Biol, 2005. **33**(3): p. 280-9.
111. Papi, A., et al., *Rhinovirus infection induces major histocompatibility complex class I and costimulatory molecule upregulation on respiratory epithelial cells.* J Infect Dis, 2000. **181**(5): p. 1780-4.
112. Sajjan, U., et al., *Rhinovirus disrupts the barrier function of polarized airway epithelial cells.* Am J Respir Crit Care Med, 2008. **178**(12): p. 1271-81.
113. Leigh, R., et al., *Human rhinovirus infection enhances airway epithelial cell production of growth factors involved in airway remodeling.* J Allergy Clin Immunol, 2008. **121**(5): p. 1238-1245 e4.
114. Tacon, C.E., et al., *Human rhinovirus infection up-regulates MMP-9 production in airway epithelial cells via NF-{kappa}B.* Am J Respir Cell Mol Biol, 2010. **43**(2): p. 201-9.
115. Kuo, C., et al., *Rhinovirus infection induces expression of airway remodelling factors in vitro and in vivo.* Respirology, 2011. **16**(2): p. 367-77.
116. Skevaki, C.L., et al., *Rhinovirus-induced basic fibroblast growth factor release mediates airway remodeling features.* Clin Transl Allergy, 2012. **2**(1): p. 14.
117. Knipe, D.M. and P.M. Howley, *Fields Virology*. Fifth ed. Vol. One. 2007.
118. Takeuchi, O. and S. Akira, *Innate immunity to virus infection.* Immunol Rev, 2009. **227**(1): p. 75-86.
119. Haller, O., G. Kochs, and F. Weber, *The interferon response circuit: induction and suppression by pathogenic viruses.* Virology, 2006. **344**(1): p. 119-30.
120. Kotenko, S.V., *IFN-lambdas.* Curr Opin Immunol, 2011. **23**(5): p. 583-90.
121. Xiao, C., et al., *Defective epithelial barrier function in asthma.* J Allergy Clin Immunol, 2011. **128**(3): p. 549-56 e1-12.
122. Ordonez, C.L., et al., *Mild and moderate asthma is associated with airway goblet cell hyperplasia and abnormalities in mucin gene expression.* Am J Respir Crit Care Med, 2001. **163**(2): p. 517-23.
123. Sackesen, C., et al., *A comprehensive evaluation of the enzymatic and nonenzymatic antioxidant systems in childhood asthma.* J Allergy Clin Immunol, 2008. **122**(1): p. 78-85.
124. Sousa, A.R., et al., *Increased expression of the monocyte chemoattractant protein-1 in bronchial tissue from asthmatic subjects.* Am J Respir Cell Mol Biol, 1994. **10**(2): p. 142-7.
125. Sekiya, T., et al., *Inducible expression of a Th2-type CC chemokine thymus- and activation-regulated chemokine by human bronchial epithelial cells.* J Immunol, 2000. **165**(4): p. 2205-13.
126. Coleman, J.M., et al., *Epithelial eotaxin-2 and eotaxin-3 expression: relation to asthma severity, luminal eosinophilia and age at onset.* Thorax, 2012. **67**(12): p. 1061-6.
127. Pichavant, M., et al., *Impact of bronchial epithelium on dendritic cell migration and function: modulation by the bacterial motif KpOmpA.* J Immunol, 2006. **177**(9): p. 5912-9.

128. Wark, P.A., et al., *IFN-gamma-induced protein 10 is a novel biomarker of rhinovirus-induced asthma exacerbations.* J Allergy Clin Immunol, 2007. **120**(3): p. 586-93.
129. Hackett, T.L., et al., *Intrinsic phenotypic differences of asthmatic epithelium and its inflammatory responses to respiratory syncytial virus and air pollution.* Am J Respir Cell Mol Biol, 2011. **45**(5): p. 1090-100.
130. Danahay, H., et al., *Notch2 is required for inflammatory cytokine-driven goblet cell metaplasia in the lung.* Cell Rep, 2015. **10**(2): p. 239-52.
131. Filley, W.V., et al., *Identification by immunofluorescence of eosinophil granule major basic protein in lung tissues of patients with bronchial asthma.* Lancet, 1982. **2**(8288): p. 11-6.
132. Bousquet, J., et al., *Eosinophilic inflammation in asthma.* N Engl J Med, 1990. **323**(15): p. 1033-9.
133. Holgate, S.T., W.R. Roche, and M.K. Church, *The role of the eosinophil in asthma.* Am Rev Respir Dis, 1991. **143**(3 Pt 2): p. S66-70.
134. Frigas, E., et al., *Elevated levels of the eosinophil granule major basic protein in the sputum of patients with bronchial asthma.* Mayo Clin Proc, 1981. **56**(6): p. 345-53.
135. Hastie, A.T., et al., *The effect of purified human eosinophil major basic protein on mammalian ciliary activity.* Am Rev Respir Dis, 1987. **135**(4): p. 848-53.
136. Motojima, S., et al., *Toxicity of eosinophil cationic proteins for guinea pig tracheal epithelium in vitro.* Am Rev Respir Dis, 1989. **139**(3): p. 801-5.
137. Chow, A.W., et al., *Polarized secretion of interleukin (IL)-6 and IL-8 by human airway epithelia 16HBE14o- cells in response to cationic polypeptide challenge.* PLoS One, 2010. **5**(8): p. e12091.
138. Zhang, S., et al., *Growth factors secreted by bronchial epithelial cells control myofibroblast proliferation: an in vitro co-culture model of airway remodeling in asthma.* Lab Invest, 1999. **79**(4): p. 395-405.
139. Pegorier, S., et al., *Eosinophil-derived cationic proteins activate the synthesis of remodeling factors by airway epithelial cells.* J Immunol, 2006. **177**(7): p. 4861-9.
140. Bucchieri, F., et al., *Asthmatic bronchial epithelium is more susceptible to oxidant-induced apoptosis.* Am J Respir Cell Mol Biol, 2002. **27**(2): p. 179-85.
141. Leino, M.S., et al., *Barrier disrupting effects of alternaria alternata extract on bronchial epithelium from asthmatic donors.* PLoS One, 2013. **8**(8): p. e71278.
142. Puddicombe, S.M., et al., *Involvement of the epidermal growth factor receptor in epithelial repair in asthma.* FASEB J, 2000. **14**(10): p. 1362-74.
143. Chu, H.W., et al., *Transforming growth factor-beta2 induces bronchial epithelial mucin expression in asthma.* Am J Pathol, 2004. **165**(4): p. 1097-106.
144. Bedke, N., et al., *Transforming growth factor-beta promotes rhinovirus replication in bronchial epithelial cells by suppressing the innate immune response.* PLoS One, 2012. **7**(9): p. e44580.

145. Bentley, A.M., et al., *Expression of endothelial and leukocyte adhesion molecules intercellular adhesion molecule-1, E-selectin, and vascular cell adhesion molecule-1 in the bronchial mucosa in steady-state and allergen-induced asthma.* Journal of Allergy and Clinical Immunology, 1993. **92**(6): p. 857-868.
146. Jakiela, B., et al., *Basal cells of differentiated bronchial epithelium are more susceptible to rhinovirus infection.* Am J Respir Cell Mol Biol, 2008. **38**(5): p. 517-23.
147. Lachowicz-Scroggins, M.E., et al., *Interleukin-13-Induced Mucous Metaplasia Increases Susceptibility of Human Airway Epithelium to Rhinovirus Infection.* American Journal of Respiratory Cell and Molecular Biology, 2010. **43**(6): p. 652-661.
148. Wark, P.A., et al., *Asthmatic bronchial epithelial cells have a deficient innate immune response to infection with rhinovirus.* J Exp Med, 2005. **201**(6): p. 937-47.
149. Contoli, M., et al., *Role of deficient type III interferon-lambda production in asthma exacerbations.* Nat Med, 2006. **12**(9): p. 1023-6.
150. Cakebread, J.A., et al., *Rhinovirus-16 Induced Release of IP-10 and IL-8 Is Augmented by Th2 Cytokines in a Pediatric Bronchial Epithelial Cell Model.* PLoS One, 2014. **9**(4): p. e94010.
151. Uller, L., et al., *Double-stranded RNA induces disproportionate expression of thymic stromal lymphopoietin versus interferon-beta in bronchial epithelial cells from donors with asthma.* Thorax, 2010. **65**(7): p. 626-32.
152. Grainge, C., et al., *Asthmatic and normal respiratory epithelial cells respond differently to mechanical apical stress.* Am J Respir Crit Care Med, 2014. **190**(4): p. 477-80.
153. Evans, M.J., et al., *The attenuated fibroblast sheath of the respiratory tract epithelial-mesenchymal trophic unit.* Am J Respir Cell Mol Biol, 1999. **21**(6): p. 655-7.
154. Myerburg, M.M., et al., *Hepatocyte growth factor and other fibroblast secretions modulate the phenotype of human bronchial epithelial cells.* Am J Physiol Lung Cell Mol Physiol, 2007. **292**(6): p. L1352-60.
155. Skibinski, G., J.S. Elborn, and M. Ennis, *Bronchial epithelial cell growth regulation in fibroblast cocultures: the role of hepatocyte growth factor.* Am J Physiol Lung Cell Mol Physiol, 2007. **293**(1): p. L69-76.
156. Kurokawa, M., et al., *Expression and effects of IL-33 and ST2 in allergic bronchial asthma: IL-33 induces eotaxin production in lung fibroblasts.* Int Arch Allergy Immunol, 2011. **155 Suppl 1**: p. 12-20.
157. Suwara, M.I., et al., *IL-1alpha released from damaged epithelial cells is sufficient and essential to trigger inflammatory responses in human lung fibroblasts.* Mucosal Immunol, 2014. **7**(3): p. 684-93.
158. Donaldson, J.E., *ANALYSIS OF THE EXPRESSION OF THYMIC STROMAL LYMPHOPOIETIN AND ITS VARIANTS IN CELLS OF THE ASTHMATIC AIRWAY*, in *Faculty of medicine*2015, University of Southampton.
159. Datta, A., et al., *Evidence for a functional thymic stromal lymphopoietin signaling axis in fibrotic lung disease.* J Immunol, 2013. **191**(9): p. 4867-79.
160. Tracy, E.C., et al., *Interleukin-1alpha is the major alarmin of lung epithelial cells released during photodynamic therapy to induce*

inflammatory mediators in fibroblasts. Br J Cancer, 2012. **107**(9): p. 1534-46.
161. Osei, E.T., et al., *Interleukin-1alpha drives the dysfunctional cross-talk of the airway epithelium and lung fibroblasts in COPD.* Eur Respir J, 2016.
162. Morishima, Y., et al., *Triggering the induction of myofibroblast and fibrogenesis by airway epithelial shedding.* Am J Respir Cell Mol Biol, 2001. **24**(1): p. 1-11.
163. Thompson, H.G., et al., *Epithelial-derived TGF-beta2 modulates basal and wound-healing subepithelial matrix homeostasis.* Am J Physiol Lung Cell Mol Physiol, 2006. **291**(6): p. L1277-85.
164. Desmouliere, A., et al., *Transforming growth factor-beta 1 induces alpha-smooth muscle actin expression in granulation tissue myofibroblasts and in quiescent and growing cultured fibroblasts.* J Cell Biol, 1993. **122**(1): p. 103-11.
165. Hinz, B., et al., *Recent developments in myofibroblast biology: paradigms for connective tissue remodeling.* Am J Pathol, 2012. **180**(4): p. 1340-55.
166. Davies, D.E., *The role of the epithelium in airway remodeling in asthma.* Proc Am Thorac Soc, 2009. **6**(8): p. 678-82.
167. Vignola, A.M., et al., *Sputum metalloproteinase-9/tissue inhibitor of metalloproteinase-1 ratio correlates with airflow obstruction in asthma and chronic bronchitis.* Am J Respir Crit Care Med, 1998. **158**(6): p. 1945-50.
168. Mautino, G., et al., *Tissue inhibitor of metalloproteinase-1 levels in bronchoalveolar lavage fluid from asthmatic subjects.* Am J Respir Crit Care Med, 1999. **160**(1): p. 324-30.
169. Maisi, P., et al., *Soluble membrane-type 1 matrix metalloproteinase (MT1-MMP) and gelatinase A (MMP-2) in induced sputum and bronchoalveolar lavage fluid of human bronchial asthma and bronchiectasis.* APMIS, 2002. **110**(11): p. 771-82.
170. Redington, A.E., et al., *Transforming growth factor-beta 1 in asthma. Measurement in bronchoalveolar lavage fluid.* Am J Respir Crit Care Med, 1997. **156**(2 Pt 1): p. 642-7.
171. Redington, A.E., et al., *Basic fibroblast growth factor in asthma: measurement in bronchoalveolar lavage fluid basally and following allergen challenge.* J Allergy Clin Immunol, 2001. **107**(2): p. 384-7.
172. Hoshino, M., Y. Nakamura, and Q.A. Hamid, *Gene expression of vascular endothelial growth factor and its receptors and angiogenesis in bronchial asthma.* J Allergy Clin Immunol, 2001. **107**(6): p. 1034-8.
173. Hoshino, M., M. Takahashi, and N. Aoike, *Expression of vascular endothelial growth factor, basic fibroblast growth factor, and angiogenin immunoreactivity in asthmatic airways and its relationship to angiogenesis.* J Allergy Clin Immunol, 2001. **107**(2): p. 295-301.
174. Reeves, S.R., et al., *Asthmatic airway epithelial cells differentially regulate fibroblast expression of extracellular matrix components.* J Allergy Clin Immunol, 2014.
175. Reeves, S.R., et al., *Fibroblast-myofibroblast transition is differentially regulated by bronchial epithelial cells from asthmatic children.* Respir Res, 2015. **16**(1): p. 21.

176. Michalik, M., et al., *Asthmatic bronchial fibroblasts demonstrate enhanced potential to differentiate into myofibroblasts in culture.* Med Sci Monit, 2009. **15**(7): p. BR194-201.
177. Del Vecchio, A.M., et al., *Utility of animal and in vivo experimental infection of humans with rhinoviruses in the development of therapeutic agents for viral exacerbations of asthma and chronic obstructive pulmonary disease.* Pulm Pharmacol Ther, 2015. **30**: p. 32-43.
178. Bartlett, N.W., et al., *Mouse models of rhinovirus-induced disease and exacerbation of allergic airway inflammation.* Nat Med, 2008. **14**(2): p. 199-204.
179. Rosenthal, L.A., et al., *A rat model of picornavirus-induced airway infection and inflammation.* Virol J, 2009. **6**: p. 122.
180. Gruenert, D.C., et al., *Characterization of human tracheal epithelial cells transformed by an origin-defective simian virus 40.* Proc Natl Acad Sci U S A, 1988. **85**(16): p. 5951-5.
181. Pezzulo, A.A., et al., *The air-liquid interface and use of primary cell cultures are important to recapitulate the transcriptional profile of in vivo airway epithelia.* Am J Physiol Lung Cell Mol Physiol, 2011. **300**(1): p. L25-31.
182. Whitcutt, M.J., K.B. Adler, and R. Wu, *A biphasic chamber system for maintaining polarity of differentiation of cultured respiratory tract epithelial cells.* In Vitro Cell Dev Biol, 1988. **24**(5): p. 420-8.
183. Jacobs, J.P., C.M. Jones, and J.P. Baille, *Characteristics of a human diploid cell designated MRC-5.* Nature, 1970. **227**(5254): p. 168-70.
184. Jones, H.W., Jr., et al., *George Otto Gey. (1899-1970). The HeLa cell and a reappraisal of its origin.* Obstet Gynecol, 1971. **38**(6): p. 945-9.
185. Gey, G.O., W.D. Coffman, and M.T. Kubicek, *Tissue culture studies of the proliferative capacity of cervical carcinoma and normal epithelium.* Cancer Research, 1952. **12**(4): p. 264.
186. Kato, H., et al., *Length-dependent recognition of double-stranded ribonucleic acids by retinoic acid-inducible gene-I and melanoma differentiation-associated gene 5.* J Exp Med, 2008. **205**(7): p. 1601-10.
187. Parker, L.C., C.A. Stokes, and I. Sabroe, *Rhinoviral infection and asthma: the detection and management of rhinoviruses by airway epithelial cells.* Clin Exp Allergy, 2014. **44**(1): p. 20-8.
188. Puxeddu, I., et al., *The role of eosinophil major basic protein in angiogenesis.* Allergy, 2009. **64**(3): p. 368-74.
189. Shahana, S., C. Kampf, and G.M. Roomans, *Effects of the cationic protein poly-L-arginine on airway epithelial cells in vitro.* Mediators Inflamm, 2002. **11**(3): p. 141-8.
190. Abu-Ghazaleh, R.I., G.J. Gleich, and F.G. Prendergast, *Interaction of eosinophil granule major basic protein with synthetic lipid bilayers: a mechanism for toxicity.* J Membr Biol, 1992. **128**(2): p. 153-64.
191. Boraschi, D. and A. Tagliabue, *The interleukin-1 receptor family.* Semin Immunol, 2013. **25**(6): p. 394-407.
192. Papi, A. and S.L. Johnston, *Rhinovirus infection induces expression of its own receptor intercellular adhesion molecule 1 (ICAM-1) via increased NF-kappaB-mediated transcription.* J Biol Chem, 1999. **274**(14): p. 9707-20.
193. Hubert, J., *Spearman-Karber method. Bioassay.* 2nd ed. 1984, Dubuque (Iowa): Hunt Publishing.

194. Garlanda, C., C.A. Dinarello, and A. Mantovani, *The interleukin-1 family: back to the future.* Immunity, 2013. **39**(6): p. 1003-18.
195. Theofilopoulos, A.N., et al., *Type I interferons (alpha/beta) in immunity and autoimmunity.* Annu Rev Immunol, 2005. **23**: p. 307-36.
196. Wrana, J.L., et al., *TGF beta signals through a heteromeric protein kinase receptor complex.* Cell, 1992. **71**(6): p. 1003-14.
197. Alberts, B., A. Johnson, and J. Lewis, *Molecular Biology of the Cell*, 2002, Garland Science.
198. Salic, A. and T.J. Mitchison, *A chemical method for fast and sensitive detection of DNA synthesis in vivo.* Proc Natl Acad Sci U S A, 2008. **105**(7): p. 2415-20.
199. LifeTechnologiesCorporation, *Click-iT EdU Imaging Kit manual.* 2011.
200. Promega. *CytoTox 96® Non-Radioactive Cytotoxicity Assay Protocol*. 2015 [cited 2015 2nd Feb]; Available from: http://www.promega.co.uk/resources/protocols/technical-bulletins/0/cytotox-96-non-radioactive-cytotoxicity-assay-protocol/.
201. R&DSystems. *ELISA Developement Guide*. 2014 [cited 2015 2nd Feb]; Available from: http://www.rndsystems.com/resources/images/5670.pdf.
202. Berg, J.M., J.L. Tymoczko, and L. Stryer, *Biochemistry*. 6th Edition ed. 2007, New York: W H Freeman.
203. R&DSystems. *Luminex®Screening Assay Product Data Sheet*. 2014 [cited 2015 2nd Feb]; Available from: http://www.rndsystems.com/pdf/LXSAH.pdf.
204. Luminex. *xMAP® Technology*. 2015 [cited 2015 2nd Feb]; Available from: http://www.luminexcorp.com/TechnologiesScience/xMAPTechnology/.
205. MesoScaleDiscovery®. *Literature - Meso Scale Discovery®*. 2015 [cited 2015 2nd Feb]; Available from: http://www.mesoscale.com/CatalogSystemWeb/WebRoot/literature.aspx.
206. MesoScaleDiscovery®, *MSD® 96-Well MULTI-ARRAY® Human IFN-□ Assay protocol*, 2015.
207. Comstock, A.T., et al., *Rhinovirus-induced barrier dysfunction in polarized airway epithelial cells is mediated by NADPH oxidase 1.* J Virol, 2011. **85**(13): p. 6795-808.
208. Piper, S.C., et al., *The role of interleukin-1 and interleukin-18 in pro-inflammatory and anti-viral responses to rhinovirus in primary bronchial epithelial cells.* PLoS One, 2013. **8**(5): p. e63365.
209. Jackson, D.J., et al., *IL-33-dependent type 2 inflammation during rhinovirus-induced asthma exacerbations in vivo.* Am J Respir Crit Care Med, 2014. **190**(12): p. 1373-82.
210. Hui, C.C., et al., *T cell-mediated induction of thymic stromal lymphopoietin in differentiated human primary bronchial epithelial cells.* Clin Exp Allergy, 2014. **44**(7): p. 953-64.
211. Nagarkar, D.R., et al., *Airway epithelial cells activate TH2 cytokine production in mast cells through IL-1 and thymic stromal lymphopoietin.* J Allergy Clin Immunol, 2012. **130**(1): p. 225-32 e4.

212. Rezaee, F., et al., *Polyinosinic:polycytidylic acid induces protein kinase D-dependent disassembly of apical junctions and barrier dysfunction in airway epithelial cells.* J Allergy Clin Immunol, 2011. **128**(6): p. 1216-1224 e11.
213. Cakebread, J.A., et al., *Exogenous IFN-beta has antiviral and anti-inflammatory properties in primary bronchial epithelial cells from asthmatic subjects exposed to rhinovirus.* J Allergy Clin Immunol, 2011. **127**(5): p. 1148-54 e9.
214. Korpi-Steiner, N.L., et al., *Human monocytic cells direct the robust release of CXCL10 by bronchial epithelial cells during rhinovirus infection.* Clin Exp Allergy, 2010. **40**(8): p. 1203-13.
215. Sumida, A., et al., *TH1/TH2 immune response in lung fibroblasts in interstitial lung disease.* Arch Med Res, 2008. **39**(5): p. 503-10.
216. Heijink, I.H., et al., *Budesonide and fluticasone propionate differentially affect the airway epithelial barrier.* Respir Res, 2016. **17**: p. 2.
217. Unger, B.L., et al., *Nod-like receptor X-1 is required for rhinovirus-induced barrier dysfunction in airway epithelial cells.* J Virol, 2014. **88**(7): p. 3705-18.
218. Spurrell, J.C., et al., *Human airway epithelial cells produce IP-10 (CXCL10) in vitro and in vivo upon rhinovirus infection.* Am J Physiol Lung Cell Mol Physiol, 2005. **289**(1): p. L85-95.
219. Morris, G.E., et al., *A novel electrospun biphasic scaffold provides optimal three-dimensional topography for in vitro co-culture of airway epithelial and fibroblast cells.* Biofabrication, 2014. **6**(3): p. 035014.
220. Harrington, H., et al., *Immunocompetent 3D Model of Human Upper Airway for Disease Modeling and In Vitro Drug Evaluation.* Mol Pharm, 2014.
221. Pohl, C., et al., *Acute morphological and toxicological effects in a human bronchial coculture model after sulfur mustard exposure.* Toxicol Sci, 2009. **112**(2): p. 482-9.
222. Wiszniewski, L., et al., *Long-term cultures of polarized airway epithelial cells from patients with cystic fibrosis.* Am J Respir Cell Mol Biol, 2006. **34**(1): p. 39-48.
223. Vermeer, P.D., et al., *Differentiation of human airway epithelia is dependent on erbB2.* Am J Physiol Lung Cell Mol Physiol, 2006. **291**(2): p. L175-80.
224. Campbell-Harding, G., et al., *The innate antiviral response upregulates IL-13 receptor alpha2 in bronchial fibroblasts.* J Allergy Clin Immunol, 2013. **131**(3): p. 849-55.
225. Bedke, N., et al., *Contribution of bronchial fibroblasts to the antiviral response in asthma.* J Immunol, 2009. **182**(6): p. 3660-7.
226. Ito, Y., et al., *Influenza induces IL-8 and GM-CSF secretion by human alveolar epithelial cells through HGF/c-Met and TGF-alpha/EGFR signaling.* Am J Physiol Lung Cell Mol Physiol, 2015. **308**(11): p. L1178-88.
227. Alkhouri, H., et al., *Regulation of pulmonary inflammation by mesenchymal cells.* Pulm Pharmacol Ther, 2014. **29**(2): p. 156-65.
228. Kitamura, H., et al., *Mouse and human lung fibroblasts regulate dendritic cell trafficking, airway inflammation, and fibrosis through integrin alphavbeta8-mediated activation of TGF-beta.* J Clin Invest, 2011. **121**(7): p. 2863-75.

229. Kobayashi, Y., et al., *Identification of calcium-activated neutral protease as a processing enzyme of human interleukin 1 alpha.* Proc Natl Acad Sci U S A, 1990. **87**(14): p. 5548-52.
230. Chen, C.J., et al., *Identification of a key pathway required for the sterile inflammatory response triggered by dying cells.* Nat Med, 2007. **13**(7): p. 851-6.
231. Chen, G.Y. and G. Nunez, *Sterile inflammation: sensing and reacting to damage.* Nat Rev Immunol, 2010. **10**(12): p. 826-37.
232. Dinarello, C.A., *Immunological and inflammatory functions of the interleukin-1 family.* Annu Rev Immunol, 2009. **27**: p. 519-50.
233. Wilkinson, E., *The Effect of Rhinovirus 16 on Human Bronchial Barrier Integrity and Mucosal IL-6 Responses.* , in *Faculty of Medicine*2013, University of Southampton.
234. Willart, M.A., et al., *Interleukin-1alpha controls allergic sensitization to inhaled house dust mite via the epithelial release of GM-CSF and IL-33.* J Exp Med, 2012. **209**(8): p. 1505-17.
235. Proud, D., S.P. Sanders, and S. Wiehler, *Human rhinovirus infection induces airway epithelial cell production of human beta-defensin 2 both in vitro and in vivo.* J Immunol, 2004. **172**(7): p. 4637-45.
236. Shi, L., et al., *Rhinovirus-induced IL-1beta release from bronchial epithelial cells is independent of functional P2X7.* Am J Respir Cell Mol Biol, 2012. **47**(3): p. 363-71.
237. Wessendorf, J.H., et al., *Identification of a nuclear localization sequence within the structure of the human interleukin-1 alpha precursor.* J Biol Chem, 1993. **268**(29): p. 22100-4.
238. Werman, A., et al., *The precursor form of IL-1alpha is an intracrine proinflammatory activator of transcription.* Proc Natl Acad Sci U S A, 2004. **101**(8): p. 2434-9.
239. Melkamu, T., H. Kita, and S.M. O'Grady, *TLR3 activation evokes IL-6 secretion, autocrine regulation of Stat3 signaling and TLR2 expression in human bronchial epithelial cells.* J Cell Commun Signal, 2013. **7**(2): p. 109-18.
240. Coulter, K.R., et al., *Extracellular regulation of interleukin (IL)-1beta through lung epithelial cells and defective IL-1 type II receptor expression.* Am J Respir Cell Mol Biol, 1999. **20**(5): p. 964-75.
241. Yang, Y., et al., *Regulation of interleukin-1beta and interleukin-1beta inhibitor release by human airway epithelial cells.* Eur Respir J, 2004. **24**(3): p. 360-6.
242. Di Paolo, N.C., et al., *Virus binding to a plasma membrane receptor triggers interleukin-1 alpha-mediated proinflammatory macrophage response in vivo.* Immunity, 2009. **31**(1): p. 110-21.
243. Mazzarella, G., et al., *Phenotypic features of alveolar monocytes/macrophages and IL-8 gene activation by IL-1 and TNF-alpha in asthmatic patients.* Allergy, 2000. **55 Suppl 61**: p. 36-41.
244. Allakhverdi, Z., et al., *Cutting edge: The ST2 ligand IL-33 potently activates and drives maturation of human mast cells.* J Immunol, 2007. **179**(4): p. 2051-4.

245. Nagarkar, D.R., et al., *Airway epithelial cells activate T(H)2 cytokine production in mast cells through IL-1 and thymic stromal lymphopoietin.* J Allergy Clin Immunol, 2012. **130**(1): p. 225-232.
246. Pesci, A., et al., *Histochemical characteristics and degranulation of mast cells in epithelium and lamina propria of bronchial biopsies from asthmatic and normal subjects.* Am Rev Respir Dis, 1993. **147**(3): p. 684-9.
247. Bradding, P., A.F. Walls, and S.T. Holgate, *The role of the mast cell in the pathophysiology of asthma.* J Allergy Clin Immunol, 2006. **117**(6): p. 1277-84.
248. Monteseirin, J., *Neutrophils and asthma.* J Investig Allergol Clin Immunol, 2009. **19**(5): p. 340-54.
249. Shepherd, J., et al., *Systematic review and economic analysis of the comparative effectiveness of different inhaled corticosteroids and their usage with long-acting beta2 agonists for the treatment of chronic asthma in adults and children aged 12 years and over.* Health Technol Assess, 2008. **12**(19): p. iii-iv, 1-360.
250. Mertens, M. and J.A. Singh, *Anakinra for rheumatoid arthritis: a systematic review.* J Rheumatol, 2009. **36**(6): p. 1118-25.
251. Dinarello, C.A. and J.W. van der Meer, *Treating inflammation by blocking interleukin-1 in humans.* Semin Immunol, 2013. **25**(6): p. 469-84.
252. Hernandez, M.L., et al., *IL-1 receptor antagonist reduces endotoxin-induced airway inflammation in healthy volunteers.* J Allergy Clin Immunol, 2015. **135**(2): p. 379-85.
253. Seki, E., et al., *Cytokine profiles, signalling pathways and effects of fluticasone propionate in respiratory syncytial virus-infected human foetal lung fibroblasts.* Cell Biol Int, 2013.
254. Edwards, M.R., M.W. Johnson, and S.L. Johnston, *Combination therapy: Synergistic suppression of virus-induced chemokines in airway epithelial cells.* Am J Respir Cell Mol Biol, 2006. **34**(5): p. 616-24.
255. Oshita, Y., et al., *Increased circulating 92 kDa matrix metalloproteinase (MMP-9) activity in exacerbations of asthma.* Thorax, 2003. **58**(9): p. 757-60.
256. Psarras, S., et al., *Vascular endothelial growth factor-mediated induction of angiogenesis by human rhinoviruses.* J Allergy Clin Immunol, 2006. **117**(2): p. 291-7.
257. Lee, K.Y., et al., *Clinical significance of plasma and serum vascular endothelial growth factor in asthma.* J Asthma, 2008. **45**(9): p. 735-9.
258. Dosanjh, A., *Transforming growth factor-beta expression induced by rhinovirus infection in respiratory epithelial cells.* Acta Biochim Biophys Sin (Shanghai), 2006. **38**(12): p. 911-4.
259. Xatzipsalti, M., et al., *Modulation of the epithelial inflammatory response to rhinovirus in an atopic environment.* Clin Exp Allergy, 2008. **38**(3): p. 466-72.
260. Xu, J., et al., *Matrix metalloproteinase-2 from bronchial epithelial cells induces the proliferation of subepithelial fibroblasts.* Clin Exp Allergy, 2002. **32**(6): p. 881-8.
261. Iskandar, A.R., et al., *Impact Assessment of Cigarette Smoke Exposure on Organotypic Bronchial Epithelial Tissue Cultures: A Comparison of Mono-Culture and Coculture Model Containing Fibroblasts.* Toxicol Sci, 2015.

262. Chakrabarti, S. and K.D. Patel, *Matrix metalloproteinase-2 (MMP-2) and MMP-9 in pulmonary pathology.* Exp Lung Res, 2005. **31**(6): p. 599-621.
263. Simcock, D.E., et al., *Proangiogenic activity in bronchoalveolar lavage fluid from patients with asthma.* Am J Respir Crit Care Med, 2007. **176**(2): p. 146-53.
264. Bodo, M., et al., *Bronchial epithelial cell matrix production in response to silica and basic fibroblast growth factor.* Mol Med, 2001. **7**(2): p. 83-92.
265. Brown, K.R., et al., *VEGF induces airway epithelial cell proliferation in human fetal lung in vitro.* Am J Physiol Lung Cell Mol Physiol, 2001. **281**(4): p. L1001-10.
266. Lee, H.S., A. Myers, and J. Kim, *Vascular endothelial growth factor drives autocrine epithelial cell proliferation and survival in chronic rhinosinusitis with nasal polyposis.* Am J Respir Crit Care Med, 2009. **180**(11): p. 1056-67.
267. Perng, D.W., et al., *Matrix metalloprotease-9 induces transforming growth factor-beta(1) production in airway epithelium via activation of epidermal growth factor receptors.* Life Sci, 2011. **89**(5-6): p. 204-12.
268. McCawley, L.J. and L.M. Matrisian, *Matrix metalloproteinases: they're not just for matrix anymore!* Curr Opin Cell Biol, 2001. **13**(5): p. 534-40.
269. Wang, J., et al., *Double-stranded RNA poly(I:C) enhances matrix metalloproteinase mRNA expression in human nasal polyp epithelial cells.* Acta Otolaryngol Suppl, 2009(562): p. 105-9.
270. Kubota, Y., et al., *Interleukin-1alpha-dependent regulation of matrix metalloproteinase-9(MMP-9) secretion and activation in the epithelial cells of odontogenic jaw cysts.* J Dent Res, 2000. **79**(6): p. 1423-30.
271. Kubota, Y., et al., *Interleukin-1alpha enhances type I collagen-induced activation of matrix metalloproteinase-2 in odontogenic keratocyst fibroblasts.* J Dent Res, 2002. **81**(1): p. 23-7.
272. Turner, N.A., et al., *Modulatory effect of interleukin-1alpha on expression of structural matrix proteins, MMPs and TIMPs in human cardiac myofibroblasts: role of p38 MAP kinase.* Matrix Biol, 2010. **29**(7): p. 613-20.
273. Ko, J.A., et al., *Downregulation of matrix metalloproteinase-2 in corneal fibroblasts by interleukin-1 receptor antagonist released from corneal epithelial cells.* Invest Ophthalmol Vis Sci, 2010. **51**(12): p. 6286-93.
274. Tang, R.F., et al., *Interleukin-1alpha, 6 regulate the secretion of vascular endothelial growth factor A, C in pancreatic cancer.* Hepatobiliary Pancreat Dis Int, 2005. **4**(3): p. 460-3.
275. Sato, N. and A. Fujii, *Effects of interleukin-1alpha on the production and release of basic fibroblast growth factor in cultured nifedipine-reactive gingival fibroblasts.* J Oral Sci, 2008. **50**(1): p. 83-90.
276. Bando, Y., et al., *Cyclooxygenase-2-derived prostaglandin E2 is involved in vascular endothelial growth factor production in interleukin-1alpha-stimulated human periodontal ligament cells.* J Periodontal Res, 2009. **44**(3): p. 395-401.
277. Moodley, Y.P., et al., *Fibroblasts isolated from normal lungs and those with idiopathic pulmonary fibrosis differ in interleukin-6/gp130-*

mediated cell signaling and proliferation. Am J Pathol, 2003. **163**(1): p. 345-54.
278. Liu, X., et al., *The CC chemokine ligand 2 (CCL2) mediates fibroblast survival through IL-6.* Am J Respir Cell Mol Biol, 2007. **37**(1): p. 121-8.
279. Shelfoon, C., et al., *Chemokine release from human rhinovirus-infected airway epithelial cells promotes fibroblast migration.* J Allergy Clin Immunol, 2016.
280. Hung, C.F., et al., *Role of IGF-1 pathway in lung fibroblast activation.* Respir Res, 2013. **14**: p. 102.
281. Gibbs, J.D., et al., *Cell cycle arrest by transforming growth factor beta1 enhances replication of respiratory syncytial virus in lung epithelial cells.* J Virol, 2009. **83**(23): p. 12424-31.
282. Li, N., et al., *Influenza viral neuraminidase primes bacterial coinfection through TGF-beta-mediated expression of host cell receptors.* Proc Natl Acad Sci U S A, 2015. **112**(1): p. 238-43.
283. Mazzieri, R., J.S. Munger, and D.B. Rifkin, *Measurement of active TGF-beta generated by cultured cells.* Methods Mol Biol, 2000. **142**: p. 13-27.
284. Wakefield, L.M., et al., *Latent transforming growth factor-beta from human platelets. A high molecular weight complex containing precursor sequences.* J Biol Chem, 1988. **263**(16): p. 7646-54.
285. Munger, J.S., et al., *The integrin alpha v beta 6 binds and activates latent TGF beta 1: a mechanism for regulating pulmonary inflammation and fibrosis.* Cell, 1999. **96**(3): p. 319-28.
286. Boxall, C., S.T. Holgate, and D.E. Davies, *The contribution of transforming growth factor-beta and epidermal growth factor signalling to airway remodelling in chronic asthma.* Eur Respir J, 2006. **27**(1): p. 208-29.
287. Annes, J.P., J.S. Munger, and D.B. Rifkin, *Making sense of latent TGFbeta activation.* J Cell Sci, 2003. **116**(Pt 2): p. 217-24.
288. Wipff, P.J. and B. Hinz, *Integrins and the activation of latent transforming growth factor beta1 - an intimate relationship.* Eur J Cell Biol, 2008. **87**(8-9): p. 601-15.
289. Yu, Q. and I. Stamenkovic, *Cell surface-localized matrix metalloproteinase-9 proteolytically activates TGF-beta and promotes tumor invasion and angiogenesis.* Genes Dev, 2000. **14**(2): p. 163-76.
290. Finlay, G.A., et al., *Transforming growth factor-beta 1-induced activation of the ERK pathway/activator protein-1 in human lung fibroblasts requires the autocrine induction of basic fibroblast growth factor.* J Biol Chem, 2000. **275**(36): p. 27650-6.
291. Burgess, H.A., et al., *PPARgamma agonists inhibit TGF-beta induced pulmonary myofibroblast differentiation and collagen production: implications for therapy of lung fibrosis.* Am J Physiol Lung Cell Mol Physiol, 2005. **288**(6): p. L1146-53.
292. Kobayashi, T., et al., *Smad3 mediates TGF-beta1 induction of VEGF production in lung fibroblasts.* Biochem Biophys Res Commun, 2005. **327**(2): p. 393-8.
293. Proud, D., et al., *Gene expression profiles during in vivo human rhinovirus infection: insights into the host response.* Am J Respir Crit Care Med, 2008. **178**(9): p. 962-8.

294. Wardlaw, A.J., et al., *Eosinophils and mast cells in bronchoalveolar lavage in subjects with mild asthma. Relationship to bronchial hyperreactivity.* Am Rev Respir Dis, 1988. **137**(1): p. 62-9.
295. Ohtake, K., et al., *Poly-L-arginine predominantly increases the paracellular permeability of hydrophilic macromolecules across rabbit nasal epithelium in vitro.* Pharm Res, 2003. **20**(2): p. 153-60.
296. Ohtake, K., et al., *Poly-L-arginine enhances paracellular permeability via serine/threonine phosphorylation of ZO-1 and tyrosine dephosphorylation of occludin in rabbit nasal epithelium.* Pharm Res, 2003. **20**(11): p. 1838-45.
297. Uchida, D.A., et al., *Cationic proteins increase the permeability of cultured rabbit tracheal epithelial cells: modification by heparin and extracellular calcium.* Exp Lung Res, 1996. **22**(1): p. 85-99.
298. Rochester, C.L., et al., *Eosinophil-fibroblast interactions. Granule major basic protein interacts with IL-1 and transforming growth factor-beta in the stimulation of lung fibroblast IL-6-type cytokine production.* J Immunol, 1996. **156**(11): p. 4449-56.
299. Arseneault, D., K. Maghni, and P. Sirois, *Selective inflammatory response induced by intratracheal and intravenous administration of poly-L-arginine in guinea pig lungs.* Inflammation, 1999. **23**(3): p. 287-304.
300. Thomas, L.L., et al., *Peptide-based analysis of amino acid sequences important to the biological activity of eosinophil granule major basic protein.* Immunol Lett, 2001. **78**(3): p. 175-81.
301. Zagai, U., et al., *The effect of eosinophils on collagen gel contraction and implications for tissue remodelling.* Clin Exp Immunol, 2004. **135**(3): p. 427-33.
302. Kato, Y., et al., *Leukotriene D4 induces production of transforming growth factor-beta1 by eosinophils.* Int Arch Allergy Immunol, 2005. **137 Suppl 1**: p. 17-20.
303. Flood-Page, P., et al., *Anti-IL-5 treatment reduces deposition of ECM proteins in the bronchial subepithelial basement membrane of mild atopic asthmatics.* J Clin Invest, 2003. **112**(7): p. 1029-36.
304. Vancheri, C., et al., *Intranasal heparin reduces eosinophil recruitment after nasal allergen challenge in patients with allergic rhinitis.* J Allergy Clin Immunol, 2001. **108**(5): p. 703-8.
305. Mousavi, S., et al., *Anti-Inflammatory Effects of Heparin and Its Derivatives: A Systematic Review.* Adv Pharmacol Sci, 2015. **2015**: p. 507151.
306. Takizawa, H., et al., *Interleukin 6-receptor expression on human bronchial epithelial cells: regulation by IL-1 and IL-6.* Am J Physiol, 1996. **270**(3 Pt 1): p. L346-52.
307. Hackett, T.L., *Epithelial-mesenchymal transition in the pathophysiology of airway remodelling in asthma.* Curr Opin Allergy Clin Immunol, 2012. **12**(1): p. 53-9.
308. Freynet, O., et al., *Human lung fibroblasts may modulate dendritic cell phenotype and function: results from a pilot in vitro study.* Respir Res, 2016. **17**: p. 36.

309. Hammad, H., et al., *House dust mite allergen induces asthma via Toll-like receptor 4 triggering of airway structural cells.* Nat Med, 2009. **15**(4): p. 410-6.
310. Fukumoto, A., et al., *Induction of TARC production by lipopolysaccharide and interleukin-4 in nasal fibroblasts.* Int Arch Allergy Immunol, 2008. **145**(4): p. 291-7.
311. Nonaka, M., et al., *Combined stimulation with Poly(I:C), TNF-alpha and Th2 cytokines induces TARC production by human fibroblasts from the nose, bronchioles and lungs.* Int Arch Allergy Immunol, 2010. **152**(4): p. 327-41.
312. Darveau, M.E., et al., *Increased T-cell survival by structural bronchial cells derived from asthmatic subjects cultured in an engineered human mucosa.* J Allergy Clin Immunol, 2008. **121**(3): p. 692-9.
313. Pompen, M., et al., *Lung epithelial H292 cells induce differentiation of immature human HMC-1 mast cells by interleukin-6 and stem cell factor.* Clin Exp Allergy, 2000. **30**(8): p. 1104-12.
314. Saito, H., et al., *Selective growth of human mast cells induced by Steel factor, IL-6, and prostaglandin E2 from cord blood mononuclear cells.* J Immunol, 1996. **157**(1): p. 343-50.
315. Park, C.S., et al., *Granulocyte macrophage colony-stimulating factor is the main cytokine enhancing survival of eosinophils in asthmatic airways.* Eur Respir J, 1998. **12**(4): p. 872-8.
316. Holgate, S.T., *Epithelial damage and response.* Clin Exp Allergy, 2000. **30 Suppl 1**: p. 37-41.
317. Pelaia, G., et al., *Cellular mechanisms underlying eosinophilic and neutrophilic airway inflammation in asthma.* Mediators Inflamm, 2015. **2015**: p. 879783.
318. Huang, G., Y. Wang, and H. Chi, *Regulation of TH17 cell differentiation by innate immune signals.* Cell Mol Immunol, 2012. **9**(4): p. 287-95.
319. Burgler, S., et al., *Differentiation and functional analysis of human T(H)17 cells.* J Allergy Clin Immunol, 2009. **123**(3): p. 588-95, 595 e1-7.
320. Malavia, N.K., et al., *Airway epithelium stimulates smooth muscle proliferation.* Am J Respir Cell Mol Biol, 2009. **41**(3): p. 297-304.
321. Hirst, S.J., C.H. Twort, and T.H. Lee, *Differential effects of extracellular matrix proteins on human airway smooth muscle cell proliferation and phenotype.* Am J Respir Cell Mol Biol, 2000. **23**(3): p. 335-44.
322. Benam, K.H., et al., *Small airway-on-a-chip enables analysis of human lung inflammation and drug responses in vitro.* Nat Methods, 2016. **13**(2): p. 151-7.
323. Huh, D., et al., *Reconstituting organ-level lung functions on a chip.* Science, 2010. **328**(5986): p. 1662-8.
324. Ahdieh, M., T. Vandenbos, and A. Youakim, *Lung epithelial barrier function and wound healing are decreased by IL-4 and IL-13 and enhanced by IFN-gamma.* Am J Physiol Cell Physiol, 2001. **281**(6): p. C2029-38.
325. Laoukili, J., et al., *IL-13 alters mucociliary differentiation and ciliary beating of human respiratory epithelial cells.* J Clin Invest, 2001. **108**(12): p. 1817-24.

326. Swartz, M.A., et al., *Mechanical stress is communicated between different cell types to elicit matrix remodeling.* Proc Natl Acad Sci U S A, 2001. **98**(11): p. 6180-5.
327. Tschumperlin, D.J., et al., *Mechanotransduction through growth-factor shedding into the extracellular space.* Nature, 2004. **429**(6987): p. 83-6.
328. Choe, M.M., P.H. Sporn, and M.A. Swartz, *Extracellular matrix remodeling by dynamic strain in a three-dimensional tissue-engineered human airway wall model.* Am J Respir Cell Mol Biol, 2006. **35**(3): p. 306-13.
329. Ishioka, T., et al., *Effects of respiratory syncytial virus infection and major basic protein derived from eosinophils in pulmonary alveolar epithelial cells (A549).* Cell Biol Int, 2011. **35**(5): p. 467-74.
330. Jones, R.L., et al., *Airway remodelling in COPD: It's not asthma!* Respirology, 2016.
331. Aoshiba, K. and A. Nagai, *Differences in airway remodeling between asthma and chronic obstructive pulmonary disease.* Clin Rev Allergy Immunol, 2004. **27**(1): p. 35-43.
332. Hoenderdos, K. and A. Condliffe, *The neutrophil in chronic obstructive pulmonary disease.* Am J Respir Cell Mol Biol, 2013. **48**(5): p. 531-9.
333. Amitani, R., et al., *Effects of human neutrophil elastase and Pseudomonas aeruginosa proteinases on human respiratory epithelium.* Am J Respir Cell Mol Biol, 1991. **4**(1): p. 26-32.
334. Cardell, L.O., et al., *LTB(4)-induced nasal gland serous cell secretion mediated by neutrophil elastase.* Am J Respir Crit Care Med, 1999. **160**(2): p. 411-4.
335. Ganesan, S. and U.S. Sajjan, *Repair and Remodeling of airway epithelium after injury in Chronic Obstructive Pulmonary Disease.* Curr Respir Care Rep, 2013. **2**(3).
336. Heijink, I.H., et al., *Abnormalities in airway epithelial junction formation in chronic obstructive pulmonary disease.* Am J Respir Crit Care Med, 2014. **189**(11): p. 1439-42.
337. Muller, K.C., et al., *Lung fibroblasts from patients with emphysema show markers of senescence in vitro.* Respir Res, 2006. **7**: p. 32.
338. Tang, A.C., et al., *Current concepts: host-pathogen interactions in cystic fibrosis airways disease.* Eur Respir Rev, 2014. **23**(133): p. 320-32.
339. Hendricks, M.R. and J.M. Bomberger, *Digging through the Obstruction: Insight into the Epithelial Cell Response to Respiratory Virus Infection in Patients with Cystic Fibrosis.* J Virol, 2016. **90**(9): p. 4258-61.
340. Regamey, N., et al., *Airway remodelling and its relationship to inflammation in cystic fibrosis.* Thorax, 2011. **66**(7): p. 624-9.
341. Tiddens, H.A., et al., *Cystic fibrosis lung disease starts in the small airways: can we treat it more effectively?* Pediatr Pulmonol, 2010. **45**(2): p. 107-17.
342. Rossi, G.A. and A.A. Colin, *Infantile respiratory syncytial virus and human rhinovirus infections: respective role in inception and persistence of wheezing.* Eur Respir J, 2015. **45**(3): p. 774-89.
343. Patel, J.A., et al., *Interleukin-1 alpha mediates the enhanced expression of intercellular adhesion molecule-1 in pulmonary epithelial cells*

infected with respiratory syncytial virus. Am J Respir Cell Mol Biol, 1995. **13**(5): p. 602-9.
344. Patel, J.A., et al., *Autocrine regulation of interleukin-8 by interleukin-1alpha in respiratory syncytial virus-infected pulmonary epithelial cells in vitro.* Immunology, 1998. **95**(4): p. 501-6.
345. Chang, C.H., Y. Huang, and R. Anderson, *Activation of vascular endothelial cells by IL-1alpha released by epithelial cells infected with respiratory syncytial virus.* Cell Immunol, 2003. **221**(1): p. 37-41.
346. Oshansky, C.M., et al., *Respiratory syncytial virus F and G proteins induce interleukin 1alpha, CC, and CXC chemokine responses by normal human bronchoepithelial cells.* J Infect Dis, 2010. **201**(8): p. 1201-7.
347. Villenave, R., et al., *In vitro modeling of respiratory syncytial virus infection of pediatric bronchial epithelium, the primary target of infection in vivo.* Proc Natl Acad Sci U S A, 2012. **109**(13): p. 5040-5.
348. Wang, J.H., et al., *Effect of co-culturing human primary basic fibroblasts with respiratory syncytial virus-infected 16-HBE cells.* Genet Mol Res, 2016. **15**(1).
349. Chang, C.H., et al., *Interleukin-1alpha released from epithelial cells after adenovirus type 37 infection activates intercellular adhesion molecule 1 expression on human vascular endothelial cells.* J Virol, 2002. **76**(1): p. 427-31.
350. Kurt-Jones, E.A., et al., *Pattern recognition receptors TLR4 and CD14 mediate response to respiratory syncytial virus.* Nat Immunol, 2000. **1**(5): p. 398-401.
351. Borthwick, L.A., et al., *Pseudomonas aeruginosa Induced Airway Epithelial Injury Drives Fibroblast Activation: A Mechanism in Chronic Lung Allograft Dysfunction.* Am J Transplant, 2016. **16**(6): p. 1751-65.
352. Jacobsen, J.N., A.S. Andersen, and K.A. Krogfelt, *Impact of Pseudomonas aeruginosa quorum sensing on cellular wound healing responses in vitro.* Scand J Infect Dis, 2012. **44**(8): p. 615-9.
353. Brothers, K.M., et al., *Putting on the brakes: Bacterial impediment of wound healing.* Sci Rep, 2015. **5**: p. 14003.
354. Yang, J.J., D.D. Wang, and T.Y. Sun, *Flagellin of Pseudomonas aeruginosa induces transforming growth factor beta 1 expression in normal bronchial epithelial cells through mitogen activated protein kinase cascades.* Chin Med J (Engl), 2011. **124**(4): p. 599-605.
355. Datta, A., C.J. Scotton, and R.C. Chambers, *Novel therapeutic approaches for pulmonary fibrosis.* Br J Pharmacol, 2011. **163**(1): p. 141-72.
356. Scotton, C.J. and R.C. Chambers, *Molecular targets in pulmonary fibrosis: the myofibroblast in focus.* Chest, 2007. **132**(4): p. 1311-21.
357. Smoktunowicz, N., et al., *The anti-fibrotic effect of inhibition of TGFbeta-ALK5 signalling in experimental pulmonary fibrosis in mice is attenuated in the presence of concurrent gamma-herpesvirus infection.* Dis Model Mech, 2015. **8**(9): p. 1129-39.
358. Morris, J.C., et al., *Phase I study of GC1008 (fresolimumab): a human anti-transforming growth factor-beta (TGFbeta) monoclonal antibody in patients with advanced malignant melanoma or renal cell carcinoma.* PLoS One, 2014. **9**(3): p. e90353.

Appendix A: Supplementary data

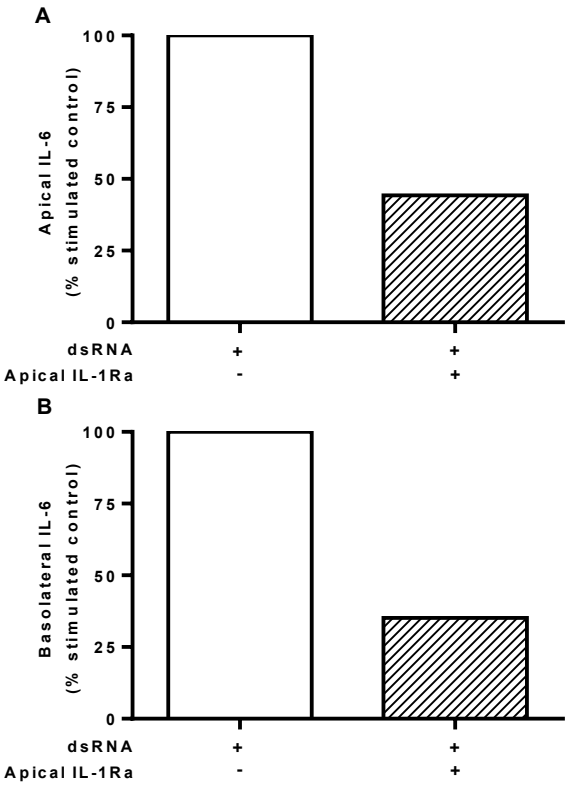

Figure A1 The effect of IL-1R antagonism on dsRNA-induced IL-6 release in HBEC monocultures. HBECs was cultured in the absence or presence of IL-1Ra (500ng/ml) applied either apically for 1h prior to stimulation with dsRNA (poly(I:C); 1µg/ml). Apical (A) and basolateral (B) cell-free supernatants were harvested 24h after stimulation and assayed for IL-6 by ELISA. To investigate the effects of IL-1Ra on dsRNA-dependent responses, control mediator levels were subtracted from stimulated levels and expressed as a percentage of the response to dsRNA. (n=1)

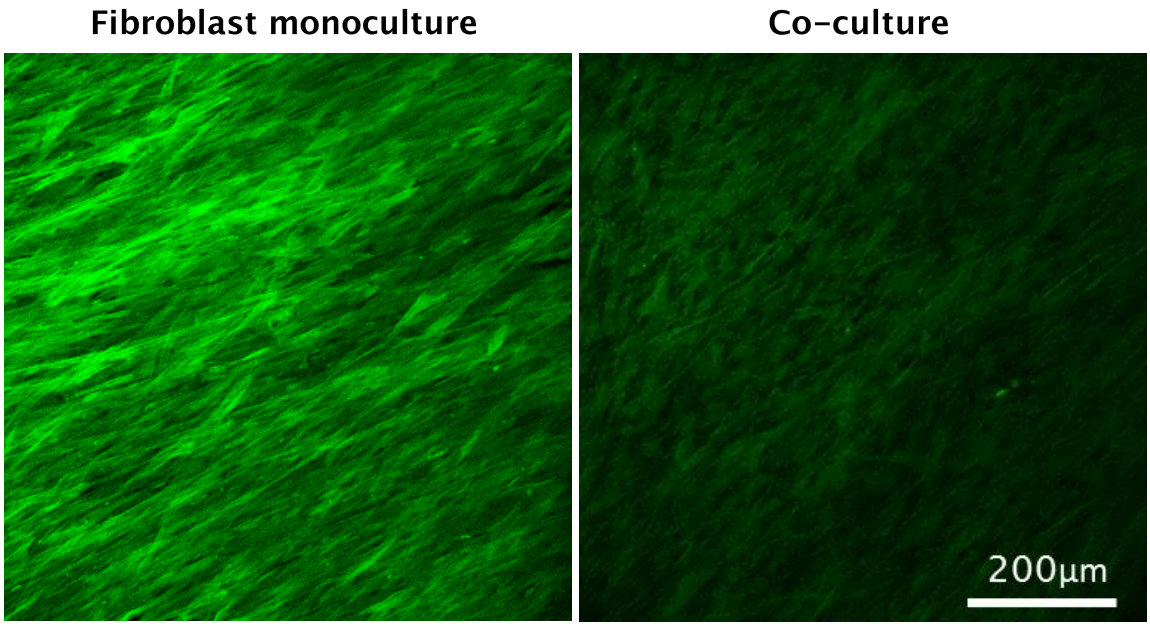

Figure A2 Fibroblasts have reduced α-SMA staining in co-culture with epithelial cells. Seven days after seeding cultures were fixed and stained for α-SMA (green) (magnification x10, representative of 6 independent experiments)

Table A1 The effect of IL-1R antagonism on dsRNA-induced cytokine and chemokine release in the polarized EMTU co-culture model. The EMTU co-culture model was cultured in the absence or presence of IL-1Ra (500ng/ml) applied either apically, basolaterally or both for 1h prior to stimulation with dsRNA (poly(I:C); 1µg/ml). Apical and basolateral cell-free supernatants were harvested 24h after stimulation and assayed for IL-6, CXCL8, CXCL10 and GM-CSF by ELISA. Results are means ±SD, n=3-6. b.d. indicates levels below the detection limit of the assay.

	IL-6 (ng/ml)				CXCL8 (ng/ml)				CXCL10 (ng/ml)				GM-CSF (pg/ml)			
	Apical		Basolateral		Apical		Basolateral		Apical		Basolateral		Apical		Basolateral	
dsRNA	-	+	-	+	-	+	-	+	-	+	-	+	-	+	-	+
- IL-1Ra	1.8±1.9	33.9±28.2	25.6±22.3	207.7±194.7	1.7±0.7	9.3±4.1	58.8±24.7	172±68.5	b.d.	0.8±0.5	0.1±0.1	6.6±3.1	b.d.	b.d.	74±87	276±105
+ IL-Ra apical	1.3±1.4	16.0±14.0	24.8±19.5	93.9±90.4	1.1±0.5	4.0±1.4	41.8±14.1	93.2±38.9	b.d.	0.7±0.6	b.d.	6.3±4.9	b.d.	b.d.	40±20	113±103
+ IL-Ra basolateral	1.4±1.5	21.2±18.8	15.9±14.8	19.3±18.2	1.0±0.5	5.9±2.9	27.2±13.9	47.7±20.6	b.d.	0.7±0.6	b.d.	8.5±8.9	b.d.	b.d.	22±19	66±27
+ IL-1Ra apical and basolateral	1.2±1.3	14.6±11.9	14.2±13.5	15.6±13.6	0.9±0.5	3.1±1.1	24.0±10.1	34.9±9.2	b.d.	0.8±6	b.d.	7.3±6.9	b.d.	b.d.	18±16	62±36

Table A2 Effect of IL-1α stimulation on IL-6 and CXCL8 release from fibroblast and HBEC monocultures. Fibroblast and HBEC monocultures were stimulated with IL-1α either apically (10ng/ml), basolaterally (1ng/ml) or in combination, or with dsRNA (poly(I:C); 1µg/ml) as a positive control. After 24h, cell-free supernatants were assayed for IL-6 and CXCL8 by ELISA. Results are means ± SD, n=4-5.

	IL-6 (ng/ml)				**CXCL8 (ng/ml)**			
	Apical		**Basolateral**		**Apical**		**Basolateral**	
	Fibroblast	**Epithelial**	**Fibroblast**	**Epithelial**	**Fibroblast**	**Epithelial**	**Fibroblast**	**Epithelial**
control	0.4±0.4	0.4±0.2	0.7±0.7	0.6±0.3	0.3±0.2	0.8±0.2	0.3±0.1	1.4±0.3
dsRNA	0.6±0.6	6.1±3.7	0.9±0.8	1.9±1.1	0.5±0.4	5.3±0.8	0.4±0.2	2.6±0.2
IL-1α	49.8±42.4	0.4±0.2	72.5±58.8	0.7±0.3	146.6±113.7	1.1±0.2	137.1±125.6	1.7±0.4

Table A3 Effect of IL-1Ra on HRV16-induced proinflammatory responses in the primary EMTU co-culture model. Co-cultures were treated with IL-1Ra (500ng/ml) basolaterally for 1h prior to HRV16 (MOI=2) or UV-HRV16 infection as a negative control. After 24h, cell-free supernatants were assayed for IL-6, CXCL8, and CXCL10 by ELISA. Results are shown for each separate epithelial cell donor. *$P \leq 0.05$, **$P \leq 0.05$ for HRV16 compared to UV-HRV16; $^{+}P \leq 0.05$ for IL-1Ra compared to control (two-way ANOVA with Bonferroni correction). b.d. indicates levels below the detection limit of the assay.

	IL-6 (pg/ml)				**CXCL8 (pg/ml)**				**CXCL10 (pg/ml)**			
	UV-HRV16		**HRV16**		**UV-HRV16**		**HRV16**		**UV-HRV16**		**HRV16**	
IL-1Ra	-	+	-	+	-	+	-	+	-	+	-	+
Donor 1: GA1-006	12	13	73	30	3526	1726	5799	2976	b.d.	b.d.	2416	1818
Donor 2: IL17HC17TH	35	37	53	24	1494	793	3707	1570	b.d.	b.d.	1043	759
Donor 3: GA1-001	6	1	17	7	3194	1804	6951	2802	b.d.	b.d.	2095	1743
Means± SD	17.7±15	17.1±18	47.5±28	21.5±10	2738±1090	1441±563	5486±1644*	2449±766^{+}	b.d.	b.d.	1851±718**	1440±590**

Table A4 Epithelial cell donor information for each experiment.

Experiment	Study	Pt ID	Non-asthmatic (NA)/severe asthmatic (SA)	Sex	Age	Ethnicity	Height	Weight	Fev1	Fev1 %	Fvc	Fvc%	Atopy	Smoker	Meds
Primary co-culture vs. ALI monoculture	GORD	GA1-006	NA	M	42		183cm	96kg	5.25	126.2	6.58	128.8	Y Grass	Never	None
Co-culture HRV16 &IL-1Ra	GORD	GA1-001	NA	F	59		177cm	68.2kg	3.54	121.2	4.55	133.1	N	0.6pkyr	Levothyroxine
	GORD	GA1-006	NA	M	42		183cm	96kg	5.25	126.2	6.58	128.8	Y Grass	Never	None
	Cross sectional study Interleukin-17 (IL17) in asthma	IL17HC17TH	NA	M	34	white	178.5cm	63.2kg	4.7		5.7		N	Never	None
ALI freeze thaw exp.	GORD	GA1-006	NA	M	42		183cm	96kg	5.25	126.2	6.58	128.8	Y Grass	Never	None
	Cross sectional study Interleukin-17 (IL17) in asthma	IL17HC17TH	NA	M	34	white	178.5cm	63.2kg	4.7		5.7		N	Never	None
	Cross sectional study Interleukin-17 (IL17) in asthma	IL17HC39KC	NA	F	46	white	165	88.8	2.5		3.25		N	Former 0.5pkyr	
	COPD MAP	SOTON-EV189	NA	F	61									Non-smoker	
	COPD MAP	SOTON-EV206	NA												
Non-asthmatic compared to asthmatic	GORD	GA1-006	NA	M	42		183cm	96kg	5.25	126.2	6.58	128.8	Y Grass	Never	
	Cross sectional study Interleukin-17 (IL17) in asthma	IL17HC17TH	NA	M	34	white	178.5cm	63.2kg	4.7		5.7		N	Never	
	Cross sectional study Interleukin-17 (IL17) in asthma	IL17HC39KC	NA	F	46	white	165	88.8	2.5		3.25		N	Former 0.5pkyr	
	COPD MAP	SOTON-EV189	NA	F	61									Non-smoker	
	COPD MAP	SOTON-EV206	NA												

	GORD	GA3-003	SA	F	65		155cm	106kg	1.96	103.5	2.52	110.4	N	Never	Symbicort,Terbutaline,Citalopram,Co-amilofruse,Domperidone,Montelukast,Ranitidine
	Cross sectional study Interleukin-17 (IL17) in asthma	L17SA19KG	SA	F	41	white	156.0	125.4	2.5	96.5	2.9		N	Never	Salbutamol inh, Tiotropium resipmat 2.5 ii, qvar 4 bd, fluoxetine 40mg, atimos 12mcg bd, mometasone nasal ii bd, montelukast 10mg od, clarithromycin 500mg od
	Pathophysiology of airway diseases such as asthma and COPD	DS157	SA	F	66				0.8	33.2			N	Never	
	Pathophysiology of airway diseases such as asthma and COPD	DS174	SA	M	33		174	71							Inhaled corticosteroid, LABA, antileukotriene, antihistamine

Appendix B: Publications

TISSUE BARRIERS
2016, VOL. 4, NO. 3, e1206378 (12 pages)
http://dx.doi.org/10.1080/21688370.2016.1206378

Taylor & Francis
Taylor & Francis Group

RESEARCH PAPER

OPEN ACCESS

IL-1α mediates cellular cross-talk in the airway epithelial mesenchymal trophic unit

Alison R. Hill[a], Jessica E. Donaldson[a], Cornelia Blume[a], Natalie Smithers[a], Liku Tezera[a], Kamran Tariq[b], Patrick Dennison[b], Hitasha Rupani[a,b], Matthew J. Edwards[c], Peter H. Howarth[a,b], Christopher Grainge[a,¶], Donna E. Davies[a,b,d], and Emily J. Swindle[a,b,d]

[a]Clinical and Experimental Sciences, Faculty of Medicine, University of Southampton, University Hospital Southampton, Southampton, UK; [b]NIHR Southampton Respiratory Biomedical Research Unit, University Hospital Southampton, Southampton, UK; [c]Novartis Institutes for BioMedical Research, Horsham, UK; [d]Institute for Life Sciences, Highfield Campus, University of Southampton, Southampton, UK

ABSTRACT

The bronchial epithelium and underlying fibroblasts form an epithelial mesenchymal trophic unit (EMTU) which controls the airway microenvironment. We hypothesized that cell-cell communication within the EMTU propagates and amplifies the innate immune response to respiratory viral infections.

EMTU co-culture models incorporating polarized (16HBE14o-) or differentiated primary human bronchial epithelial cells (HBECs) and fibroblasts were challenged with double-stranded RNA (dsRNA) or rhinovirus.

In the polarized EMTU model, dsRNA affected ionic but not macromolecular permeability or cell viability. Compared with epithelial monocultures, dsRNA-stimulated pro-inflammatory mediator release was synergistically enhanced in the basolateral compartment of the EMTU model, with the exception of IL-1α which was unaffected by the presence of fibroblasts. Blockade of IL-1 signaling with IL-1 receptor antagonist (IL-1Ra) completely abrogated dsRNA-induced basolateral release of mediators except CXCL10. Fibroblasts were the main responders to epithelial-derived IL-1 since exogenous IL-1α induced pro-inflammatory mediator release from fibroblast but not epithelial monocultures. Our findings were confirmed in a differentiated EMTU model where rhinovirus infection of primary HBECs and fibroblasts resulted in synergistic induction of basolateral IL-6 that was significantly abrogated by IL-1Ra. This study provides the first direct evidence of integrated IL-1 signaling within the EMTU to propagate inflammatory responses to viral infection.

ARTICLE HISTORY
Received 18 May 2016
Revised 17 June 2016
Accepted 21 June 2016

KEYWORDS
cross-talk; epithelial cells; fibroblasts; *in vitro* models of the airway; viral infection

Introduction

The structural cells of the conducting airways control the tissue microenvironment and are critical in the maintenance of homeostasis. Central to this is the bronchial epithelium which forms a protective barrier against the external environment, with functions including secretion of a protective layer of mucus, control of paracellular permeability and production of immunomodulatory growth factors and cytokines.[1] Below the epithelium, the attenuated fibroblast sheath directs immune responses and it has been proposed that these cells work together as an epithelial mesenchymal-trophic unit (EMTU) to co-ordinate appropriate responses to environmental stimuli.[2]

Evidence of cellular cross-talk has already been demonstrated in simple experiments using epithelial-derived conditioned media or in epithelial-fibroblast co-cultures where fibroblasts respond to epithelial-derived signals to drive inflammatory or remodelling responses. For example, conditioned media from human bronchial epithelial cells (HBECs) subjected to endoplasmic reticulum stress can cause proinflammatory mediator release from human lung fibroblasts (HLFs) via a mechanism involving the alarmin, IL-1α.[3] In other studies, scrape-wounding of HBECs induced α-smooth muscle actin expression in fibroblasts in a co-culture model via TGFβ.[4] While several

CONTACT Emily J. Swindle E.J.Swindle@soton.ac.uk Clinical and Experimental Sciences, Henry Wellcome Laboratories, Level F, South Academic Block, Mailpoint 810, Faculty of Medicine, University Hospital Southampton, Southampton SO16 6YD, UK.
¶ Present address: School of Medicine and Public Health, The University of Newcastle, Newcastle, NSW, Australia.

Supplemental data for this article can be accessed on the publisher's website.

studies have examined cross-talk in response to chemical or mechanical damage to the epithelium, none have examined the effects of human rhinovirus (HRV) infection of the epithelium on the EMTU.

HRV infects the upper airways and causes symptoms of the common cold in healthy adults but in chronic respiratory diseases such as asthma and chronic obstructive pulmonary disease (COPD) it is a major cause of viral-induced exacerbations, causing increased lower respiratory tract symptoms.[5,6] The bronchial epithelium is the major target for HRV infection and replication in chronic airways disease.[7] Following *in vitro* stimulation of either monolayer or fully differentiated HBECs with HRV or pathogen associated molecular patterns (PAMPs), such as double stranded RNA (dsRNA), increases in ionic permeability[7,8] and release of proinflammatory mediators are observed.[6,7,9,10] A critical role for some of these epithelial-derived mediators on immune cell activation has been demonstrated following incubation of immune cells with epithelial conditioned medium from virus or dsRNA-treated cultures. For example, HRV-dependent epithelial IL-33 causes Th2 cytokine release from T cells and group 2 innate lymphoid cells,[11] while dsRNA-dependent epithelial-derived thymic stromal lymphopoietin promotes CCL17 production from monocyte-derived dendritic cells[12] and Th2 cytokine release from mast cells.[13] HRV also induces HBECs to release growth factors such as amphiregulin, activin A, and vascular endothelial growth factor (VEGF);[14-16] such conditioned medium can result in VEGF-dependent angiogenesis in endothelial cells[14] and basic fibroblast growth factor-dependent proliferation of fibroblasts.[16]

A key feature of the epithelial barrier is its polarized structure due to the expression of tight junction proteins, leading to the vectorial release of mediators. This not only allows establishment of chemotactic gradients, required for immune cell recruitment and retention, but also controls signaling to underlying fibroblasts which orchestrate responses within the local tissue microenvironment. Here we investigated, for the first time, the integrated responses to HRV infection of the epithelial barrier in co-culture with fibroblasts. Within this system, the polarized epithelium ensured apical delivery to the epithelium of HRV (or dsRNA), as occurs *in vivo*, and enabled direct assessment of vectorial cytokine signaling. We report that challenge of polarized HBECs with dsRNA results in enhanced release of fibroblast-derived proinflammatory mediators in the EMTU model. Furthermore, blockade of IL-1 signaling revealed a key role for basolateral IL-1α release in mediating epithelial-fibroblast cross-talk. These observations of direct epithelial-mesenchymal signaling via IL-1α were confirmed utilizing fully differentiated primary HBECs infected with HRV and in co-culture with fibroblasts.

Materials and methods

A full description of the methods can be found in the online supplement.

Cell culture

The human bronchial epithelial (16HBE14o$^-$) and fibroblast (MRC5) cell lines used in this study were a gift from Professor D. C. Grunert (San Francisco, USA) and from the European Collection of Authenticated Cell Cultures (ECACC) respectively. Normal primary HBECs were obtained by epithelial brushing using fiberoptic bronchoscopy. All procedures were approved by the Southampton and South West Hampshire Research Ethics Committee (Rec codes 13/SC/0182, 09/H0504/109 and 10/H0504/2) and were undertaken following written informed consent.

Establishment and challenge of the EMTU co-culture models

For the polarized EMTU model, fibroblasts (MRC5) were seeded onto the basolateral surface of an inverted Transwell® insert and incubated for 2h at 37°C before the addition of 16HBE cells into the apical compartment. Co-cultures were placed into 24-well plates containing 16HBE medium and cultured for 5 d. On day 6, cultures were challenged apically with 1 μg/ml synthetic dsRNA (polyinosinic:polycytidylic acid (poly(I:C)); Invivogen); this concentration had minimal effects on cell viability (Fig. S1A-C). Where required, 16HBE or MRC5 monocultures were similarly treated.

For the primary differentiated EMTU co-culture model, fibroblasts (MRC5) were seeded onto the basolateral surface of inverted Transwell®inserts containing primary fully differentiated air-liquid interface (ALI) (21 day) cultures as previously described.[17] The primary EMTU models were infected apically with HRV16 for 6h at 33°C, then the apical surface was washed (3X, HBSS) before

culturing at 37°C. Twenty four hours post-infection the apical secretions (200 μl) were harvested by washing with HBSS and the basolateral (500 μl) supernatants collected. Controls of UV-irradiated HRV16 (1200mJ/cm^2 on ice for 50min) were included in all experiments. The viral titer of cell-free supernatants was determined by $TCID_{50}$ assay.[18,19]

For IL-1 blocking experiments, cultures were pre-incubated with IL-1 receptor antagonist (IL-1Ra; 500ng/ml, R&D systems) apically and/or basolaterally for 1h prior to challenge.

MRC5 and 16HBE monocultures were challenged with human recombinant IL-1α (Miltenyi Biotec,) apically (10 ng/ml) and basolaterally (1 ng/ml).

Epithelial permeability

Ionic permeability was measured as transepithelial electrical resistance (TER) using chopstick electrodes with an EVOM voltohmeter (World Precision Instruments, Aston, UK). Data are expressed as ohms.cm^2 and have been corrected for the resistance of an empty Transwell®. Macromolecular permeability was measured 3 and 21 hours after dsRNA challenge by adding FITC-labeled dextran to the apical compartment of co-cultures; FITC-dextran flux into the basolateral compartment was quantified 3h later by spectrofluorometry.

Detection of cytokines and chemokines

Cell-free supernatants were assayed for IL-1α, IL-1β and IL-1Ra using a Luminex®multiplex assay according to the manufacturer's instructions (R&D systems). IL-6, CXCL8, CXCL10, GM-CSF and IL-1α were determined by ELISA according to the manufacturer's protocol (R&D Systems).

Statistical analysis

Normality of distribution was assessed using the Shapiro-Wilk test (Sigma-Plot version 12.5, Systat Software) and the appropriate parametric or non-parametric tests used. Results are expressed as means $\pm$ SD or as box plots representing the median with 25% and 75% interquartiles and whiskers representing minimum and maximum values, as appropriate. All data were analyzed using Prism (GraphPad, CA, USA). $P < 0.05$ were considered significant.

Results

DsRNA increases ionic permeability but not macromolecular permeability in the polarized EMTU model

Compared to equivalent HBEC monocultures, ionic permeability at baseline was significantly lower in the polarized EMTU model as measured by an increase in TER (Fig. 1A $P \leq 0$ .05). The polarized EMTU model was stimulated with dsRNA (poly(I:C)), a molecular pattern associated with viral replication,[20] at a concentration (1 μg/ml) that induced significant effects on ionic permeability and cytokine release with minimal effects on cell viability in HBEC monocultures (Fig. S1). DsRNA increased ionic permeability of either HBEC monocultures or the polarized EMTU model, with a significant decrease in TER

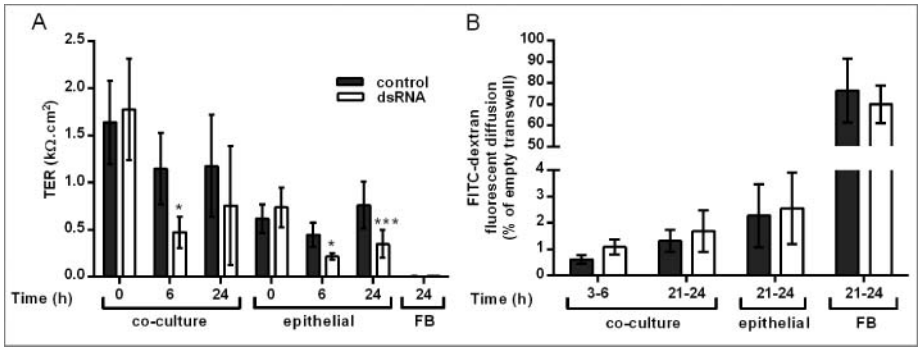

Figure 1. Effect of double-stranded RNA (dsRNA) on epithelial barrier function in the polarized epithelial mesenchymal trophic unit (EMTU) co-culture model. The EMTU co-culture model or HBEC or fibroblast monoculture controls were challenged with poly(I:C) (1μg/ml) and ionic or macromolecular permeability determined by transepithelial resistance (TER) measurements (A) or FITC-dextran diffusion (B) respectively. Results are means $\pm$ SD, n = 7 (A) and n = 3–5 (B). $^{*}P \leq 0.05$, $^{***}P \leq 0$ .001 compared to unstimulated controls (2-way ANOVA with Bonferroni correction).

by 6h (Fig. 1A). This increase in permeability was sustained 24h after dsRNA stimulation in HBEC monocultures, but partially recovered in the EMTU model. Macromolecular permeability of the epithelium was not significantly affected by co-culture with fibroblasts or following challenge with dsRNA (Fig. 1B). These data suggest that even after dsRNA treatment, epithelial polarization is maintained in the polarized EMTU model.

DsRNA induces polarized release of proinflammatory mediators which is enhanced in the basolateral compartment

Consistent with the restricted movement of macromolecules across the epithelial barrier, dsRNA induced vectorial proinflammatory mediator release in the polarized EMTU model. In the apical compartment, dsRNA induced significant increases in IL-6, CXCL8, and CXCL10 release which was comparable with HBEC monocultures (Fig. 2A–C). In contrast, in the basolateral compartment, dsRNA-stimulated cytokine levels were synergistically enhanced compared to dsRNA-stimulated HBEC monocultures (Fig. 2D–F, Fig. S2). At the concentration of dsRNA tested (1 μg/ml), fibroblast monocultures were unresponsive to stimulation (Fig. 2A–F). Taken together, these data suggest that epithelial-fibroblast cross-talk is occurring within the EMTU model.

In contrast with IL-6, CXCL8, GM-CSF and CXCL10 release, the polarity of dsRNA-dependent IL-1α release was mainly apical (Fig. 3A–B), even when corrected for differences in volume between the apical and basolateral compartments (data not shown), and was comparable between HBEC monocultures and the polarized EMTU model. No IL-1β was detected. Since IL-1α levels were similar in cultures containing HBECs alone this strongly suggests that HBECs are the primary source of IL-1α following dsRNA stimulation.

IL-1 mediates dsRNA-dependent proinflammatory responses

IL-1 has previously been shown to drive autocrine mediator release in epithelial[10] or fibroblast[3] monocultures. To test whether epithelial-derived IL-1α was responsible for augmenting responses in the EMTU model, we used IL-1 receptor antagonist (IL-Ra). In unstimulated cultures, IL-1Ra caused a small decrease in constitutive proinflammatory mediator release (Fig. S3). In dsRNA-stimulated co-cultures, pre-incubation with IL-1Ra significantly reduced dsRNA-induced IL-6, CXCL8 and GM-CSF release (Fig. 4,

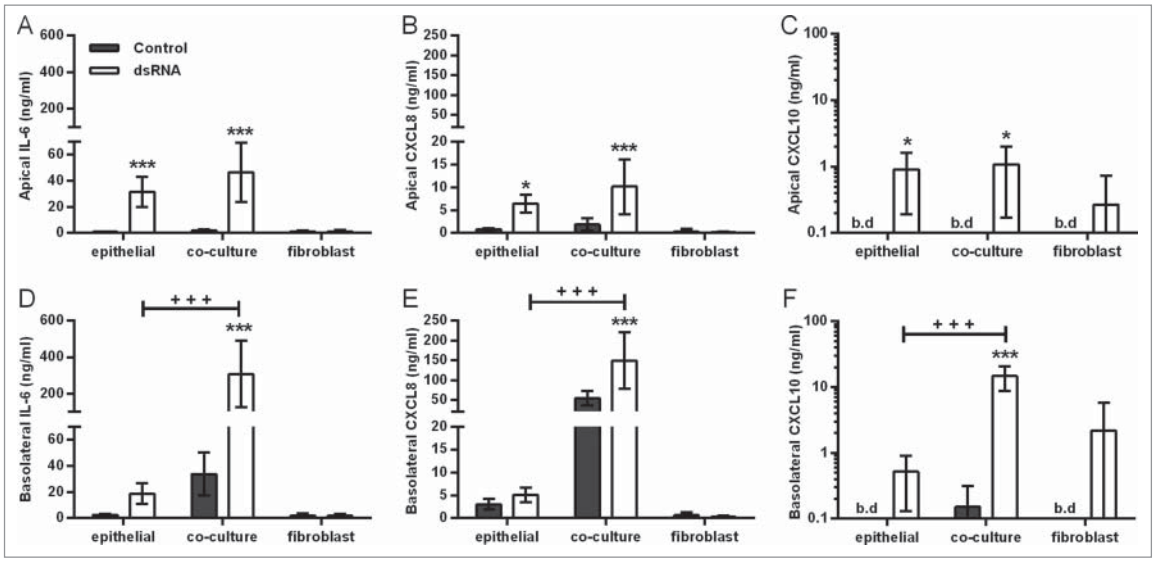

Figure 2. Effect of double-stranded RNA (dsRNA) on proinflammatory mediator release in the polarized epithelial mesenchymal trophic unit (EMTU) co-culture model. Apical (A-C) and basolateral (D-F) cell-free supernatants were harvested from the EMTU co-culture model or human bronchial epithelial cell (HBEC) and fibroblast monocultures 24h after challenge with poly(I:C) (1 μg/ml) and assayed for IL-6 (A,D), CXCL8 (B,E), and CXCL10 (C,F) by ELISA. Results are means $\pm$ SD, n = 3–5. $^{*}P \leq 0.05$, and $^{***}P \leq 0.001$ for comparison between control and poly(I:C)-stimulated cultures and $^{+++}P \leq 0$ .001 for comparison with HBEC monocultures and EMTU co-culture model (2-way ANOVA with Bonferroni correction). b.d. indicates levels below the detection limit of the assay.

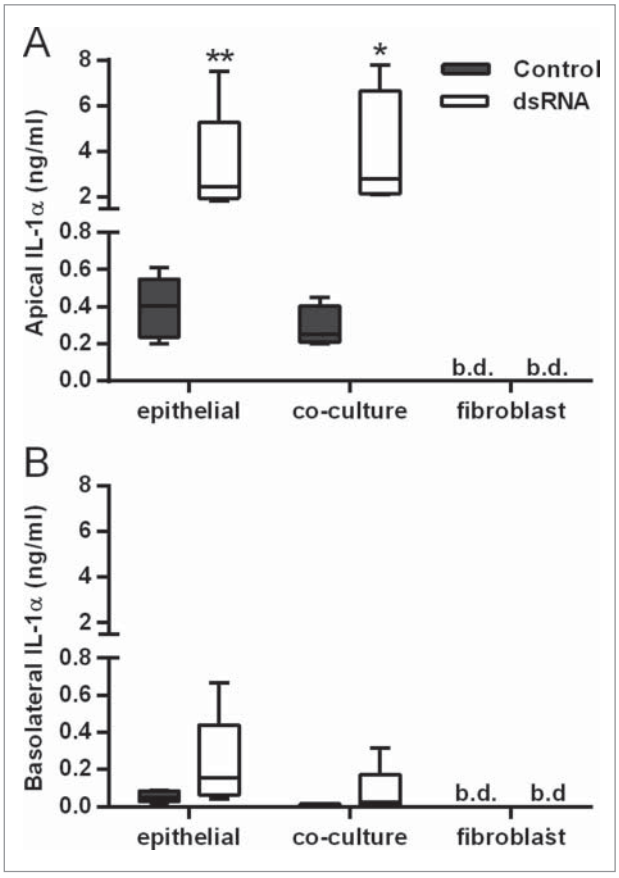

Figure 3. Comparison of IL-1α release from double-stranded RNA (dsRNA)-stimulated human bronchial epithelial cell (HBEC) and fibroblast monocultures with the polarized epithelial mesenchymal trophic unit (EMTU) co-culture model. Apical (A) and basolateral (B) cell-free supernatants were harvested 24 h after challenge with poly(I:C) (1 μg/ml) and assayed for IL-1α and IL-1β by Luminex®. Results for IL-1α release are shown as box plots representing the median with 25% and 75% interquartiles, and whiskers representing minimum and maximum values, n = 3–5. $^{*}P \leq 0.05$, $^{**}P \leq 0.01$ for comparison between control and poly(I:C) stimulated cultures (Mann-Whitney U test). b.d. indicates levels below the detection limit of the assay. IL-1β was below the level of detection of the assay.

Fig. S4 and Table S1). For apical cytokine release, IL-1Ra only partially reduced dsRNA-dependent IL-6 and CXCL8 (Fig. 4A–B) release and was most effective when added apically or to both compartments. For basolateral cytokine release, IL-1Ra had the greatest effect when added basolaterally or to both compartments with complete abrogation of dsRNA-dependent IL-6, CXCL8 and GM-CSF (Fig. 4D–E & Fig. S4). The partial inhibitory effect of IL-1Ra when added apically could be explained by a small (0.1–1%) but significant passage of exogenously applied IL-1Ra to the basolateral compartment regardless of dsRNA stimulation (Fig. S5). Neither apical nor basolateral dsRNA-dependent CXCL10 release was affected by IL-1Ra (Fig. 4C, F). Since IL-1β could not be detected in any cultures, these data suggest that epithelial-derived IL-1α is absolutely required to drive a subset of proinflammatory responses by the underlying fibroblasts.

Fibroblasts are the main responders to IL-1α

To investigate the direct effect of IL-1α on the different cell types, HBEC and fibroblast monocultures were directly stimulated with IL-1α at concentrations similar to those measured apically (10 ng/ml) or basolaterally (1 ng/ml) following dsRNA challenge (See Fig. 3). In fibroblast monocultures IL-1α significantly induced IL-6 and CXCL8 release (Fig. 5A–B and Table S2). In HBEC monocultures, IL-1α responses were low relative to those observed in the fibroblasts (Fig. 5C–D & Table S2) suggesting that within the polarized EMTU model, fibroblasts are the main responders to dsRNA-induced IL-1α.

A role for IL-1alpha in epithelial-fibroblast signaling in response to rhinovirus infection in a primary EMTU co-culture model

As HBECs are the primary source of IL-1α, we initially characterized the response of fully differentiated primary HBECs to HRV16 infection. Similar to the dsRNA-challenged polarized EMTU model, HRV16 infection induced IL-1α release from HBEC ALIs which was higher in the apical compared to the basolateral compartment (Fig. 6). IL-1α was also detected intracellularly and was significantly increased following HRV16 infection. Of note, the amount of intracellular IL-1α production was 50-100X greater than that detected extracellularly following HRV infection.

In either HBEC mono- or co-cultures with fibroblasts, HRV16 infection resulted in polarized release of mediators. HRV16-dependent basolateral IL-6 release was significantly augmented in the primary EMTU co-culture model compared to HBEC monocultures (Fig. 7A–B). This enhancement was not due to differences in viral replication (median $TCID_{50}$ of 17.6×10^{6}/ml in both primary HBEC monocultures and differentiated EMTU model). As observed with dsRNA, HRV16-dependent IL-1α release was higher in the apical compartment and levels were comparable in both the primary EMTU co-culture model and HBEC monocultures (Fig. 7C–D). HRV16-dependent IL-1β release was not detected. The importance of IL-

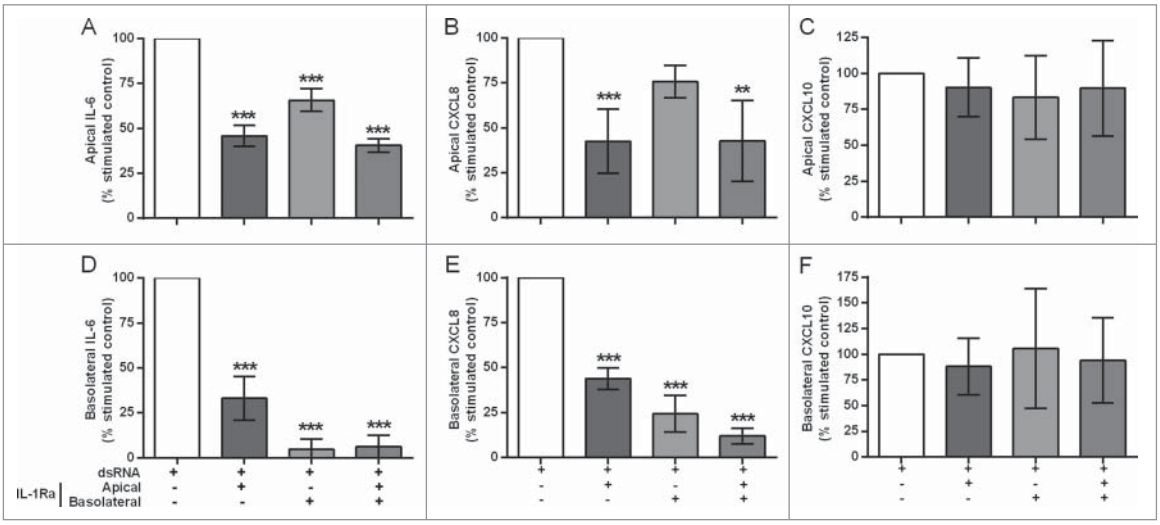

Figure 4. The effect of IL-1R antagonism on double-stranded RNA (dsRNA)-induced cytokine and chemokine release in the polarized epithelial mesenchymal trophic unit (EMTU) co-culture model. The EMTU co-culture model was cultured in the absence or presence of IL-1Ra (500 ng/ml) applied either apically, basolaterally or both for 1h prior to stimulation with poly(I:C) (1 μg/ml). Apical (A-C) and basolateral (D-F) cell-free supernatants were harvested 24 h after stimulation and assayed for IL-6 (A, D), CXCL8 (B, E), and CXCL10 (C, F) by ELISA. To investigate the effects of IL-1Ra on dsRNA-dependent responses, control mediator levels were subtracted from stimulated levels and expressed as a percentage of the response to dsRNA. Results are mean responses compared to the poly(I:C)-induced response in the absence of IL-1Ra (100%) $\pm$ SD, n = 3–6. $^{**}P \leq 0.01$, $^{***}P \leq 0.001$ for comparison between poly(I:C)-stimulated cultures in the absence or presence of IL-1Ra (one-way ANOVA with Bonferroni correction).

1 in epithelial-fibroblast cross-talk was confirmed by blocking IL-1 signaling using IL-1Ra. This significantly reduced basolateral HRV16-dependent IL-6 and CXCL8 release (Fig. 8A–B) to levels comparable to the non-replicating UV-irradiated HRV control. CXCL10 release was only modestly reduced (Fig. 8C)

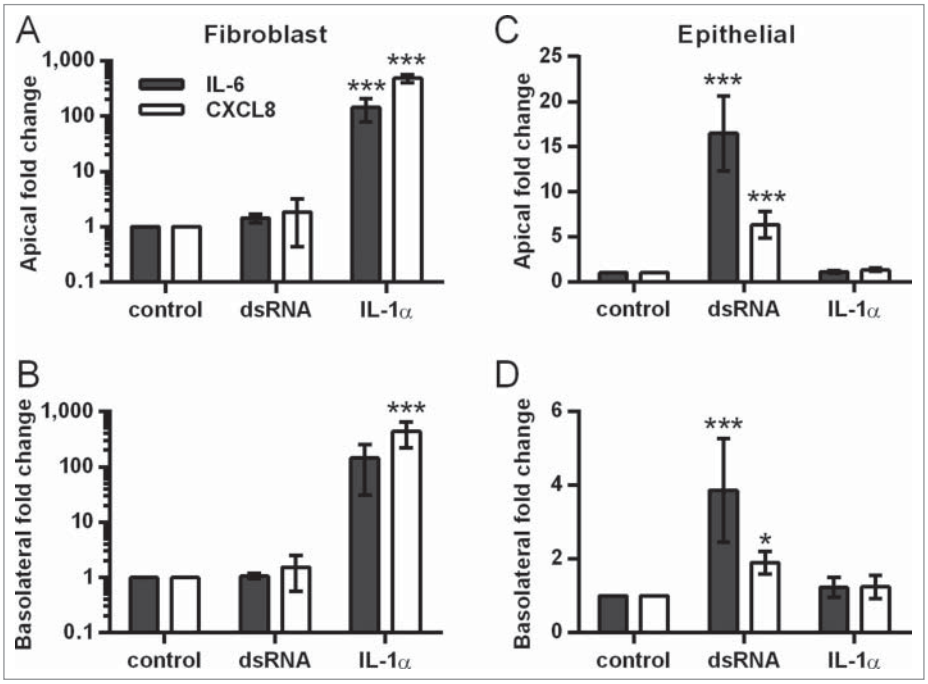

Figure 5. Effect of IL-1α stimulation on IL-6 and CXCL8 release from fibroblast and human bronchial epithelial cell (HBEC) monocultures. Fibroblast (A-B) and HBEC (C-D) monocultures were stimulated with IL-1α either apically (10 ng/ml), basolaterally (1ng/ml) or in combination, or with poly(I:C) (1 μg/ml) as a positive control. After 24 h, cell-free supernatants were assayed for IL-6 and CXCL8 by ELISA. Fold change in mediator release compared to the unstimulated control was calculated for each experiment. Results are mean fold changes $\pm$ SD, n = 4–5. $^{*}P \leq 0.05$, $^{***}P \leq 0.001$ compared to untreated control (2-way ANOVA with Bonferroni correction).

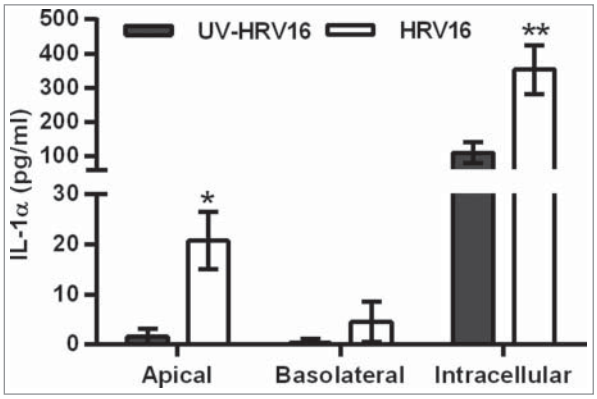

Figure 6. Increased extracellular and intracellular IL-1α release from human bronchial epithelial cell (HBEC) monocultures infected with human rhinovirus (HRV)16. ALI monocultures were infected apically with HRV16 (MOI = 2) or UV-HRV16 as a negative control. After 24h, apical and basolateral supernatants were removed and the remaining cells went through 3 cycles of freeze/thaw before cell-free supernatants were assayed for IL-1α by ELISA. Results are means ± range, n = 5. $^{*}P \leq 0.05$, $^{**}P \leq 0.01$ compared to UV-HRV16 control (ANOVA with Bonferroni correction).

and viral replication was unaffected (median $TCID_{50}$ of 17.6×10^{6}/ml in both control and IL-1Ra-treated cultures). Together these data demonstrate an essential role for IL-1α in mediating paracrine proinflammatory signaling following viral infection of primary differentiated epithelium.

Discussion

Although cell-cell communication is essential for normal function of all tissues, the relationship between structural organization and function is not addressed in most *in vitro* studies. Here we examined this relationship using an integrated co-culture system in which fully differentiated (or polarized HBECs) were apically challenged with HRV (or dsRNA) and demonstrated clear evidence of a synergistic interaction between the infected bronchial epithelium and fibroblasts. This interaction was mediated, in part, by epithelial-derived IL-1α which drives a marked proinflammatory response from the underlying fibroblasts. To our knowledge this is the first study to demonstrate direct epithelial-fibroblast cross-talk in response to HRV infection or dsRNA and it highlights the importance of epithelial barrier function and integrity.

An advantage of the EMTU models is the ability to investigate polarized epithelial function which is essential for development of chemotactic gradients for

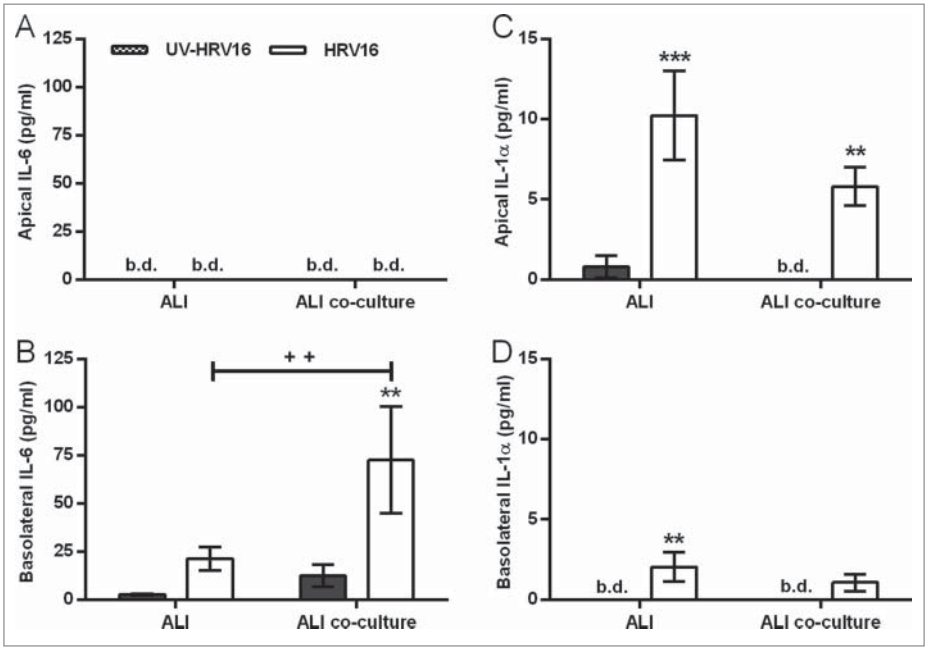

Figure 7. Increased human rhinovirus (HRV)16-induced IL-6 and IL-1α release from the primary differentiated epithelial mesenchymal trophic unit (EMTU) co-culture model compared to air-liquid interface (ALI) monocultures. ALI mono- or co-cultures with fibroblasts were infected apically with human rhinovirus (HRV)16 (MOI = 2) or UV-HRV16 as a negative control. After 24 h, apical (A, C) and basolateral (B, D) cell-free supernatants were assayed for IL-6 (A-B) or IL-1α (C-D). Results are means ± SD, 3 separate experiments from one epithelial cell donor and are representative of 3 donors. $^{**}P \leq 0.01$, $^{***}P \leq 0.001$ compared to UV-HRV16 control and $^{++}P \leq 0.01$ comparing HRV16-treated mono- and co-cultures (2-way ANOVA with Bonferroni correction). b.d. indicates levels below the detection limit of the assay.

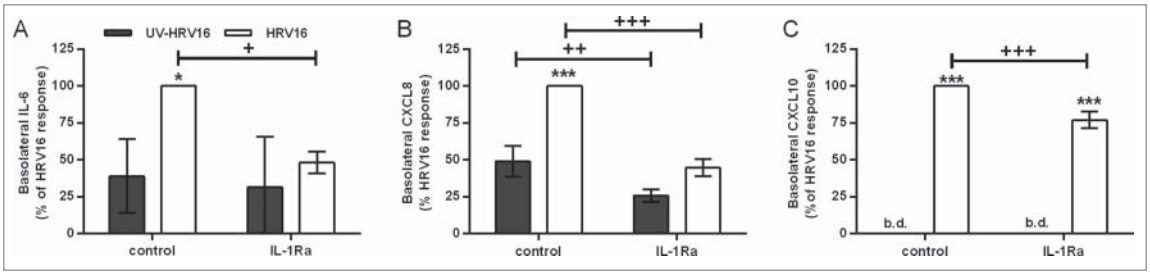

Figure 8. Role for IL-1α in human rhinovirus (HRV)16-induced proinflammatory responses in the primary differentiated epithelial mesenchymal trophic unit (EMTU) co-culture model. Co-cultures were treated with IL-1Ra (500 ng/ml) basolaterally for 1 h prior to HRV16 (MOI = 2) or UV-HRV16 as a negative control. After 24 h, cell-free supernatants were assayed for IL-6 (A), CXCL8 (B), and CXCL10 (C) by ELISA. To examine the effect of IL-1Ra on HRV16-induced cytokine release, cytokine levels are expressed as % of HRV16-induced control response (100%). Results are means ± SD, n = 3 separate epithelial cell donors. $^{***}P \leq 0.001$ compared to UV-HRV16 control and $^{+}P \leq 0.05$, $^{++}P \leq 0.01$ or $^{+++}P \leq 0.01$ comparing control and IL-1Ra-treated cultures (2-way ANOVA with Bonferroni correction). b.d. indicates levels below the detection limit of the assay.

immune cell trafficking and/or retention. In contrast with previous studies using epithelial monocultures, where HRV (or dsRNA) increased both ionic and macromolecular permeability,[7,8,21,22] we show that only ionic permeability is affected in the EMTU models. Consistent with the absence of any effects on paracellular permeability, apical challenge of the epithelium with HRV or dsRNA resulted in polarized inflammatory mediator release. Most notably, a synergistic enhancement in the basolateral compartment of the EMTU models suggests a coordinated response to viral infection. This was observed in both the polarized and primary EMTU models but the magnitude of the enhanced responses was different between cultures. The less robust response observed in the primary EMTU model may be due to the use of HRV instead of dsRNA. For a response to HRV, the virus first needs to infect the epithelial cells and replicate to generate dsRNA, in contrast with the bolus treatment with exogenously added dsRNA. Furthermore, the fully differentiated epithelial culture has a protective mucus layer which may reduce accessibility of the epithelial surface to the virus and, even if the HRV reaches the cell surface, differentiated epithelial cells are less susceptible to infection than basal cells.[23] Irrespective of the differences in the magnitude of response, synergistic enhancements in basolateral mediator release in both models suggest cross-talk between epithelial cells and fibroblasts following viral infection. This adds to previous studies where influenza virus infection enhanced mediator release in alveolar epithelial cell and fibroblast co-cultures, however polarized responses were not examined.[24] The ability of fibroblasts to respond to and amplify signals from a virally-infected epithelium reflects their role as sentinels of the immune system.[2,25,26]

In the EMTU models we determined a key role for epithelial-derived IL-1α in mediating cellular cross-talk and amplifying innate immune responses following viral stimulation. IL-1α is constitutively expressed in the cytoplasm of cells and is released in a mature form following necrotic cell death, however it can also be released in the absence of cell death.[10,27-29] While we found no evidence of epithelial cell death in the co-culture model following dsRNA (Fig. S1C), we observed approximately 10% cell death in HRV-infected ALI cultures. However we also observed upregulation of intracellular IL-1α in HBECs following exposure to HRV or dsRNA suggesting intracellular IL-1α protein is induced by viral challenge and may be actively released, as reported previously.[10] We also concluded that the IL-1α was epithelial-derived since it was detected equivalently in HBEC mono- and co-cultures but not in fibroblast monocultures. This is consistent with immunohistochemical staining of bronchial tissue showing that the epithelium is a major site of IL-1α expression,[3] with localization toward the apical surface of the epithelium.

The polarized nature of the models also gave us the opportunity to investigate the importance of apical and basolateral IL-1 signaling. Thus, basolateral application of IL-1Ra was sufficient to completely suppress basolateral release of IL-6, CXCL8 and GM-CSF, but had minimal effect on CXCL10 release. As CXCL10 is strongly induced by Type I and III interferons, it is of considerable interest that this anti-viral response can be separated from the IL-1α mediated proinflammatory response. In contrast with its potency in the

basolateral compartment, apical application of IL-1Ra was less effective with only a partial suppression of mediator release. Although both IL-1α and IL-1β can be inhibited by the use of IL-1Ra,[30] in our system it is likely that IL-1Ra primarily blocks IL-1α signaling as we could not detect IL-1β in the EMTU co-culture models. IL-1β has previously been detected from primary HBEC monolayer cultures following viral infection,[10,31,32] however we could not detect it in our models using differentiated HBEC cultures. This may be due to use of undifferentiated cells versus polarized or fully differentiated cultures. Our data suggest that in response to dsRNA or HRV, epithelial cells release IL-1α basolaterally and that this is required to drive IL-6, CXCL8 and GM-CSF release from fibroblasts. Consistent with this, we showed that the fibroblasts were highly sensitive to direct stimulation with IL-1α. These results are consistent with previous findings that IL-1α present in conditioned medium from damaged epithelial cells induces IL-6 and CXCL8 production from fibroblasts.[3,33]

Given the relatively high levels of apically released IL-1α, it was surprising that the low levels of basolateral IL-1α measured in the EMTU co-culture models were not only sufficient, but essential, for dsRNA-induced proinflammatory mediator release in this compartment. This may be explained by the close proximity of the fibroblasts to the basolateral surface of the epithelium resulting in high localized concentrations of IL-1α. Also IL-1R1 is highly expressed by fibroblasts[3] suggesting that they are highly sensitive to activation, even at low concentrations of IL-1α. Furthermore IL-6 is known to act as an autocrine factor that can drive its own release,[34] thus IL-1α may be a trigger for this effect. In contrast to the marked sensitivity of fibroblasts to exogenous or paracrine IL-1α, HBECs were relatively unresponsive to direct IL-1α stimulation. Thus, we observed little response using a concentration similar to that measured in the cell-free supernatants of challenged cultures; however, at higher concentrations of IL-1α, IL-6 production could be observed (data not shown). Furthermore, when HBEC monocultures were challenged with dsRNA in the presence of IL-1Ra, partial inhibition of dsRNA-dependent cytokine release was observed, similar to findings with HRV-infected HBECs.[10] In such a complex antiviral response, it is possible that other factors synergize with IL-1α to promote an epithelial inflammatory response.

Although out of the scope of the current study, the high levels of IL-1α in the apical compartment are of considerable interest as they have the potential to amplify local innate and adaptive immunity through direct activation or enhancement of luminal immune cell functions. Macrophages are the first line of cellular defense against invading pathogens and the IL-1α-IL-1RI pathway has been identified as a key driver of inflammatory cytokine and chemokine activation after adenovirus infection.[35] However, direct evidence for IL-1α-mediated cross talk with infected epithelium has not been investigated. The human monocytic cell line, THP-1, expresses IL-1R1 and alveolar macrophages have reduced LPS-dependent CXCL8 release in the presence of IL-1Ra.[3,36] Mast cells also respond to IL-1α with enhanced Th2 cytokine production.[37,38]

In conclusion, we provide evidence of direct cellular cross-talk in an integrated model of the EMTU where apical HRV infection or exposure to dsRNA of the epithelium results in the maintenance of polarized responses and drives synergistic basolateral proinflammatory mediator release from underlying fibroblasts. Epithelial-derived IL-1α plays a key role in enhancing proinflammatory but not anti-viral responses of the underlying fibroblasts. In chronic respiratory diseases, such as asthma and COPD, where respiratory viral infections are a major cause of acute exacerbations[6] targeting IL-1α may suppress airway inflammation while maintaining anti-viral signaling. The IL-1R1 antagonist anakinra is already FDA-approved[39] and clinical trials have shown its effectiveness in inflammatory diseases[40] and LPS-induced airway inflammation in healthy volunteers without adverse effects.[41]

Abbreviations

16HBE	the 16HBE14o$^-$ human bronchial epithelial cell line
ALI	air-liquid interface
BEC	bronchial epithelial cell
dsRNA	double-stranded RNA
EMTU	epithelial-mesenchymal trophic unit
HBEC	human bronchial epithelial cell
HLF	human lung fibroblast
HRV	human rhinovirus
IL-1R1	IL-1 receptor
IL-R2	IL-1 decoy receptor
IL-1Ra	IL-1 receptor antagonist
MOI	multiplicity of infection
poly(I:C)	polyinosinic:polycytidylic acid

$TCID_{50}$ tissue culture infective dose resulting in 50% death
TER transepithelial electrical resistance

Disclosure of potential conflicts of interest

Prof. Donna Davies reports personal fees from Synairgen, other from Synairgen, outside the submitted work and has a patent for use of Inhaled interferon β for virus-induced exacerbations of asthma and COPD with royalties paid. Dr. Grainge reports personal fees from Astra Zeneca Pharmaceuticals and Boehringer Ingleheim and grants from Boehringer Ingelheim, outside the submitted work. Prof. Peter Howarth reports part time employment as Global Medical Expert by GSK since 2016.

Acknowledgments

We thank Graham Berreen (University of Southampton) for technical support.

Funding

Support for the work was provided by a joint studentship from The Gerald Kerkut Charitable Trust and the University of Southampton, Faculty of Medicine to ARH, the Asthma, Allergy and Inflammation Research (AAIR) Charity, the Medical Research Council, UK (MRC) (G0900453) and an MRC CASE studentship (G100187) to JED sponsored by Novartis.

References

[1] Swindle EJ, Collins JE, Davies DE. Breakdown in epithelial barrier function in patients with asthma: identification of novel therapeutic approaches. J Allergy Clin Immunol 2009; 124:23-34; quiz 5-6; PMID:19560576; http://dx.doi.org/10.1016/j.jaci.2009.05.037

[2] Evans MJ, Van Winkle LS, Fanucchi MV, Plopper CG. The attenuated fibroblast sheath of the respiratory tract epithelial-mesenchymal trophic unit. Am J Respir Cell Mol Biol 1999; 21:655-7; PMID:10572061; http://dx.doi.org/10.1165/ajrcmb.21.6.3807

[3] Suwara MI, Green NJ, Borthwick LA, Mann J, Mayer-Barber KD, Barron L, Corris PA, Farrow SN, Wynn TA, Fisher AJ, et al. IL-1alpha released from damaged epithelial cells is sufficient and essential to trigger inflammatory responses in human lung fibroblasts. Mucosal Immunol 2014; 7:684-93; PMID:24172847; http://dx.doi.org/10.1038/mi.2013.87

[4] Morishima Y, Nomura A, Uchida Y, Noguchi Y, Sakamoto T, Ishii Y, Goto Y, Masuyama K, Zhang MJ, Hirano K, et al. Triggering the induction of myofibroblast and fibrogenesis by airway epithelial shedding. Am J Respir Cell Mol Biol 2001; 24:1-11; PMID:11152644; http://dx.doi.org/10.1165/ajrcmb.24.1.4040

[5] Kennedy JL, Turner RB, Braciale T, Heymann PW, Borish L. Pathogenesis of rhinovirus infection. Curr Opin Virol 2012; 2:287-93; PMID:22542099; http://dx.doi.org/10.1016/j.coviro.2012.03.008

[6] Gavala ML, Bertics PJ, Gern JE. Rhinoviruses, allergic inflammation, and asthma. Immunol Rev 2011; 242:69-90; PMID:21682739; http://dx.doi.org/10.1111/j.1600-065X.2011.01031.x

[7] Sajjan U, Wang Q, Zhao Y, Gruenert DC, Hershenson MB. Rhinovirus disrupts the barrier function of polarized airway epithelial cells. Am J Respir Crit Care Med 2008; 178:1271-81; PMID:18787220; http://dx.doi.org/10.1164/rccm.200801-136OC

[8] Comstock AT, Ganesan S, Chattoraj A, Faris AN, Margolis BL, Hershenson MB, Sajjan US. Rhinovirus-induced barrier dysfunction in polarized airway epithelial cells is mediated by NADPH oxidase 1. J Virol 2011; 85:6795-808; PMID:21507984; http://dx.doi.org/10.1128/JVI.02074-10

[9] Wark PA, Bucchieri F, Johnston SL, Gibson PG, Hamilton L, Mimica J, Zummo G, Holgate ST, Attia J, Thakkinstian A, et al. IFN-gamma-induced protein 10 is a novel biomarker of rhinovirus-induced asthma exacerbations. J Allergy Clin Immunol 2007; 120:586-93; PMID:17628646; http://dx.doi.org/10.1016/j.jaci.2007.04.046

[10] Piper SC, Ferguson J, Kay L, Parker LC, Sabroe I, Sleeman MA, Briend E, Finch DK. The role of interleukin-1 and interleukin-18 in pro-inflammatory and anti-viral responses to rhinovirus in primary bronchial epithelial cells. PLoS One 2013; 8:e63365; PMID:23723976; http://dx.doi.org/10.1371/journal.pone.0063365

[11] Jackson DJ, Makrinioti H, Rana BM, Shamji BW, Trujillo-Torralbo MB, Footitt J, Jerico Del-Rosario, Telcian AG, Nikonova A, Zhu J, et al. IL-33-dependent type 2 inflammation during rhinovirus-induced asthma exacerbations in vivo. Am J Respir Crit Care Med 2014; 190:1373-82; PMID:25350863; http://dx.doi.org/10.1164/rccm.201406-1039OC

[12] Hui CC, Murphy DM, Neighbour H, Al-Sayegh M, O'Byrne S, Thong B, Denburg JA, Larché M. T cell-mediated induction of thymic stromal lymphopoietin in differentiated human primary bronchial epithelial cells. Clin Exp Allergy 2014; 44:953-64; PMID:24773145; http://dx.doi.org/10.1111/cea.12330

[13] Nagarkar DR, Poposki JA, Comeau MR, Biyasheva A, Avila PC, Schleimer RP, Kato A. Airway epithelial cells activate TH2 cytokine production in mast cells through IL-1 and thymic stromal lymphopoietin. J Allergy Clin Immunol 2012; 130:225-32 e4; PMID:22633328; http://dx.doi.org/10.1016/j.jaci.2012.04.019

[14] Psarras S, Volonaki E, Skevaki CL, Xatzipsalti M, Bossios A, Pratsinis H, Tsigkos S, Gourgiotis D, Constantopoulos AG, Papapetropoulos A, et al. Vascular endothelial growth factor-mediated induction of angiogenesis by human rhinoviruses. J Allergy Clin Immunol 2006; 117:291-7; PMID:16461129; http://dx.doi.org/10.1016/j.jaci.2005.11.005

[15] Leigh R, Oyelusi W, Wiehler S, Koetzler R, Zaheer RS, Newton R, Proud D. Human rhinovirus infection enhances airway epithelial cell production of growth factors

involved in airway remodeling. J Allergy Clin Immunol 2008; 121:1238-45 e4; PMID:18355907; http://dx.doi.org/10.1016/j.jaci.2008.01.067

[16] Skevaki CL, Psarras S, Volonaki E, Pratsinis H, Spyridaki IS, Gaga M, Georgiou V, Vittorakis S, Telcian AG, Maggina P, et al. Rhinovirus-induced basic fibroblast growth factor release mediates airway remodeling features. Clin Transl Allergy 2012; 2:14; PMID:22908984; http://dx.doi.org/10.1186/2045-7022-2-14

[17] Blume C, Swindle EJ, Dennison P, Jayasekera NP, Dudley S, Monk P, Behrendt H, Schmidt-Weber CB, Holgate ST, Howarth PH, et al. Barrier responses of human bronchial epithelial cells to grass pollen exposure. Eur Respir J 2013; 42:87-97; PMID:23143548; http://dx.doi.org/10.1183/09031936.00075612

[18] Papi A, Johnston SL. Rhinovirus infection induces expression of its own receptor intercellular adhesion molecule 1 (ICAM-1) via increased NF-kappaB-mediated transcription. J Biol Chem 1999; 274:9707-20; PMID:10092659; http://dx.doi.org/10.1074/jbc.274.14.9707

[19] Bedke N, Sammut D, Green B, Kehagia V, Dennison P, Jenkins G, Tatler A, Howarth PH, Holgate ST, Davies DE. Transforming growth factor-β promotes rhinovirus replication in bronchial epithelial cells by suppressing the innate immune response. PloS One 2012; 7:e44580; PMID:22970254; http://dx.doi.org/10.1371/journal.pone.0044580

[20] Takeuchi O, Akira S. Innate immunity to virus infection. Immunol Rev 2009; 227:75-86; PMID:19120477; http://dx.doi.org/10.1111/j.1600-065X.2008.00737.x

[21] Rezaee F, Meednu N, Emo JA, Saatian B, Chapman TJ, Naydenov NG, De Benedetto A, Beck LA, Ivanov AI, Georas SN. Polyinosinic:polycytidylic acid induces protein kinase D-dependent disassembly of apical junctions and barrier dysfunction in airway epithelial cells. J Allergy Clin Immunol 2011; 128:1216-24 e11; PMID:21996340; http://dx.doi.org/10.1016/j.jaci.2011.08.035

[22] Unger BL, Ganesan S, Comstock AT, Faris AN, Hershenson MB, Sajjan US. Nod-like receptor X-1 is required for rhinovirus-induced barrier dysfunction in airway epithelial cells. J Virol 2014; 88:3705-18; PMID:24429360; http://dx.doi.org/10.1128/JVI.03039-13

[23] Jakiela B, Brockman-Schneider R, Amineva S, Lee WM, Gern JE. Basal cells of differentiated bronchial epithelium are more susceptible to rhinovirus infection. Am J Respir Cell Mol Biol 2008; 38:517-23; PMID:18063839; http://dx.doi.org/10.1165/rcmb.2007-0050OC

[24] Ito Y, Correll K, Zemans RL, Leslie CC, Murphy RC, Mason RJ. Influenza induces IL-8 and GM-CSF secretion by human alveolar epithelial cells through HGF/c-Met and TGF-α/EGFR signaling. Am J Physiol Lung Cell Mol Physiol 2015; 308:L1178-88; PMID:26033355; http://dx.doi.org/10.1152/ajplung.00290.2014

[25] Alkhouri H, Poppinga WJ, Tania NP, Ammit A, Schuliga M. Regulation of pulmonary inflammation by mesenchymal cells. Pulm Pharmacol Ther 2014; 29:156-65; PMID:24657485; http://dx.doi.org/10.1016/j.pupt.2014.03.001

[26] Kitamura H, Cambier S, Somanath S, Barker T, Minagawa S, Markovics J, Goodsell A, Publicover J, Reichardt L, Jablons D, et al. Mouse and human lung fibroblasts regulate dendritic cell trafficking, airway inflammation, and fibrosis through integrin alphav-beta8-mediated activation of TGF-β. J Clin Invest 2011; 121:2863-75; PMID:21646718; http://dx.doi.org/10.1172/JCI45589

[27] Chen CJ, Kono H, Golenbock D, Reed G, Akira S, Rock KL. Identification of a key pathway required for the sterile inflammatory response triggered by dying cells. Nat Med 2007; 13:851-6; PMID:17572686; http://dx.doi.org/10.1038/nm1603

[28] Chen GY, Nunez G. Sterile inflammation: sensing and reacting to damage. Nat Rev Immunol 2010; 10:826-37; PMID:21088683; http://dx.doi.org/10.1038/nri2873

[29] Dinarello CA. Immunological and inflammatory functions of the interleukin-1 family. Annu Rev Immunol 2009; 27:519-50; PMID:19302047; http://dx.doi.org/10.1146/annurev.immunol.021908.132612

[30] Garlanda C, Dinarello CA, Mantovani A. The interleukin-1 family: back to the future. Immunity 2013; 39:1003-18; PMID:24332029; http://dx.doi.org/10.1016/j.immuni.2013.11.010

[31] Proud D, Sanders SP, Wiehler S. Human rhinovirus infection induces airway epithelial cell production of human β-defensin 2 both in vitro and in vivo. J Immunol 2004; 172:4637-45; http://dx.doi.org/10.4049/jimmunol.172.7.4637

[32] Shi L, Manthei DM, Guadarrama AG, Lenertz LY, Denlinger LC. Rhinovirus-induced IL-1beta release from bronchial epithelial cells is independent of functional P27. Am J Respir Cell Mol Biol 2012; 47:363-71; PMID:22493010; http://dx.doi.org/10.1165/rcmb.2011-0267OC

[33] Tracy EC, Bowman MJ, Henderson BW, Baumann H. Interleukin-1alpha is the major alarmin of lung epithelial cells released during photodynamic therapy to induce inflammatory mediators in fibroblasts. Br J Cancer 2012; 107:1534-46; PMID:22996613; http://dx.doi.org/10.1038/bjc.2012.429

[34] Melkamu T, Kita H, O'Grady SM. TLR3 activation evokes IL-6 secretion, autocrine regulation of Stat3 signaling and TLR2 expression in human bronchial epithelial cells. J Cell Commun Signal 2013; 7:109-18; PMID:23232980; http://dx.doi.org/10.1007/s12079-012-0185-z

[35] Di Paolo NC, Miao EA, Iwakura Y, Murali-Krishna K, Aderem A, Flavell RA, Papayannopoulou T, Shayakhmetov DM. Virus binding to a plasma membrane receptor triggers interleukin-1 α-mediated proinflammatory macrophage response in vivo. Immunity 2009; 31:110-21; PMID:19576795; http://dx.doi.org/10.1016/j.immuni.2009.04.015

[36] Mazzarella G, Grella E, D'Auria D, Paciocco G, Perna F, Petillo O, Peluso G. Phenotypic features of alveolar monocytes/macrophages and IL-8 gene activation by IL-

1 and TNF-α in asthmatic patients. Allergy 2000; 55 Suppl 61:36-41; PMID:10919504; http://dx.doi.org/10.1034/j.1398-9995.2000.00505.x

[37] Allakhverdi Z, Smith DE, Comeau MR, Delespesse G. Cutting edge: The ST2 ligand IL-33 potently activates and drives maturation of human mast cells. J Immunol 2007; 179:2051-4; http://dx.doi.org/10.4049/jimmunol.179.4.2051

[38] Nagarkar DR, Poposki JA, Comeau MR, Biyasheva A, Avila PC, Schleimer RP, Kato A. Airway epithelial cells activate T(H)2 cytokine production in mast cells through IL-1 and thymic stromal lymphopoietin. J Allergy Clin Immunol 2012; 130:225-32; PMID:22633328; http://dx.doi.org/10.1016/j.jaci.2012.04.019

[39] Mertens M, Singh JA. Anakinra for rheumatoid arthritis: a systematic review. J Rheumatol 2009; 36:1118-25; PMID:19447938; http://dx.doi.org/10.3899/jrheum.090074

[40] Dinarello CA, van der Meer JW. Treating inflammation by blocking interleukin-1 in humans. Semin Immunol 2013; 25:469-84; PMID:24275598; http://dx.doi.org/10.1016/j.smim.2013.10.008

[41] Hernandez ML, Mills K, Almond M, Todoric K, Aleman MM, Zhang H, Zhou H, Peden DB. IL-1 receptor antagonist reduces endotoxin-induced airway inflammation in healthy volunteers. J Allergy Clin Immunol 2015; 135:379-85; PMID:25195169; http://dx.doi.org/10.1016/j.jaci.2014.07.039